AFFDL-TR-66-163

FLIGHT INVESTIGATION OF LONGITUDINAL SHORT PERIOD FREQUENCY REQUIREMENTS AND PIO TENDENCIES

DANTE A. DiFRANCO

CORNELL AERONAUTICAL LABORATORY, INC.
BUFFALO, NEW YORK 14221

TECHNICAL REPORT AFFDL-TR-66-163

JUNE 1967

Distribution of This Document Is Unlimited

AIR FORCE FLIGHT DYNAMICS LABORATORY
RESEARCH AND TECHNOLOGY DIVISION
AIR FORCE SYSTEMS COMMAND
WRIGHT-PATTERSON AIR FORCE BASE, OHIO 45433

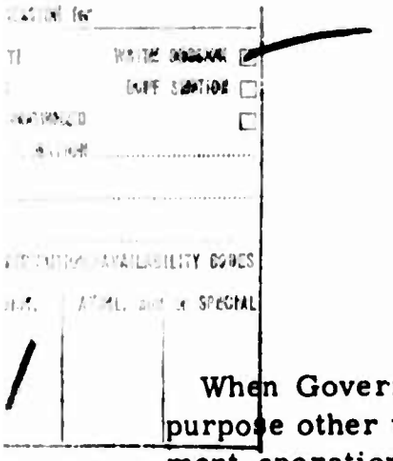

NOTICES

When Government drawings, specifications, or other data are used for any purpose other than in connection with a definitely related Government procurement operation, the United States Government thereby incurs no responsibility nor any obligation whatsoever; and the fact that the Government may have formulated, furnished, or in any way supplied the said drawings, specifications, or other data, is not to be regarded by implication or otherwise as in any manner licensing the holder or any other person or corporation, or conveying any rights or permission to manufacture, use, or sell any patented invention that may in any way be related thereto.

Copies of this report should not be returned to the Research and Technology Division unless return is required by security considerations, contractual obligations, or notice on a specific document.

FLIGHT INVESTIGATION OF LONGITUDINAL SHORT PERIOD FREQUENCY REQUIREMENTS AND PIO TENDENCIES

DANTE A. DiFRANCO

CORNELL AERONAUTICAL LABORATORY, INC.
BUFFALO, NEW YORK 14221

ABSTRACT

The results of a flight test program to investigate longitudinal short period frequency requirements and PIO tendencies are presented and discussed. Short period frequency requirements were investigated with a damping ratio (ζ_{sp}) of approximately 0.7 at three fixed values of n_z/α (16.9, 30.4, and 63.4 g/rad). PIO tendencies were investigated with various values of the parameter $2\zeta_{sp}\omega_{sp}/L_\alpha$. The feel system dynamic characteristics were held essentially constant throughout the program. A variable stability T-33 airplane was used as an in-flight simulator. Approximately 150 configurations were evaluated by two experienced test pilots. Each configuration was evaluated as a fighter in "up and away" flight. The evaluation pilots commented on each configuration and rated each numerically. An analysis of pilot ratings and pilot comments was made, and these in turn were related to various handling qualities parameters. In the analysis and interpretation of the handling qualities results, feel system dynamics and pilot-selected stick force gradients (F_{es}/n_z) were also important considerations.

FOREWORD

This report was prepared for the United States Air Force by the Cornell Aeronautical Laboratory, Inc., Buffalo, New York, in partial fulfillment of Contract AF 33(615)-2536.

The flight test program reported herein was performed by the Flight Research Department of the Cornell Aeronautical Laboratory under sponsorship of the Air Force Flight Dynamics Laboratory, Research and Technology Division, Wright-Patterson Air Force Base, Ohio, as Task 821905 of Project No. 8219. Flt. Lt. T. M. Harris and Capt. J. R. Pruner were project engineers for the Flight Dynamics Laboratory.

This report is also being published as Cornell Aeronautical Laboratory Report No. TC-2083-F-1.

The work reported in this document is the result of the combined efforts of a number of members of the Cornell Flight Research Department. The planning of the flight test program, the direction of the calibrations. and the first half of the in-flight evaluation program was under the supervision of Charles R. Chalk. Mr. Peter Neal participated as a flight test engineer through the flight test phase of the investigation. Messrs. R. Harper and J. Meeker acted as safety pilots and in-flight test conductors. Mr. N. Infanti was the Cornell evaluation pilot, and Major Michael Adams was the Air Force evaluation pilot. Mr. R. Huber was responsible for modifications, calibration, and maintenance of the T-33 variable stability system.

This manuscript was released 7 April 1967 for publication as an RTD Technical Report.

This technical report has been reviewed and is approved.

C. B. Westbrook
Chief, Control Criteria Branch
Air Force Flight Dynamics Laboratory

CONTENTS

FIGURES

FIGURES (Cont.)

TABLES

LIST OF SYMBOLS

A_i Constants in transfer functions as defined in Appendix I ($i = \alpha, \theta, n_z$)

B_i Constants in transfer functions as defined in Appendix I ($i = \alpha, \theta, n_z$)

c Wing chord, ft

C_i Constants in transfer functions as defined in Appendix I ($i = 1, 2, 3, n_z$)

$C_L = L/\frac{1}{2}\rho V_0^2 S$, Airplane lift coefficient

$C_{L_\alpha} = \partial C_L/\partial\alpha$, Nondimensional airplane lift curve slope, 1/rad

$C_{L_{\delta_e}} = \partial C_L/\partial\delta_e$, Nondimensional lift coefficient derivative due to elevator control, 1/rad

$C_m = M/\frac{1}{2}\rho V_0^2 Sc$, Airplane pitching moment coefficient

$C_{m_\alpha} = \partial C_m/\partial\alpha$, Nondimensional airplane pitching moment curve slope, 1/rad

$C_{m_{\dot\alpha}} = \partial C_m/\partial\left(\frac{\dot\alpha c}{2V_0}\right)$, Nondimensional pitching moment coefficient damping derivative with respect to angle of attack rate, 1/rad

$C_{m_q} = \partial C_m/\partial\left(\frac{\dot\theta c}{2V}\right)$, Nondimensional pitching moment coefficient damping derivative with respect to angular pitch velocity, 1/rad

$C_{m_{\delta_e}} = \partial C_m/\partial\delta_e$, Nondimensional pitching moment coefficient derivative due to elevator control, 1/rad

$CAP = \omega_{SP}^2/\left(\frac{n_z}{\alpha}\right)$, Control anticipation parameter, $1/sec^2$

$(CAP)' = \frac{\omega_{SP}^2(\ddot\theta_{nd})_{MAX}}{\left(\frac{n_z}{\alpha}\right)}$, Control anticipation parameter modified by control system dynamics, $1/sec^2$

F_i Control force of elevator, aileron, or rudder ($i = AS, ES, RP$), lbs

g Acceleration of gravity, ft/sec^2

h_p Pressure altitude, ft

I_x, I_y, I_z Moments of inertia about airplane body x, y, and z axes, respectively, slug-ft^2

LIST OF SYMBOLS (Cont.)

$K_{\omega_{\dot{\alpha}}}$ Least-squares-fit coefficient as defined in Appendix I

L Airplane lift, lbs

$L_\alpha = \frac{\rho V_0 S}{2m} C_{L_\alpha}$, Dimensional lift force derivative with respect to angle of attack, 1/sec

M Airplane moment, ft-lbs

m Mass of airplane, slugs

$M_\alpha = \frac{\rho V_0^2 Sc}{2I_y} C_{m_\alpha}$, Dimensional pitching moment derivative with respect to angle of attack, $1/sec^2$

$M_{\dot{\alpha}} = \frac{\rho V_0 Sc^2}{4I_y} C_{m_{\dot{\alpha}}}$, Dimensional damping moment in pitch with respect to angle of attack rate, 1/sec

$M_{\dot{\theta}} = \frac{\rho V_0 Sc^2}{4I_y} C_{m_q}$, Dimensional damping moment in pitch due to angular pitch rate, 1/sec

$M_{\delta_e} = \frac{\rho V_0^2 Sc}{2I_y} C_{m_{\delta_e}}$, Dimensional pitching moment derivative with respect to elevator deflection, $1/sec^2$

$M_{\delta_{ES}} = \frac{\rho V_0^2 Sc}{2I_y}\left(\frac{\delta_e}{\delta_{ES}}\right) C_{m_{\delta_e}}$, Dimensional pitching moment derivative with respect to elevator stick deflection, $1/in.\text{-}sec^2$

n_z Normal acceleration, g

s Laplace operator

LIST OF SYMBOLS (Cont.)

S	Wing area, sq ft
t	Time, sec
V	True velocity, knots or ft/sec
Z_α	$= -L_\alpha = -\frac{\rho V_0 S}{2m} C_{L_\alpha}$, Dimensional force derivative along the z -body axis with respect to angle of attack, 1/sec
Z_{δ_e}	$= -L_{\delta_e} = -\frac{\rho V_0 S}{2m} C_{L_{\delta_e}}$, Dimensional control force derivative along the z -body axis with respect to elevator control deflection, 1/sec
α	Airplane angle of attack from trim level flight, rad
γ	Flight path angle from horizontal, rad
Δ	Small incremental change
δ_i	Control surface deflection, in radians, or control stick deflection, in inches, from trim level flight ($i = AS, AT, e, ES, r, RP$)
ζ_i	Damping ratio ($i = d, e, FS, P, SP$)
θ	Pitch angle from trim level flight, rad
ρ	Air density, slugs/ft^3
τ_R	Roll mode time constant, sec
ω_i	Undamped natural frequency ($i = d, e, FS, P, SP$), rad/sec
$(\dot{})$	$= d( )/dt$, First derivative with respect to time, 1/sec
$(\ddot{})$	$= d^2( )/dt^2$, Second derivative with respect to time, 1/sec

Subscripts:

AS	Refers to aileron stick deflection at grip in inches, positive to the right
AT	Refers to total aileron deflection in degrees, positive with right aileron down and left aileron up
c	Refers to random interference command input to tracking task

LIST OF SYMBOLS (Cont.)

d	Refers to Dutch roll
e	Refers to elevator deflection or elevator servo
ES	Refers to elevator stick deflection in inches, positive rearward
FS	Refers to elevator feel system
MAX	Maximum
nd	Refers to ratio of pitch angle, pitch velocity, and pitch acceleration, including feel system dynamics, to initial pitch acceleration, excluding feel system dynamics. The pitch responses are those resulting from a step stick force input (see Section 6.2)
0	Refers to initial value or value at time zero
p	Refers to phugoid
r	Refers to rudder deflection in degrees, positive clockwise when viewed from above airplane
RP	Refers to rudder pedal deflection in inches, right rudder pedal positive
SP	Refers to longitudinal short period
ss	Refers to steady-state values
$T\text{-}33$	Refers to basic, unaugmented T-33 airplane
ϵ	Refers to error

Abbreviations:

AF	Air Force
CAL	Cornell Aeronautical Laboratory, Inc.
CAP	control anticipation parameter
cps	cycles per second
FR	fuel remaining

LIST OF SYMBOLS (Cont.)

ft	feet
IAS	indicated airspeed
in.	inch
kts	knots
lbs	pounds
LSF	least-squares-fit
PIO	pilot-induced oscillation
PIOR	pilot-induced oscillation rating
PR	pilot rating
rad/sec	radians per second
RMS	root mean square

Section I

INTRODUCTION

A number of experimental, longitudinal handling qualities investigations of short period frequency requirements have been made in the past in both fixed-base and in-flight simulators (References 1 through 9). These handling qualities results, when interpreted in terms of undamped short period frequency (ω_{sp}) and damping (ζ_{sp}) requirements for satisfactory handling qualities, show considerable differences. More recent examinations of these data indicate that n_z/α or L_α may be the important parameters which will explain and resolve these discrepancies (Reference 5, for example).

Flight test results (References 1, 2, 3, and 4), although limited at high frequencies, also indicate that there is an upper limit on the short period frequency that is acceptable to the pilot, but this trend has not been substantiated by ground simulators (Reference 6). The ground simulator results lack some important pilot cues, especially pitch motion.

An additional area of interest is those factors which contribute to pilot-induced oscillation (PIO) tendencies during demanding tasks such as tracking, formation, and low-level flying. This problem is obviously concerned with a more precise understanding of the closed-loop pilot-airplane combination. The dynamics of the control system are also important factors. References 10 through 15 examine various aspects of the PIO tendencies problem. A detailed analytic treatment of PIO tendencies is contained in Reference 10. With good control system dynamics, it has been postulated that PIO's can occur only when $2\zeta_{sp}\omega_{sp} < L_\alpha$. This postulate is based on the assumption that the pilot acts as a pure gain controller and is responsive only to θ in a single loop compensatory tracking situation.

These short period, longitudinal handling qualities problems were investigated in a flight test program conducted by the Flight Research Department of Cornell Aeronautical Laboratory (CAL) during the summer of 1965, and the results of this study are presented in this report. The USAF/CAL variable stability T-33 was used in the flight simulations. Both Air Force and CAL evaluation pilots participated in this program.

A total of 64 evaluation flights was flown, and 177 configurations were evaluated; 136 of these configurations investigated short period frequency requirements as influenced by n_z/α or L_α at a damping ratio of approximately 0.7. Three essentially fixed n_z/α values (16.9, 30.4, 63.4 g/rad) were investigated through a range of short period undamped frequencies ($\omega_{sp} \approx 2$ to 16 rad/sec). The remaining 41 configurations were concerned primarily with an investigation of PIO tendencies with essentially fixed control system

dynamics. The PIO configurations were simulated by varying the airplane damping ratio ($\zeta_{SP} \approx 0.1$ to 0.7) at reasonably fixed undamped frequencies ($\omega_{SP} \approx 2$, 4, and 6 rad/sec). The L_α values during these tests were essentially fixed at 1.36, 1.78, and 3.07.

In the analysis of pilot rating and pilot comment data, feel system dynamics and pilot-selected stick force gradients were also important handling qualities considerations.

Section II

EVALUATION PROGRAM

2.1 GENERAL DISCUSSION

For a number of years, the Flight Research Department of Cornell Aeronautical Laboratory has been engaged in variable stability and handling qualities research. Part of this research has been concerned with longitudinal, short period handling qualities requirements of a variety of aircraft performing specific tasks under specified flight conditions. Much of this short period research was concerned primarily with the frequency and damping requirements. The research was done using variable stability airplanes performing in-flight simulation and is documented in numerous reports (e.g., References 1, 2, 3, and 4).

As a result of this research, boundaries of frequency and damping with various degrees of acceptance (iso-opinion lines) have been established. Good, satisfactory, and unsatisfactory boundaries have been delineated based on pilot ratings and pilot comments. Some of the boundaries or iso-opinion lines were not well established at higher frequencies. Indications were that these boundaries would close at the higher frequencies even with satisfactory damping ($\zeta_{sp} \approx 0.7$), but this conclusion was tentative. In Reference 3, reasonably accurate simulation of short period response was limited to short period frequencies of 0.78 cps. In References 1 and 2, the limiting frequency was approximately 1.15 cps. Variable stability equipment limitations made higher frequency simulations questionable because of the significant influence of the variable stability system on the character of the airplane short period response. More recent research in a ground-based simulator (Reference 6) disagrees with these "tentative" in-flight results. The "G-seat" in which the ground-based simulations of Reference 6 were performed was capable of vertical movements and, thus, simulation of normal acceleration. However, it lacked the pitch degree of freedom of an airplane in flight. In References 1, 2, and 3, pilot objections at high frequencies were directed at the abruptness of the initial pitch response. One of the purposes of the present flight test program is to further investigate this problem in flight. The USAF/CAL variable stability T-33, with an improved elevator servo, is capable of simulating longitudinal short period frequencies of 2 cps or better.

Discrepancies exist between the iso-opinion ("thumbprint") boundaries of References 1, 2, 3, and 4. Frequency and damping are denominator parameters that enter into the transfer functions of the various airplane responses to control inputs. But the magnitude of any given response and the relation between amplitude and phasing of the responses will depend on other variables such as true speed (V_0), L_α, and M_{δ_e} of the airplane. The parameters L_α and M_{δ_e} appear in the numerator of the pitch angle transfer function. All

three parameters appear in the normal acceleration transfer function. A ground simulator program was conducted (Reference 5) to determine the probable effect of these variables on short period handling qualities. The results of Reference 5 indicated that short period iso-opinion lines are also associated with another parameter, the variation of normal acceleration with angle of attack (n_z/α). This parameter is related to V and L_α by the relationship $n_z/\alpha = V_0 L_\alpha / g$. The results of Reference 5 indicate that the most satisfactory ratings occurred for n_z/α's between 5 and 80 g/rad.

The importance of L_α and velocity (V_0) in airplane handling qualities has also been investigated more recently by others (References 7, 8, and 9). Methods have been suggested for relating iso-opinion lines or "thumbprints" for various size and types of airplanes (fighters, bombers, transports). All of the suggested parameters involve relationships between ω_{sp}, ζ_{sp}, L_α, and V_0. The present flight test program was undertaken to study some of these problems with the proper pilot cues in a more realistic physical environment.

Some investigators have pointed out the importance of the initial pitch acceleration, pitch velocity, and the shape of the response curve on the short period handling qualities (References 7 and 16). The importance of pitch acceleration, and the pilot objections associated with it are also described much earlier in the in-flight investigations of References 3 and 4. In Reference 16, the author points out the importance of CAP (control anticipation parameter) in longitudinal handling qualities. CAP is the ratio of the initial pitch acceleration ($\ddot{\theta}_0$) to the steady-state normal acceleration ($n_{z_{ss}}$) following a step elevator input from trimmed level flight (CAP = $\ddot{\theta}_0/n_{z_{ss}}$). It is suggested in Reference 7 that the pilot is responsive to a blend of normal acceleration, pitch rate, and pitch acceleration of the airplane. The handling qualities results of the flight test program presented in this report are interpreted in the light of these suggested handling qualities parameters.

The effect of feel and control system dynamics and stick forces on the closed-loop pilot-airplane handling qualities has been recognized for some time. (See References 3, 12, 13, and 15.) No attempt was made in the present program to determine the effects on handling qualities of different feel system characteristics. A set of essentially fixed feel system characteristics that were acceptable to the pilot was simulated in the variable stability T-33 for this flight test program. However, the attenuation effects of the feel system on the initial response of the airplane were significant and have been accounted for in interpreting the results and relating them to pilot ratings and comments as a function of airplane frequency. It is worth noting that the feel system in the present test is in series with the control servo and the airplane elevator control. In References 1, 2, 3, and 4, strain gauge force commands from the stick were used to actuate the control servo directly. This arrangement essentially eliminated the attenuating effects of a slow feel system on the airplane initial response, but not the attenuating

effects of the control surface servos. Obviously, a proper comparison and interpretation of past and present handling qualities results can only be made if such differences are adequately considered.

The pilot was also allowed to select what he considered to be an optimum stick force per g (F_{es}/n_z) for every configuration simulated. The stick force selected, its variability, and the pilot's reasons for the selection become an important aspect of this longitudinal short period investigation.

A rather extensive review and analytical investigation of pilot induced oscillation (PIO's) is presented in Reference 10. A study of the conditions for PIO requires an intimate understanding of the complete closed-loop pilot-airplane control system. Some aspects of the PIO tendencies in airplanes are also discussed in References 6, 11, and 14. For a linear system, with negligible effects of control system dynamics, it is postulated in Reference 10 that longitudinal PIO can occur if $2\zeta_{sp}\omega_{sp} < L_\alpha$. It is this condition of PIO tendencies that was investigated in this flight test program. The feel system frequency and damping simulated for this investigation were the same as those used in the longitudinal short period investigation ($\omega_{FS} = 23$ rad/sec, $\zeta_{FS} = 0.66$). Since the pilot was also allowed to select the elevator gearing or stick force per g for the PIO simulations, the effects of stick forces on PIO tendencies became a part of the investigation.

2.2 SHORT PERIOD FREQUENCY REQUIREMENTS

The effects of L_α and V_0, or n_z/α, on short period handling qualities requirements were investigated by both a CAL pilot and an Air Force evaluation pilot. A total of 136 configurations was investigated; 76 of these were evaluated by the CAL pilot, and 60 by the Air Force pilot. Some of these evaluations were repeat evaluations of the same configuration.

The short period investigation was at essentially constant damping ratio ($\zeta_{sp} \approx 0.7$), as ω_{sp} was varied at essentially three fixed values of L_α (1.36, 1.78, and 3.07). The variation in L_α was obtained by flying the T-33 variable stability airplane at indicated airspeeds of 220 kts, 300 kts, and 365 kts at 5500 feet pressure altitude. The true airspeeds were 238 kts, 324 kts, and 394 kts, and the corresponding values of n_z/α were 16.9, 30.4, and 63.4, respectively.

The primary factor responsible for small variations in the fixed values of L_α and n_z/α during the in-flight simulation was variation in airplane weight as fuel was consumed. These effects were kept to a minimum by simulating and evaluating three different configurations during each flight with the 220 kts simulation first, the 300 kts second, and the 365 kts third. The minimum L_α simulated ($L_\alpha = 1.36$) was determined by the minimum speed at which the evaluation pilot could pull 2 g's without entering stall buffet. The evaluation

pilots felt that a maneuver of at least 2 g's was required to adequately evaluate a configuration. The high speed and high L_α was determined by the maximum speed at which sufficient excess thrust was available to permit fighter maneuvers.

The degree of variation possible in the simulated natural frequencies is determined by the elevator servo frequency (ω_e = 63 rad/sec) and elevator gain setting limitations. The highest airplane frequencies could be simulated at the highest velocity flown (365 kts IAS). Variations in damping ratio from a ζ_{sp} of 0.7 were a function primarily of the accuracy to which airplane gain setting could be estimated to vary the frequency and keep the damping ratio constant.

The range of variables tested and the standard deviation of those variables held essentially constant are summarized in Table I.

2.3 INVESTIGATION OF PIO TENDENCIES

PIO tendencies were investigated by simulating PIO configurations under the same flight conditions (V, L_α, and n_z/α) used in the investigation of short period handling qualities. The mission, tasks, comments, and ratings associated with the short period handling qualities investigation were also the bases for the PIO investigation. Since the conditions for PIO are not clearly understood, the pilots evaluated all configurations for PIO tendencies and were not aware of which configurations were specifically simulated to induce PIO's.

Only PIO tendencies with fixed control system dynamics were investigated during this flight program. Configurations with PIO tendencies were simulated based on the PIO criterion $2\zeta_{sp}\omega_{sp} < L_\alpha$. Thus, configurations with $2\zeta_{sp}\omega_{sp}$ somewhat larger and smaller than L_α were simulated for three fixed values of L_α (1.36, 1.78, and 3.07). Variations in $2\zeta_{sp}\omega_{sp}$ at a fixed L_α were obtained by simulating various ζ_{sp} below 0.6 at three essentially fixed values of short period frequency (2, 4, and 6 rad/sec). The pilot was allowed to select the stick force per g that was most acceptable for the PIO configurations. PIO tendencies were thus attenuated by the pilot-selected stick forces and this effect is also reflected in the PIO ratings and comments.

Table XIII shows all the short period configurations simulated with damping ratios $\leq$ 0.6. These configurations were obtained from Tables VII, VIII, and IX. A few of the configurations listed in Table XIII have short period frequencies considerably higher than 6.0 radians per second, and some of these also show PIO tendencies. Listing configurations in Table XIII with $\zeta_{sp} \leq 0.6$ as PIO configurations is obviously somewhat arbitrary. The range of PIO variables investigated based on Table XIII is summarized in Table II. Most of the configurations in Table XIII, a total of 41, satisfy the condition $\omega_{sp} \leq 6.0$ radians per second and $\zeta_{sp} \leq 0.6$. Of these, 21 were

evaluated by the CAL pilot, and the remainder by the Air Force pilot. Of the total PIO configurations simulated, only 24 satisfied the criterion $2\zeta_{sp}\omega_{sp} < \angle\alpha$. Some of the PIO configurations were repeats of previously simulated configurations.

Section III

IN-FLIGHT SIMULATION

3.1 GENERAL DISCUSSION

The USAF/CAL variable stability T-33 airplane with standard 230 gallon wing tanks was used as the simulation and test vehicle. The simulation capabilities and limitations of the airplane, and the characteristics of its variable stability system are presented in Reference 17.

The lateral-directional characteristics of the airplane were augmented at each of the three test speeds (220 kts, 300 kts, 365 kts) to levels deemed satisfactory for a fighter by the CAL evaluation pilot. The lateral-directional characteristics (Table VI) were then held fixed throughout the program.

The center stick and rudder pedals were used to control the airplane for this program. The control feel and control authority for rudder and aileron controls were selected by the CAL evaluation pilot at the beginning of the program and remained constant throughout the evaluation (Table VI).

The spring rate of the elevator stick (F_{ES}/δ_{ES}) was set at 30 lbs/in., and the control gearing (δ_e/δ_{ES}) was optimized by the pilot at the beginning of the evaluation of each configuration.

The simulation included random disturbance inputs to all three controls (ailerons, rudder, and elevators). A tracking task was also a part of the evaluation. The tracking error was presented to the pilot on an all-attitude indicator.

The longitudinal short period frequency and damping of the airplane were varied through the variable stability elevator gains as a function of angle of attack and pitch rate (δ_e/α, $\delta_e/\dot{\alpha}$, and $\delta_e/\dot{\theta}$).

Each of these factors is discussed in the sections that follow.

3.2 SIMULATION OF SHORT PERIOD FREQUENCY AND DAMPING

Assuming negligible velocity changes, and negligible elevator lift, the longitudinal short period equations of motion for an airplane can be written as:

$$-\dot{\alpha} + Z_\alpha \alpha + \dot{\theta} = 0 \tag{3.1}$$

$$M_{\dot{\alpha}} \dot{\alpha} + M_\alpha \alpha - \ddot{\theta} + M_{\dot{\theta}} \dot{\theta} + M_{\delta_e} \delta_e = 0 \tag{3.2}$$

$$n_z = \frac{V_o}{g} \dot{\gamma} = \frac{V_o}{g} (\dot{\theta} - \dot{\alpha}) \tag{3.3}$$

Equation (3.3) is not an independent equation of motion but simply a relationship between normal acceleration in g (n_z), flight path angle rate ($\dot{\gamma}$), and the pitch and angle of attack rates ($\dot{\theta}$ and $\dot{\alpha}$). In terms of the dimensional derivatives in Equations (3.1) and (3.2), defined in the List of Symbols, the undamped natural frequency (ω_{sp}) and damping ratio (ζ_{sp}) of the short period assume the following form:

$$\omega_{sp}^2 = Z_\alpha M_{\dot{\theta}} - M_\alpha \tag{3.4}$$

$$2\zeta_{sp}\omega_{sp} = -Z_\alpha - M_{\dot{\theta}} - M_{\dot{\alpha}} \tag{3.5}$$

$$\zeta_{sp} = \frac{-(Z_\alpha + M_{\dot{\theta}} + M_{\dot{\alpha}})}{2\sqrt{Z_\alpha M_{\dot{\theta}} - M_\alpha}} \tag{3.6}$$

By varying the values of the derivatives in Equations (3.1) and (3.2), it is possible to vary the longitudinal short period undamped frequency and damping ratio. It is not possible to vary Z_α of the variable stability T-33 independently of the other derivatives; that is, Z_α can only be varied by varying the airplane flight condition which also varies the other derivatives. The T-33 elevator lift capability (Z_{δ_e}) is negligibly small. Neglecting Z_{δ_e}, it can be shown that the other derivatives can be varied independently by changing the gain settings to the elevator of the T-33 airplane.

$$M_\alpha = (M_\alpha)_{T-33} + \left(\frac{\delta_e}{\alpha}\right)\left(M_{\delta_e}\right)_{T-33} \tag{3.7}$$

$$M_{\dot{\alpha}} = (M_{\dot{\alpha}})_{T-33} + \left(\frac{\delta_e}{\dot{\alpha}}\right)\left(M_{\delta_e}\right)_{T-33} \tag{3.8}$$

$$M_{\dot{\theta}} = (M_{\dot{\theta}})_{T-33} + \left(\frac{\delta_e}{\dot{\theta}}\right)\left(M_{\delta_e}\right)_{T-33} \tag{3.9}$$

The quantities δ_e/α, $\delta_e/\dot{\alpha}$, and $\delta_e/\dot{\theta}$ are the constant static gain settings to the elevator as a function of the airplane α, $\dot{\alpha}$, and $\dot{\theta}$ responses. The derivatives in Equations (3.7), (3.8), and (3.9) are the T-33 derivatives for a given flight condition. By varying the simulated derivatives through the gain settings, the simulated frequencies and damping ratios can be varied. It is interesting to note that larger derivatives and larger frequencies can be simulated for the same gain settings when the T-33 derivatives are larger, especially M_{δ_e}. The derivative M_{δ_e} for the T-33 is larger when the airplane is flying at a higher free stream dynamic pressure. Assuming no gain limits as a function of flight condition, the highest frequencies simulated occur for the flight condition with the highest IAS, 365 kts.

Equations (3.7), (3.8), and (3.9) are true only when the elevator servo frequency is very high compared to the simulated frequencies and the lags of the sensors of the airplane are negligible. In actual fact, the problem is more complex, and each derivative is not an independent function of only one gain setting. Once the required gain settings are determined analytically, they are checked out through calibration flights. The frequency and damping ratios simulated in flight for various gain settings are determined from oscillograph traces of the actual airplane responses. The results of the calibration flights are used to determine gain settings to simulate particular frequencies and the damping ratios for each flight condition of the airplane.

The results of these calibration flights were used to determine gain setting curves at essentially constant damping ratio ($\zeta_{sp} \approx 0.7$) with varying frequency for each of the flight conditions (220 kts, 300 kts, and 365 kts IAS). These curves were used in the simulation of a spectrum of short period frequency configurations at three fixed values of L_α (1.36, 1.78, and 3.07).

In the simulation of PIO configurations, it was necessary to vary the damping ratio at three nominal values of frequency (ω_{sp} = 2, 4, and 6 rad/sec) for each of the flight conditions. Similar calibration flights were run to determine gain setting curves to simulate a spectrum of damping ratios for each of the flight conditions.

3.3 SIMULATION OF L_α AND n_z/α

As previously stated, it is not possible to vary L_α (or $-Z_\alpha$) independently in the variable stability T-33 airplane. The variable stability system does not incorporate variable lift as a function of angle of attack. The parameter L_α was varied by varying the indicated airspeed (220 kts, 300 kts, and 365 kts) at 5500 feet pressure altitude. The reasons for selecting these speeds were discussed in Section 2.2. The relationship between L_α and n_z/α is therefore fixed and determined by the equation, $n_z/\alpha = V_0 L_\alpha / g$. Some small variation in L_α and n_z/α occurred for each flight condition due to variations in fuel remaining for the T-33 airplane.

3.4 SIMULATION OF STICK FORCE PER g

The variable stability T-33 has a completely separate feel system whose characteristics can be varied independently from the airplane parameters simulated.

A spring rate (F_{ES}/δ_{ES}) of 30 lbs/in. was selected as satisfactory by the evaluation pilot during the calibration flight. The spring rate, with a few minor variations, was held constant throughout the evaluation flights. The control gearing (δ_e/δ_{ES}) was selected by the evaluation pilot for each configuration simulated. By changing the control gearing, the pilot could vary the δ_e/F_{ES}. By this means, the pitch response of the airplane to stick

force input could be changed, but not without a corresponding change in F_{ES}/n_z of the airplane. A reduction in gearing results in a reduction in pitch sensitivity and an increase in the steady-state F_{ES}/n_z. The actual airplane pitch response is, of course, a function also of the feel system and airplane dynamics.

For several configurations simulated, it was not possible to give the evaluation pilot the control gearing that he desired because of practical limitations in the simulation procedure. For these cases, the spring rate was changed slightly to give the pilot the desired δ_e/F_{ES}. Table III shows the spring rates actually used for the various flights.

Elevator stick position commands (δ_{ES}) from the feel system were used to operate the elevator through the elevator servo. Pilot force commands at the stick are not felt immediately as elevator stick commands to the elevator servo because of the design characteristics of the feel system (see Reference 17). The elevator stick (δ_{ES}) to stick force (F_{ES}) transfer function can be represented as a second order system.

$$\frac{\delta_{ES}}{F_{ES}}(s) = \frac{\omega_{FS}^2 \left(\frac{\delta_{ES}}{F_{ES}}\right)_{SS}}{(s^2 + 2\zeta_{FS}\omega_{FS}s + \omega_{FS}^2)} \qquad (3.10)$$

The numerator contains the constant steady-state spring rate gain, and the denominator contains the feel system frequency and damping. The feel system frequency and damping simulated for the spring rate of 30 lbs/in are $\omega_{FS} = 23$ rad/sec and $\zeta_{FS} = 0.66$. The feel system characteristics for the other spring rates are shown in Table III.

The method for determining the feel system characteristics is discussed in Appendix II. The effect of the feel system characteristics on the initial pitch response of the airplane is discussed in Section VI. The effect of the feel system on the pilot's evaluation of the simulated configurations is discussed in Section VII.

3.5 SIMULATION OF TRACKING TASK

A tracking task was included in the evaluation of each configuration simulated. The task was presented to the pilot by means of a cross-pointer on the all-attitude indicator (Figure 1). The pointer was driven by the difference between the command signal (θ_c) from the filtered random noise generator and a signal obtained from the pitch angle gyro. The display to the pilot thus consisted of the attitude error (θ_ϵ) together with the actual attitude of the airplane (θ). At the beginning of the tracking task, before the random noise was turned on, the gyro position, the airplane, and the cross-pointer could all be adjusted so that they coincided in trimmed level flight. Thus, the tracking errors and the airplane pitch angle displayed were plus and minus

angles from the trim attitude. The pilot's tracking task was one of reducing the error by getting the horizon and cross-pointer to coincide. The pitch angle error displayed on the indicator (Figure 1) was magnified with respect to the actual airplane pitch angle displayed. One inch of movement of the cross-pointer represented 5 degrees of change in attitude error. One inch of movement of the gyro horizon with respect to center-line represented about 20 degrees of airplane pitch attitude change. This magnification of tracking error was selected as reasonable by the evaluation pilot for tracking.

The level of pitch angle command that results from the random noise source varies with time. A realistic and reasonable root mean square (RMS) level was selected by the CAL evaluation pilot during the calibration flights for each flight condition of the airplane (220 kts, 300 kts, and 365 kts). The levels of pitch command gains remained constant for each flight condition throughout the evaluation program. Some typical RMS values of θ_c and θ_ϵ were measured for two evaluation flights at each flight condition during the pilot's performance of one minute of tracking. These RMS values are shown in Table IV.

The random noise source used for the tracking task was the same one used for random noise inputs to the controls. The output of the random noise source was filtered before it was used as an input to either the tracking task or the airplane controls. The amplitude versus frequency of the random noise filter is shown in Figure 2. The amplitude of the high frequency content of this filtered noise, although satisfactory as a random noise input to the controls, was unsatisfactory as a pitch angle tracking error. The random noise input to the tracking task was therefore filtered a second time using a low pass filter with a corner at 0.5 cycle per second. The modification of the filter frequency response resulting from this low pass filter is also shown on Figure 2. This modification made the tracking task appear reasonable to the evaluation pilot. There were still some complaints during the evaluation flights by both pilots that the frequency content of the pitch attitude error was high.

3.6 SIMULATION OF RANDOM NOISE

Each configuration simulated was also evaluated with random noise inputs to all three controls (ailerons, rudder, and elevators). Reasonable random noise levels were selected by the CAL evaluation pilot during the preliminary calibration flights.

The random noise levels to the ailerons and rudder remained fixed for each of the three flight conditions during the evaluation. This is based on the fact that the lateral-directional characteristics remained essentially fixed for each flight condition as discussed in Section 3.7.

Satisfactory values of random noise inputs to the elevator required that these inputs be a function of the simulated longitudinal short period frequency. A stiffer airplane (high ω_{sp}) is more difficult to disturb with the same elevator inputs. During the preliminary flights, a pilot evaluation of acceptable levels of random noise inputs to the elevator, as a function of the short period undamped natural frequency, was determined for each of the three flight conditions. These functional relationships were used throughout the evaluation program and are shown in Figure 3.

Some scatter exists in the curves of random noise level shown in Figure 3. The explanation is as follows: The short period frequencies plotted are the best estimates of the simulated frequencies determined by the analysis of flight test data after the completion of the flight test program. This analysis is based on parameter identification and correlation techniques explained and presented in Section V and Appendix I. The random noise level inputs to the elevator used during the evaluation flights were based on estimates of the frequencies being simulated during a particular evaluation. These estimates were in turn determined from gain setting curves based on flight test data obtained from calibration flights. With a few exceptions, which will be discussed later, the deviations of the points from the faired curves are not large.

3.7 CHARACTERISTICS OF THE LONGITUDINAL PHUGOID

No attempt was made to alter the longitudinal phugoid. The phugoid undamped natural frequency (ω_p) and damping ratio (ζ_p) for a given flight condition are essentially those of the T-33 airplane. For the three flight conditions under investigation, measurements of the phugoid characteristics were made during one of the evaluation flights. The phugoid has a period in the vicinity of one minute for all three flight conditions and is lightly damped (see Table V).

3.8 LATERAL-DIRECTIONAL CHARACTERISTICS

As stated previously, the lateral-directional characteristics of the variable stability T-33 airplane were augmented at each of the three test conditions to levels deemed satisfactory for a fighter by the evaluation pilot. Satisfactory values of aileron and rudder gearing and aileron stick and rudder pedal force gradients were also selected by the CAL evaluation pilot and remained unchanged throughout the evaluation.

The lateral-directional characteristics selected by the pilot were measured in flight and are shown in Table VI. These characteristics included Dutch roll undamped frequency (ω_d), damping ratio (ζ_d), roll mode time constant (τ_R), aileron and rudder gearing ($\delta_{AT}/\delta_{AS}, \delta_r/\delta_{RP}$), and aileron stick and rudder pedal spring rates ($F_{AS}/\delta_{AS}, F_{RP}/\delta_{RP}$). The values shown should only be considered as representative values, since some variation in the lateral-directional characteristics occurs for any flight condition due to variations in fuel remaining. The effect of fuel remaining on the lateral-

directional characteristics is more pronounced than the effect of different fuel conditions on the longitudinal characteristics. This is because of the significant changes in the lateral-directional moments of inertia (I_x and I_z) as the tip tank fuel is consumed (see Reference 17). These inertia effects were kept to a minimum during the flight test program by always simulating the three different flight conditions during each flight in the following sequence: 300 kts, 220 kts, and 365 kts IAS.

Section IV

IN-FLIGHT EVALUATION

4.1 GENERAL DISCUSSION

In-flight evaluations of longitudinal short period frequency requirements and PIO tendencies were made by both the CAL and Air Force evaluation pilots. The handling qualities parameters simulated for both pilots covered the same range of variables.

For each flight, a different configuration was simulated at each of the following flight conditions; 300 kts, 220 kts, and 365 kts IAS at 5500 feet pressure altitude. The sequence of flight conditions was the same for each flight in order to keep the effects of variations in fuel remaining to a minimum.

Each configuration was simulated by variable stability gain settings of the T-33 airplane. These gain settings took the form of variable stability system knob settings that could be adjusted by the safety pilot in the rear cockpit. The evaluation pilot in the front cockpit was not told the configuration being simulated. Short period frequency configurations with $\zeta_{sp} \approx 0.7$ and PIO configurations were sometimes simulated during the same flight.

After performing maneuvers to select the "optimum" gear ratio for a specific configuration, the evaluation pilot was asked to perform specific tasks, and any other tasks he thought appropriate o properly evaluate the configuration. The evaluation pilot was supplied with a comment check list, the CAL rating scale, and a PIO rating scale. His comments and ratings were recorded as part of the flight records.

Oscillograph records were taken of the airplane response to specific inputs, to properly identify the handling qualities parameters actually simulated. One minute of tracking performance was also recorded for each configuration. In a few cases, records were taken of the evaluation pilot's selection of F_{ES}/n_z. The evaluation pilot was not aware that these records were taken. The records were later analyzed for stick pumping and are discussed elsewhere in the report.

4.2 EVALUATION MANEUVERS

For each configuration, the pilot first performed whatever maneuvers he thought necessary to properly select the elevator gearing. The elevator gearing was varied by the safety pilot in the rear cockpit in response to the requests of the evaluation pilot.

After selecting the gear ratio, the pilot was asked to perform the following maneuvers which include the compensatory tracking task previously discussed. During these maneuvers, the configuration was evaluated as a fighter in "up and away" flight.

Evaluation Maneuvers (Smooth Air)

1. Trim airplane.
2. Straight and level flight, including small pilot-initiated disturbances about level flight.
3. Heading changes maintaining constant altitude.
   a. Small bank angles
   b. Large bank angles (up to 60°)
4. Symmetrical pull-up and push-over to specific normal acceleration.
5. Climbing and descending turns.
6. Tracking task.
7. Maneuvers with random noise inputs.

4.3 PILOT COMMENTS AND PILOT RATINGS SCALES

During and after the performance of the evaluation maneuvers, the pilot commented on the configuration. These comments, as well as the comments on the selection of the gear ratio, were recorded on a wire recorder. To aid the pilot in making comments, he was provided with the following comment check list:

Pilot Comment Check List

1. Is the airplane difficult to trim?
2. Is attitude control satisfactory?
3. Is normal acceleration control a problem?
4. Is holding altitude a problem?
   a. Straight and level?
   b. Turns?
5. What is maximum usable bank angle?
6. Is maintaining airspeed a problem?
7. Are there any problems associated with the tracking task?
   a. How well can you accomplish the task?
   b. How much fatigue is involved?

8. What are the effects of random noise inputs on handling qualities?

9. Are special piloting techniques required for the configuration? What are they?

10. What instruments are used the most?

11. Are any of the instruments inadequate for this configuration?

12. What are the good features of the configuration?

13. What are the bad features of the configuration?

14. Pilot rating - adjectives - number - why?

Comments on question 14 were based on the standard CAL rating scale.

CAL RATING SCALE

CATEGORY	ADJECTIVE DESCRIPTION WITHIN CATEGORY		NUMERICAL RATING
ACCEPTABLE	SATISFACTORY	EXCELLENT	1
		GOOD	2
		FAIR	3
		(ASK THAT IT BE FIXED)	
	UNSATISFACTORY	FAIR	4
		POOR	5
		BAD	6
		(WON'T BUY IT)	
UNACCEPTABLE	FLYABLE	BAD[a]	7
		VERY BAD[b]	8
		DANGEROUS[c]	9
		(WON'T FLY IT)	
	UNFLYABLE	UNFLYABLE	10

[a] REQUIRED MAJOR PORTION OF PILOT'S ATTENTION

[b] CONTROLLABLE ONLY WITH A MINIMUM OF COCKPIT DUTIES.

[c] AIRCRAFT JUST CONTROLLABLE WITH COMPLETE ATTENTION.

One objective of the in-flight evaluation program was the investigation of PIO conditions with fixed control system dynamics. A PIO rating scale was established for this program for the purpose of defining categories of PIO tendencies for all the configurations simulated (PIO configurations and short period frequency configurations). The PIO rating scale supplements the comment data and the CAL rating scale and is defined as follows:

PIO TENDENCY RATING SCALE

DESCRIPTION	NUMERICAL RATING
NO TENDENCY FOR PILOT TO INDUCE UNDESIRABLE MOTIONS.	1
UNDESIRABLE MOTIONS TEND TO OCCUR WHEN PILOT INITIATES ABRUPT MANEUVERS OR ATTEMPTS TIGHT CONTROL. THESE MOTIONS CAN BE PREVENTED OR ELIMINATED BY PILOT TECHNIQUE.	2
UNDESIRABLE MOTIONS EASILY INDUCED WHEN PILOT INITIATES ABRUPT MANEUVERS OR ATTEMPTS TIGHT CONTROL. THESE MOTIONS CAN BE PREVENTED OR ELIMINATED BUT ONLY AT SACRIFICE TO TASK PERFORMANCE OR THROUGH CONSIDERABLE PILOT ATTENTION AND EFFORT.	3
OSCILLATIONS TEND TO DEVELOP WHEN PILOT INITIATES ABRUPT MANEUVERS OR ATTEMPTS TIGHT CONTROL. PILOT MUST REDUCE GAIN OR ABANDON TASK TO RECOVER.	4
DIVERGENT OSCILLATIONS TEND TO DEVELOP WHEN PILOT INITIATES ABRUPT MANEUVERS OR ATTEMPTS TIGHT CONTROL. PILOT MUST OPEN LOOP BY RELEASING OR FREEZING THE STICK.	5
DISTURBANCE OR NORMAL PILOT CONTROL MAY CAUSE DIVERGENT OSCILLATION. PILOT MUST OPEN CONTROL LOOP BY RELEASING OR FREEZING THE STICK.	6

4.4 TURBULENCE CONSIDERATIONS

The response of an airplane to atmospheric turbulence is an important aspect of handling qualities research. Much of the turbulence effect on airplanes is associated with the gust induced angle of attack changes and their effect on the riding and handling qualities. Unfortunately, the variable stability T-33 is not capable of simulating variable lift due to angle of attack at a fixed flight condition. Such a capability would be required for simulating gust induced angle of attack changes. In this flight test program, the effects of turbulence were judged from natural turbulence and the pitch response of the airplane to random noise inputs to the elevator. Random noise inputs to the elevator are only an approximation of the pitching motion that will result from gusts.

4.5 IN-FLIGHT DATA RECORDS

In order to properly identify the handling qualities parameters simulated and the pilot's closed-loop performance, oscillograph records were taken of the airplane response to specific control inputs or control tasks for each configuration simulated. These records were analyzed during and after the completion of the flight test program. Oscillograph records were taken under the following conditions:

Oscillograph Data Records

1. Variable stability system engage at each speed (flight condition).
2. Response to automatic elevator doublets, pulses, and steps.
3. Response to manual elevator stick doublets, pulses, and steps.
4. One minute of tracking of pitch attitude command.
5. Rapid and precise 1 and 2 g pull and hold.
6. Pilot initiated attitude changes of the airplane.
7. Selection of elevator gearing (on four flights only).

Section V

IDENTIFICATION OF SIMULATED PARAMETERS

The oscillograph records of the airplane response to specific inputs were used to identify the longitudinal short period parameters actually simulated for each configuration evaluated by the pilot. Doublet, pulse, and step responses were used to identify ω_{sp} and ζ_{sp}. The short period frequency investigation at various values of L_α was conducted at essentially fixed damping ratio ($\zeta_{sp} \approx 0.7$). For these well damped configurations, frequency and damping were generally identified using the so called "time ratio" method for a second-order response. For the low damping configurations when $\zeta_{sp} < 0.5$, the "transient peak ratio" method for a second-order response was used. Both methods are presented and discussed in Reference 18.

From the airplane response to various fixed control inputs, it was possible to identify a number of steady-state parameters such as α/δ_{ES}, F_{ES}/n_z, n_z/α, and F_{ES}/δ_{ES}.

There are some problems associated with the identification of short period characteristics. For well damped high frequencies, the airplane response is very rapid, and it becomes difficult to determine frequency and damping ratio accurately by the "time ratio" method. In addition, the shape of the response is not quite that of a second-order system because of the distortion due to sensor and servo lags. However, under such conditions, measurements of steady-state parameters are quite good. At the low short period frequencies simulated ($\omega_{sp} \approx 2$ rad/sec) the airplane response is slow, and measurements of frequency, damping, and steady-state parameters are contaminated by the effects of the phugoid association with velocity changes. The stick "bobweight" effect (that is the inertia effects of the free stick in response to airplane dynamics) also somewhat alters the measurements of frequency and damping. Bobweight effects on the measurements were minimized by properly selecting records to be analyzed.

At the completion of the flight test program, methods were devised for correlating the measured parameters to the gain settings used in the simulation. These correlations determined the degree of consistency and accuracy in the measured parameters. In addition, on the basis of these correlations, it was possible to establish alternate methods of identifying questionable parameters, especially at the high and low frequencies simulated. The correlation and alternate parameter identification techniques are discussed in Appendix I.

The parameters simulated for each of the three flight conditions are shown in Tables VII, VIII, and IX. The PIO configurations simulated at low damping are also shown in these tables. The "measured" values in the tables were obtained from the oscillograph records of the flight using the techniques previously described. The least-squares-fit (LSF) values were determined

using the least-squares-fit correlation techniques of Appendix I. The "best estimate" values represent the best estimate of what parameters were simulated. In some cases, the "best estimate" value is simply the directly measured value using the oscillograph traces. This is the case when the "measured" and "LSF" values are in good agreement. In some cases, the "best estimate" values were determined by other methods, such as determining short period frequency indirectly from measured steady-state values of α/δ_{es} and the least-squares-fit value of $M_{\delta_{es}}$, as discussed in Appendix I. "Best estimate" values determined indirectly as discussed in Appendix I are identified in the tables by a double asterisk. In a few instances, the "best estimate" value is simply considered to be the least-squares-fit value.

Section VI

EFFECT OF FEEL SYSTEM DYNAMICS ON AIRPLANE PITCH RESPONSE

6.1 GENERAL DISCUSSION

The importance of the magnitude of the pitch response of an airplane to control inputs, and the effect of this response on the closed-loop handling qualities, have been recognized for some time. Assuming velocity changes and elevator lift (Z_{δ_e}) to be negligibly small, the short period longitudinal equations of motion of the airplane are represented by Equations (3.1) and (3.2). These equations are equally valid for the variable stability T-33 simulating another airplane, when the simulated derivatives are described by Equations (3.7), (3.8), and (3.9). These same results can be obtained from Equations (I.5) and (I.6) in Appendix I by neglecting the small terms containing elevator lift (Z_{δ_e}). Thus, in terms of simulated derivatives, and control stick inputs (δ_{ES}), the two-degree-of-freedom equations of motion become:

$$-\dot{\alpha} + Z_\alpha \alpha + \dot{\theta} = 0 \tag{6.1}$$

$$M_{\dot{\alpha}} \dot{\alpha} + M_\alpha \alpha - \ddot{\theta} + M_{\dot{\theta}} \dot{\theta} + M_{\delta_e} \left(\frac{\delta_e}{\delta_{ES}}\right) \delta_{ES} = 0 \tag{6.2}$$

Under these same assumptions, the transfer functions $\theta(s)/\delta_{ES}(s)$ and $n_z(s)/\delta_{ES}(s)$ assume the following form in terms of the simulated frequency and damping ratio:

$$\frac{\theta(s)}{\delta_{ES}(s)} = \frac{M_{\delta_e}\left(\frac{\delta_e}{\delta_{ES}}\right)(s - Z_\alpha)}{s(s^2 + 2\zeta_{SP}\omega_{SP}s + \omega_{SP}^2)} \tag{6.3}$$

$$\frac{n_z(s)}{\delta_{ES}(s)} = \frac{-\frac{V_o}{g} Z_\alpha M_{\delta_e}\left(\frac{\delta_e}{\delta_{ES}}\right)}{s^2 + 2\zeta_{SP}\omega_{SP}s + \omega_{SP}^2} \tag{6.4}$$

These expressions can also be obtained from Equations (I.8) and (I.10), using Equations (I.19) and (I.20) of Appendix I.

It is assumed in Equations (6.3) and (6.4) that the elevator-to-stick gain (δ_e/δ_{ES}) is independent of frequency. This is reasonably true at the simulated airplane frequencies since the elevator servo frequency is relatively high (63 rad/sec). This assumption is less true under transient conditions, such as the airplane response to rapid stick inputs.

An even more important factor in the simulations of this program is the response of the airplane to stick force commands. The response of the elevator stick to stick force commands is determined by the following transfer function for the variable stability T-33 feel system:

$$\frac{\delta_{ES}(s)}{F_{ES}(s)} = \frac{\omega_{FS}^2 \left(\frac{\delta_{ES}}{F_{ES}}\right)_{ss}}{s^2 + 2\zeta_{FS}\omega_{FS}s + \omega_{FS}^2} \tag{6.5}$$

The feel system characteristics that were used in this program are summarized in Table III. These characteristics were determined as indicated in Appendix II based on ground and in-flight records. The elevator servo characteristics are also analyzed briefly in Appendix II.

The following section discusses how the elevator and feel system characteristics affect the initial pitch response of the airplane to stick force inputs.

6.2 AIRPLANE TRANSFER FUNCTIONS AND RESPONSE CHARACTERISTICS INCLUDING FEEL SYSTEM

The pitch response and normal acceleration response of the airplane to stick force inputs (including elevator servo and feel system characteristics) can be written as follows:

$$\frac{\theta(s)}{F_{ES}(s)} = \frac{\theta(s)}{\delta_e(s)} \frac{\delta_e(s)}{\delta_{ES}(s)} \frac{\delta_{ES}(s)}{F_{ES}(s)} \tag{6.6}$$

$$\frac{n_z(s)}{F_{ES}(s)} = \frac{n_z(s)}{\delta_e(s)} \frac{\delta_e(s)}{\delta_{ES}(s)} \frac{\delta_{ES}(s)}{F_{ES}(s)} \tag{6.7}$$

If the $\delta_e(s)/\delta_{ES}(s)$ transfer function can also be represented as a second-order system (Appendix II), then:

$$\frac{\delta_e(s)}{\delta_{ES}(s)} = \frac{\omega_e^2 \left(\frac{\delta_e}{\delta_{ES}}\right)_{ss}}{s^2 + 2\zeta_e\omega_e s + \omega_e^2} \tag{6.8}$$

Substituting Equations (6.3), (6.4), (6.5), and (6.8) in Equations (6.6) and (6.7) results in the following transfer functions:

$$\frac{\theta(s)}{F_{ES}(s)} = \frac{\omega_{FS}^2 \omega_e^2 M_{\delta_e} \left(\frac{\delta_e}{\delta_{ES}}\right)_{ss} \left(\frac{\delta_{ES}}{F_{ES}}\right)_{ss} (s - Z_\alpha)}{s(s^2 + 2\zeta_{SP}\omega_{SP}s + \omega_{SP}^2)(s^2 + 2\zeta_{FS}\omega_{FS}s + \omega_{FS}^2)(s^2 + 2\zeta_e\omega_e s + \omega_e^2)} \tag{6.9}$$

$$\frac{n_z(s)}{F_{ES}(s)} = \frac{-\omega_{FS}^2 \omega_e^2 \left(\frac{V_0}{g} Z_\alpha M_{\delta_e}\right) \left(\frac{\delta_e}{\delta_{ES}}\right)_{ss} \left(\frac{\delta_{ES}}{F_{ES}}\right)_{ss}}{(s^2 + 2\zeta_{SP}\omega_{SP}s + \omega_{SP}^2)(s^2 + 2\zeta_{FS}\omega_{FS}s + \omega_{FS}^2)(s^2 + 2\zeta_e\omega_e s + \omega_e^2)} \tag{6.10}$$

The subscript ss refers to the gain values under steady-state conditions, or the asymptotic value at low frequencies. Assuming the elevator servo frequency (ω_e) is high compared to the feel system frequency (ω_{FS}), the transfer functions can be reduced to the following:

$$\frac{\theta(s)}{F_{ES}(s)} = \frac{\omega_{FS}^2 M_{\delta e}\left(\frac{\delta_e}{\delta_{ES}}\right)_{ss}\left(\frac{\delta_{ES}}{F_{ES}}\right)_{ss}(s - Z_\alpha)}{s(s^2 + 2\zeta_{SP}\omega_{SP}s + \omega_{SP}^2)(s^2 + 2\zeta_{FS}\omega_{FS}s + \omega_{FS}^2)} \tag{6.11}$$

$$\frac{n_z(s)}{F_{ES}(s)} = \frac{-\omega_{FS}^2\left(\frac{V_0}{g}Z_\alpha M_{\delta e}\right)\left(\frac{\delta_e}{\delta_{ES}}\right)_{ss}\left(\frac{\delta_{ES}}{F_{ES}}\right)_{ss}}{(s^2 + 2\zeta_{SP}\omega_{SP}s + \omega_{SP}^2)(s^2 + 2\zeta_{FS}\omega_{FS}s + \omega_{FS}^2)} \tag{6.12}$$

The initial pitch response of the airplane was analyzed using the transfer functions of Equations (6.9) and (6.11). The results were nearly identical, indicating little effect of the elevator servo lags on the transient response. This is attributable to the high elevator servo frequency compared to feel system frequency (63 rad/sec compared to 23 rad/sec).

Based on Equation (6.11), the pitch velocity and pitch acceleration transfer functions can be written as follows:

$$\frac{\dot{\theta}(s)}{F_{ES}(s)} = \frac{\omega_{FS}^2 M_{\delta e}\left(\frac{\delta_e}{\delta_{ES}}\right)_{ss}\left(\frac{\delta_{ES}}{F_{ES}}\right)_{ss}(s - Z_\alpha)}{(s^2 + 2\zeta_{SP}\omega_{SP}s + \omega_{SP}^2)(s^2 + 2\zeta_{FS}\omega_{FS}s + \omega_{FS}^2)} \tag{6.13}$$

$$\frac{\ddot{\theta}(s)}{F_{ES}(s)} = \frac{\omega_{FS}^2 M_{\delta e}\left(\frac{\delta_e}{\delta_{ES}}\right)_{ss}\left(\frac{\delta_{ES}}{F_{ES}}\right)_{ss}s(s - Z_\alpha)}{(s^2 + 2\zeta_{SP}\omega_{SP}s + \omega_{SP}^2)(s^2 + 2\zeta_{FS}\omega_{FS}s + \omega_{FS}^2)} \tag{6.14}$$

Without feel system dynamics included, the pitch acceleration transfer function, $\ddot{\theta}(s)/F_{ES}(s)$ becomes:

$$\frac{\ddot{\theta}(s)}{F_{ES}(s)} = \frac{M_{\delta e}\left(\frac{\delta_e}{\delta_{ES}}\right)_{ss}\left(\frac{\delta_{ES}}{F_{ES}}\right)_{ss}s(s - Z_\alpha)}{(s^2 + 2\zeta_{SP}\omega_{SP}s + \omega_{SP}^2)} \tag{6.15}$$

For a step stick force input (F_{ES}) where $F_{ES}(s) = F_{ES}/s$, the airplane initial pitch acceleration can be found from Equation (6.15).

$$\begin{aligned}\ddot{\theta}_0 &= \lim_{s\to\infty} s\,\frac{\ddot{\theta}(s)}{F_{ES}(s)}\,F_{ES}(s) = \lim_{s\to\infty}\frac{\ddot{\theta}(s)}{F_{ES}(s)}\,F_{ES} \\ &= M_{\delta e}\left(\frac{\delta_e}{\delta_{ES}}\right)_{ss}\left(\frac{\delta_{ES}}{F_{ES}}\right)_{ss}F_{ES}\end{aligned} \tag{6.16}$$

The actual pitch response of the airplane to a step stick force input, with feel system dynamics included, can be found from Equations (6.11), (6.13), and (6.14).

$$\theta(s) = \frac{\omega_{FS}^2 M_{\delta_e} \left(\frac{\delta_e}{\delta_{ES}}\right)_{ss} \left(\frac{\delta_{ES}}{F_{ES}}\right)_{ss} F_{ES} (s - z_\alpha)}{s^2(s^2 + 2\zeta_{SP}\omega_{SP}s + \omega_{SP}^2)(s^2 + 2\zeta_{FS}\omega_{FS}s + \omega_{FS}^2)} \tag{6.17}$$

$$\dot{\theta}(s) = \frac{\omega_{FS}^2 M_{\delta_e} \left(\frac{\delta_e}{\delta_{ES}}\right)_{ss} \left(\frac{\delta_{ES}}{F_{ES}}\right)_{ss} F_{ES} (s - z_\alpha)}{s(s^2 + 2\zeta_{SP}\omega_{SP}s + \omega_{SP}^2)(s^2 + 2\zeta_{FS}\omega_{FS}s + \omega_{FS}^2)} \tag{6.18}$$

$$\ddot{\theta}(s) = \frac{\omega_{FS}^2 M_{\delta_e} \left(\frac{\delta_e}{\delta_{ES}}\right)_{ss} \left(\frac{\delta_{ES}}{F_{ES}}\right)_{ss} F_{ES} (s - z_\alpha)}{(s^2 + 2\zeta_{SP}\omega_{SP}s + \omega_{SP}^2)(s^2 + 2\zeta_{FS}\omega_{FS}s + \omega_{FS}^2)} \tag{6.19}$$

The actual airplane response to a step stick force input can be related to the initial pitch acceleration response without feel system dynamics, Equation (6.16). Dividing Equations (6.17), (6.18), and (6.19) by $\ddot{\theta}_0$ or $M_{\delta_e}(\delta_e/\delta_{ES})_{ss}(\delta_{ES}/F_{ES})_{ss}F_{ES}$, we have,

$$\theta_{nd}(s) = \frac{\omega_{FS}^2 (s - z_\alpha)}{s^2(s^2 + 2\zeta_{SP}\omega_{SP}s + \omega_{SP}^2)(s^2 + 2\zeta_{FS}\omega_{FS}s + \omega_{FS}^2)} \tag{6.20}$$

$$\dot{\theta}_{nd}(s) = \frac{\omega_{FS}^2 (s - z_\alpha)}{s(s^2 + 2\zeta_{SP}\omega_{SP}s + \omega_{SP}^2)(s^2 + 2\zeta_{FS}\omega_{FS}s + \omega_{FS}^2)} \tag{6.21}$$

$$\ddot{\theta}_{nd}(s) = \frac{\omega_{FS}^2 (s - z_\alpha)}{(s^2 + 2\zeta_{SP}\omega_{SP}s + \omega_{SP}^2)(s^2 + 2\zeta_{FS}\omega_{FS}s + \omega_{FS}^2)} \tag{6.22}$$

where

$$\theta_{nd} = \theta \Big/ M_{\delta_e} \left(\frac{\delta_e}{\delta_{ES}}\right)_{ss} \left(\frac{\delta_{ES}}{F_{ES}}\right)_{ss} F_{ES} \tag{6.23}$$

$$\dot{\theta}_{nd} = \dot{\theta} \Big/ M_{\delta_e} \left(\frac{\delta_e}{\delta_{ES}}\right)_{ss} \left(\frac{\delta_{ES}}{F_{ES}}\right)_{ss} F_{ES} \tag{6.24}$$

$$\ddot{\theta}_{nd} = \ddot{\theta} \Big/ M_{\delta_e} \left(\frac{\delta_e}{\delta_{ES}}\right)_{ss} \left(\frac{\delta_{ES}}{F_{ES}}\right)_{ss} F_{ES} \tag{6.25}$$

The expression $\ddot{\theta}_{nd}$ is a nondimensional pitch acceleration. It is the ratio of pitch acceleration, including the effects of feel system dynamics, to the pitch acceleration at time $t = 0^+$, excluding feel system dynamics, following a step stick force input.

Without elevator or feel system dynamics, the maximum pitch acceleration following a step stick force input occurs at time zero and is equal to $\ddot{\theta}_0 = M_{\delta_e}(\delta_e/\delta_{ES})_{ss}(\delta_{ES}/F_{ES})_{ss} F_{ES}$. With feel system dynamics included, the pitch acceleration response is defined by Equation (6.19). At time zero, the pitch acceleration is zero, and the maximum occurs at some time after $t=0$.

It is difficult to determine analytically from Equations (6.19) or (6.22) the time at which maximum pitch acceleration occurs and its magnitude. By transforming Equation (6.20) to a differential equation in the time domain and performing a step by step integration with time, it is possible to obtain a time history of θ_{nd}, $\dot{\theta}_{nd}$, and $\ddot{\theta}_{nd}$. From these time histories, it is possible to determine maximum values of $\dot{\theta}_{nd}$ and $\ddot{\theta}_{nd}$. Then $\dot{\theta}_{MAX}$ and $\ddot{\theta}_{MAX}$ can be determined from Equations (6.24) and (6.25).

$$\dot{\theta}_{MAX} = (\dot{\theta}_{nd})_{MAX} M_{\delta_e} \left(\frac{\delta_e}{\delta_{ES}}\right)_{ss} \left(\frac{\delta_{ES}}{F_{ES}}\right)_{ss} F_{ES} \tag{6.26}$$

$$\ddot{\theta}_{MAX} = (\ddot{\theta}_{nd})_{MAX} M_{\delta_e} \left(\frac{\delta_e}{\delta_{ES}}\right)_{ss} \left(\frac{\delta_{ES}}{F_{ES}}\right)_{ss} F_{ES} \tag{6.27}$$

The θ_{nd} response, and therefore $(\dot{\theta}_{nd})_{MAX}$ and $(\ddot{\theta}_{nd})_{MAX}$, are a function of the feel system frequency and damping, simulated airplane frequency and damping, and the value of Z_α. When the feel system frequency and damping, Z_α, and the airplane damping are fixed, then the pitch response θ_{nd} to a step stick force input is only a function of the airplane frequency.

Plots of $(\ddot{\theta}_{nd})_{MAX}$ obtained from time histories of the pitch response are shown as Figures 4, 6, and 7. Figure 7 examines the effects of elevator servo lags as well as feel system lags on the maximum pitch acceleration. This figure should be compared to Figure 4 with only feel system lags included. The effect of the elevator servo on the maximum pitch acceleration is negligible. Figures 4 and 6 show the effect of slightly different feel system characteristics on the maximum pitch accelerations. The differences are not large, and should not significantly affect the pitch acceleration response of the simulated airplane. The different feel system characteristics used during some of the simulated configurations are indicated in Table III. It is evident from Figure 4 that the feel system dynamics used in this flight test program caused very significant attenuation on the pitch acceleration response of the airplane, especially at the higher frequencies simulated.

The steady-state value of pitch velocity, $\dot{\theta}_{ss}$, following a step stick force input, can be obtained from Equation (6.18).

$$\dot{\theta}_{ss} = \lim_{s \to 0} s\dot{\theta}(s) = - \frac{M_{\delta_e} \left(\frac{\delta_e}{\delta_{ES}}\right)_{ss} \left(\frac{\delta_{ES}}{F_{ES}}\right)_{ss} F_{ES} Z_\alpha}{\omega_{sp}^2} \tag{6.28}$$

From Equation (6.21), $(\dot{\theta}_{nd})_{ss} = -Z_\alpha/\omega_{sp}^2$. Obviously $\dot{\theta}_{ss}$ and $(\dot{\theta}_{nd})_{ss}$ are related by Equation (6.24).

$$\dot{\theta}_{ss} = (\dot{\theta}_{nd})_{ss} \; M_{\delta_e} \left(\frac{\delta_e}{\delta_{ES}}\right)_{ss} \left(\frac{\delta_{ES}}{F_{ES}}\right)_{ss} F_{ES} \tag{6.29}$$

From Equations (6.26) and (6.29), we have:

$$\frac{\dot{\theta}_{MAX}}{\dot{\theta}_{ss}} = \frac{(\dot{\theta}_{nd})_{MAX}}{(\dot{\theta}_{nd})_{ss}} \tag{6.30}$$

Plots of pitch velocity overshoot ratio are shown as Figure 5 following a step stick force input. These curves include the attenuating effects of the feel system.

6.3 ATTENUATION OF AIRPLANE RESPONSE DUE TO FEEL SYSTEM

Once the attenuating effects of the feel system are known, as presented in Figures 4 through 7, then the airplane pitch response with feel system effects included can easily be determined.

The feel system dynamics had no effect on the steady-state parameters of the simulated airplane, such as $(F_{ES}/n_z)_{ss}$ and $(n_z/\alpha)_{ss}$. From Equations (I.18), (I.19), and (I.22) in Appendix I, it is possible to determine these parameters, provided it is assumed that terms containing Z_{δ_e} are negligibly small.

$$\left(\frac{F_{ES}}{n_z}\right)_{ss} = \frac{\omega_{sp}^2}{-\frac{V_o}{g} Z_\alpha M_{\delta_e} \left(\frac{\delta_e}{\delta_{ES}}\right)_{ss} \left(\frac{\delta_{ES}}{F_{ES}}\right)_{ss}} \tag{6.31}$$

$$\left(\frac{n_z}{\alpha}\right)_{ss} = -\frac{V_o}{g} Z_\alpha \tag{6.32}$$

Substituting in Equation (6.16), we can derive the following expression:

$$\frac{\ddot{\theta}_o}{F_{ES}} = \frac{\omega_{sp}^2}{\left(\frac{n_z}{\alpha}\right)_{ss} \left(\frac{F_{ES}}{n_z}\right)_{ss}} \tag{6.33}$$

Equation (6.33) is the initial pitch acceleration per unit step stick force input at time $t = 0^+$, if the lag of the feel and elevator servos are ignored. The maximum pitch acceleration per unit step stick force including feel system dynamics can easily be obtained from Equations (6.27), (6.16), and (6.33).

$$\frac{\ddot{\theta}_{MAX}}{F_{ES}} = \frac{\omega_{sp}^2 (\ddot{\theta}_{nd})_{MAX}}{\left(\frac{n_z}{\alpha}\right)_{ss} \left(\frac{F_{ES}}{n_z}\right)_{ss}} \tag{6.34}$$

It is interesting to note that maximum pitch acceleration per unit stick force, Equation (6.34), involves the feel system dynamics and all the parameters varied in the short period handling qualities investigated in this report. The parameter F_{ES}/n_z was selected by the pilot for each configuration simulated.

Bihrle's control anticipation parameter, CAP, Reference 16, can easily be derived from Equation (6.33):

$$CAP = \left(\frac{\ddot{\theta}_o}{F_{ES}}\right)\left(\frac{F_{ES}}{n_z}\right)_{ss} = \frac{\ddot{\theta}_o}{n_{z_{ss}}} = \frac{\omega_{sp}^2}{\left(\frac{n_z}{\alpha}\right)_{ss}} \qquad (6.35)$$

CAP, including the effect of feel system dynamics (CAP)', can be obtained from Equation (6.34).

$$(CAP)' = \left(\frac{\ddot{\theta}_{MAX}}{F_{ES}}\right)\left(\frac{F_{ES}}{n_z}\right)_{ss} = \frac{\ddot{\theta}_{MAX}}{n_{z_{ss}}} = \frac{\omega_{sp}^2 (\ddot{\theta}_{nd})_{MAX}}{\left(\frac{n_z}{\alpha}\right)_{ss}} \qquad (6.36)$$

It has been suggested that $\dot{\theta}_{MAX}/\dot{\theta}_{ss}$ may be of some importance in defining the shape of the desired pitch response to step control inputs, and therefore of some significance as a handling qualities parameter. It is evident from Figure 5 that pitch velocity overshoot is a strong function of Z_α as well as simulated ω_{sp}. The question naturally arises as to whether $\dot{\theta}_{MAX}/\dot{\theta}_{ss}$ and (CAP)' are really independent parameters. Figure 8 is a plot of $\dot{\theta}_{MAX}/\dot{\theta}_{ss}$ versus (CAP)' for various fixed values of Z_α. Figure 8 was obtained from Figures 4 and 5. It is evident from Figure 8 that a functional relationship does indeed exist between these two parameters. Within the range of Z_α's and ω_{sp}'s simulated for this flight test program, the two parameters are not really independent. It is interesting to note that $\ddot{\theta}_{MAX}/F_{ES}$, Equation (6.34), is an independent parameter from $\dot{\theta}_{MAX}/\dot{\theta}_{ss}$ since it is inversely proportional to F_{ES}/n_z.

Section VII

HANDLING QUALITIES RESULTS

7.1 GENERAL DISCUSSION

Pilot rating data and pilot comment data are presented and discussed in this section for both the investigation of short period frequency requirements and PIO tendencies.

Pilot numerical ratings for the short period frequency investigation are related to various short period frequency parameters such as ω_{SP}, n_z/α, CAP, (CAP)', $\dot{\theta}_{MAX}/F_{ES}$, and F_{ES}/n_z. These pilot ratings are also interpreted in terms of the pilot comments.

Pilot numerical PIO ratings for the PIO configurations investigated are interpreted in terms of several parameters that have been suggested, such as $2\zeta_{SP}\omega_{SP}$, $2\zeta_{SP}\omega_{SP}/L_\alpha$, and F_{ES}/n_z. The PIO ratings are also related to the pilot comments.

It became apparent in the flight test program and in the analysis of pilot ratings and pilot comment data that the pilot-selected steady-state stick force gradient formed an important part of this handling qualities investigation. This is true of both the short period and PIO configurations. By his selection of stick force, the pilot tended to optimize the short period frequency response requirements and minimize the PIO tendencies. This optimization was often a compromise of conflicting requirements; that is, one requirement could be improved only to the detriment of one or more of the others. The pilot's compromise was not always an easy one, and it did differ from time to time for the same configuration. The variability in pilot-optimized stick force gradients accounts for some of the variation that exists in a given pilot's ratings. In addition, the optimization of stick force gradient differed in some cases between the CAL pilot and the Air Force pilot. This fact also accounts for some of the variation of ratings between pilots.

One of the handling characteristics of importance to the pilots was the initial pitch response to control inputs. The attenuation of this response, due to the feel system characteristics simulated, was also accounted for in the interpretation of pilot ratings and pilot comments.

The results for the two pilots are compared and interpreted in terms of the simulated handling qualities parameters and the pilot comments.

Comparisons are made between the results of this flight test program and previous results obtained in fixed base and in-flight simulation of longitudinal short period requirements and PIO tendencies. Some of these earlier results were obtained by the Flight Research Department of Cornell Aeronautical Laboratory under previous programs.

7.2 SHORT PERIOD FREQUENCY REQUIREMENTS

Figures 9 and 10 are plots of pilot rating as a function of frequency for fixed values of n_z/α (16.9, 30.4, and 63.4 g/rad). These ratings are for a short period damping ratio (ζ_{SP}) of approximately 0.7.

7.2.1 Ratings and Comments of the Air Force Pilot

The ratings and comments of the Air Force pilot will be discussed and interpreted first. It is evident from Figure 9 that, with $\zeta_{SP} \approx 0.7$, pilot ratings do indeed become worse at high as well as low short period frequencies. It is also evident from the figure that the rate of deterioration of pilot ratings with frequency from the optimum frequency is largest at the lowest n_z/α (16.9 g/rad). This makes the satisfactory frequency range (PR < 3.5) largest at the largest n_z/α tested (63.4 g/rad). Based on the faired curves of Figure 9, the satisfactory frequency range for the Air Force pilot can be tabulated as follows:

n_z/α	Range of Satisfactory Frequencies (ω_d) PR < 3.5
16.9	2.4 to 6.9 rad/sec
30.4	2.7 to 9.0 rad/sec
63.4	4.1 to 13.9 rad/sec

In this program, the pilot was allowed to optimize F_{ES}/n_z by adjusting δ_e/δ_{ES}. The stick gradient, with a few exceptions, was held essentially constant ($F_{ES}/\delta_{ES} = 30$ lbs/in). At the higher frequencies simulated, the pilot's continual complaint was of the abruptness or sensitivity of the airplane for small control inputs about trim. He stated that this sensitivity or abruptness could be reduced by lowering δ_e/δ_{ES}, which of course increased the steady-state F_{ES}/n_z. The elevator gearing ratio selected was therefore a compromise between an acceptable level of sensitivity and the high steady-state maneuvering forces.

The manner in which this compromise was made is shown by the F_{ES}/n_z selected by the pilot as a function of ω_{SP} at a fixed n_z/α (Figure 9). It is evident from the figure that the pilot-selected "optimum" F_{ES}/n_z increased with an increase in short period frequency and a decrease in n_z/α. It is also evident from the selected F_{ES}/n_z at $V = 365$ kts IAS ($n_z/\alpha = 63.4$) that the airplane did not feel too sensitive to the pilot, even though the simulated short period frequencies were quite high ($\omega_{SP} = 16$ rad/sec).

There is reason to believe, as will be explained later, that the sensitivity or abruptness of which the pilot complains may be primarily related to the pitch acceleration response of the airplane to control inputs. The maximum pitch acceleration response, $\dot{\theta}_{MAX}$, following a step stick force input is described by Equation (6.34), which is repeated here for convenience.

$$\frac{\ddot{\theta}_{MAX}}{F_{ES}} = \frac{\omega_{SP}^2 (\dot{\theta}_{nd})_{MAX}}{\left(\frac{n_z}{\alpha}\right)_{ss}\left(\frac{F_{ES}}{n_z}\right)_{ss}} \qquad (6.34)$$

Equation (6.34) contains many of the essential handling qualities parameters that enter into the longitudinal short period simulations under discussion. It is evident from the equation that the "sensitivity," or maximum pitch acceleration response of an airplane, varies directly as ω_{SP}^2 and inversely as n_z/α. The highest pitch acceleration or sensitivity thus occurs at high frequencies and low values of n_z/α. This pitch acceleration per unit stick force can be reduced with a higher steady state F_{ES}/n_z. This explains much of the reason for the pilot's "compromising" with higher stick forces as the short period frequency increased and n_z/α decreased (Figure 9).

Equation (6.34) contains a factor $(\ddot{\theta}_{nd})_{MAX}$, which accounts for the feel system attenuation of the maximum pitch acceleration response following a step stick force input. This factor is a result of the feel system dynamics explained in Section VI and shown on Figures 4 and 6. The relatively low "optimum" stick force gradients selected by the Air Force pilot at the highest n_z/α appear to be due to the high n_z/α and the pronounced attenuation effects of the feel system.

At the low frequencies simulated, the pilot objected to the sluggish or slow response of the airplane. This was also described as a "digging in" quality; that is, the initial response was slow, causing the pilot first to increase his input. The pilot was next aware of a buildup in pitch velocity which was difficult to check in order to obtain a desired new attitude position. The result was an unsatisfactory and highly objectionable overcontrol tendency which caused the pilot to downgrade the configuration.

In many respects, the low frequencies involve a threshold-of-perception problem for the pilot. It is evident from Equation (6.34) that, for a given F_{ES}/n_z, the same pitch acceleration response will occur at a lower frequency, provided n_z/α is reduced. This is evident from the pilot rating curves of Figure 9. Good pilot ratings occur at lower frequencies as n_z/α is reduced. The decrease in pitch acceleration response ($\ddot{\theta}_{MAX}/F_{ES}$) with a reduction in frequency is more rapid at lower fixed values of n_z/α. This fact probably accounts for the more rapid deterioration of pilot rating with a reduction in frequency below the optimum frequency when n_z/α is small (Figure 9).

Equation (6.34) also indicates that $\ddot{\theta}_{MAX}/F_{ES}$ can be increased at low frequencies by reducing $(F_{ES}/n_z)_{ss}$. But such a procedure results in an airplane with objectionable light maneuver forces and a strong overcontrol tendency.

Some scatter does exist in the pilot rating and pilot-selected stick force data of Figure 9. The scatter in PR and F_{es}/n_z at the higher frequencies with $n_z/\alpha = 30.4$ is associated with the excitation of the T-33 structural modes at these simulated frequencies. The structural excitation occurred when the wing tip tanks were essentially full of fuel. The 300 kts IAS configuration was always the first configuration simulated during the flight. The pilot commented on and objected to the structural mode excitation, and later examination of oscillograph traces of a wing tip accelerometer confirmed that the excitation was present. The excitation is probably associated primarily with wing bending, but may also be a result of some wing torsion. The structural modes tended to increase the sensitivity of the airplane at these frequencies. This somewhat erratic change in sensitivity colored the pilot-selected $(F_{es}/n_z)_{ss}$ to correct for the sensitivity. The result was an increased variability in pilot rating. The pilot ratings in this region are open to some question and are shown as solid points on Figure 9.

For the flight condition of 220 kts IAS, certain pilot ratings and stick force points that deviate significantly from the faired curves are also shown as solid points. The flight number for each of these points is also indicated. The poorer pilot ratings for flights 583, 588, and 614 are probably associated with the marked deviation of the pilot-selected steady-state F_{es}/n_z from the "optimum" curve. On flights 583 and 588, the pilot commented on the excessively high steady-state stick forces, and that this fact entered into downgrading the configuration. Flight 581 was the Air Force evaluation pilot's first evaluation at this flight condition, and this fact may account for the low rating.

For the configurations simulated at 220 kts IAS, the evaluations were somewhat limited since the airplane was only capable of pulling one incremental g in maneuvers before the onset of maximum lift buffet. Both pilots often commented on this limitation. It may be that the pilot-selected optimum stick force gradient is somewhat high because of it. The optimization was probably weighted more on the basis of attenuating the sensitivity around trim because of the limited maneuverability at this flight condition.

On flight 602 at 300 kts IAS, the pilot stated that he liked the configuration, but he still objected to the amount of longitudinal sensitivity. As a result, he downgraded the configuration.

On flights 584 and 616, for V = 365 kts IAS, the pilot complained of a lag in control response, sluggishness of the configurations, a tendency to overshoot, and the heavy forces required to get the airplane to respond. He gave both of these configurations poor ratings of 6 and 7. On flight 588, the pilot also spoke of the low frequency of the configuration and the overshoot tendencies, but he liked the handling characteristics. He said the stick forces were good and rated the configuration 3.0. The only explanation that can be offered for this discrepancy is that pilot rating is very sensitive to small changes in frequency in the low short period frequency range below optimum frequency.

7.2.2 Ratings and Comments of CAL Pilot

Figure 10 is a similar presentation of pilot ratings and pilot-selected stick force gradients for the CAL evaluation pilot. The data show many similarities to those of the Air Force pilot and some significant differences. Based on the faired curves of Figure 10, the satisfactory frequency range for the CAL pilot can be tabulated as follows:

n_z/α	Range of Satisfactory Frequencies (ω_d) PR < 3.5
16.9	3.7 to 6.5 rad/sec
30.4	4.2 to 7.5 rad/sec
63.4	6.0 to 11 rad/sec

The CAL pilot also downgraded the high as well as low frequencies. The deterioration of pilot ratings with increasing frequency from the optimum tends to be larger at lower values of n_z/α. The trend is also for the acceptable frequency range to be largest at the greatest value of n_z/α (n_z/α = 63.4). The optimum short period frequency also increases with an increase in n_z/α. The deterioration of pilot rating with a decrease in frequency below the optimum is also greatest for the lowest n_z/α simulated (16.9 g/rad). At frequencies above the optimum, the CAL pilot also compromised on higher stick force gradients to reduce the sensitivity or abruptness of the initial response of the airplane. The CAL pilot comments about the handling characteristics of the configurations in the various frequency ranges were similar to those of the AF pilot, and the explanations previously offered for the Air Force pilot also apply for the CAL pilot.

There are some significant differences between Figure 10 and Figure 9 that bear closer examination in the low frequency range below optimum frequency. The CAL pilot also complained of the slow or sluggish response and the tendency to overcontrol. This concern with overcontrol, and the possibility of overstressing the airplane, led the CAL pilot to select higher stick forces at the low frequencies. The CAL pilot's "optimum" stick force gradient curves are therefore parabolic in shape, with the minimum stick force of the 6 to 8 lbs/g occurring at the frequency for best pilot rating.

The higher scatter in the pilot-selected stick force gradients as a function of frequency reflects a greater difficulty for the CAL pilot in optimizing his stick force gradient. The compromise between excessive abruptness or sensitivity and excessive steady state F_{es}/n_z was not always an easy one to make. This is especially true of the flight condition of V = 220 kts IAS (n_z/α = 16.9). The greater scatter in pilot-selected F_{es}/n_z is reflected in the larger scatter in pilot ratings. It is interesting to note that optimum pilot ratings at the optimum frequency were always poorer for the CAL evaluation pilot (3.0 rather than the 2.0 given by the Air Force pilot).

Frequency ranges in which structural modes were excited are also indicated in Figure 10. The CAL evaluation pilot commented on this excitation and indicated that it was difficult to determine how much of the excitation was structural and how much was due to the high short period frequency simulated. The structural excitation was again substantiated by an examination of the oscillograph trace of a wing tip accelerometer. Considerably more scatter exists in the pilot rating data in this region. The scatter is undoubtedly influenced by the degree of structural excitation that was present during the evaluation, and by the pilot's ability to attenuate the excitation by proper selection of stick force gradient.

Some of the other pilot rating points that deviate significantly from the faired curves (for explainable reasons) are also shown as solid in Figure 10. Pilot comment data were examined to determine the reasons for these deviations.

An examination of pilot comments for V = 220 kts (n_z/α = 16.9) leads to the following explanations. On flight 577, the pilot commented that the configuration felt "loose," and the pilot's tendency was to overcontrol and overdrive the airplane. He also commented that the configuration was sluggish and tended to "dig in." He felt that the stick force gradient (F_{es}/n_z) was a little high, and he rated the configuration as 7 because of its poor tracking. The only explanation that can be offered for the scatter in pilot rating in this low frequency range is that the rating is very sensitive to small changes in frequency. No explanation exists for the poor pilot rating of 5 for flight 595; the pilot comment of poor tracking and sluggish response is inconsistent with the comments for other configurations in this frequency range. The large variation in pilot ratings in the frequency range of 8.3 to 10.6 rad/sec is undoubtedly due to the excitation of some structural modes in the T-33 airplane. The pilot often commented that the sensitivity of the airplane was probably a combination of aerodynamic and structural factors. The degree to which the structural modes influenced the pilot ratings is not known. On flights 564, 576, and 579, the pilot complained of the existence of some noise in the variable stability system, as well as the excitation of the airplane's structural modes.

The pilot comments for V = 300 kts (n_z/α = 30.4) leads to the following explanations for some of the more significant deviations in pilot rating. On flight 578, the weather was quite poor, and the pilot commented that a satisfactory evaluation of the configuration was not possible. Structural modes were excited in the frequency range of 9.0 to 11.5 rad/sec. On flight 565, the pilot commented that the structure seemed to be excited by the airplane's short period frequency, and the "bobble" tendency of the configuration made tracking poor. Also, there was a PIO tendency. On flight 577, the pilot did not feel confident about rating the configuration because of the significant structural excitation. On flights 624 and 626, the evaluation pilot first commented on the structural excitation, and then tried to rate the configuration assuming the structural excitation did not exist.

At the flight condition of V = 365 kts (n_z/α = 63.4), several of the pilot rating points show marked deviation from the faired curves. On the first evaluation flight, flight 564, the pilot was somewhat rushed because of a shortage of fuel. During this flight, the pilot also questioned his subjective weighting of tracking and maneuverability in arriving at a final evaluation and numerical rating. The evaluations of flights 570 and 596 were also rushed because of a shortage of fuel. The pilot did not feel confident about either evaluation. In addition, on flight 570, the weather was poor, and on flight 596, the stick force gradient selected was high (F_{es}/n_z = 11.7 lbs/g). No satisfactory explanation can be offered for the poor rating on flight 592. The pilot complained of PIO tendencies and that the damping was less with the pilot in the loop. Based on the poor tracking and PIO tendencies, the pilot rating was 6.5. On flight 575, the pilot stated that the tracking performance was quite satisfactory. He stated that a slight PIO tendency existed and that the airplane was somewhat abrupt in response. The rating of 4.5 was based primarily on the slight abruptness of response and the somewhat heavy stick forces. The discrepancy in rating between flight 575 and 592 cannot be explained except to note that the pilot-selected stick force gradient is different -- 9.3 as compared to 6.8 for flights 575 and 592, respectively.

7.2.3 Initial Pitch Response and Handling Qualities

The importance of pitch response on longitudinal handling qualities has been recognized for some time. Special attention has often been directed at the characteristics of the early part of the pitch response, especially that portion which includes the maximum pitch acceleration and maximum pitch velocity following an abrupt control input. Just how these initial aspects of the response influence the pilot, and how they can be defined by one or more simple handling qualities parameters, is at present not clearly understood.

It has been stated in Reference 16 that a pilot will resort to stick "pumping" when performing precise maneuvers such as landing, tracking, or formation flying. By pumping the stick, the pilot is able to sense the longitudinal responsiveness of the airplane under a given flight condition, and he is able to establish confidence in the level of control available. It is further stated that stick pumping will occur at a frequency that results in a maximum pitch acceleration response for a given control input. Under this condition, the pitch acceleration and control input are in phase.

In the present flight test program, both pilots did indeed resort to stick pumping as a means of sensing the sensitivity or sluggishness of the pitch response of the airplane. Stick pumping was resorted to by both the Air Force and CAL pilots in selecting the optimum or best compromise of stick force gradient. As observed by the safety pilot, stick pumping was used especially by the Air Force pilot. This may explain the greater consistency in the stick forces selected as a function of frequency by the Air Force pilot (compare Figures 9 and 10).

In order to further establish the importance of pitch acceleration response as a pilot cue, oscillograph records were taken of stick pumping during selection by both pilots of the optimum stick force gradient. These records were taken by the safety pilot without the knowledge of the evaluation pilot. From these records, pumping frequencies were measured.

Figure 11 shows frequency response plots of the $\ddot{\theta}(s)/F_{ES}(s)$ transfer function for those configurations in which pumping frequencies were measured. This transfer function, including feel system dynamics, is defined by Equation (6.14), repeated here for convenience.

$$\frac{\ddot{\theta}(s)}{F_{ES}(s)} = \frac{\omega_{FS}^2 M_{\delta_e} \left(\frac{\delta_e}{\delta_{ES}}\right)_{ss} \left(\frac{\delta_{ES}}{F_{ES}}\right)_{ss} s\left(s - Z_\alpha\right)}{\left(s^2 + 2\zeta_{sp}\omega_{sp}s + \omega_{sp}^2\right)\left(s^2 + 2\zeta_{FS}\omega_{FS}s + \omega_{FS}^2\right)} \tag{6.14}$$

Feel system frequency and damping for various flight conditions are presented in Table III. The airplane frequencies and damping are shown on Figure 11 as defined in Tables VII, VIII, and IX.

The range of measured pilot pumping frequencies is spotted on each of these frequency response curves. It is evident from Figure 11 that stick pumping, with stick force as the control input, does indeed occur at a frequency where pitch acceleration is a maximum and the pitch acceleration and stick force are essentially in phase. The small deviations from the conditions for maximum pitch acceleration indicated on Figure 11 are not considered significant.

The importance to longitudinal short period handling qualities of the maximum pitch acceleration during the initial pitch response of an airplane can be further illustrated by examining the time history of pitch response following a step stick force input, as defined by Equation (6.22). The nondimensional pitch acceleration response is a function only of the feel system frequency and damping, and the airplane frequency, damping and Z_α. Time histories of $\ddot{\theta}_{nd}$, $\dot{\theta}_{nd}$, and θ_{nd} were obtained by integrating Equation (6.22) in the time domain using a digital computer. The actual pitch response as a function of time is then related to these time histories by equations analogous to Equation (6.34). Thus,

$$\frac{\ddot{\theta}(t)}{F_{ES}} = \frac{\omega_{sp}^2 \ddot{\theta}_{nd}(t)}{\left(\frac{n_g}{\alpha}\right)_{ss}\left(\frac{F_{ES}}{n_g}\right)_{ss}} \tag{7.1}$$

$$\frac{\dot{\theta}(t)}{F_{ES}} = \frac{\omega_{sp}^2 \dot{\theta}_{nd}(t)}{\left(\frac{n_g}{\alpha}\right)_{ss}\left(\frac{F_{ES}}{n_g}\right)_{ss}} \tag{7.2}$$

$$\frac{\theta(t)}{F_{ES}} = \frac{\omega_{sp}^2 \theta_{nd}(t)}{\left(\frac{n_g}{\alpha}\right)_{ss}\left(\frac{F_{ES}}{n_g}\right)_{ss}} \tag{7.3}$$

Time histories of the pitch responses for three frequencies and the three simulated values of n_z/α are shown in Figure 12 for a step stick force input. All responses are for a stick force gradient of 6 lbs/g.

It is evident from Figure 12 that maximum pitch acceleration is a strong function of frequency. From Equation (6.34), it is evident that the maximum pitch acceleration is a function of the frequency squared, except for the very significant attenuating effects of the feel system, as indicated in Figure 4. It is also evident from Figure 4 that the maximum nondimensional pitch acceleration response is not a strong function of Z_α. It can therefore be concluded from Equations (7.1), (7.2), and (7.3) that the magnitude of the initial pitch response is nearly inversely proportional to n_z/α. This may be checked by comparing the peak values of pitch acceleration and pitch velocity for high short period frequency in Figure 12 at the three values of n_z/α.

The shape of the pitch angle response as a function of frequency is of some interest. The pitch angle curves all show a small initial delay in the pitch response. At the highest frequency and lowest n_z/α, the pitch angle first increases rapidly and then tapers off to a steady rate of increase. For the lowest frequency tested, the pitch angle increases slowly at first, and then more rapidly to the same steady rate as the higher frequencies. At the intermediate frequency, the pitch angle increase is fairly linear. These effects are attenuated as n_z/α increases.

In this flight test program, if the pilot was dissatisfied with the magnitude of pitch response for a given stick force input, he could change the response by adjusting F_{ES}/n_z. When the response was abrupt or sensitive to the pilot, he could increase F_{ES}/n_z to reduce the abruptness at the expense of higher steady-state maneuvering forces. As indicated by Equation (6.34), the maximum pitch acceleration response is inversely proportional to F_{ES}/n_z for a step stick force input.

If one assumes that for the condition of satisfactory short period damping ($\zeta_{SP} \approx 0.7$), the maximum initial pitch acceleration is an important longitudinal short period handling qualities parameter, then this parameter is defined by Equation (6.34), which is repeated here for convenience.

$$\frac{\ddot{\theta}_{MAX}}{F_{ES}} = \frac{\omega_{SP}^2 (\ddot{\theta}_{nd})_{MAX}}{\left(\frac{n_z}{\alpha}\right)_{ss} \left(\frac{F_{ES}}{n_z}\right)_{ss}} \qquad (6.34)$$

If it is further assumed that, for given longitudinal short period and feel system characteristics, F_{ES}/n_z can be consistently optimized by the pilot, then F_{ES}/n_z as such can be eliminated from Equation (6.34). Multiplying both sides of Equation (6.34) by F_{ES}/n_z, we have the following parameter:

$$(CAP)' = \frac{\ddot{\theta}_{MAX}}{(n_z)_{ss}} = \frac{\omega_{sp}^2 (\ddot{\theta}_{nd})_{MAX}}{\left(\frac{n_z}{\alpha}\right)_{ss}} \qquad (6.36)$$

Equation (6.36) is Bihrle's control anticipation parameter with the attenuating effects of the feel system included. This parameter was previously discussed in Section 6.3.

Figures 13 and 14 are plots of pilot ratings versus (CAP)' for the Air Force and CAL pilots, respectively. The solid points on these figures, which represent questionable data, are identical to the solid points on Figures 9 and 10. The faired curves of Figure 9 as a function of ω_{sp} are mapped on Figure 13 as a function of (CAP)'. The same mapping occurred between curves of Figures 10 and 14.

An examination of Figure 13 for the Air Force pilot indicates that the pilot rating curves are very similar in shape when plotted as a function of (CAP)' for the three simulated flight conditions, n_z/α = 16.9, 30.4, and 63.4 g/rad. The same can be said of the curves of optimum stick force gradient. It appears that the optimum stick force gradient selected does decrease somewhat at a given (CAP)' as n_z/α increases. As noted previously, the same is true of optimum F_{ES}/n_z at a given ω_{sp} . The significant scatter in pilot ratings and pilot-selected F_{ES}/n_z at the high (CAP)' values for V = 300 kts IAS is associated with excitation of the airplane structural modes. Some of the deviation in pilot ratings as a function of (CAP)' is undoubtedly associated with variations in pilot-selected F_{ES}/n_z as a function of (CAP)'.

Figure 14 is a similar plot for the CAL evaluation pilot. Again, the data points for the questionable pilot ratings are shown solid. The significant scatter in pilot ratings at high values of (CAP)' at V = 220 kts and 300 kts IAS is again associated with the excitation of structural modes. It is worth noting that, although the character of CAL pilot rating data variation with (CAP)' is similar to that of the Air Force pilot, the plotted data exhibit more scatter. The greater scatter in pilot rating data probably reflects the larger scatter in pilot-selected optimum F_{ES}/n_z . It is interesting to note that, in the case of the CAL pilot, higher stick force gradients were selected at the low frequencies. In his comments, the CAL pilot stated that at low frequencies the airplane was slow or sluggish in initial response. The tendency to overcontrol under these conditions led him to select high stick forces to prevent overcontrol or overstressing of the airplane. Even with the higher stick forces, the pilot ratings were as poor, or poorer, than those of the Air Force pilot in the low frequency range.

If it is assumed that the initial pitch acceleration response of the airplane is the most important longitudinal short period handling qualities parameter for the condition with satisfactory damping ($\zeta_{sp} \approx 0.7$), then it should be

possible to plot pilot rating as a function of (CAP)' only. Such a plot also assumes that the optimum F_{ES}/n_z is selected in a consistent fashion as a function of (CAP)'.

Figures 15 and 16 are such plots for the Air Force pilot using data for all three flight conditions. Corresponding results for the CAL pilot are plotted as Figures 17 and 18. Data points associated with questionable pilot ratings are again shown as solid points and are identified by flight number.

Figure 15, for the Air Force pilot, indicates a significant degree of correlation between (CAP)' and pilot rating. Optimum pilot ratings occur in the vicinity of (CAP)' of 0.5. The plot further indicates that the satisfactory boundary (PR $\leq$ 3.5) is confined to (CAP)' values between 0.25 and 1.40. Pilot ratings better than 6.5 lie between (CAP)' values of 0.15 and 2.6. Some of the scatter that exists in the pilot rating data of Figure 15 may reflect variations in optimum F_{ES}/n_z shown in Figure 16.

7.2.4 Summary of Pilot Comments - Low Frequencies

A summary of the pilot comments at low frequencies is presented below. Based on pilot comments and pilot ratings, the low frequency regions are a function of flight condition, and they can be approximated as follows:

1. $\omega_{SP} <$ 2.5 to 3.0 rad/sec for n_z/α = 16.9 g/rad
2. $\omega_{SP} <$ 3.0 to 3.5 rad/sec for n_z/α = 30.4 g/rad
3. $\omega_{SP} <$ 4.0 to 4.5 rad/sec for n_z/α = 63.4 g/rad

As the short period frequencies decreased below the values indicated above, both pilots began complaining about the slow response of the airplane. The handling qualities of this slow response were described in the following general way. The initial response to a control input was slow and even showed characteristics of a response lag. This initial response was followed by a pitch-up tendency or "digging-in" quality which was unanticipated and difficult to stop or control in any precise manner. The final result was a tendency to overcontrol or overdrive the airplane. These characteristics became progressively worse as the frequency was reduced. Performance in the tracking task deteriorated rapidly, but the degradation in ground tracking was less rapid. The airplane became more difficult to trim as the frequency was reduced. Precise normal acceleration control and attitude control became progressively more difficult.

In general, the Air Force pilot chose progressively lower stick force gradients as the frequency was reduced. This made it easier for him to increase the initial response of the airplane to control force inputs. He then modulated the input to prevent overcontrol. He often complained of the lightening of the stick force gradient as the g-force was increased. This was sometimes described as a tendency to tighten up in a turn when the frequency was low.

The CAL pilot increased his stick force gradient as the frequency was reduced. This was done to prevent overcontrol or overstressing of the airplane.

As the frequency was decreased, both pilots said that the airplane was less sensitive to random disturbance inputs to the elevator.

The CAL pilot complained often of a lack of control harmony as the frequency was reduced. The airplane became increasingly more responsive to aileron control than to elevator control. This mismatch was accentuated by the increased stick force gradients selected as the short period frequency was reduced. The Air Force pilot complained much less about the lack of control harmony, since his selected stick force gradient was low at low frequencies.

Both pilots rapidly downgraded the configurations as the short period longitudinal frequency was reduced, even though they selected different stick force gradients.

The basis for the pilot comments at low short period frequencies becomes readily apparent when one observes the shape and magnitude of the pitch rate and pitch angle response at low frequencies (ω_{sp} = 2 rad/sec) shown in Figure 12. The pitch rate builds up gradually, almost linearly, to the steady-state value with little overshoot. The pitch angle increase with time is parabolic, slow at first and much more rapid later.

7.2.5 Summary of Pilot Comments - High Frequencies

A summary of pilot comments at high frequencies is presented below. Based on the pilot comments and pilot ratings, the high frequency regions as a function of flight condition can be approximated as follows:

1. $\omega_{sp} >$ 5.0 to 5.5 rad/sec for n_z/α = 16.9 g/rad
2. $\omega_{sp} >$ 6.0 to 7.0 rad/sec for n_z/α = 30.4 g/rad
3. $\omega_{sp} >$ 8.80 to 9.0 rad/sec for n_z/α = 63.4 g/rad

As the short period frequencies increased above the values indicated, both pilots began to complain about the fast response of the airplane. The handling qualities of these fast short period frequencies were described in the following way: The initial response of the airplane to control inputs was abrupt. The airplane was very responsive and sensitive to small control inputs about trim. The airplane also had a tendency to "bobble" about trim for small inputs and also had a tendency to bobble in making precise attitude changes. These characteristics increased more rapidly with frequency at the lowest n_z/α tested (16.9 g/rad). The increase in sensitivity with frequency was attenuated by the feel system dynamics.

Although the pilots liked the rapid response of the airplane, they objected to the abruptness, sensitivity, and bobbling tendencies. These characteristics led both pilots to select higher stick force gradients with an increase in frequency to attenuate the sensitivity and bobble tendencies of the airplane. This trend was especially pronounced for the lowest n_z/α tested. Higher stick force gradients, however, resulted in higher steady-state maneuvering forces. Thus, the gradient selected was always a compromise between these two conflicting requirements. The compromise was not always an easy one to make, especially for the CAL pilot.

With increasing frequency, it was generally true that the airplane became more responsive and sensitive to random inputs to the elevator, and tracking became more difficult. Small changes in trim became more of a problem. Precise control of small changes in attitude and normal acceleration were more difficult than larger changes which required larger stick forces. Small attitude control was also better with a higher stick force gradient. All of these trends with frequency were less pronounced at the highest n_z/α tested.

At the higher frequencies, both pilots commented occasionally on a problem with control harmony; that is, control was more sensitive and control forces larger in pitch than in roll.

At 300 kts, and more often at 365 kts, both pilots commented on a greater bobble tendency that existed with negative, as compared to positive, incremental g-forces. Attitude control was more difficult with negative incremental g-forces than with positive incremental g-forces. They also commented that the dynamics of the pushovers were such that it was easier for the pilot to couple with the airplane, induce oscillations, and develop PIO tendencies.

Airplane sensitivity was more erratic and difficult to control when the structural modes of the airplane were excited. The primary structural mode excited was wing bending, which occurred at frequencies between 17 and 21 rad/sec (2.7 to 3.3 cps). These bending frequencies were observed in the oscillograph record of a wing tip mounted accelerometer and are a function of the fuel remaining in the tip tanks. Both pilots commented on the varying degree of structural excitation that occurred when the airplane undamped frequencies varied from approximately 8 to 11.5 rad/sec (approximately half the structural frequencies). The erratic nature of the pilot ratings and pilot-selected stick forces in this region are also understandable. The pilots were obviously correcting and interpreting sensitivity due to structural factors as well as the inherent airplane sensitivity.

The reasons for the airplane sensitivity at high frequencies become apparent from an examination of Figure 12. The marked increase in maximum pitch acceleration with an increase in frequency and a decrease in n_z/α for the same steady-state stick force gradient is very evident. A similar characteristic is observed in the pitch rate overshoot. The abruptness, sensitivity, and bobbling tendency of the airplane are undoubtedly associated with those

transient characteristics of the high frequency configurations. It is possible to reduce the pitch accelerations and pitch rates for a given frequency and n_z/α by simply increasing the stick force gradient. Maximum pitch acceleration and pitch velocity per unit stick force are inversely proportional to the stick force gradient.

7.2.6 Pilot Ratings and Iso-Opinion Lines

The importance of the pilot-selected "optimum" stick force gradient in the pilot rating and comments of a simulated short period configuration has been amply demonstrated. Plots of pilot rating as a function of (CAP)' assume that stick forces were optimized by the pilot always in the same manner as a function of (CAP)'. The scatter in stick force data indicates that the pilot-optimized stick forces were not always consistent. The pilot comments also indicated concern as to whether the stick force gradient selected was a proper balance between transient and steady-state requirements. The concern about stick force gradients is especially evident in the comments of the CAL pilot. It therefore appears that pilot ratings are in reality a function of F_{ES}/n_z as well as (CAP)'.

Attempts were made to obtain a least-squares fit of pilot rating data as a function of F_{ES}/n_z and (CAP)' for both pilots. Although the results were not conclusive, there was clear evidence that variation or "scatter" in pilot rating was to some extent a function of variations in F_{ES}/n_z. This appeared to be the case for the CAL pilot at all values of (CAP)'. For the Air Force pilot, the stick force dependency of pilot ratings was only evident at the higher values of (CAP)' -- generally (CAP)' values greater than one. But some of this scatter and stick force dependency is also related to the structural interactions present in the simulation.

If the steady-state maneuver forces as well as the initial pitch acceleration response are important in the pilot ratings, as the comment data indicate, then it should be possible to draw iso-opinion lines (constant rating lines) on a plot of F_{ES}/n_z versus $\ddot{\theta}_{MAX}/F_{ES}$ The quantity $\ddot{\theta}_{MAX}/F_{ES}$ is the maximum pitch acceleration for a unit step stick force input as defined by Equation (6.34) and shown in Tables X, XI, and XII. The plotted data and iso-opinion lines are shown for both pilots as Figures 19 through 22.

All data presented in the figures are based on a longitudinal short period damping ratio of $\zeta_{SP} \approx 0.7$. The numbers next to each of the points refer to the numerical pilot rating based on the CAL Rating Scale. Iso-opinion boundaries that delineate satisfactory (PR< 3.5) and unsatisfactory (3.5< PR <6.5) regions are also shown on each of the figures. Questionable points are shown solid and correspond to the questionable points shown solid on previous figures for the reasons previously discussed. Most of the solid points are considered questionable because of possible excitation of the structural modes.

Figure 19 shows a reasonably well-defined satisfactory pilot rating region for the Air Force pilot. It is evident from Figure 20 that few of the unsatisfactory pilot rating points lie in the satisfactory region. Although pilot rating line 6.5 is not well defined by the data, the general area of unsatisfactory ratings is indicated.

Several regions of unsatisfactory pilot ratings are designated on Figure 19. In Region 1, the configuration is unacceptable primarily because of sluggish initial response. In Region 2, the steady-state stick force gradients are too high. In Region 3, the high initial response to small inputs makes the airplane abrupt or sensitive. In Region 4, the configuration would be unsatisfactory because of the light stick force gradients.

Although similar characteristics are displayed by the ratings of the CAL pilot, shown in Figures 21 and 22, the trend is less clear. Many more unsatisfactory ratings lie in the satisfactory region (see Figure 22). It is interesting to note that the satisfactory region for the CAL pilot is more restricted and is shifted upward. The CAL evaluation pilot was less inclined to consider light stick force gradients as satisfactory.

It must be clearly understood that these conclusions are only tentative, since the satisfactory and unsatisfactory boundaries are not always well defined by the data. It was not the purpose of this flight test program to vary stick force gradients in a systematic manner.

7.3 PIO TENDENCIES

7.3.1 Correlation of PIO Ratings

It is postulated in Reference 10 that, with good control system dynamics, PIO tendencies can occur only for those conditions in which $2\zeta_{sp}\omega_{sp} < L_\alpha$. This condition of closed-loop instability was derived in Reference 10 for short period longitudinal motions, assuming the pilot's describing function during a sustained PIO to be a simple gain, and in addition, assuming that the pilot is responsive primarily to visual pitch attitude cues.

Figure 23 is a plot of pilot-induced oscillation rating (PIOR) as a function of $2\zeta_{sp}\omega_{sp}/L_\alpha$ for the Air Force pilot, and Figure 24 is a similar plot for the CAL pilot. The pilot-selected stick force gradients are also shown on these figures. The PIO data are presented in Table XIII, and the PIOR's are based on the PIO Tendency Rating Scale of Section 4.3. Attempts were made to simulate PIO configurations in the flight program primarily by reducing the damping ratio. Table XIII includes all configurations in Tables VII, VIII, and IX where the damping ratio was equal to or less than 0.6. Strictly speaking, many of these configurations are not PIO configurations, since they do not satisfy the criterion under investigation: $2\zeta_{sp}\omega_{sp}/L_\alpha < 1.0$. The division line for PIO configurations must of necessity be arbitrary, since the exact conditions for the occurrence of PIO's are not understood.

Figures 23 and 24 indicate a general tendency to PIO for $2\zeta_{SP}\omega_{SP}/L_\alpha < 1.0$, although a significant amount of scatter exists in the data for both pilots. It is also evident from the pilot-selected stick force gradient curves that, as PIO tendencies increased, both pilots selected higher stick force gradients to inhibit these tendencies. This trend was evident for all three flight conditions (V = 220 kts, 300 kts, and 365 kts IAS). The fact that higher values of F_{ES}/n_z were selected to inhibit PIO tendencies is also evident from the many pilot comments about PIO tendencies. The scatter in the selected stick force gradients and the discreteness of the rating scale may explain some of the scatter in PIO ratings.

The interrelationship between PIO tendencies and stick force gradients is not clearly understood. Attempts were made to extract the effect of F_{ES}/n_z by least-squares fitting of PIO ratings to various power series in $2\zeta_{SP}\omega_{SP}/L_\alpha$ and F_{ES}/n_z by assuming that

$$PIOR = f\left(\frac{2\zeta_{SP}\omega_{SP}}{L_\alpha}, \frac{F_{ES}}{n_z}\right)$$

The results were not conclusive, since the stick force gradients were selected by the pilot to inhibit, rather than induce, PIO tendencies. In the case of the CAL pilot, the fits indicated that PIO tendencies were as much a function of variations in F_{ES}/n_z as they were of $2\zeta_{SP}\omega_{SP}/L_\alpha$. This was not the case for the Air Force pilot. Based on the optimum-selected stick force gradients of Figure 23, the Air Force pilot PIO ratings were primarily determined by the PIO parameter $2\zeta_{SP}\omega_{SP}/L_\alpha$.

Figures 25, 26, and 27 show comparisons of PIO ratings and pilot-selected optimum stick force gradients for the two pilots. Each figure is for a specific flight condition. The data indicate no significant differences in PIO ratings and pilot-selected stick force gradients for the two pilots.

7.3.2 Analysis of PIO Comment Data

An examination of the PIO rating scale of Section 4.3 indicates that sustained PIO's are indicated only when the PIO rating is 4 or higher. An examination of Figures 23 and 24 and Table XIII shows PIO ratings of 4 or poorer for only five of the PIO configurations simulated. Four of these configurations were simulated at the flight condition of 365 kts IAS. A PIO rating of 4 is also indicated for a configuration not included in Table XIII: flight 583 at 365 kts IAS. The pertinent characteristics of these configurations are shown below:

FLT	V(IAS) KTS	PILOT	ω_{sp}	ζ_{sp}	$\frac{2\zeta_{sp}\omega_{sp}}{L_\alpha}$	$\frac{F_{es}}{n_z}$	PR	PIOR
583	365	AF	8.98	0.66	3.90	4.86	3	4
595	365	CAL	3.72	0.24	0.58	--	9	4.5
596	300	CAL	6.08	0.13	0.89	15.8	8	5
601	365	CAL	2.16	0.44	0.62	16.2	9	4.5
605	365	AF	3.72	0.19	0.46	4.15	7.5	4.0
610	365	AF	5.47	0.05	0.18	8.12	8.5	4.0

On flight 583, the pilot commented that the airplane was responsive to rapid inputs, displayed sensitivity, and tended to bobble for small inputs. In tracking, he said the airplane showed overcontrol tendencies and the beginning of a minor PIO. He gave the airplane a PIO rating of 4 and an overall rating of 3. These ratings appear to be inconsistent, since such a poor PIO rating should not result in as good an overall rating. This was only the third flight for the Air Force pilot, and his relative unfamiliarity with the rating scales and their use may have been a factor.

On flight 595, the pilot complained that the airplane was "touchy," "digs in," and has a sluggish initial response. He complained that the stick force selected was too heavy, but that he selected it to prevent overcontrol. He said that, with the low frequency and low damping conditions, he got a PIO while trying to track, and that the airplane had real PIO tendencies. The only usable piloting technique was either not to disturb the airplane or to initiate control slowly. He said the airplane was completely unacceptable and very bad; it could be described as "nearly dangerous" because of its PIO characteristics.

On flight 596, the pilot said the selected F_{es}/n_z was high but necessary to reduce the oscillatory tendencies of the airplane. He said that in tracking, the pilot could induce oscillations even though the selected F_{es}/n_z was high, and he attributed this condition to the combination of frequency and damping of the configuration. He further stated that the tracking performance was very, very poor and that the airplane was quite responsive to random noise or the pilot inputs in response to the random noise. The airplane was unacceptable and was "close to dangerous" with a strong PIO tendency.

On flight 601, the pilot complained of the lag in response and the overcontrol tendency of the configuration. He felt that none of the stick force gradients that he tried were satisfactory. The selected F_{es}/n_z allowed some maneuverability, but a strong tendency to overdrive the airplane still existed. In turbulence it was very difficult to track. Without turbulence, it was significantly easier, but still "not good." He said that PIO tendencies did exist and the airplane was very bad, "almost dangerous."

On flight 605, the Air Force pilot said the configuration was very susceptible to PIO, and the damping was poor. The response to control inputs was slow at first and then "took off." Higher stick force gradients decreased the tendency for the pilot to couple with the airplane, and there was less sensitivity to PIO's. In tracking, PIO tendencies were prevalent, and any effort to reduce the tracking error only resulted in a PIO. He rated the configuration flyable but unacceptable. It was "bad" or "very bad" and had real PIO tendencies.

On flight 610, the pilot complained that, in controlling attitude or making attitude changes, the pilot coupled with the airplane, and a PIO resulted. The attitude errors then became worse. Tracking was difficult because of a PIO tendency, especially when making corrections in the negative g direction. The pilot's technique for flying this configuration was to avoid overcontrolling the airplane because of the PIO tendencies. The pilot rated the configuration unacceptable, very bad, and probably dangerous because of the PIO tendencies.

On flight 630 at 300 kts IAS, and on flights 577 and 630 at 365 kts IAS, the PIO ratings were 3.5, even though the damping ratios were satisfactory (between 0.66 and 0.75). The short period frequency on flight 630 was 11.49 rad/sec, and the pilot complained of structural excitation of the airplane. Part of the excitation was probably reflected as a PIO tendency. On flight 577 at 365 kts, the frequency was 4.64 rad/sec, and the damping ratio was 0.73. The CAL pilot complained of a tendency to overdrive the airplane and of its tendency to "pitch up" and "dig in." He stated that the tracking performance was bad because of PIO tendencies and that, based on general maneuvers and not tracking, the PIO rating would be only 2. He also felt that the evaluation was not adequate, since he was rushed because of a shortage of fuel. On flight 630 at 365 kts, the frequency was high (17.90 rad/sec). The pilot complained of the abruptness and sensitivity of the configuration and the existence of a high frequency bobble. He said the PIO rating of 3.5 was a result of this high frequency bobble and the initial abruptness of response, and was not due strictly to a PIO tendency.

On many of the configurations that were simulated to investigate short period frequency requirements with satisfactory damping ($\zeta_{sp} \approx 0.7$), both pilots gave a PIO rating of 3. In most of these cases, the ratings were given because of undesirable motions induced by pilot inputs and not by actual PIO tendencies. These undesirable motions were a result of low frequency "dig in" qualities, high frequency sensitivity, or bobble, and in some cases excitation of the airplane structure. In only a very few cases did the pilot comments indicate actual PIO tendencies.

Section VIII

CONCLUSIONS AND RECOMMENDATIONS

This flight test program to investigate longitudinal short period frequency requirements with satisfactory damping ($\zeta_{sp} = 0.7$), and PIO tendencies with acceptable control system dynamics, leads to the following conclusions:

1. Longitudinal handling qualities are indeed a function of n_z/α as well as short period frequency and damping.

2. The magnitude of the stick force gradient has a major effect on the acceptability of a particular set of longitudinal dynamics. At a fixed n_z/α and with satisfactory damping ($\zeta_{sp} \approx 0.7$), a most acceptable combination of both stick force gradient and short period frequency exists. As frequency is increased and n_z/α reduced, the optimum stick force gradients selected by both pilots were heavier. At lower frequencies and higher n_z/α, higher optimum stick force gradients were more acceptable only to the CAL evaluation pilot.

3. Feel system and control system dynamic characteristics can have significant attenuating effects on the abrupt pitch response at high frequencies and therefore such characteristics are of considerable importance in the analysis of handling qualities results.

4. The maximum pitch acceleration response of an airplane to step stick force inputs appears to be a parameter of significance in the pilot's evaluation of longitudinal handling qualities. This parameter contains many of the variables found to be of significance in this and past handling qualities investigations.

$$\frac{(\ddot{\theta})_{MAX}}{F_{ES}} = \frac{\omega_{sp}^2 (\ddot{\theta}_{nd})_{MAX}}{\left(\frac{n_z}{\alpha}\right)_{ss}\left(\frac{F_{ES}}{n_z}\right)_{ss}}$$

$(\ddot{\theta}_{nd})_{MAX}$ is an attenuation factor due to feel system and control system dynamics.

5. For a ζ_{sp} of 0.7, the present flight test program suggests that short period handling qualities results may be a function of both $(\ddot{\theta})_{MAX}/F_{ES}$, and F_{ES}/n_z.

6. The importance of the parameter $(\ddot{\theta})_{MAX}/F_{ES}$ to the pilot seems to be substantiated by the pilot comment data and the stick pumping used by both pilots in selecting optimum stick force gradients for each configuration simulated.

7. As the short period frequency was increased and n_z/α reduced, the pilot objections were directed at the abruptness of initial response, the sensitivity, and the bobble tendencies of the airplane. As the short period frequency was reduced and the n_z/α increased, the pilot objected to the sluggish initial response, and the "digging in" and overcontrol tendencies after this initial response. Both types of configurations were downgraded by both evaluation pilots.

8. It has been established that high short period frequencies are objectionable to the pilot and that the satisfactory region of pilot ratings (PR < 3.5) does close at the higher frequencies. How high the frequency may be before it is objectionable is a function of n_z/α, feel system and control system dynamics, and stick force gradients.

9. The excitation of structural modes of the T-33 airplane resulted in considerable variation in pilot ratings at some simulated short period frequencies. These results suggest the considerable importance of structural modes on an airplane's short period handling qualities.

10. With satisfactory control system dynamics, PIO tendencies generally increase when $2\zeta_{SP}\omega_{SP} < L_\alpha$. Both pilots selected higher stick force gradients to attenuate the PIO tendencies of a configuration. Stick force gradient may be an important parameter in the analysis of PIO tendencies, but the present results are not conclusive.

11. Some of the variability in intra-pilot and inter-pilot rating and PIO ratings is attributable to variations in pilot-selected stick force gradients. Pilot-selected stick force gradients were more consistent for the Air Force pilot. As a result, his ratings were also more consistent.

On the basis of present and past longitudinal short period results, the following recommendations for future flight test work seem appropriate:

1. A similar investigation of longitudinal short period handling qualities should be made in which the stick force gradients are fixed at various levels. The independent effect of stick force gradients on longitudinal handling qualities can then be definitely established.
2. Linear feel system and control system dynamics should be further varied to establish the importance of feel system dynamics on longitudinal handling qualities.
3. The possible improvements that may result from a nonlinear feel system should also be investigated, such as a nonlinear F_{es}/n_z.
4. Similar investigations to those in the present report should also be performed at other damping ratios.
5. PIO tendency investigations of this flight test program should be repeated with stick force gradients fixed at various levels. Such an investigation would establish the independent effect of stick force gradient in PIO's.
6. PIO tendencies should also be investigated as influenced by variations in the feel and control system dynamics.
7. The PIO tendency evaluation results should be compared with results obtained from other PIO-inducing tasks such as formation flight and in-flight refueling.

REFERENCES

1. Chalk, Charles R.: "Additional Flight Evaluations of Various Longitudinal Handling Qualities in a Variable Stability Jet Fighter" - Part 1 - WADC TR 57-719 (CAL Report No. TB-1141-F-1), March 1958.

2. Chalk, Charles R.: "Additional Flight Evaluations of Various Longitudinal Handling Qualities in a Variable Stability Jet Fighter" - Part 2 - WADC TR 57-719 (CAL Report No. TB-1141-F-2), July 1958.

3. Harper, Robert P. Jr.: "Flight Evaluations of Various Longitudinal Handling Qualities in a Variable-Stability Jet Fighter" - WADC TR 55-299 (CAL Report No. TB-757-F-12); July 1955.

4. Newell, Fred; Campbell, Graham: "Flight Evaluations of Variable Short Period and Phugoid Characteristics in a B-26" - WADC TR 54-594 (CAL Report No. TB-757-F-11), December 1954.

5. Chalk, Charles R.: "Simulator Investigation of the Effects of L_α and True Speed on Longitudinal Handling Qualities" - Journal of Aircraft, Vol. 1 No. 6, November - December 1964.

6. A'Harrah, Ralph C.: "Low-Altitude, High-Speed Handling and Riding Qualities" - Report 443 - AGARD Flt. Mech. Meeting; Turin, Italy - April 1963.

7. Malcom, L. G. and Tobie, T. N.: "New Short Period Handling Qualities Criterion for Fighter Aircraft" - Boeing - T/N D6-17841, September 1965.

8. Shomber, H. A.; Gertsen, W. M.: "Longitudinal Handling Qualities Criteria: An Evaluation" - AIAA Paper No. 65-780 - AIAA/RAES/JSASS Aircraft Design and Technology Meeting, November 15-18, 1965.

9. Kehrer, William T.: "Longitudinal Stability and Control of Large Supersonic Aircraft at Low Speeds" - ICAS Paper No. 64-586, August 1964.

10. Ashkenas, Irving L; Jex, Henry R.; McRuer, Duane T.: "Pilot-Induced Oscillations: Their Cause and Analysis" - Systems Tech., Inc. Report No. STI TR-239-2; NORAIR Report NOR-64-143, July 1964.

11. Hirsch, D. L.: "Investigation and Elimination of PIO Tendencies in the Northrop T-38A" - Presented at SAE Meeting in New York, July 1964.

12. Sadoff, Melvin: "The Effects of Longitudinal Control - System Dynamics on Pilot Opinion and Response Characteristics as Determined from Flight Tests and from Ground Simulator Studies" - NASA Memo. 10-1-58A, October 1958.

13. Phillips, William H.; Brown, B. Porter; Matthews, James T., Jr.: "Review and Investigation of Unsatisfactory Control Characteristics Involving Instability of Pilot-Aircraft Combinations and Methods for Predicting these Difficulties from Ground Tests" - NACA TN 4064, August 1957.

14. Decker, James L.: "The Human Pilot and the High-Speed Airplane" - Journal Aeronautical Sciences, Vol. 23, No. 8, August 1956.

15. Johnson, Harold I.: "Flight Investigation to Improve the Dynamic Longitudinal Stability and Control Feel Characteristics of the P-63A-1 Airplane (AAF No. 42-68889) with Closely Balanced Experimental Elevators" - NACA MR No. L6E20, July 1946.

16. Bihrle, William Jr.: "A Handling Qualities Theory for Precise Flight Path Control" - AFFDL-TR-65-198, June 1966.

17. Key, David L.: "A Functional Description and Working Data for the Variable-Stability System - T-33 Airplane" - CAL Report No. TC-1921-F-2, October 1965.

18. Draper, Charles Stark; McKay, Walter; Lees, Sidney: "Instrument Engineering" - Vol. II, McGraw-Hill Book Co., 1953.

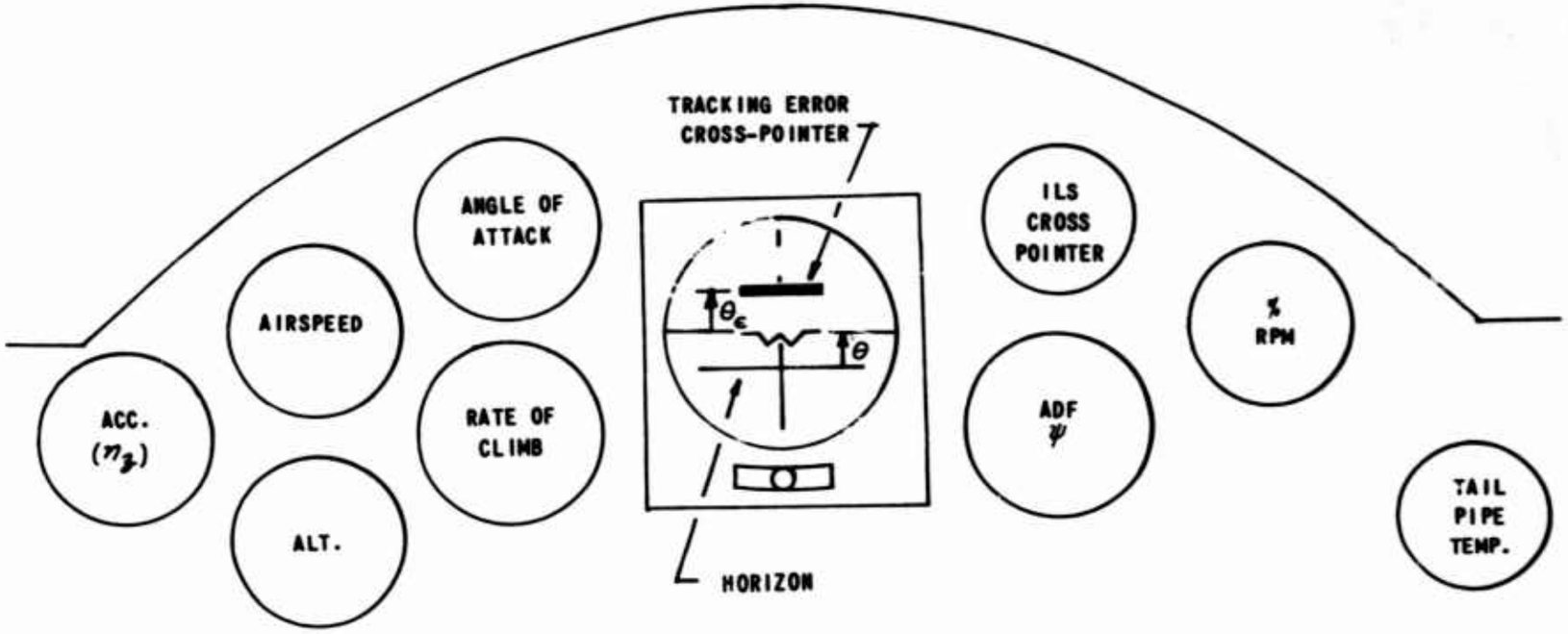

Figure 1 T-33 PANEL ARRANGEMENT WITH TRACKING TASK DISPLAY

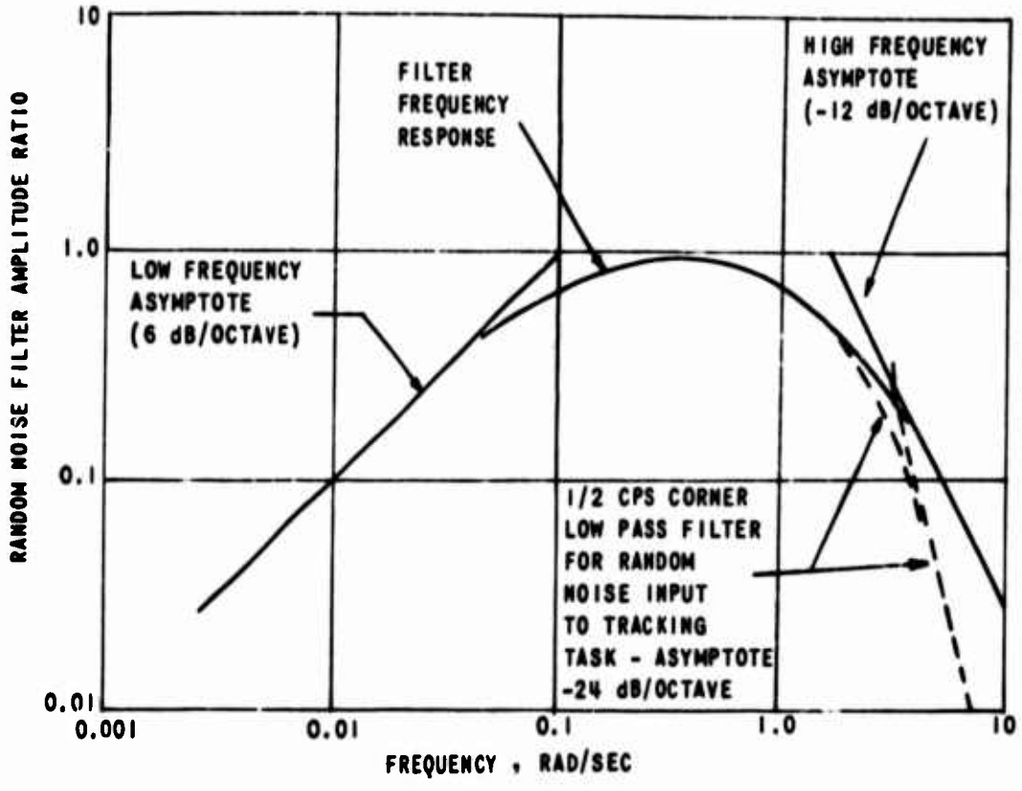

Figure 2 RANDOM NOISE FILTER FREQUENCY RESPONSE - WITH AND WITHOUT 1/2 CPS LOW PASS FILTER

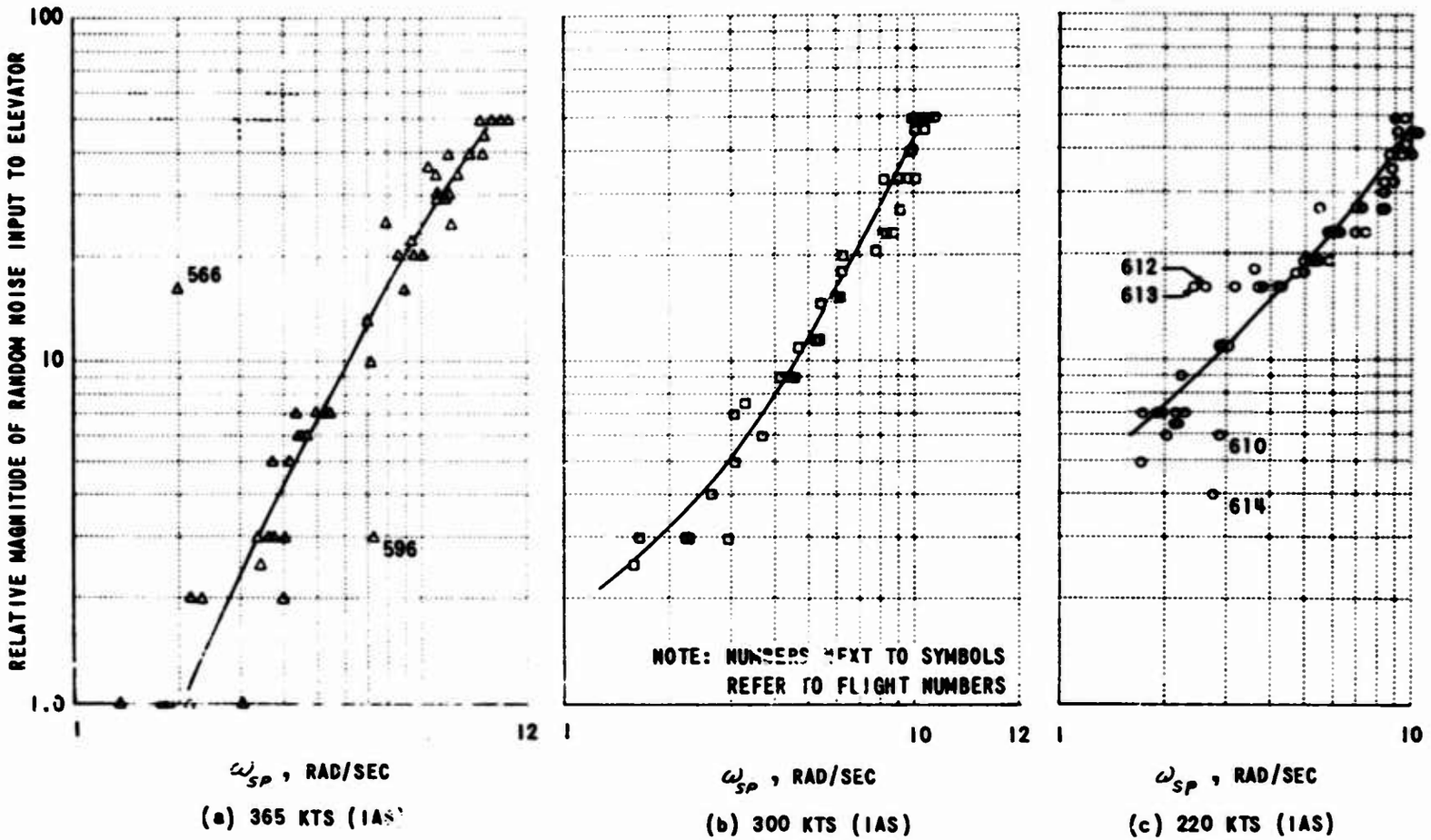

Figure 3 RELATIVE MAGNITUDE OF RANDOM NOISE INPUT TO ELEVATOR AS A FUNCTION OF SHORT PERIOD FREQUENCY

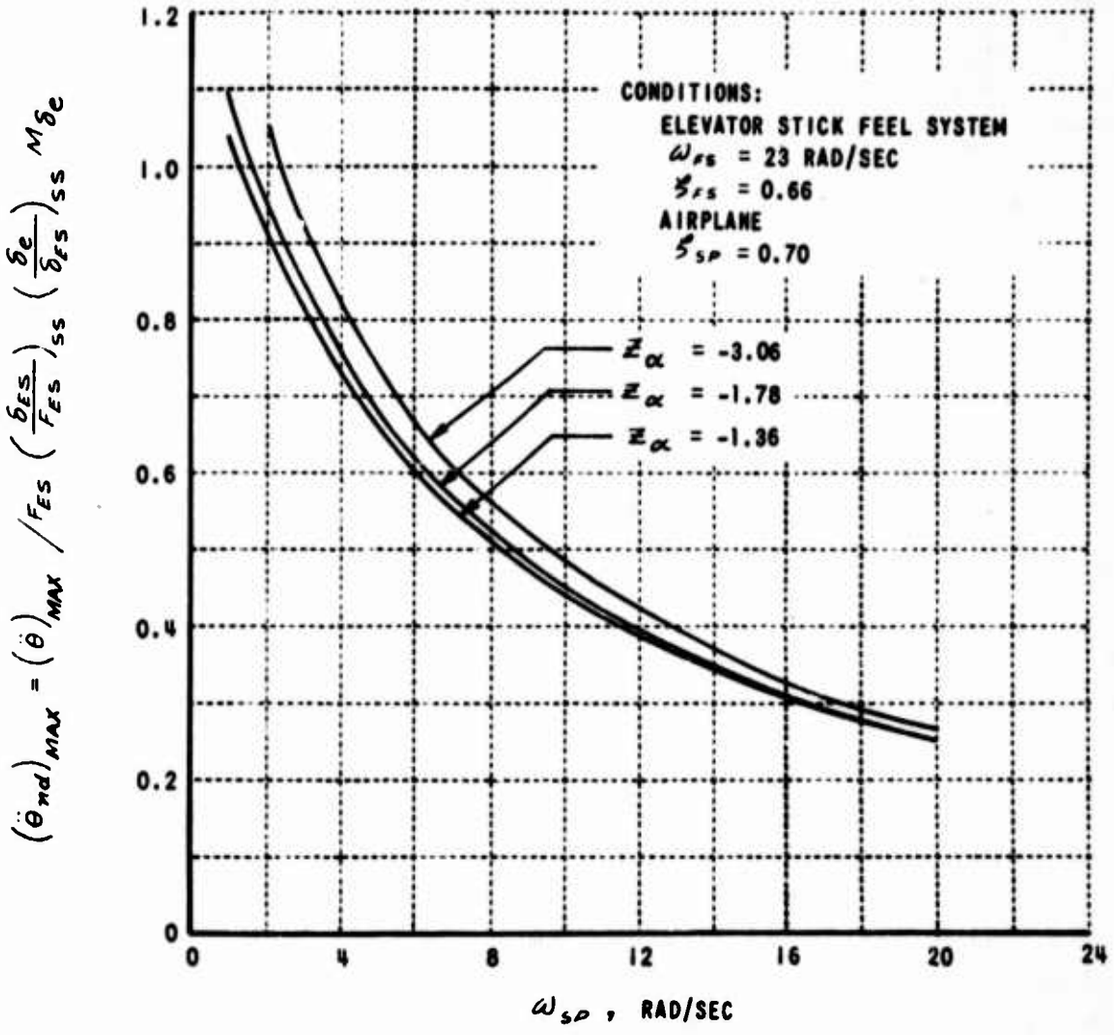

Figure 4 MAXIMUM NONDIMENSIONAL PITCH ACCELERATION $(\ddot{\theta}_{nd})_{MAX}$ FOLLOWING A STEP STICK FORCE INPUT (F_{ES}) - EFFECT OF FEEL SYSTEM LAGS INCLUDED

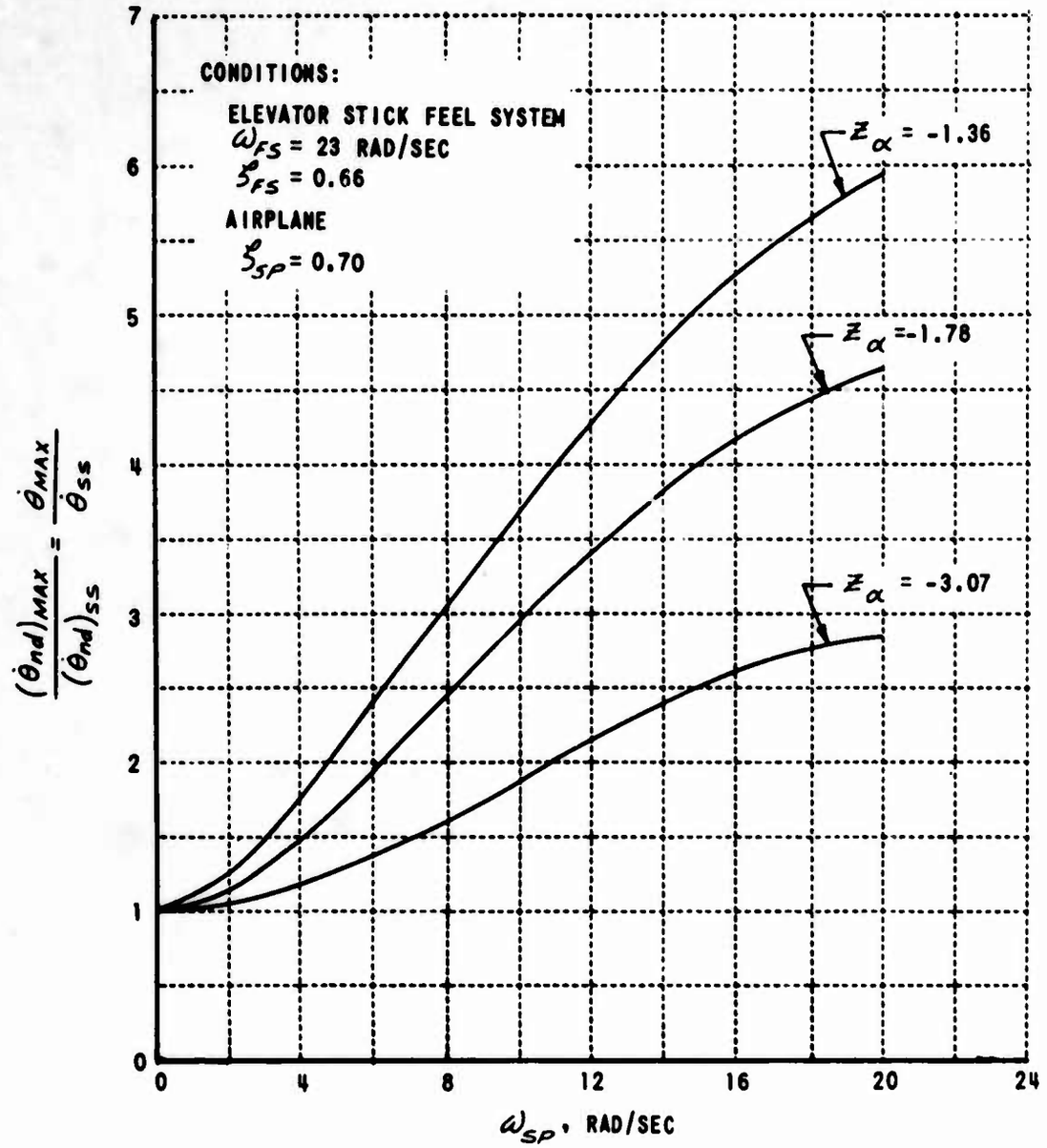

Figure 5 PITCH VELOCITY OVERSHOOT RATIO DUE TO A STEP STICK FORCE INPUT (F_{ES}) - EFFECT OF FEEL SYSTEM LAGS INCLUDED

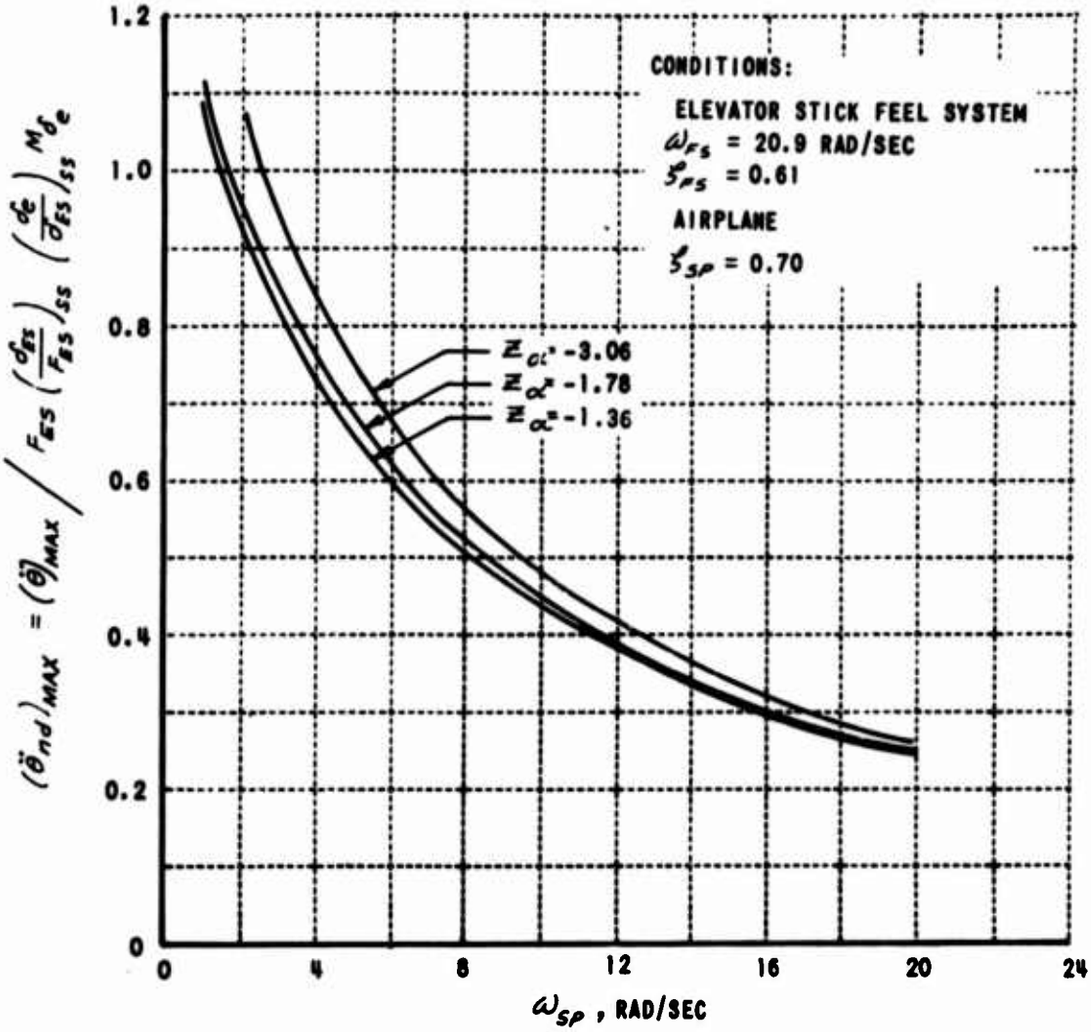

Figure 6 MAXIMUM NONDIMENSIONAL PITCH ACCELERATION $(\ddot{\theta}_{nd})_{MAX}$ FOLLOWING A STEP STICK FORCE INPUT (F_{ES}) - EFFECT OF FEEL SYSTEM LAGS INCLUDED

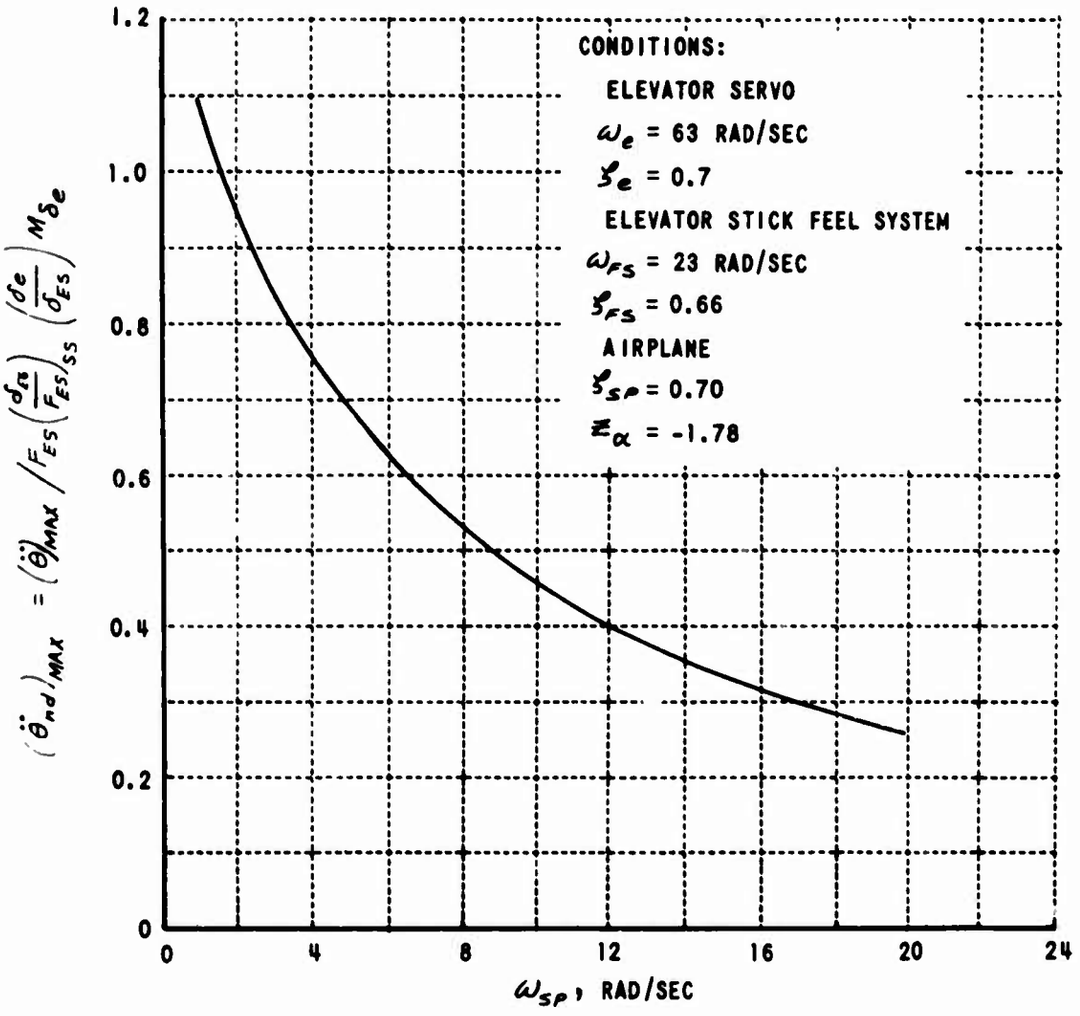

Figure 7 MAXIMUM NONDIMENSIONAL PITCH ACCELERATION $(\ddot{\theta}_{nd})_{MAX}$ FOLLOWING A STEP STICK FORCE INPUT (F_{ES}) - EFFECT OF ELEVATOR SERVO AND FEEL SYSTEM LAGS INCLUDED

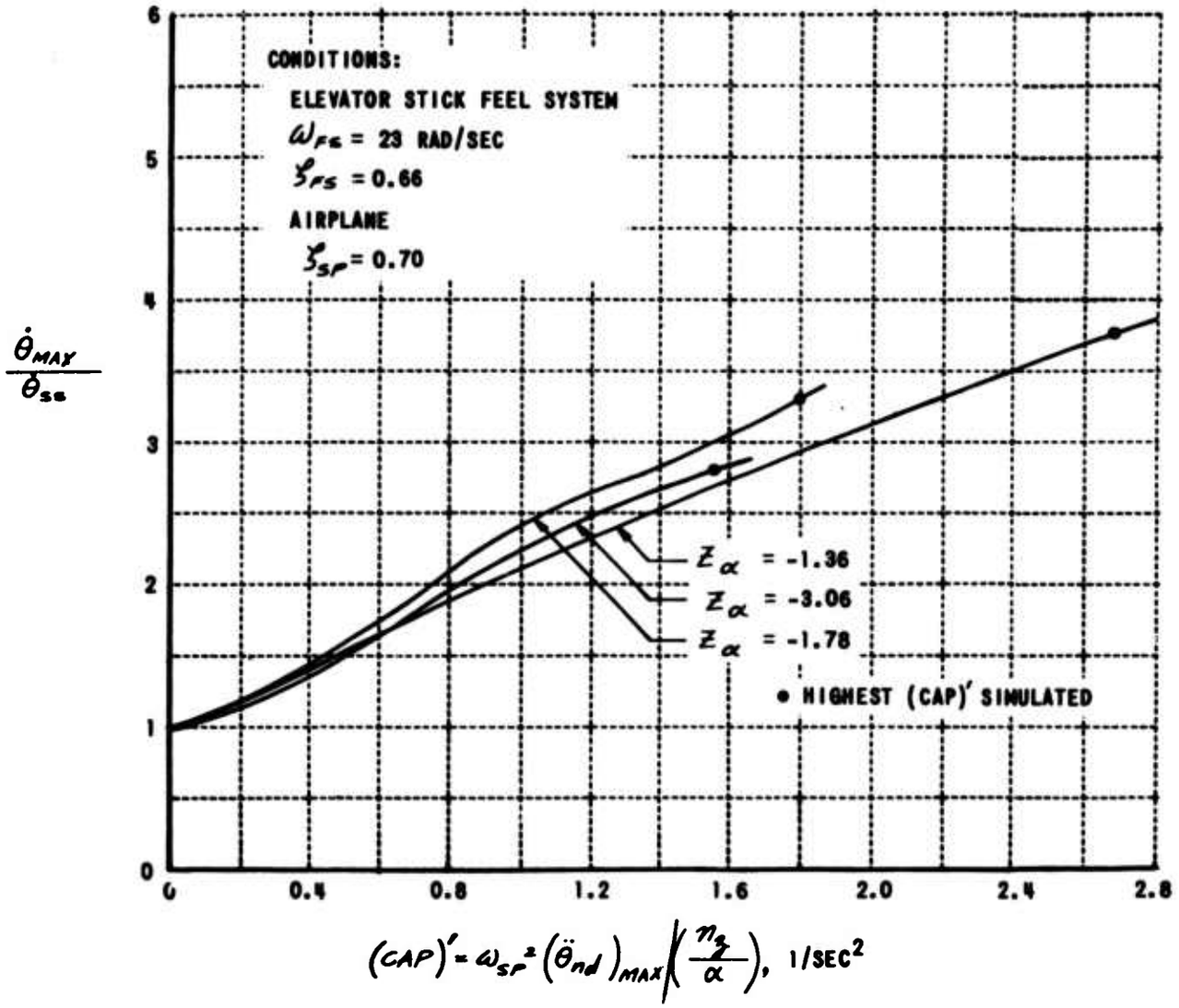

Figure 8 VARIATION OF (CAP)' WITH PITCH VELOCITY OVERSHOOT $(\dot{\theta}_{MAX}/\dot{\theta}_{ss})$

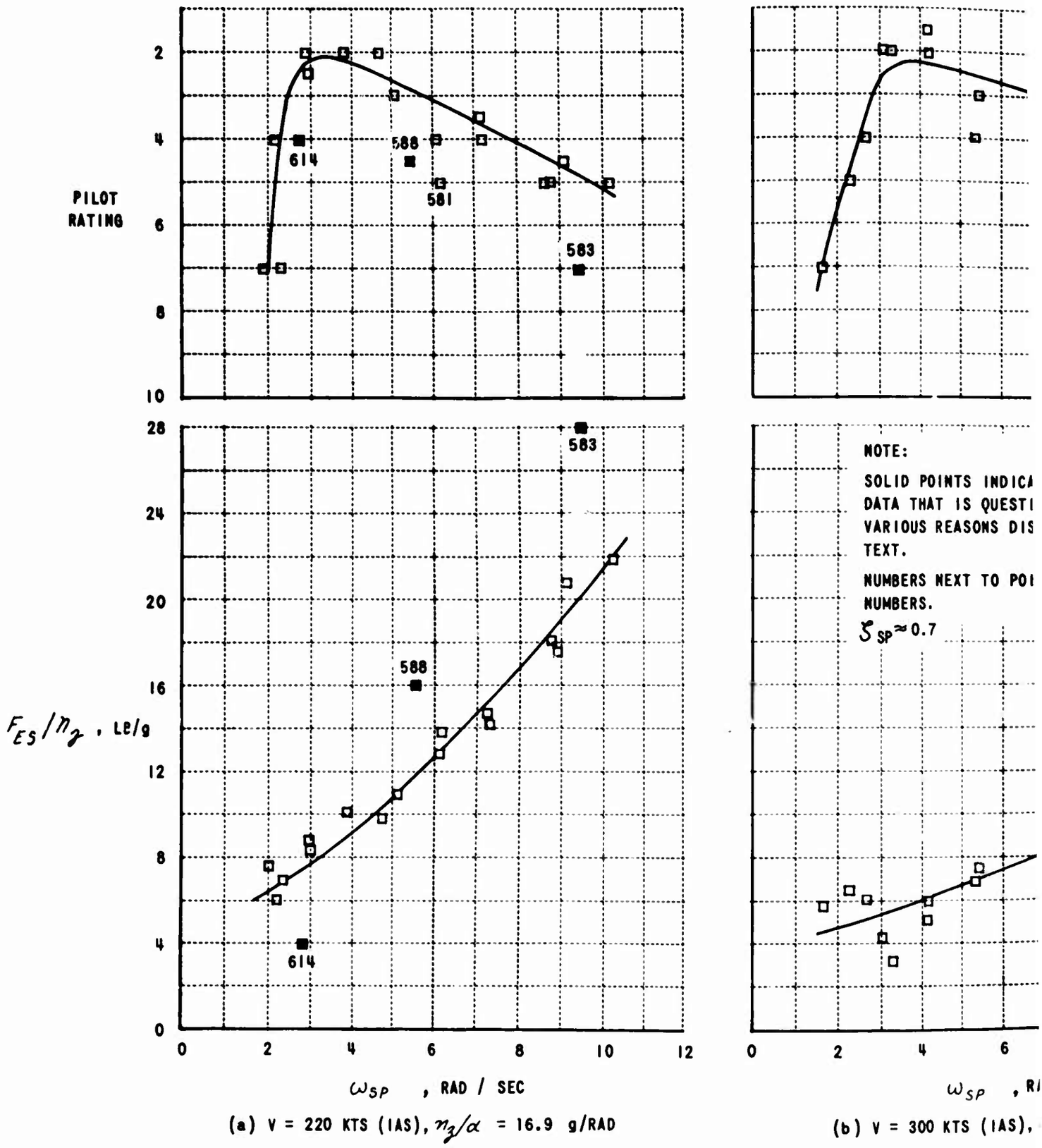

(a) V = 220 KTS (IAS), n_z/α = 16.9 g/RAD

(b) V = 300 KTS (IAS),

Figure 9
VARIATION OF PILOT RATING AND PILOT SELECTED
F_{ES}/n_z WITH SHORT PERIOD FREQUENCY
AND n_z/α - AF PILOT

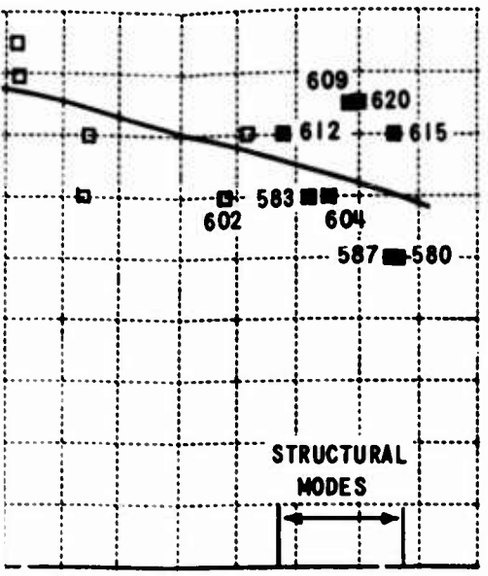

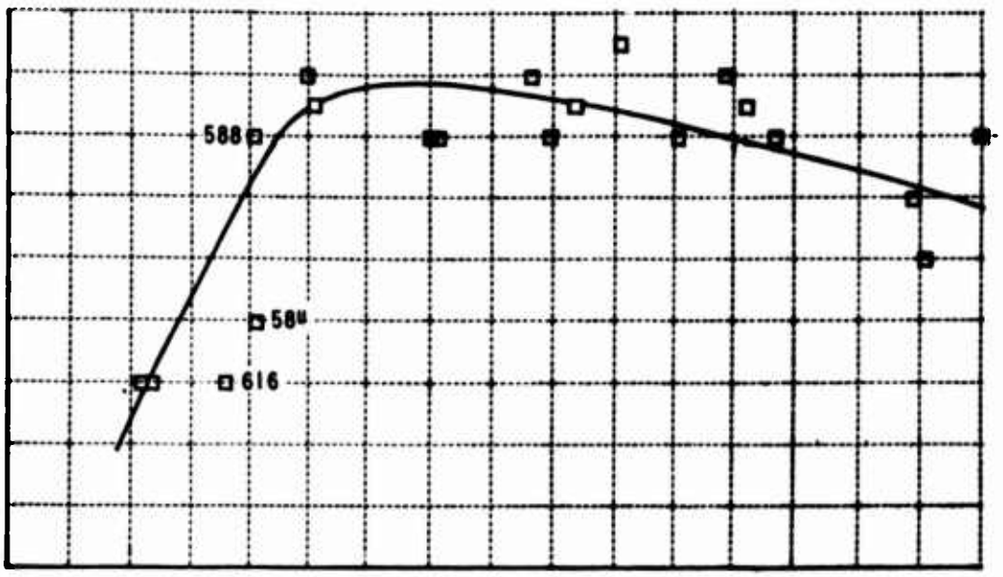

POINTS INDICATE PILOT RATING
IAT IS QUESTIONABLE FOR
REASONS DISCUSSED IN THE

NEXT TO POINTS ARE FLIGHT
.
7

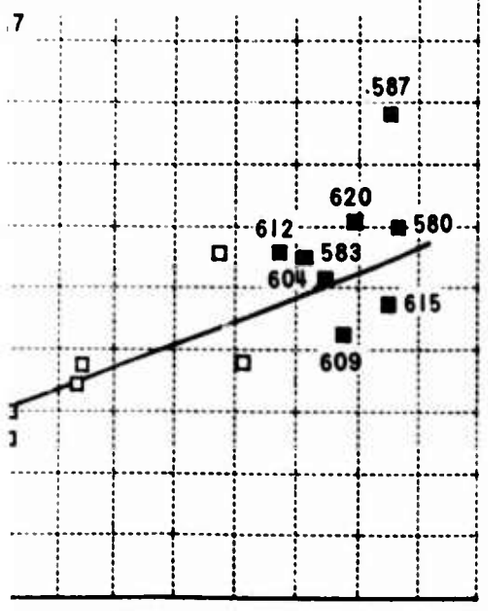

ω_{SP} , RAD / SEC

) KTS (IAS), n_z/α = 30.4 g/RAD

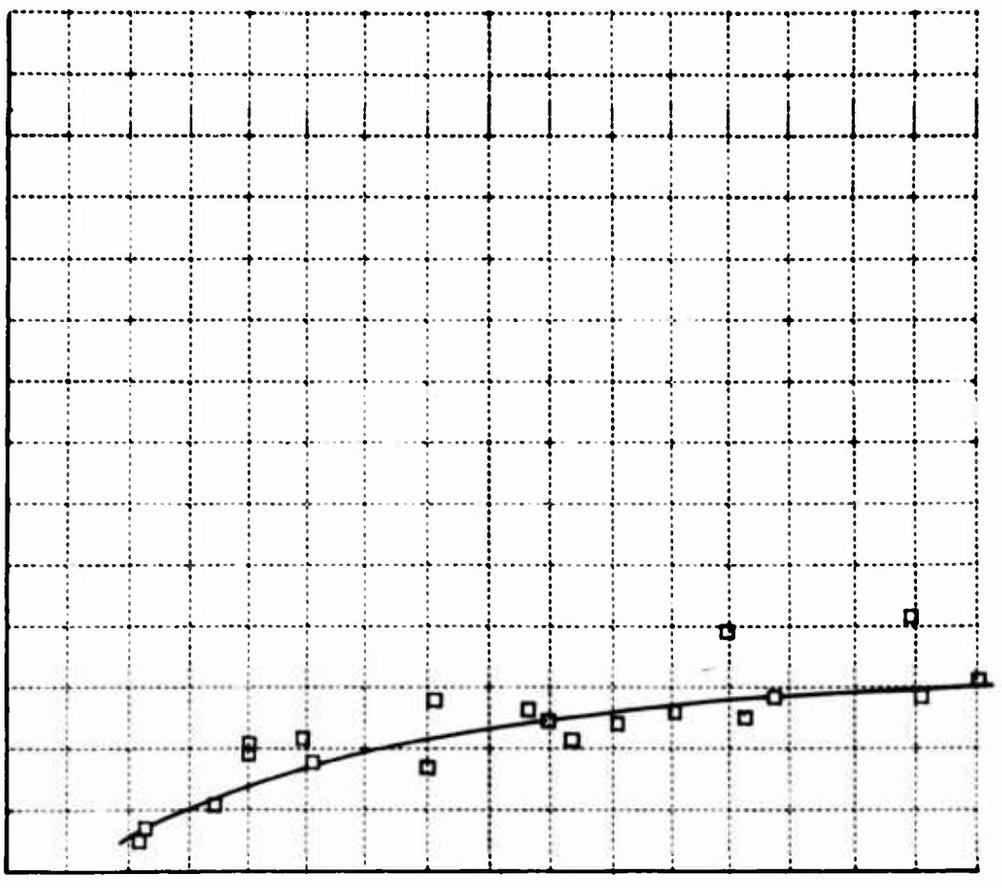

ω_{SP} , RAD / SEC

(c) V = 365 KTS (IAS), n_z/α = 63.4 g/RAD

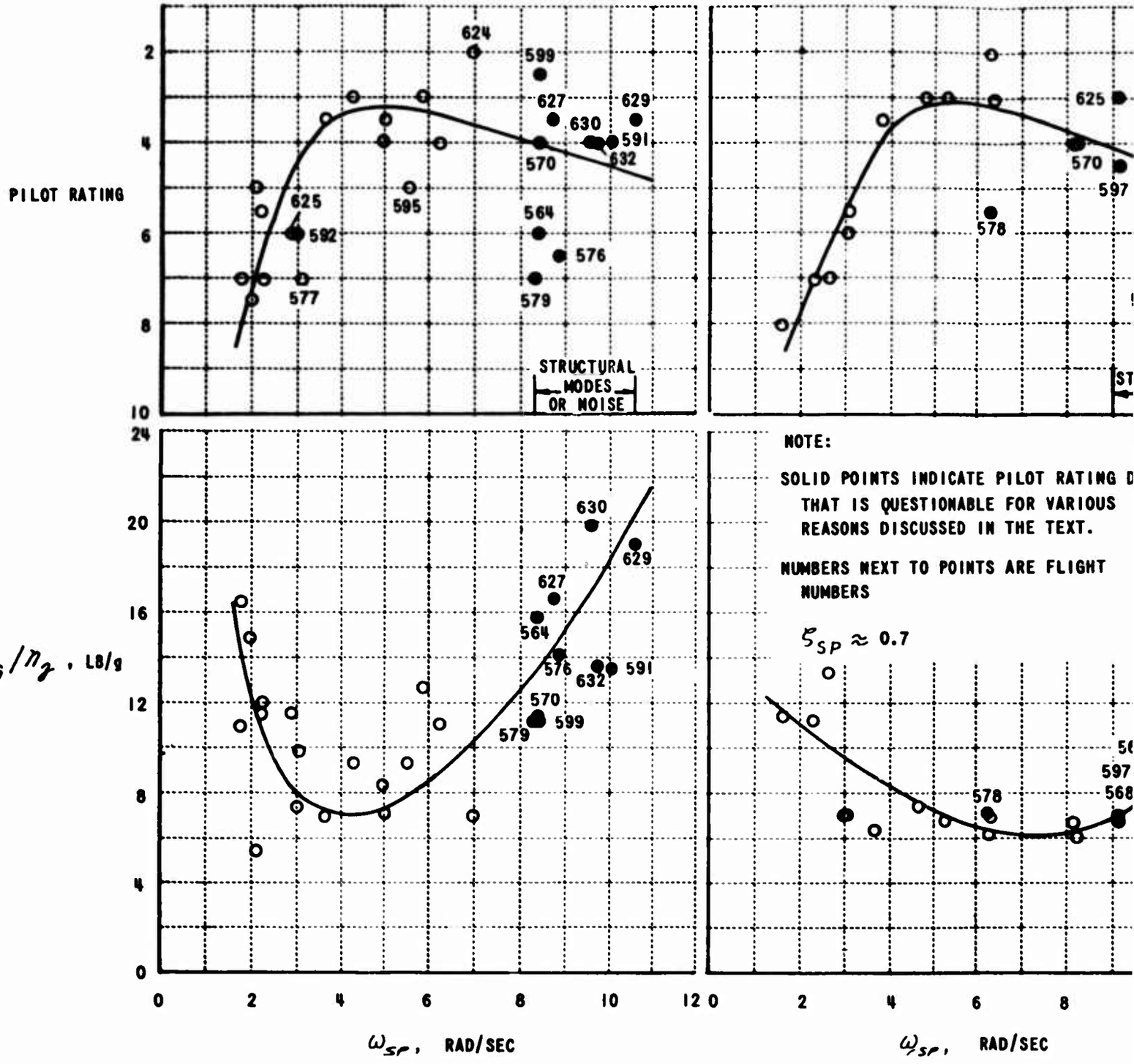

(a) V = 220 KTS (IAS), n_z/α = 16.9 g/RAD

(b) V = 300 KTS (IAS), n_z/α = 30.4

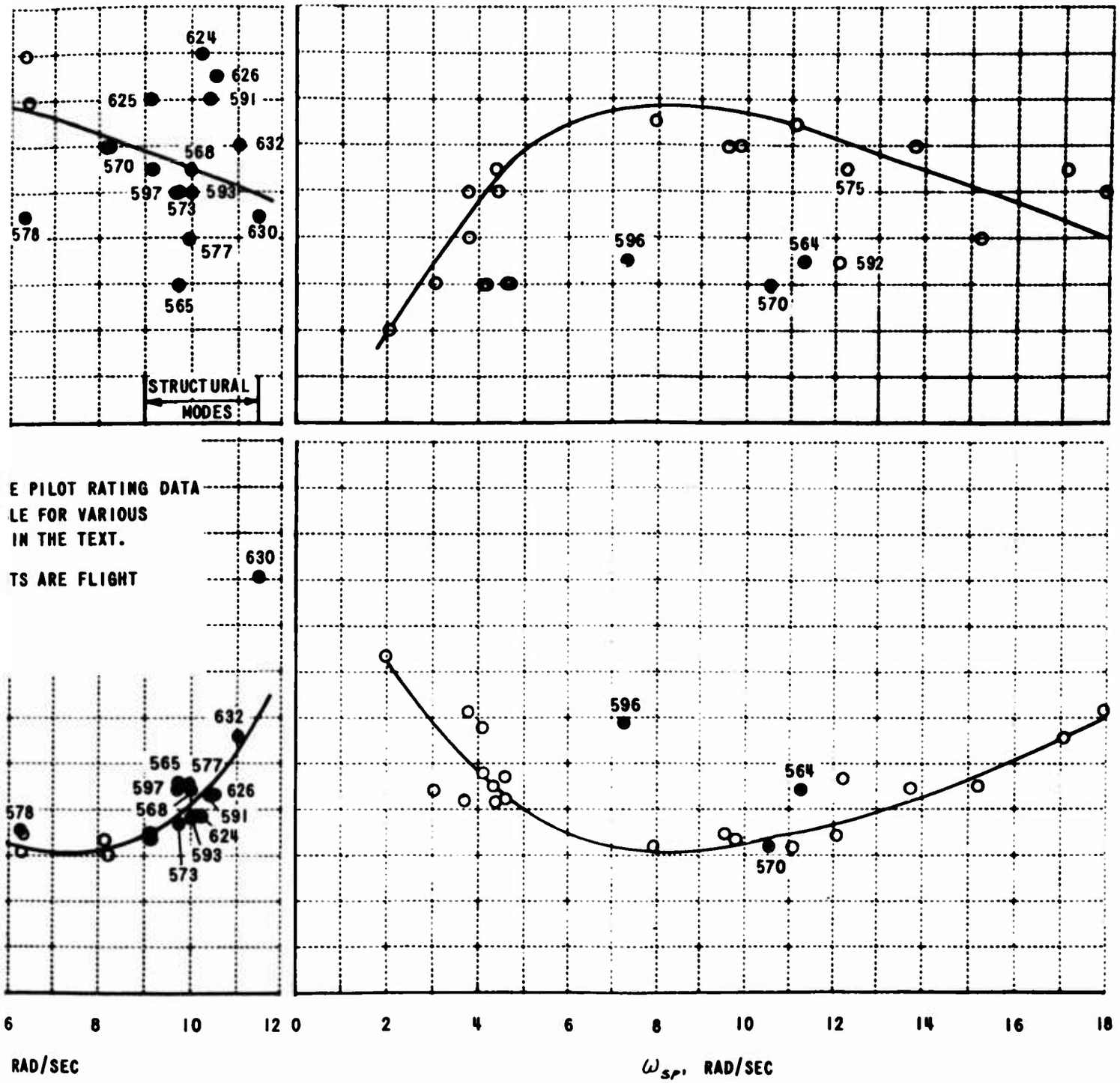

), n_z/α = 30.4 g/RAD

(c) V = 365 KTS (IAS), n_z/α = 63.4 g/RAD

Figure 10

VARIATION OF PILOT RATING AND PILOT SELECTED F_{ES}/n_z WITH SHORT PERIOD FREQUENCY AND n_z/α - CAL PILOT

B

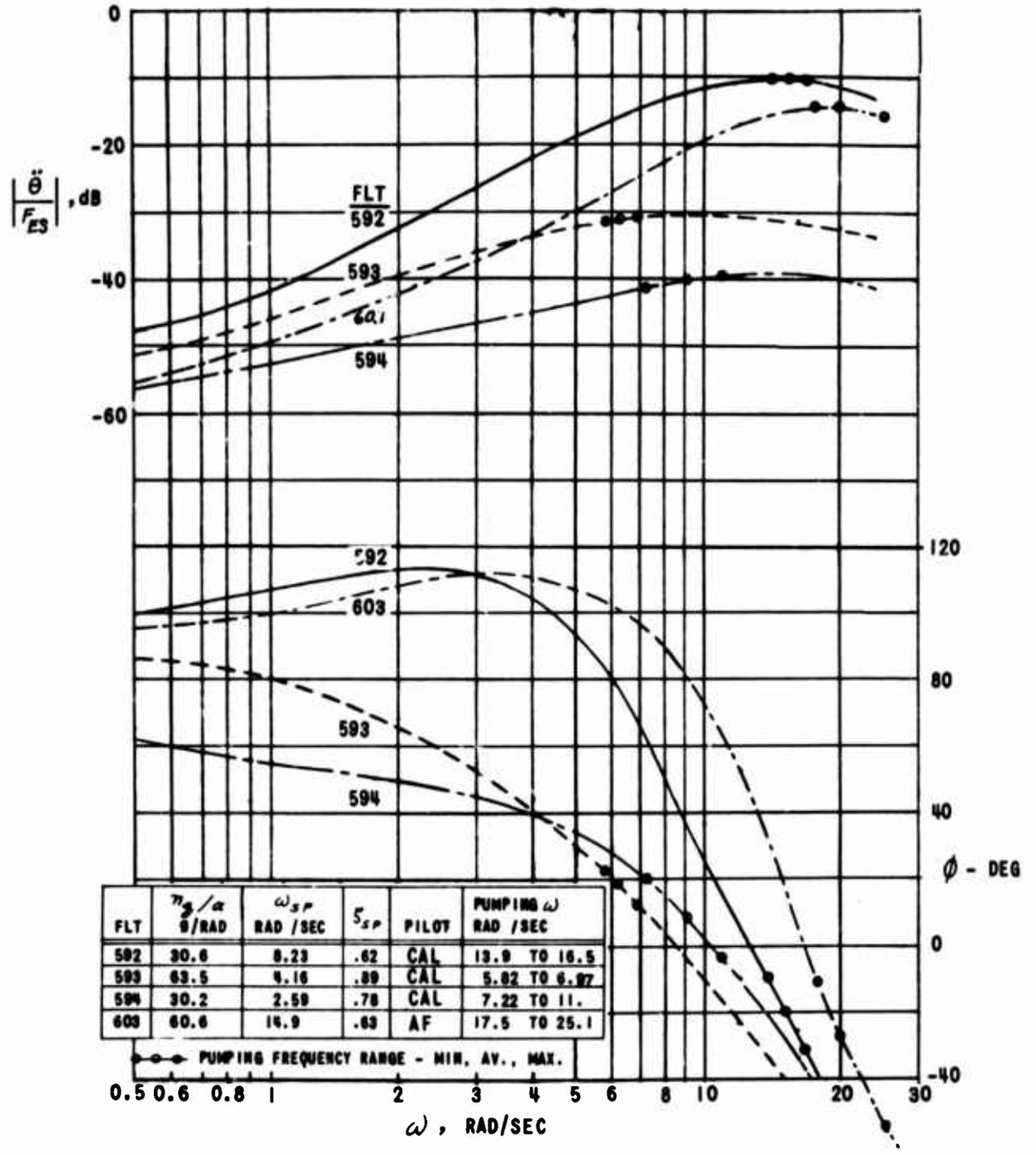

FLT	n_θ/α θ/RAD	ω_{SP} RAD/SEC	ζ_{SP}	PILOT	PUMPING ω RAD/SEC
592	30.6	8.23	.62	CAL	13.9 TO 16.5
593	63.5	4.16	.89	CAL	5.82 TO 6.97
594	30.2	2.59	.78	CAL	7.22 TO 11.
603	60.6	16.9	.63	AF	17.5 TO 25.1

Figure 11 COMPARISON OF $\frac{\ddot{\theta}(s)}{F_{ES}(s)}$ FREQUENCY RESPONSES AND PUMPING FREQUENCIES

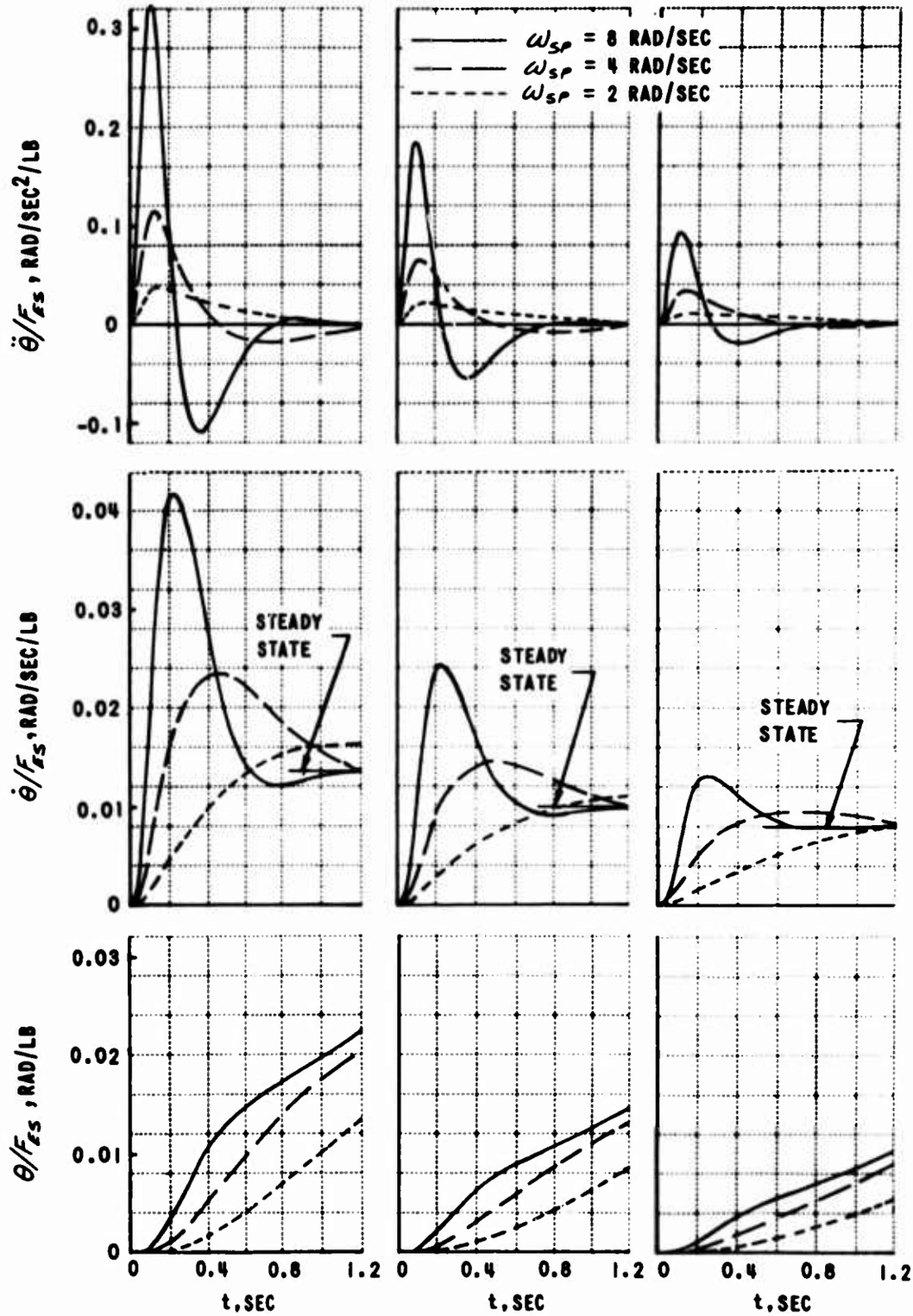

(a) n_z/α = 16.9 g/RAD (b) n_z/α = 30.4 g/RAD (c) n_z/α = 63.4 g/RAD

CONDITIONS:

F_{ES}/n_z = 6 lbs/g, ζ_{SP} = 0.70

ω_{FS} = 23 rad/sec, ζ_{FS} = 0.66

Figure 12 PITCH RESPONSE FOLLOWING A STEP STICK FORCE INPUT

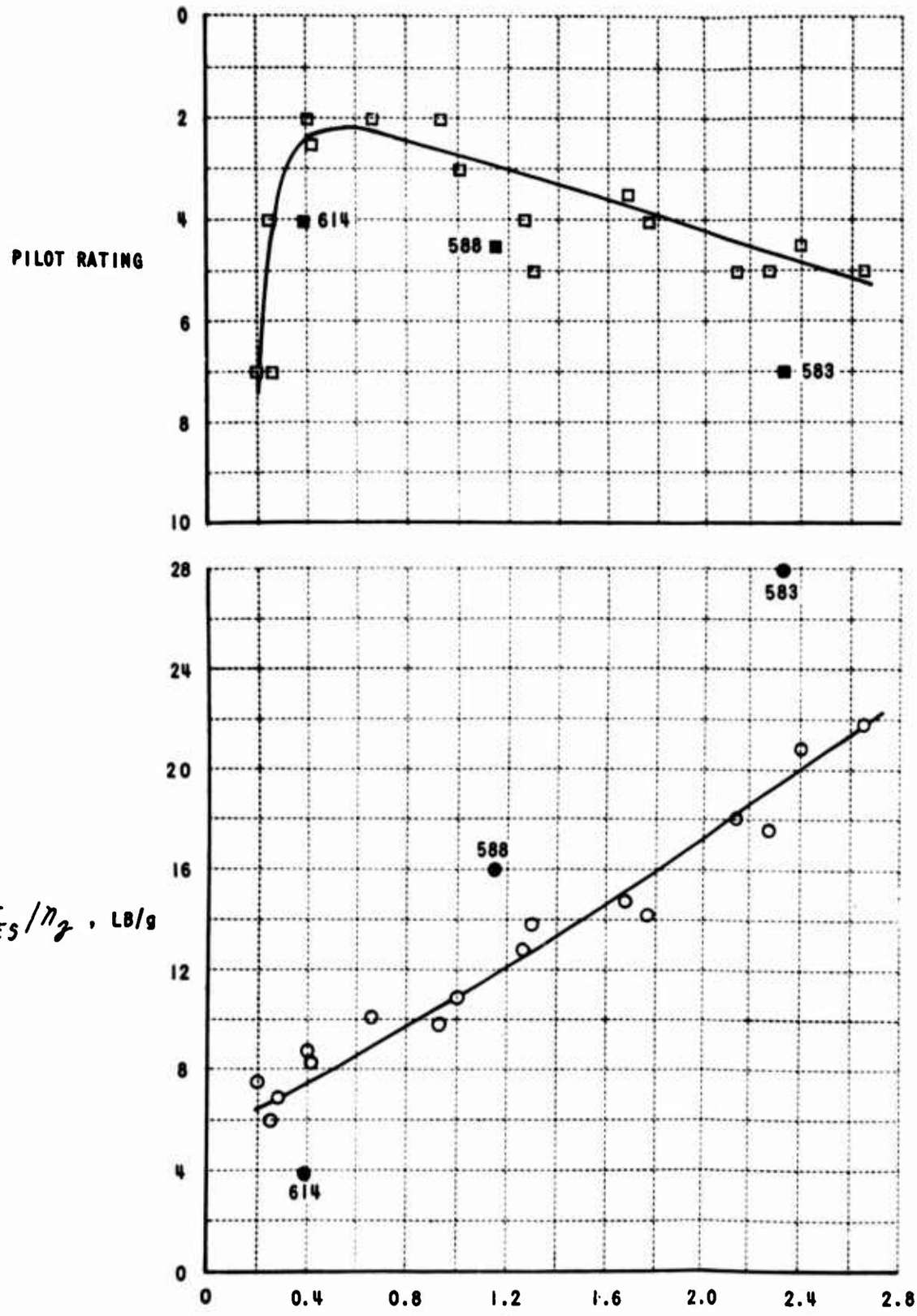

(a) V = 220 KTS(IAS), n_z/α = 16.9 g/RAD

(b) V

Figure 13
VARIATION OF PILOT RATING AND PILOT SELECTED F_{ES}/n_z WITH (CAP)' AND n_z/α - AF PILOT

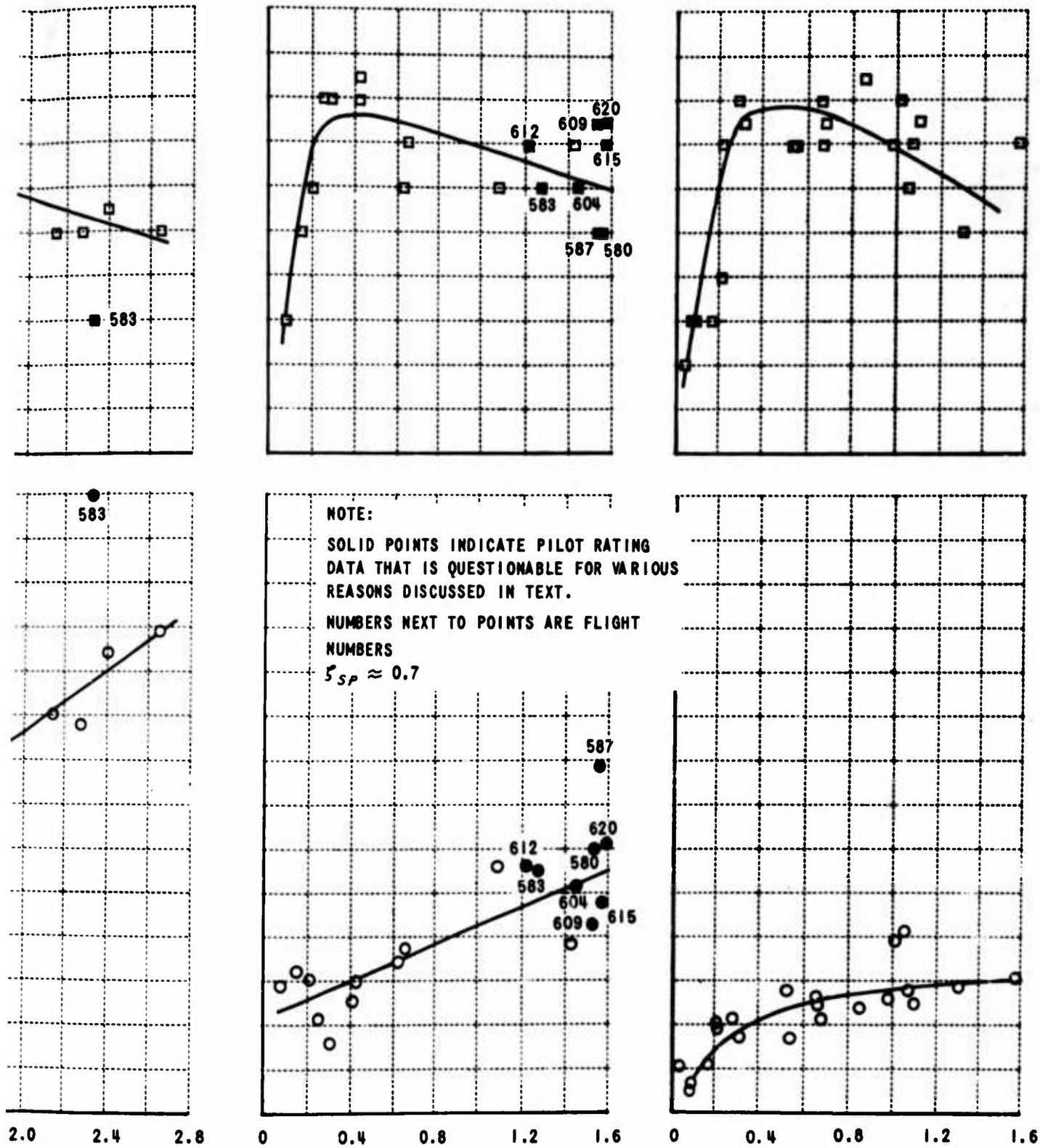

/SEC^2

9 g/RAD

$(CAP)' = \dfrac{\omega_{SP}^2 (\ddot{\theta}_{nd})_{MAX}}{n_z/\alpha}$, 1/SEC^2

(b) V = 300 KTS(IAS), n_z/α = 30.4 g/RAD

$(CAP)' = \dfrac{\omega_{SP}^2 (\ddot{\theta}_{nd})_{MAX}}{n_z/\alpha}$, 1/SEC^2

(c) V = 365 KTS(IAS), n_z/α = 63.4 g/RAD

B

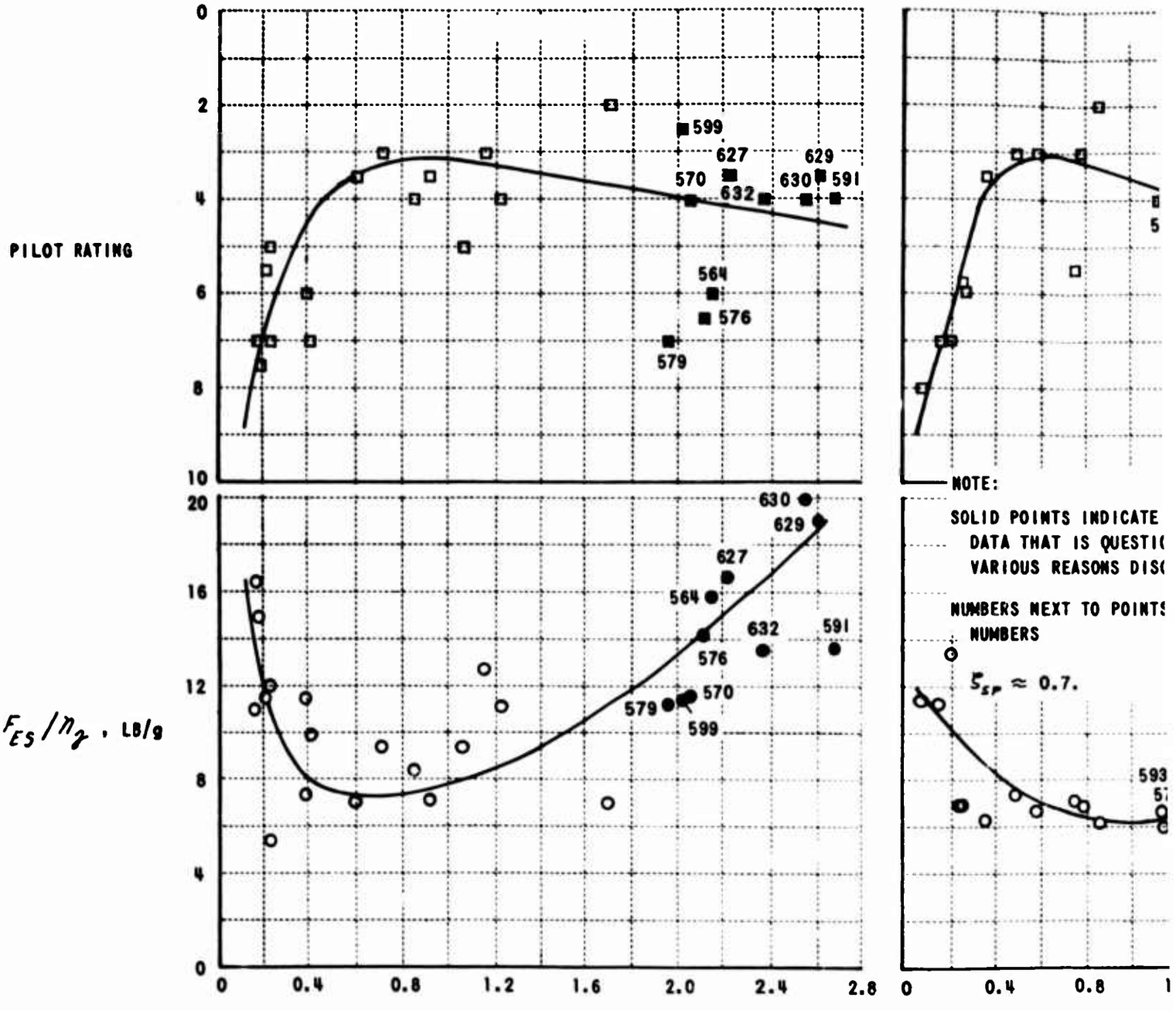

$$(CAP)' = \frac{\omega_{SP}^2 (\ddot{\theta}_{nd})_{MAX}}{n_z/\alpha}, \ 1/SEC^2$$

(a) V = 220 KTS(IAS), n_z/α = 16.9 g/RAD

$$(CAP)' = \frac{\omega_{SP}^2 (\ddot{\theta}_{nd}}{n_z/\alpha}$$

(b) V = 300 KTS(IAS),

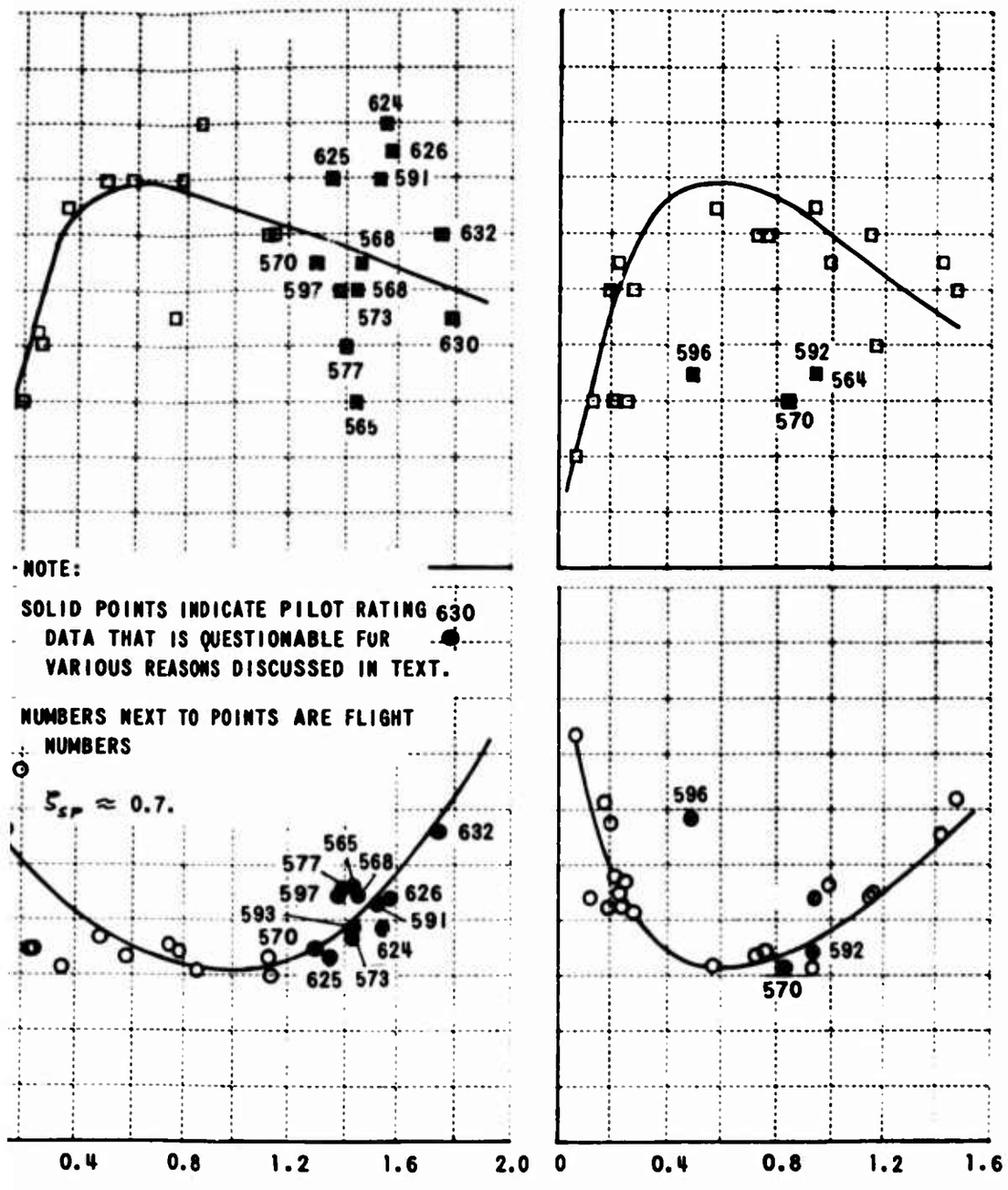

$$(CAP)' = \frac{\omega_{sp}^2 (\ddot{\theta}_{nd})_{MAX}}{n_z/\alpha}, \ 1/SEC^2$$

(b) V = 300 KTS(IAS), n_z/α = 30.4 g/RAD

$$(CAP)' = \frac{\omega_{sp} (\ddot{\theta}_{nd})_{MAX}}{n_z/\alpha}, \ 1/SEC^2$$

(c) V = 300 KTS(IAS), n_z/α = 63.4 g/RAD

Figure 14

VARIATION OF PILOT RATING AND PILOT SELECTED F_{ES}/n_z WITH (CAP)' AND n_z/α - CAL PILOT

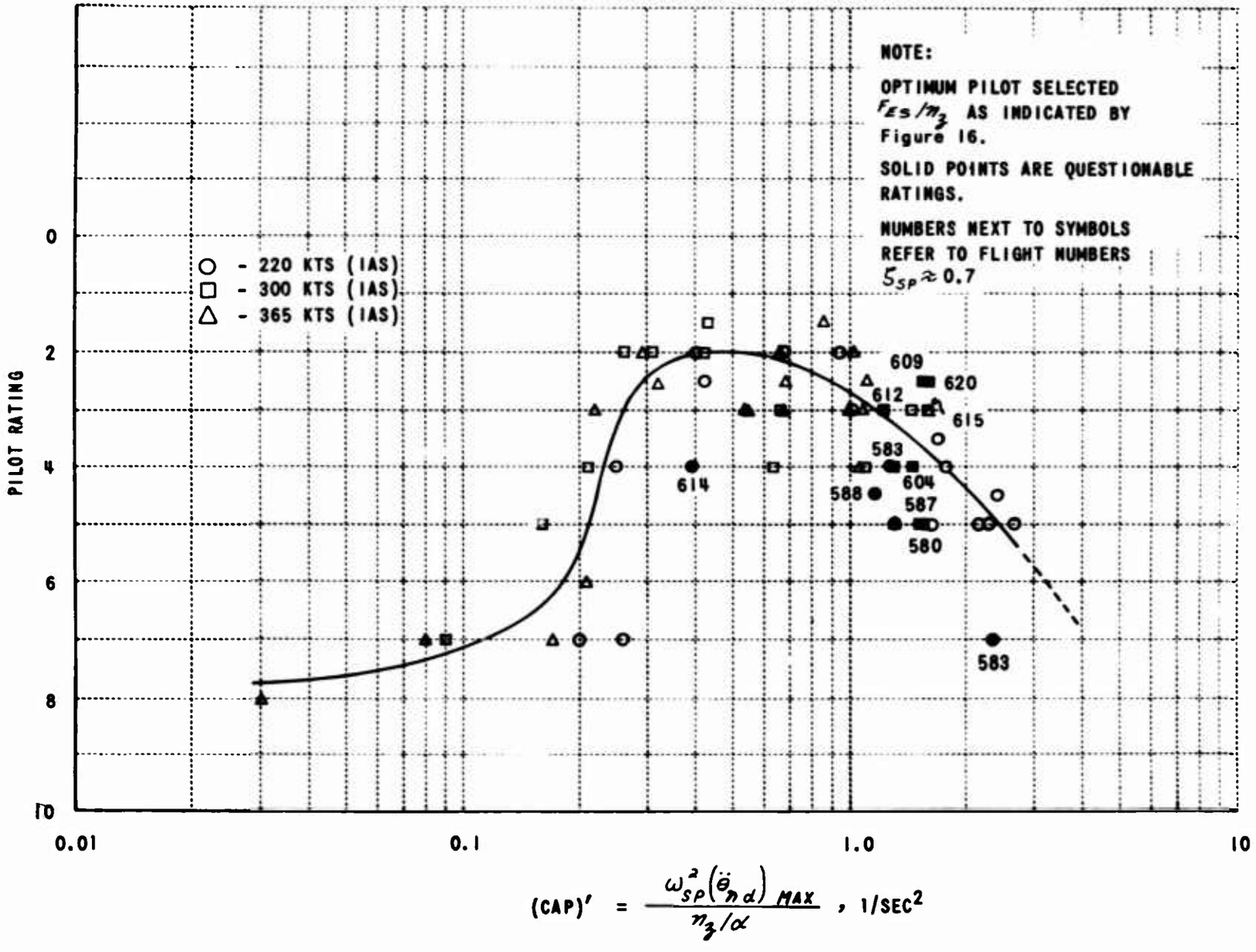

Figure 15 VARIATION OF PILOT RATING WITH (CAP)′ - AF PILOT

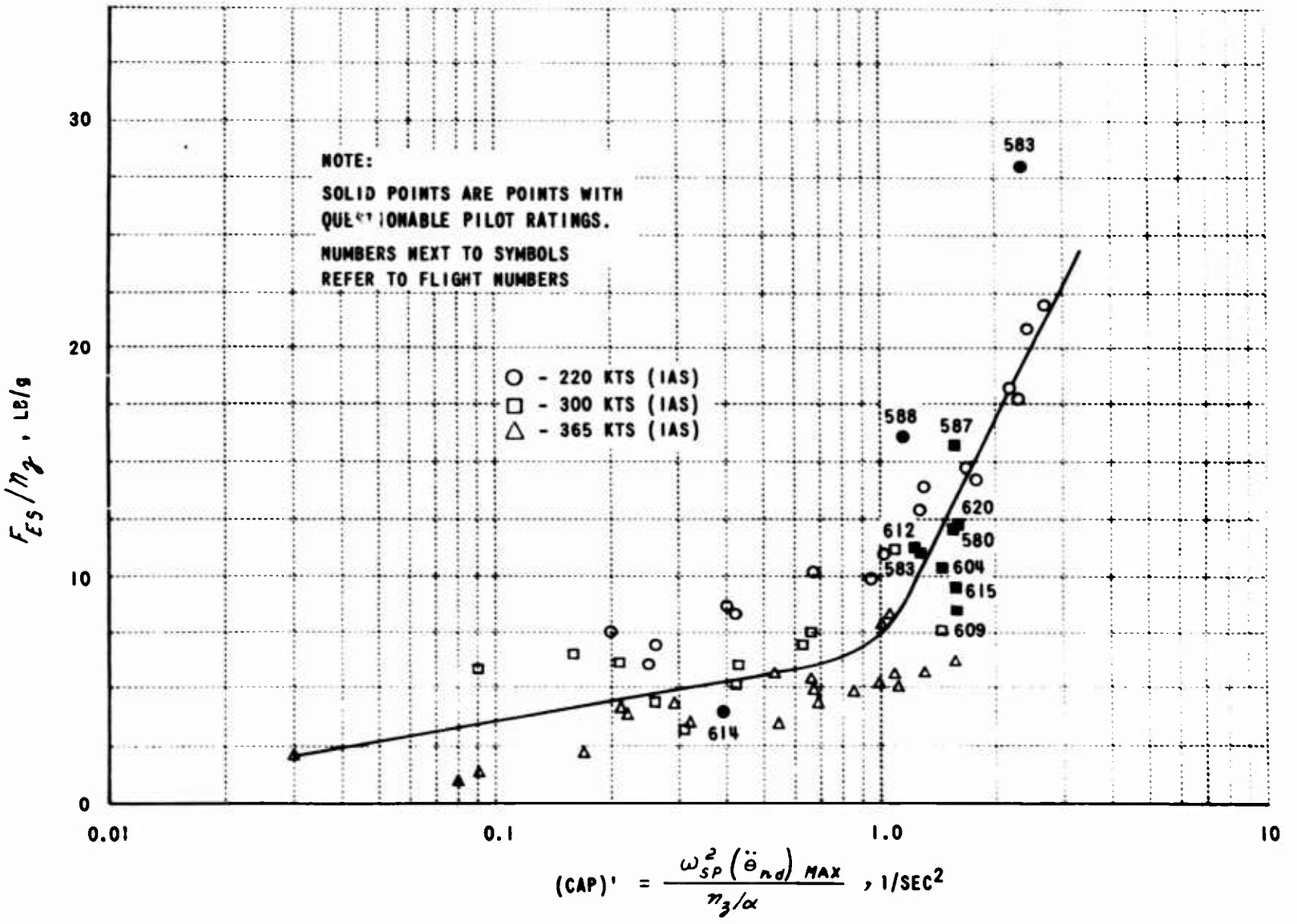

Figure 16 VARIATION OF OPTIMUM PILOT SELECTED F_{ES}/n_z WITH (CAP)' - AF PILOT

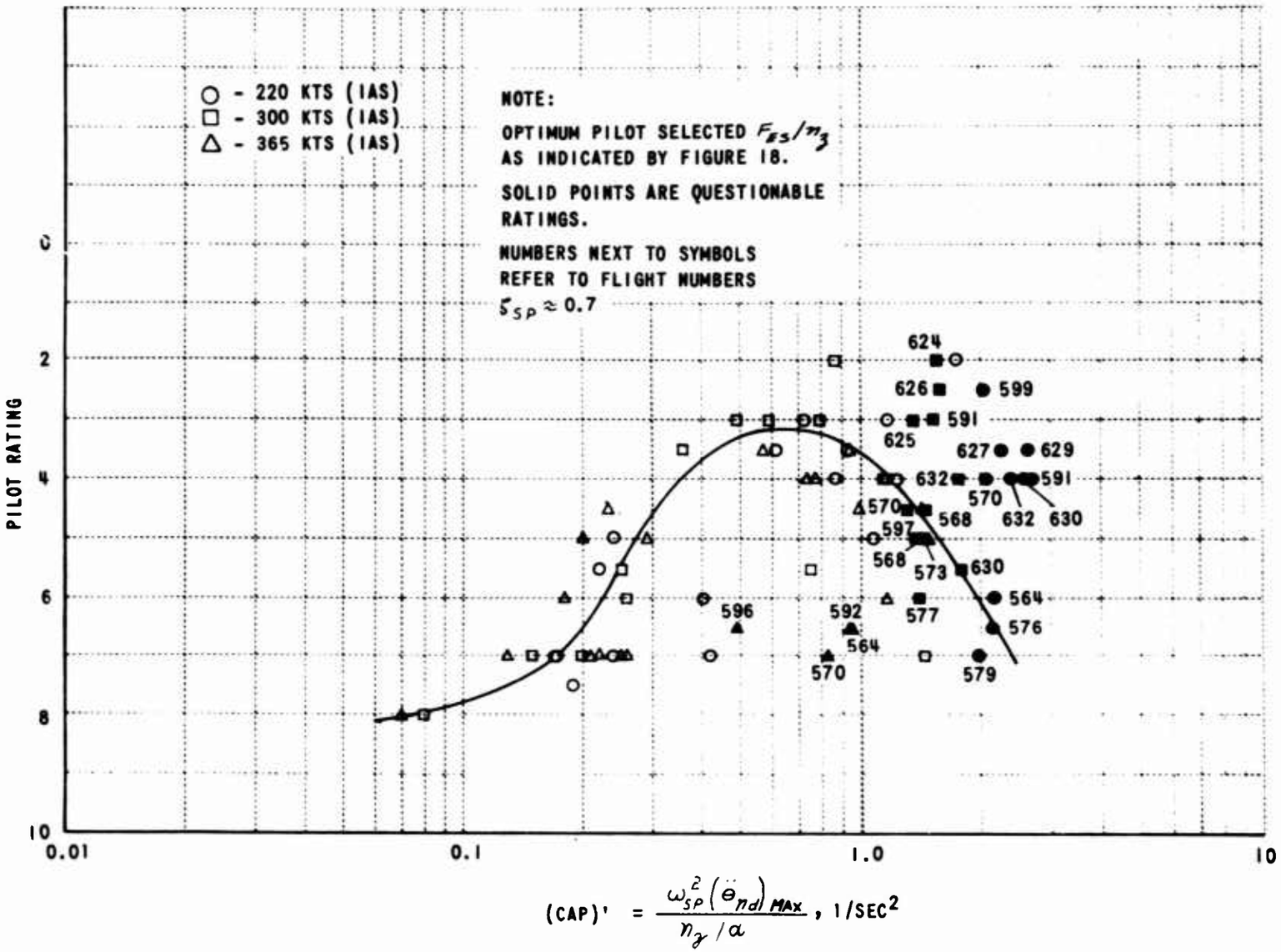

Figure 17 VARIATION OF PILOT RATING WITH (CAP)' - CAL PILOT

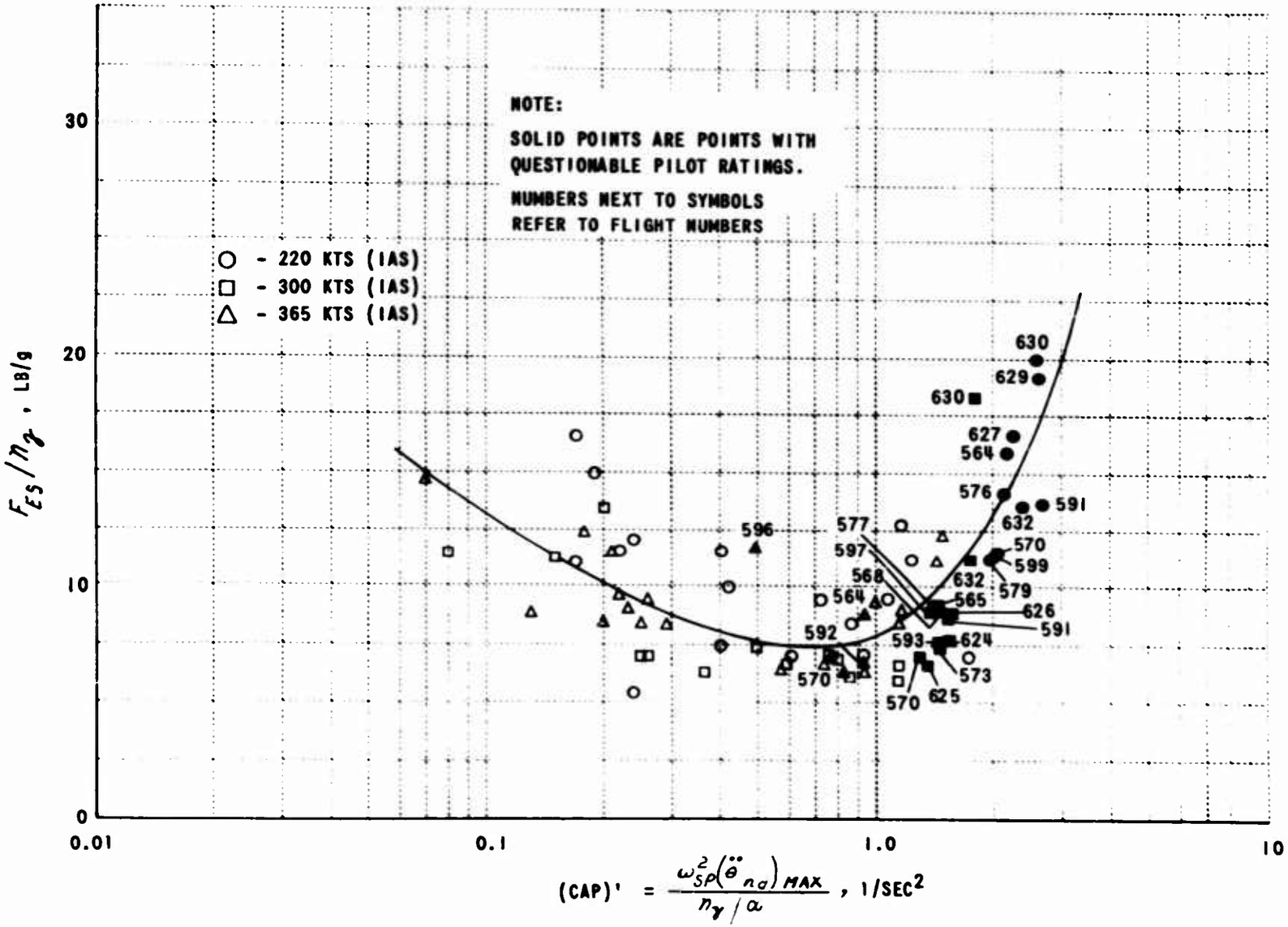

Figure 18 VARIATION OF OPTIMUM PILOT SELECTED F_{ES}/n_z WITH (CAP)' - CAL PILOT

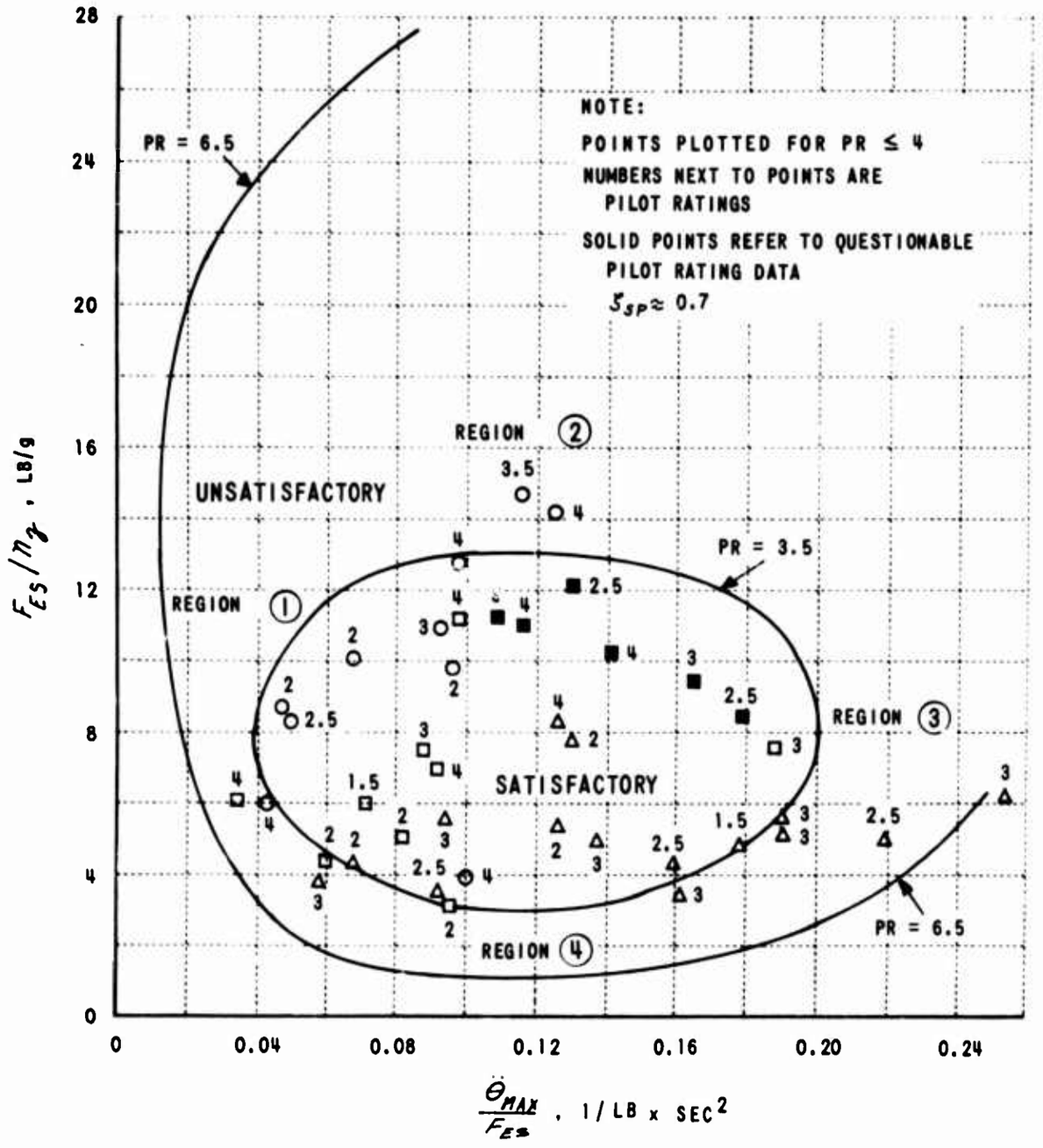

Figure 19 REGION OF SATISFACTORY PILOT RATINGS - AF PILOT

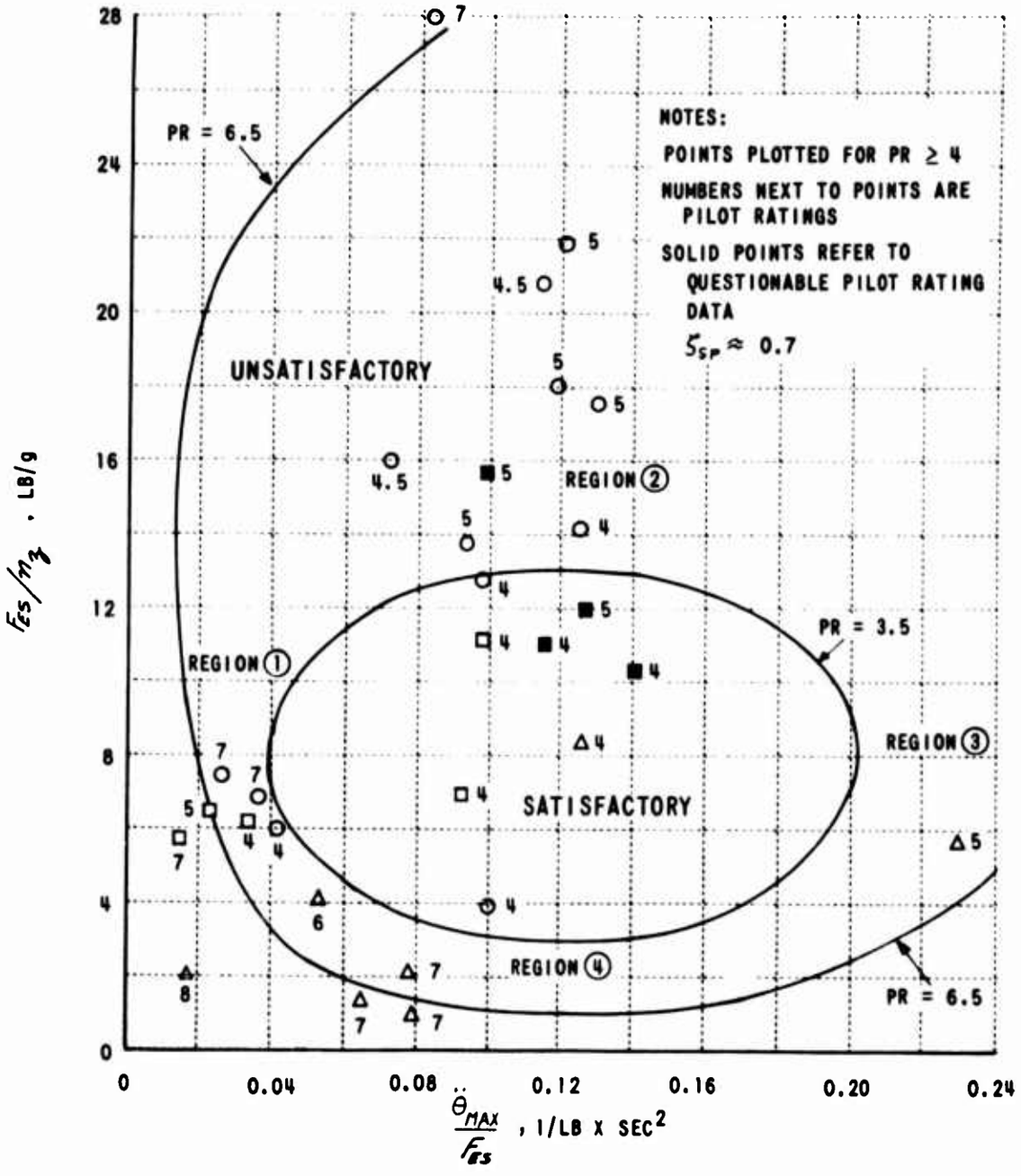

Figure 20 REGION OF UNSATISFACTORY PILOT RATINGS - AF PILOT

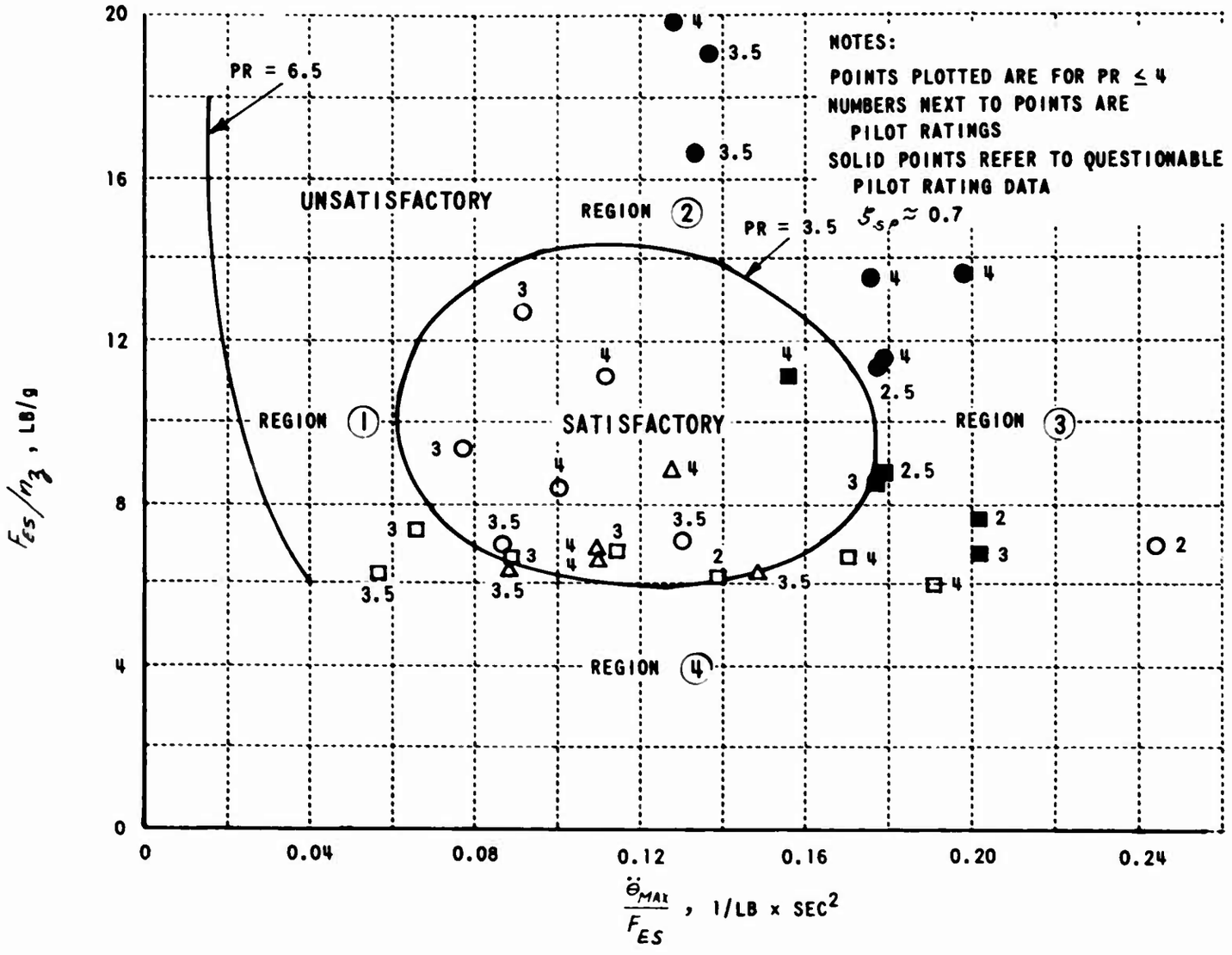

Figure 21 REGION OF SATISFACTORY PILOT RATINGS - CAL PILOT

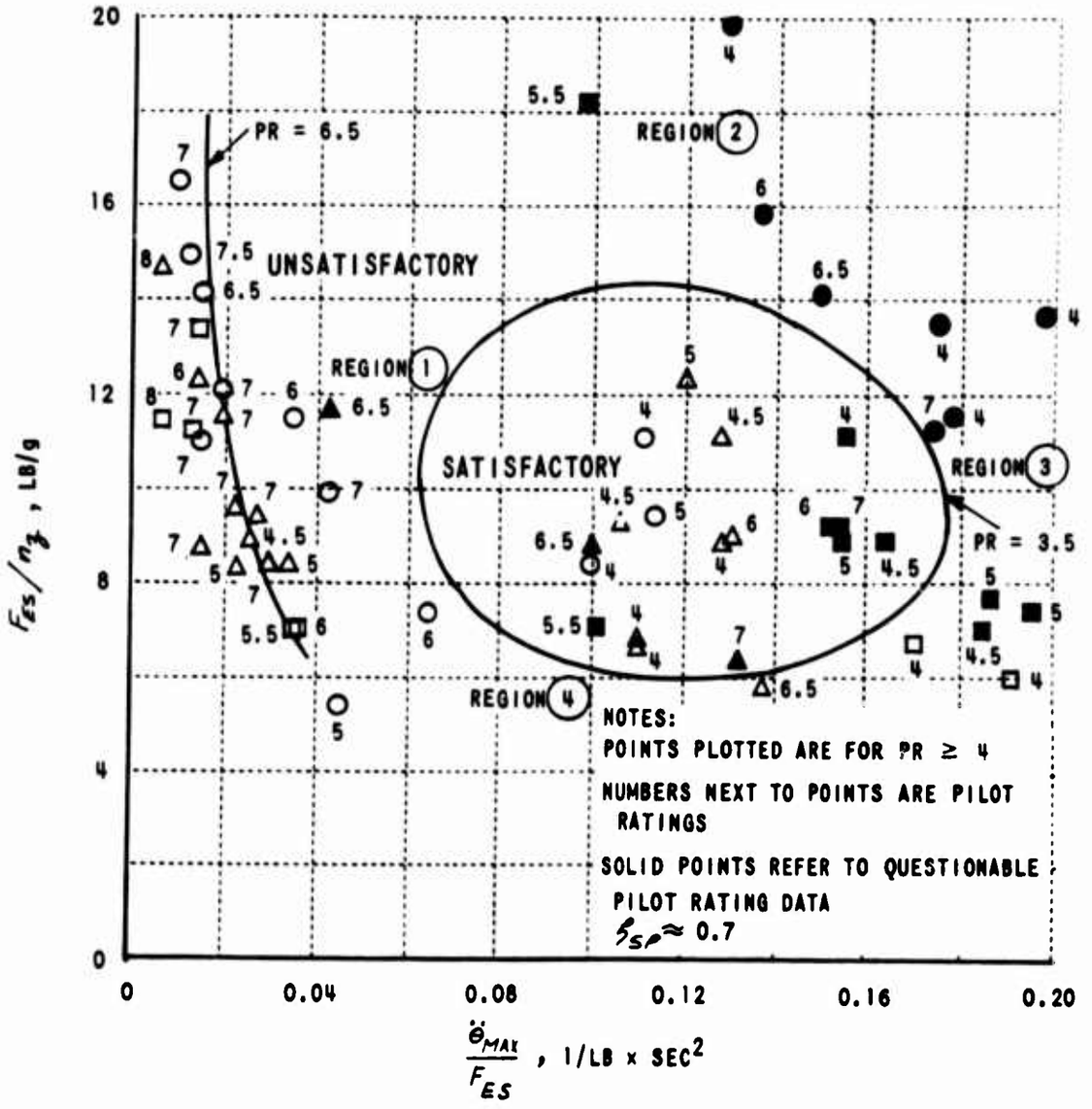

Figure 22 REGION OF UNSATISFACTORY PILOT RATINGS - CAL PILOT

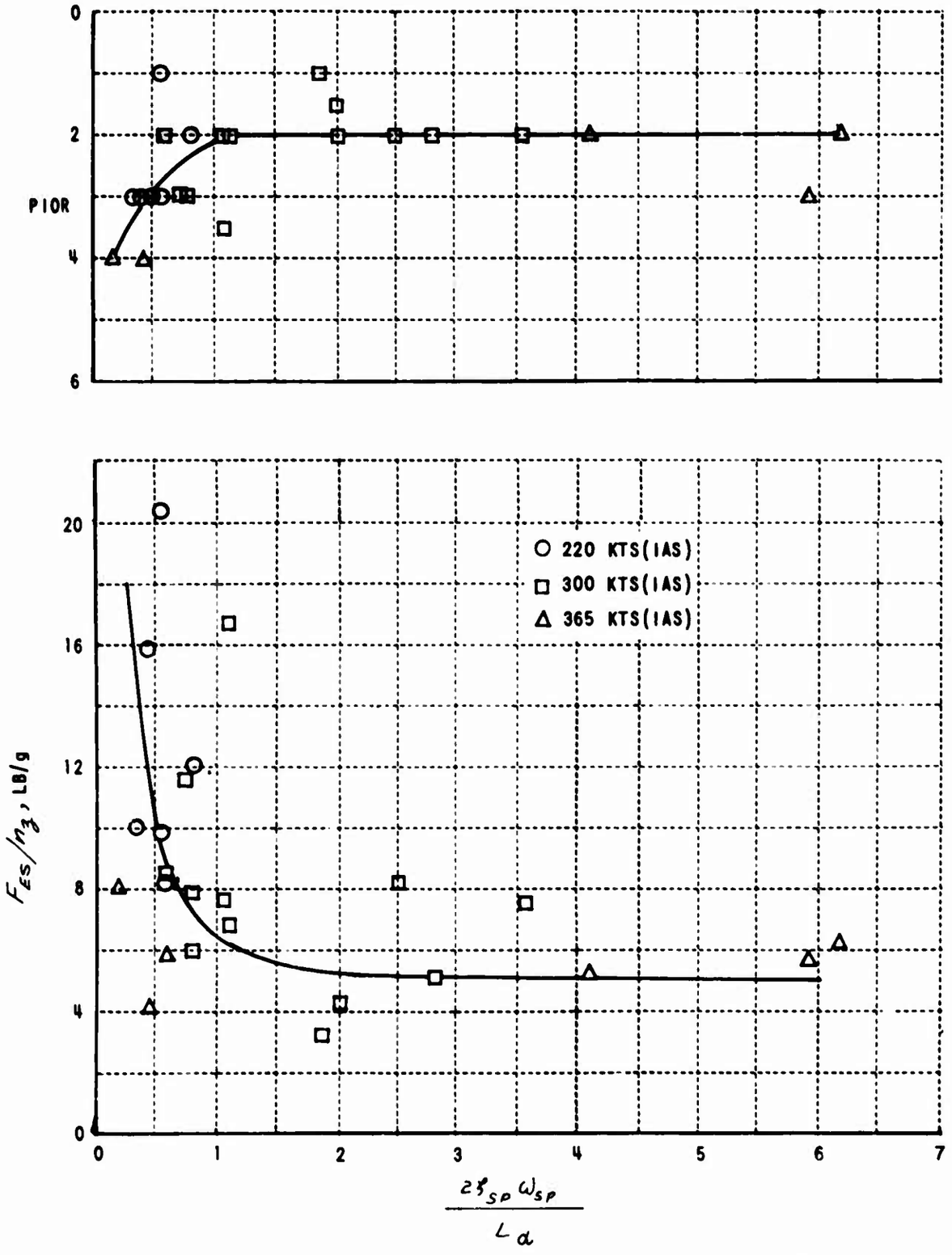

Figure 23 VARIATION OF PIOR AND F_{ES}/n_z WITH $2\zeta_{SP}\omega_{SP}/L_\alpha$ - AF PILOT

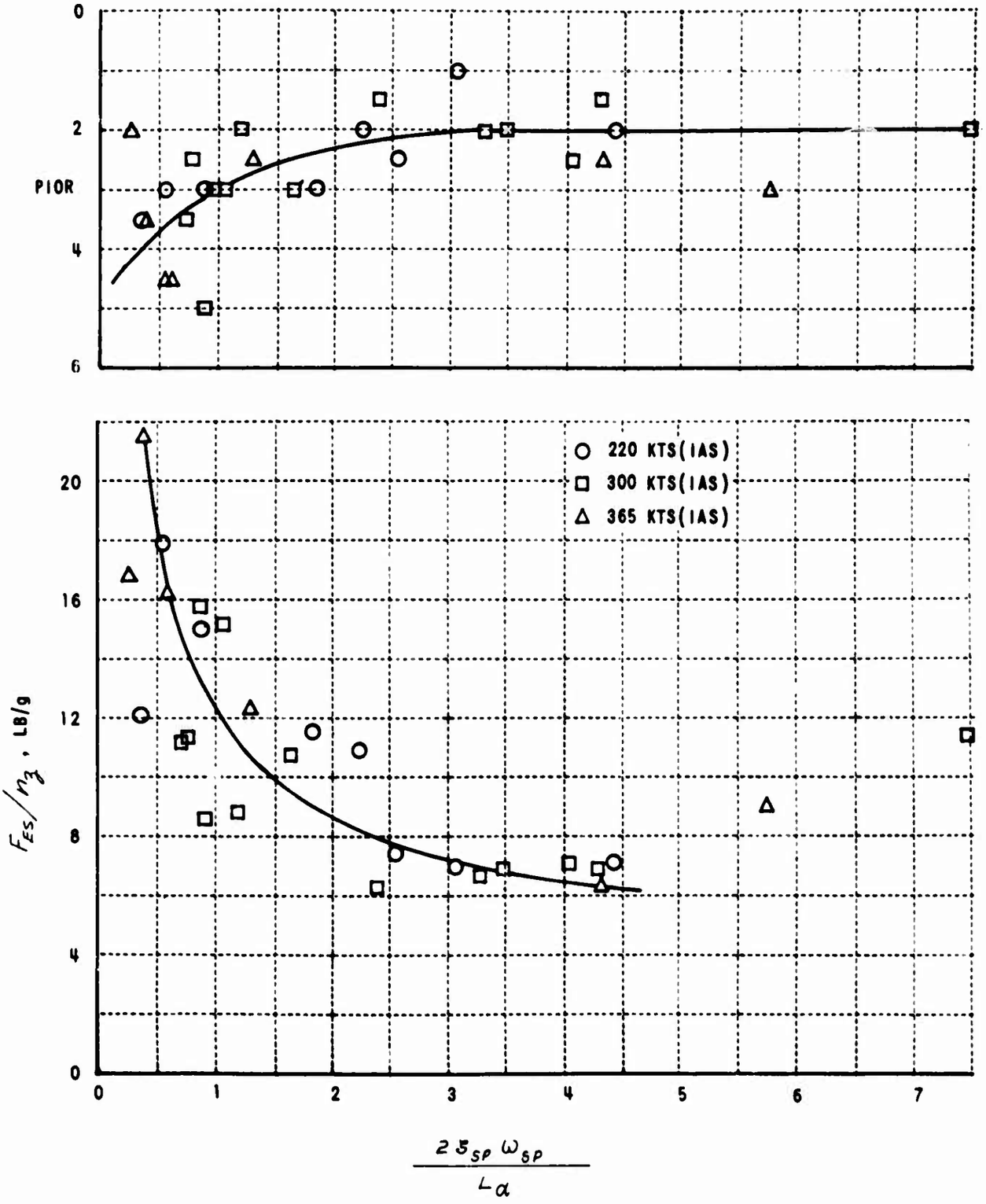

Figure 24 VARIATION OF PIOR AND F_{ES}/n_z WITH $2 S_{SP} \omega_{SP}/L_\alpha$ - CAL PILOT

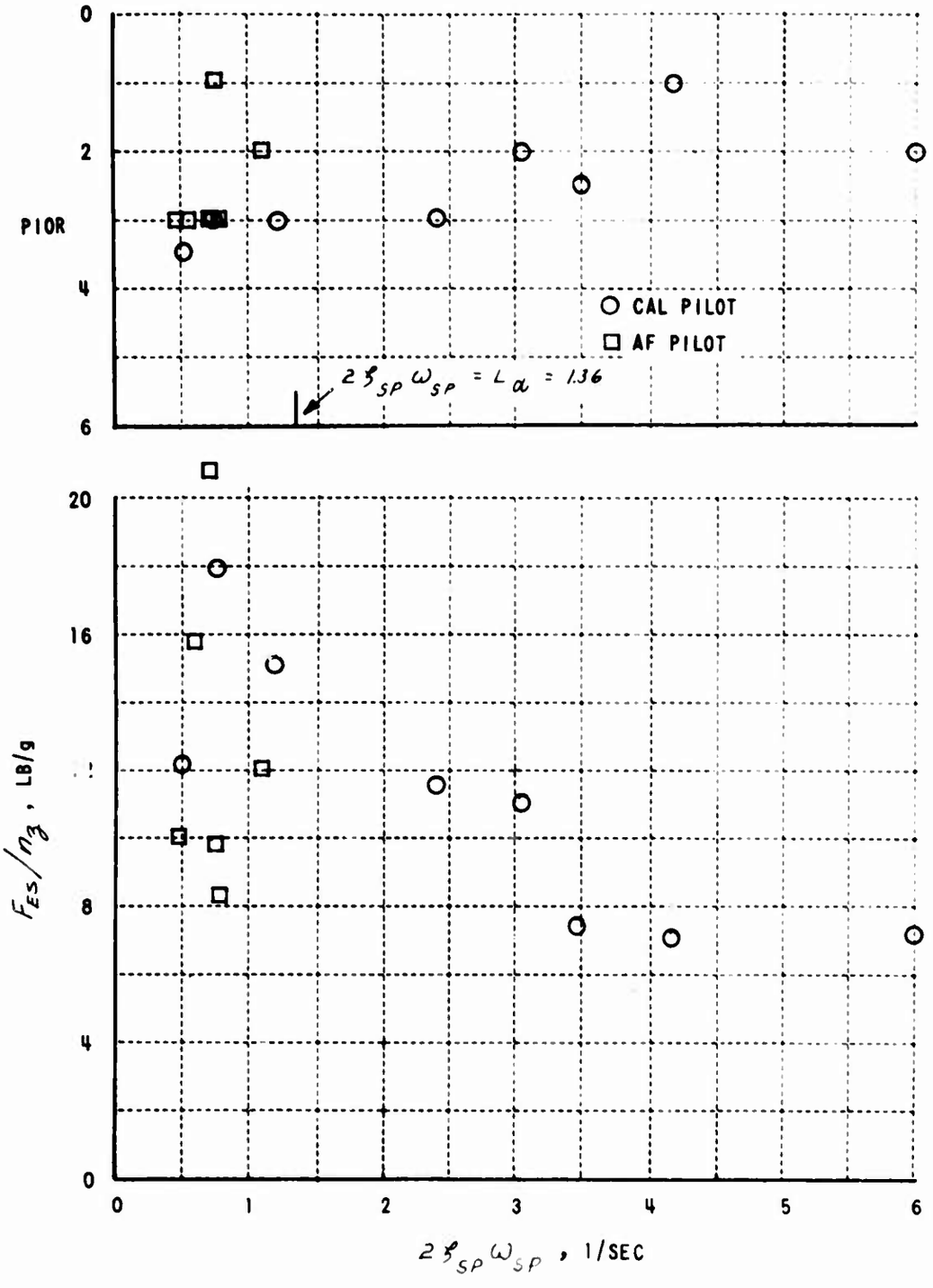

Figure 25 COMPARISON OF PIOR AND F_{ES}/n_z OF BOTH PILOTS
V = 220 KTS(IAS), n_z/α = 16.9 g/RAD

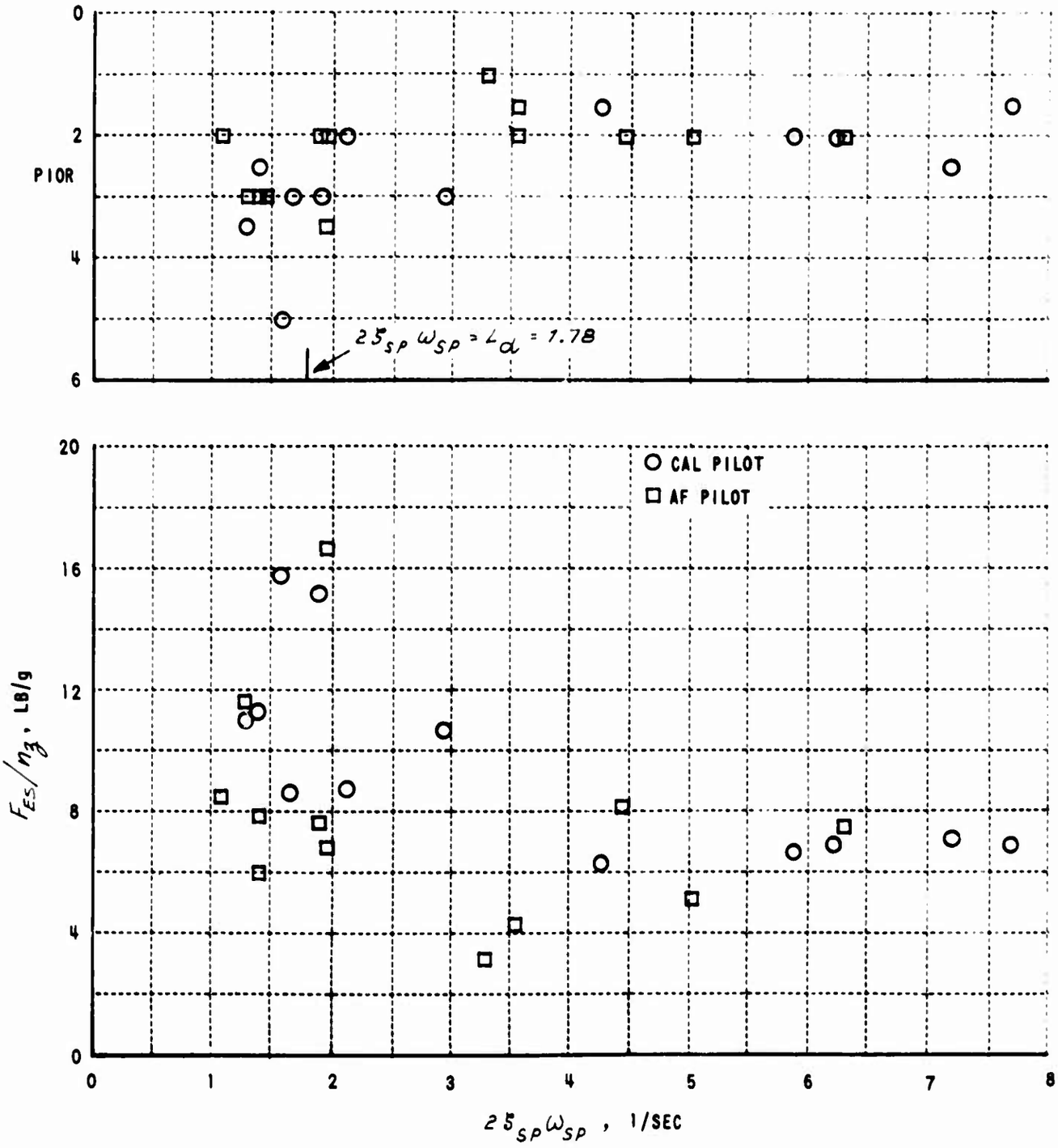

Figure 26 COMPARISON OF PIOR AND F_{ES}/n_z OF BOTH PILOTS

V = 300 KTS(IAS), n_z/α = 30.4 g/RAD

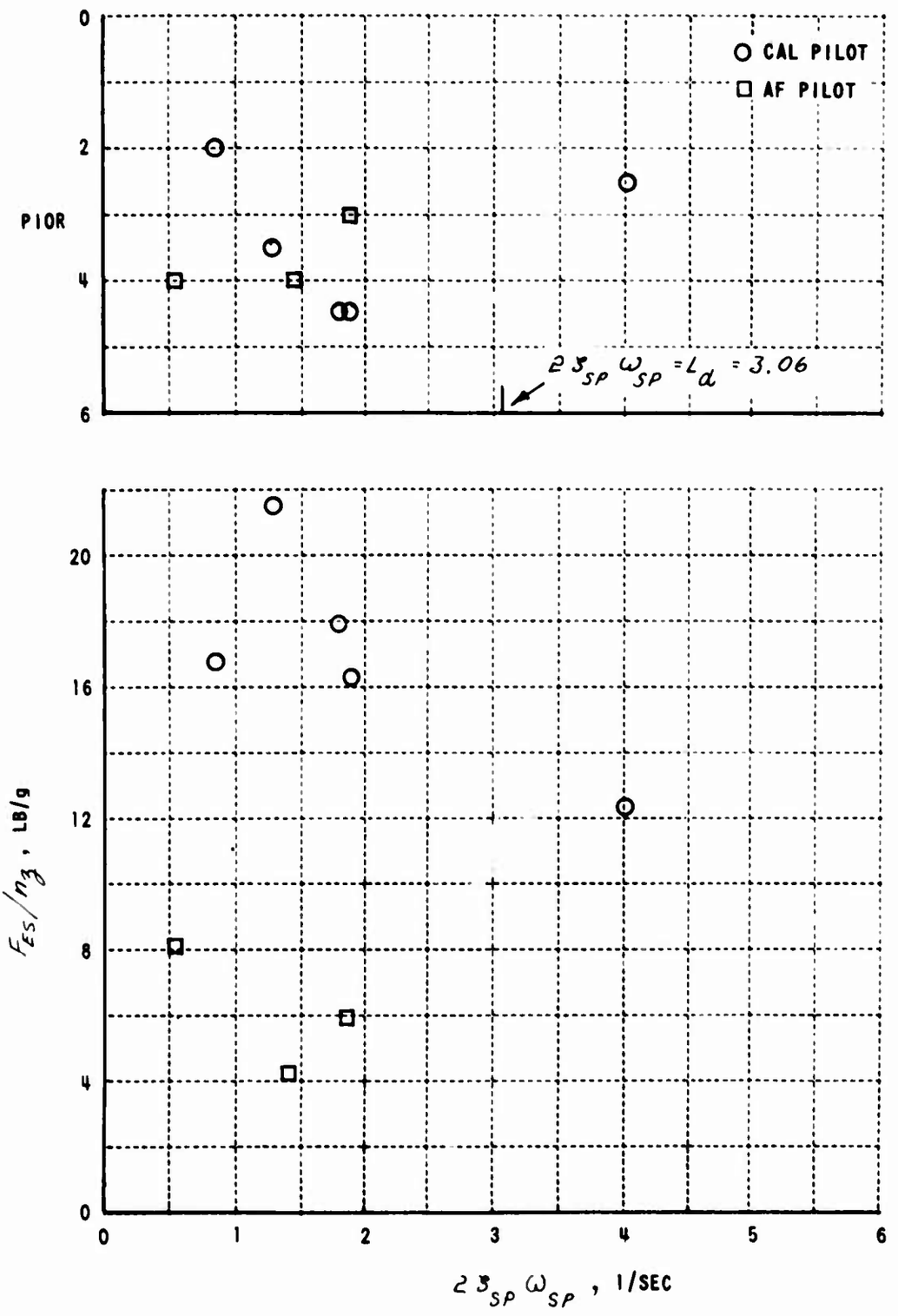

Figure 27 COMPARISON OF PIOR AND F_{ES}/n_z OF BOTH PILOTS

V = 365 KTS(IAS), n_z/α = 63.4 g/RAD

Table I

SHORT PERIOD FREQUENCY PARAMETERS SIMULATED

V (IAS) KTS	L_α			n_z/α			ζ_{sp}			ω_{sp}
	RANGE	AVERAGE	STANDARD DEVIATION	RANGE	AVERAGE	STANDARD DEVIATION	RANGE	AVERAGE	STANDARD DEVIATION	RANGE
220	1.18 TO 1.51	1.36	.068	14.7 TO 18.9	16.929	.85	.56 TO .9	.703	.0744	1.71 TO 10.59
300	1.66 TO 1.88	1.77	.0595	28.2 TO 32.0	30.142	1.012	.56 TO 1.08	.693	.103	1.59 TO 11.49
365	2.61 TO 3.32	2.97	.0152	54.0 TO 68.6	61.438	3.149	.57 TO 1.313	.728	.127	1.36 TO 17.9

Table II

PIO CONFIGURATIONS SIMULATED

V (IAS) KTS	n_z/α			ω_{sp}	ζ_{sp}	$2\zeta_{sp}\omega_{sp}$	$\frac{2\zeta_{sp}\omega_{sp}}{L_\alpha}$
	RANGE	AVERAGE	STANDARD DEVIATION	RANGE	RANGE	RANGE	RANGE
220	16.0 TO 18.9	17.307	.963	1.99 TO 6.95	.05 TO .60	.484 TO 4.176	.356 TO 3.07
300	26.8 TO 32.5	30.27	1.36	2.94 TO 11.02	.09 TO .60	1.089 TO 7.16	.612 TO 4.28
365	53.6 TO 68.8	62.091	5.07	1.8 TO 16.0	.05 TO .60	.547 TO 18.88	.178 TO 6.15

Table III

ELEVATOR FEEL SYSTEM CHARACTERISTICS

FLT NO.	V (IAS) KTS	$(F_{ES}/\delta_{ES})_{ss}$ LB/IN.	ω_{FS} RAD/SEC	ζ_{FS}
564	220	29.1	23.0*	.50*
564	300	27.9	22.5*	.50*
564	365	29.1	23.0*	.50*
576	220	23.0	20.9	.61
579	220	—	20.9	.61
581	220	30.2	23.2*	.66*
591	220	23.3	20.9	.61
599	220	23.5	20.9	.61
602	220	29.3	20.9	.61
609	300	31.4	23.5*	.66*
619	220	23.0	20.9*	.61*
619	300	23.6	20.9*	.61*
619	365	22.4	20.8*	.61*
623	220	23.7	20.9	.61
624	220	18.1	19.8	.64
626	220	30.6		

*FEEL SYSTEM ω_{FS} AND ζ_{FS} ESTIMATED BASED ON DIFFERENCES IN FEEL SYSTEM GAINS

ON ALL OTHER FLIGHTS AND SPEEDS:

ω_{FS} = 23 RAD/SEC

ζ_{FS} = 0.66

AVERAGE $(F_{ES}/\delta_{ES})_{ss}$ = 29.1 LB/IN.

Table IV

RMS PITCH ANGLE TRACKING COMMAND (θ_c)

AND ERROR (θ_ϵ) FOR VARIOUS FLIGHT CONDITIONS

FLT NO.	V (IAS) KTS	h_p FT	ω_{sp} RAD/SEC	ζ_{sp}	F_{es}/n_z	θ_c DEG RMS	θ_ϵ DEG RMS	PILOT
568	220	5500	3.60	.58	7.0	1.63	.84	CAL
577	365	5500	4.64	.73	9.4	1.66	1.05	CAL
583	300	5500	9.17	.65	11.0	1.36	.64	AF
587	220	5500	8.68	.62	18.1	1.82	1.17	AF
607	365	5500	5.11	.61	5.0	1.31	.97	AF
622	300	5500	4.40	.19	8.6	1.50	1.23	CAL

Table V

LONGITUDINAL PHUGOID CHARACTERISTICS SIMULATED

FLIGHT CONDITION		ω_p RAD/SEC	ζ_p	PERIOD SEC
V(IAS) KTS	h_p FEET			
220	5500	.111	.03	56.7
300	5500	.093	.11	67.6
365	5500	.090	.02	69.9

Table VI

CONSTANT LATERAL-DIRECTIONAL CHARACTERISTICS

FLIGHT CONDITION		ω_d RAD/SEC	ζ_d	τ_R SEC	δ_{AT}/δ_{AS} DEG/IN.	δ_R/δ_{RP} DEG/IN.	F_{AS}/δ_{AS} LB/IN.	F_{RP}/δ_{RP} LB/IN.
V(IAS) KTS	h_p FT							
220	5500	1.49	.11	.40	-3.13	-8.2	3.0	82.0
300	5500	1.83	.09	.51	-3.13	-8.2	3.0	82.0
365	5500	2.43	.17	.22	-3.13	-4.2	3.0	82.0

Table VII

PARAMETERS SIMULATED

LONGITUDINAL SHORT PERIOD AND PIO CONFIGURATIONS

V = 220 KTS(IAS)

FLT NO.	ω_{sp} RAD/SEC			$\zeta_{sp}\omega_{sp}$ RAD/SEC			ζ_{sp}			α/δ_{e_s} DEG/IN.			F_{es}/m_3 LB/Q			m_3/α Q/RAD			F_{es}/δ_{es} LB/IN.	PR	PIOR	PILOT
	MEAS.	COMP. LSF	BEST EST. VALUE	MEAS.	COMP. LSF	BEST EST. VALUE	MEAS.	COMP. LSF	BEST EST. VALUE	MEAS.	COMP. LSF	BEST EST. VALUE	MEAS.	COMP. LSF	BEST EST. VALUE	MEAS.	COMP. LSF	BEST EST. VALUE				
564	-	7.34	8.34**	-	9.98	9.98	-	.68	.68	6.57*	6.23	6.57	15.80*	16.22	15.80	16.1*	17.3	16.1	29.2	6	-	CAL
565	1.71	1.45	1.71	2.46	2.17	2.46	.72	.75	.72	8.00*	9.87	8.41**	10.98*	9.87	10.98	16.7*	17.0	16.7	27.2	7	-	
566	2.03	1.92	2.03	3.21	2.95	3.21	.79	.77	.79	17.33	19.72	17.33	6.50	5.20	5.38**	15.4	16.7	15.4	27.5	5	3	
568	3.60	3.52	3.60	4.18	4.10	4.18	.58	.58	.58	14.70	14.70	14.70	7.00	6.90	7.00	16.1	17.2	16.1	28.8	3.5	1	
570	6.60*	7.34	8.39**	8.84*	9.99	11.22**	.67*	.68	.67	8.49	8.59	8.49	11.50	11.77	11.50	17.1*	17.3	17.1	28.6	4	2	
571	5.00	5.23	5.00	6.00	6.74	6.00	.60	.65	.60	13.50	13.00	13.50	6.80	7.83	7.11**	17.7	17.8	17.7	28.3	3.5	2	
572	1.62	1.81	1.73**	2.69	2.95	2.87**	.83	.82	.83	6.24	6.18	6.24	16.50	16.60	16.60	16.5	17.1	16.5	30.2	7	1.5	
573	6.25	6.43	6.25	8.00	8.57	8.00	.64	.67	.64	8.90	9.02	8.90	10.25	11.21	11.05**	18.8	17.9	18.8	29.0	4	1.5	
574	2.22	2.37	2.22	3.20	3.41	3.20	.72	.72	.72	8.96*	7.40	8.96	11.45*	13.72	12.00**	18.0	17.3	18.0	31.7	7	2.5	
575	.94	-	-	.51		—	.27		—		10.35	—	—	10.78	—	—	16.88	—	—	9	3	
576	8.84	9.11	8.84	13.79	14.19	13.79	.78	.78	.78	5.28	5.53	5.28	14.05	13.97	14.05	17.6	17.6	17.6	23.0	6.5	3	
577	3.04	2.58	3.04	4.26	3.84	4.26	.70	.75	.70	10.23*	10.20	10.23	9.93*	9.91	9.93	17.9	17.6	17.9	30.4	7	2	
579	—	8.29	—	—	12.03	—	—	.73	-	—	7.01	—	—	11.22	—	—	17.44	—	—	7	2.5	
581	6.13	6.36	6.13	8.34	8.50	8.34	.68	.67	.68	7.04	7.29	7.04	13.82	13.79	13.82	17.4	17.6	17.4	30.2	5	2	AF
582	2.30	2.52	2.30	3.17	3.06	3.17	.69	.61	.69	14.60*	15.05	14.60	6.85*	6.79	6.85	17.7*	16.9	17.7	30.9	7	3	
583	9.44	8.95	9.44	14.92	13.55	14.92	.79	.76	.79	3.60	3.66	3.64	28.00	27.96	28.00	17.6	17.6	17.6	30.6	7	3	
584	3.82	4.07	3.82	5.20	5.44	5.20	.68	.67	.68	10.70	10.12	10.70	10.10	10.00	10.10	16.2	16.6	16.6	30.1	2	1	
585	2.19	1.90	2.19	3.68	2.93	3.68	.84	.77	.84	15.33*	18.45	16.36**	6.01*	5.56	6.01	16.8	17.1	16.8	29.0	4	1	
586	6.09	6.36	6.09	7.67	8.28	7.67	.63	.65	.63	8.29	8.06	8.29	12.75	12.55	12.75	17.6	17.5	17.6	30.2	4	2	
587	8.68	8.03	8.68	10.76	10.23	10.76	.62	.64	.62	6.05	5.78	6.05	18.10	17.51	18.10	17.1	16.7	17.1	30.5	5	2	
588	5.48	5.30	5.48	7.45	6.80	7.45	.68	.64	.68	6.32*	6.40	6.32	16.80*	15.80	15.95*	16.6	17.0	16.6	29.7	4.5	2	
591	10.02*	9.25	10.02	15.30*	13.01	15.30	.76*	.70	.76	5.46	5.67	5.46	13.50	13.68	13.50	18.5*	18.1	18.5	23.3	4	1.5	CAL
592	2.96	2.56	2.96	3.49	3.97	3.49	.59	.78	.59	14.00	14.10	14.00	7.35	7.18	7.35	17.6	17.5	17.6	32.1	6	2.5	
595	5.52	5.80	5.52	6.62	7.45	6.62	.60	.64	.60	10.39	10.70	10.39	9.44	9.44	9.44	17.9	17.4	17.9	30.8	5	2.5	
596	1.94	2.03	1.94	2.95	2.84	2.95	.76	.70	.76	6.50	6.92	6.50	14.90	14.84	14.90	18.5	17.9	18.5	29.8	7.5	2	
597	4.97	4.69	4.97	6.06	5.69	6.06	.61	.61	.61	11.30	12.05	12.60*	8.35	8.40	8.35	18.9	18.8	18.9	31.0	4	2	
598	5.54*	6.72	6.95**	2.44*	4.55	3.06**	.22*	.34	.22	6.49	9.21	9.61**	10.90	11.07	10.90	18.9	17.8	18.9	30.9	7	2	
599	8.36	8.24	8.36	12.21	11.23	12.21	.73	.68	.73	6.90	6.93	6.90	11.37	11.17	11.37	17.2	17.4	17.2	23.5	2.5	1	
600	5.83*	5.41	5.83	7.02*	6.82	7.02	.70*	.63	.70	7.55	7.84	7.55	12.65	12.88	12.65	18.1*	17.8	18.1	29.8	3	1.5	
601	2.16	2.29	2.16	2.4	2.79	2.42	.56	.61	.56	9.20*	10.79	9.79*	10.83*	11.51	11.53**	18.5	17.6	18.5	31.3	5.5	3	
602	8.85*	8.05	8.85	13.28	11.23	13.28	.75*	.70	.75	5.90	5.88	5.90	17.55	17.18	17.55	16.3*	16.6	16.3	29.3	5	2	AF

*VALUE NOT USED IN LEAST-SQUARES-FIT

**BEST VALUE COMPUTED USING STEADY-STATE (SS) PARAMETERS

Table VII (CONT'D)

FLT. NO.	ω_{sp} RAD/SEC			$\zeta_{sp}\omega_{sp}$ RAD/SEC			ζ_{sp}			α/δ_{es} DEG/IN.			F_{es}/m_3 LB/$\dot{q}$			m_3/α $\dot{q}$/RAD			$\dot{q}/\delta_{es}$	PR	PIOR	PILOT
	MEAS.	COMP. LSF	BEST EST. VALUE	MEAS.	COMP. LSF	BEST EST. VALUE	MEAS.	COMP. LSF	BEST EST. VALUE	MEAS.	COMP. LSF	BEST EST. VALUE	MEAS.	COMP. LDF	BEST EST. VALUE	MEAS.	COMP. LSF	BEST EST. VALUE	LB/IN.			
603	1.93	1.77	1.93	3.05	2.76	3.05	.79	.78	.79	13.90	12.75	13.80	7.09	8.08	7.48**	16.8	16.9	16.8	30.4	7	2	AF
604	5.08	5.27	5.08	6.71	6.81	6.71	.66	.65	.66	9.55	9.52	9.55	10.90	10.62	10.90	16.8	17.2	16.8	30.1	3	3	
605	10.20*	8.91	10.20	14.48*	12.31	14.48	.71*	.69	.71	4.37	4.39	4.37	21.90	23.03	21.90	16.9*	17.6	16.9	28.8	5	2	
606	7.22	7.37	7.22	9.67	10.07	9.67	.67	.72	.67	7.33	7.07	7.33	14.20	14.29	14.20	16.2	16.5	16.2	29.7	4	2	
607	5.95	6.01	5.95	.74	.75	.74	.06	.06	.06	4.76	4.86	4.76	20.40	21.00	20.40	18.3	17.1	18.3	30.6	7	3	
608	3.51*	2.51	2.93**	6.04*	3.90	5.05	.86*	.78	.86	12.63*	11.90	12.63	8.30*	8.49	8.30	16.7	17.0	16.7	30.9	2.5	1	
609	4.05*	2.89	3.17**	1.05*	.59	.82**	.13*	.10	.13	12.70*	12.18	12.70	8.34	8.37	8.34	17.9*	16.0	17.9	31.4	7	3	
610	2.89	2.52	2.89	3.81	3.89	3.81	.66	.77	.66	11.43	11.90	11.43	8.68	8.49	8.68	16.9	17.1	16.9	29.1	2	1	
612	9.12	8.92	9.12	12.77	12.47	12.77	.70	.70	.70	5.10	4.97	5.10	20.80	20.29	20.80	16.4	16.0	16.4	32.3	4.5	2	
613	7.18	7.32	7.18	9.48	10.05	9.48	.66	.69	.66	7.07	7.08	7.07	14.65	14.29	14.65	16.9	16.7	16.9	30.7	3.5	2	
614	2.75*	2.75	2.75	5.11*	2.93	5.11	.93	.53	.93	28.00*	25.70	26.70*	3.88	3.97	3.88	16.3*	16.4	16.3	30.6	4	1	
615	1.99	1.64	1.99	1.11	1.22	1.11	.28	.37	.28	8.77	8.88	8.77	11.98	11.52	11.98	16.1*	16.1	16.1	29.7	6	2	
616	5.89	5.96	5.89	.78	.87	.78	.07	.07	.07	7.39*	7.19	7.39	14.45*	14.65	14.45	16.0	16.0	16.0	29.6	7	3	
617	4.68	4.64	4.68	6.55	6.08	6.55	.70	.69	.70	11.05	10.15	10.50**	9.76	9.96	9.76	15.8	15.2	15.8	30.2	2	1	
618	4.21*	2.09	2.42**	.84*	—	.48**	.10*		.10	10.72*	10.00	10.72	9.32	10.22	9.96**	18.2*	16.2	18.2	31.5	7	3	
619	6.84	7.28	8.21**	9.71	10.14	11.00**	.67	.70	.67	6.60	6.41	6.60	12.10	11.15	11.82**	16.3	15.8	16.3	23.0	3	2	
620	5.95	5.95	5.95	.60	.61	.60	.05	.05	.05	6.55	6.38	6.55	15.90	15.96	15.90	16.0	15.6	16.0	29.0	8	3	†
621^	3.70	—	—	4.81			.65			13.55			8.32			14.7	—		30.6	3	2	CAL
621	4.27	4.12	4.27	5.47	5.06	5.47	.64	.61	.64	9.90	10.25	9.90	9.35	9.85	9.35	17.9	18.1	17.9	29.0	3	2	
622	4.00*	2.15	2.61**	.80*		.52**	.10		.10	8.36*	8.14	8.36	12.08*	12.54	12.08	16.8*	16.6	16.8	29.2	6.5	3.5	
623	7.87*	4.67	9.01**	10.53*	1.25	12.97**	.67*	.13	.67	7.45*	7.38	7.45	10.70*	10.48	10.70	16.9*	17.1	16.9	23.7	2	1.5	
624	6.97	7.25	6.97	10.18	9.98	10.18	.73	.69	.73	8.75	8.58	8.75	7.51	6.92	7.02**	15.8	16.3	15.8	18.1	2	1.5	
625	2.83	2.88	2.83	4.19	4.04	4.19	.74	.82	.74	8.99*	7.85	8.70**	11.54*	12.85	11.54	16.4	16.8	16.4	29.6	6	2	
626	5.90	6.01	5.90	.77	.77	.77	.07	.06	.07	5.76	5.76	5.76	17.90	17.73	17.90	17.1	16.9	17.1	30.6	7	3	
627	8.71	8.81	8.71	12.54	12.23	12.54	.72	.70	.72	6.15	6.18	6.15	16.60	16.34	16.60	16.6	16.8	16.6	30.1	3.5	2	
628	2.17	2.01	2.17	1.22	1.54	1.22	.28	.38	.28		6.83	—		14.98			17.2	—		6.5	3	
629^	7.40			13.31			.30			9.95			10.92			15.2			30.3	3	2	
629	10.59*	9.49	10.59	13.98*	12.82	13.98	.66*	.68	.66	5.30	5.51	5.30	17.22	18.38	19.02**	18.3*	19.4	18.3	29.7	3.5	2	
630	9.54	9.58	9.54	12.40	13.69	12.40	.65	.72	.65	5.25	5.24	5.25	19.85	19.31	19.85	16.5	17.2	16.5	29.9	4	2.5	
632	9.71*	8.91	9.71	14.59*	13.38	14.59	.75*	.75	.75	6.00	5.88	6.00	13.62	13.16	13.62	16.0*	17.1	16.0	22.8	4	2	
633^	5.37			7.62			.71			11.86			8.43			16.7	—	—	29.8	2	1	
633	4.25*	4.11	4.25	2.04*	1.57	2.04	.24*	.19	.24	4.90	4.97	4.90	17.13	8.62	17.13	20.5*	19.4	20.5	29.4	4.5	2.5	†

* - VALUE NOT USED IN LEAST-SQUARES FIT

** - BEST VALUE COMPUTED USING STEADY-STATE (SS) PARAMETERS

^ - FLIGHTS FLOWN AT 30,000 FT.

Table VIII

PARAMETERS SIMULATED

LONGITUDINAL SHORT PERIOD AND PIO CONFIGURATIONS

V = 300 KTS(IAS)

FLT NO.	ω_{sp} RAD/SEC			$2\zeta_{sp}\omega_{sp}$ RAD/SEC			ζ_{sp}			α/δ_{es} DEG/IN.			F_{es}/n_z LB/g			n_z/α g/RAD			F_{es}/δ_{es} LB/IN.	PR	PIOR	PILOT
	MEAS.	COMP. LSF	BEST EST. VALUE	MEAS	COMP. LSF	BEST EST. VALUE	MEAS.	COMP. LSF	BEST EST. VALUE	MEAS.	COMP. LSF	BEST EST. VALUE	MEAS.	COMP. LSF	BEST EST. VALUE	MEAS.	COMP. LSF	BEST EST. VALUE				
564	2.61	3.08	3.04**	3.55	4.76	4.13**	.68	.77	.68	7.37	8.53	7.37	7.20	6.91	7.20	30.0*	30.2	30.0	27.9	6	-	CAL
565	13.81*	9.88	9.70**	23.20*	13.66	16.31**	.84*	.69	.84	5.97	6.14	5.97	9.20	9.22	9.20	30.1*	30.3	30.1	28.2	7	-	
566	5.90*	6.34	6.30**	7.43*	8.39	7.93**	.63*	.66	.63	9.47	9.37	9.47	6.20	6.07	6.20	28.2*	29.4	28.2	28.8	2	2	
568	12.09*	10.50	9.99**	17.44*	14.76	14.40**	.70*	.70	.72	6.29*	6.16	6.29	8.92*	9.17	8.92	30.8*	30.5	30.8	29.6	4.5	-	
570	9.15	9.14	9.15	11.90	11.29	11.90	.65	.62	.65	7.73	7.74	7.73	6.98	7.31	6.98	31.0	30.2	31.0	29.0	4.5	2	
571	8.14	8.76	8.14	10.26	11.39	10.26	.63	.65	.63	9.00	8.80	9.00	6.68	6.44	6.68	30.1	29.9	30.1	31.7	4	2.5	
572	2.28*	2.50	2.28	4.92*	4.21	4.92	1.08*	.84	1.08	5.11*	4.73	5.11	11.21*	12.68	11.21	30.8*	30.1	30.8	30.5	7	1.5	
573	9.75	9.66	9.75	13.46	13.02	13.46	.69	.67	.69	7.29	7.25	7.29	7.35	7.80	7.35	30.3	30.4	30.3	29.3	5	3	
574	4.67	5.21	4.67	5.86	6.35	5.88	.63	.61	.63	7.88	6.97	7.88	7.40	8.21	7.40	31.1	29.9	31.1	30.8	3	1.5	
575	3.67*	4.12	3.67	4.26*	5.40	4.27	.58*	.66	.58	9.25	8.47	8.99**	6.30	5.98	6.30	29.1*	29.9	29.1	30.1	3.5	1.5	
576	6.36	6.71	6.36	7.63	8.13	7.63	.60	61	.60	8.00	7.80	8.00	6.89	7.28	6.89	30.6	30.1	30.6	29.5	3	1.5	
577	11.28*	10.15	9.95**	15.79*	13.35	13.95**	.70*	.66	.70	6.20	6.47	6.20	8.18	8.74	9.18**	32.0*	30.9	32.0	30.3	6	3	
578	5.70*	6.68	6.29**	6.44*	7.83	7.16*	.57*	.59	.57	7.48*	7.80	7.48	7.09*	7.28	7.09	32.0*	30.7	32.0	30.1	5.5	2.5	
579	-	3.21	-	-	4.34	-	-	.68	-	-	6.98	-	-	-	-	-	-	-	-	6.5	2	↓
580	10.68	10.27	10.68	14.74	13.65	14.74	.69	.67	.69	4.51*	5.62	4.81**	12.04*	10.05	12.04	32.0*	31.8	32.0	30.8	5	3	AF
581	3.02	3.19	3.02	3.55	4.37	3.55	.60	.69	.60	13.10	14.11	13.10	4.30	4.13	4.30	29.5*	30.3	29.5	29.0	2	2	
582	5.43	5.81	5.43	6.30	7.13	6.30	.58	.61	.58	8.01	8.04	8.01	7.48	7.09	7.48	29.5	29.8	29.5	30.5	3	2	
583	9.17	9.15	9.17	11.92	11.79	11.92	.65	.64	.65	4.94*	5.18	4.94	11.02*	10.92	11.02	31.6	30.9	31.6	29.5	4	3	
584	4.17	4.34	4.17	5.00	5.58	5.00	.60	.64	.60	12.22	11.52	11.78**	5.12	4.99	5.12	30.7	29.6	30.7	32.1	2	2	
585	2.24	2.26	2.24	4.17	3.43	4.17	.93	.76	.93	8.81*	7.96	8.81	6.52*	7.45	6.52	29.3*	29.8	29.3	30.8	5	1	
586	7.77	7.86	7.77	10.57	9.57	10.57	.68	.61	.68	5.09	5.16	5.09	12.28	10.98	11.21**	20.4	30.5	29.4	30.4	4	2	
587	13.59*	10.99	10.52**	22.56*	15.84	17.49**	.83*	.72	.83	3.60	3.61	3.60	15.70	15.65	15.70	30.6*	30.2	30.6	29.8	5	2	
588	2.63	2.76	2.63	4.26	3.96	4.26	.81	.72	.81	10.18*	9.99	10.18*	6.06*	5.91	6.06	29.4*	30.0	29.4	30.1	4	2	↓
591	12.73	10.79	10.40**	16.29*	14.50	13.31**	.64*	.67	.64	6.40	6.45	6.40	8.63	8.75	8.63	31.0*	31.2	31.0	29.9	3	1.5	CAL
592	8.23	8.31	8.23	10.21	10.42	10.21	.62	.63	.62	9.46	9.75	9.46	6.01	5.81	6.01	30.6	30.6	30.6	30.9	4	2	
593	10.00	9.47	10.00	12.60	12.20	12.60	.63	.64	.63	7.01	7.50	7.01	7.70	7.54	7.70	31.2	21.3	31.2	29.2	5	3	
594	2.59	2.64	2.59	4.04	3.77	4.04	.78	.71	.78	4.40	3.21	4.40	13.36	13.94	13.36	30.2*	30.3	30.2	29.0	7	2	
595	5.23	5.66	5.23	5.86	6.75	5.86	.56	.60	.56	8.42	8.35	8.42	6.65	6.83	6.65	30.8	30.2	30.8	30.2	3	2	
596	6.08	6.01	6.08	1.58	1.06	1.58	.13	.09	.13	3.59	3.62	3.59	14.65	15.56	15.81	33.0	31.5	33.0	30.2	8	5	
597	11.40*	9.96	9.72**	15.50*	14.13	13.23**	.66*	.71	.68	6.43*	6.88	6.43	8.87*	8.23	8.87	31.6*	31.7	31.6	31.4	5	2	
598	4.43	4.53	4.43	2.92	2.76	2.92	.33	.30	.33	5.04	5.28	5.04	10.69	10.68	10.69	31.8	30.8	31.8	30.2	7	3	
599	5.94	6.09	5.94	1.90	1.67	1.90	.16	.14	.16	3.50	3.56	3.50	15.6	15.7	15.6	31.5	30.6	31.5	31.8	7	3	↑

*VALUES NOT USED IN LEAST-SQUARE FIT

**BEST VALUES COMPUTED USING STEADY-STATE (SS) PARAMETERS

Table VIII (CONT'D)

FLT NO.	ω_{sp} RAD/SEC			$2\zeta_{sp}\omega_{sp}$ RAD/SEC			ζ_{sp}			α/δ_{FS} DEG/IN.			F_{as}/m_g LB/g			n_g/α g/RAD			F_{es}/δ_{es}	PR	PIOR	PILOT
	MEAS.	COMP. LSF	BEST EST. VALUE	MEAS.	COMP. LSF	BEST EST. VALUE	MEAS.	COMP. LSF	BEST EST. VALUE	MEAS.	COMP. LSF	BEST EST. VALUE	MEAS.	COMP. LSF	BEST EST. VALUE	MEAS.	COMP. LSF	BEST EST. VALUE	LB/IN.			
600	1.59	1.49	1.59	2.73	2.85	2.73	.86	.96	.86	5.33	5.45	5.33	11.40	11.12	11.40	31.3*	31.2	31.3	30.7	8	3	CAL
601	3.03	2.65	3.03	4.00	3.28	4.00	.66	.62	.66	8.10*	9.95	8.33	7.01*	5.81	7.01	30.8*	30.8	30.8	31.1	5.5	2.5	↓
602	5.35	5.76	5.35	6.21	7.26	6.21	.58	.63	.58	8.32	8.19	8.32	6.88	6.97	6.88	29.7	29.8	29.7	29.2	4	2	AF
603	6.07	6.10	6.07	1.94	1.89	1.94	.16	.16	.16	3.39*	3.57	3.39	16.90*	15.68	16.70*	29.7	30.2	29.7	30.1	5	3.5	↑
604	10.13	9.56	9.51**	13.98	12.86	13.11**	.69	.67	.69	5.41	5.63	5.41	10.25	10.04	10.25	29.5	30.1	29.5	28.2	4	3	
605	4.43	4.49	4.43	2.75	2.40	2.75	.31	.27	.31	6.76	6.66	6.76	8.21	8.45	8.21	30.7	31.6	30.7	29.0	3	2	
606	4.30	4.04	4.30	1.89	1.85	1.89	.22	.23	.22	7.90	7.40	7.45**	7.70	7.57	7.70	30.7	30.3	30.7	30.6	3	2	
607	1.65	1.69	1.65	2.90	2.80	2.90	.88	.83	.88	10.65	9.66	10.51**	5.82	6.18	5.82	30.3*	30.7	30.3	32.5	7	1	
608	4.11	4.03	4.11	1.97	1.83	1.97	.24	.23	.24	8.75	8.64	8.75	7.38	6.49	6.86**	26.8	30.4	26.8	32.0	4	2	
609	11.36*	10.30	9.81**	15.68*	14.49	13.53**	.69*	.70	.69	4.93	4.86	4.93	8.52	8.20	8.52	29.0*	29.6	29.0	21.4	2.5	2	
610	6.05	6.01	6.05	1.09	.91	1.09	.09	.08	.09	6.30	6.43	6.30	8.52	8.67	8.52	30.1	30.6	30.1	28.8	7	2	
612	8.78*	8.34	8.78	13.17*	10.97	13.17	.75	.66	.75	5.04	5.10	5.04	11.18	11.09	11.18	29.7*	29.5	29.7	29.2	3	2	
613	4.17	4.46	4.17	5.92	5.72	5.92	.71	.64	.71	9.56	9.57	9.56	5.85	6.01	5.85	30.2	30.1	30.2	29.6	1.5	1.5	
614	5.91	6.11	5.91	1.42	1.93	1.42	.12	.16	.12	7.92	8.03	7.92	7.90	7.78	7.90	30.4	30.1	30.4	29.9	7	3	
615	10.52	10.71	10.52	13.47	15.15	13.47	.64	.71	.64	6.06	5.86	6.06	9.50	9.63	9.50	30.3	29.4	30.3	29.8	3	2	
616	5.95	6.22	5.95	1.31	2.08	1.31	.11	.17	.11	4.93	4.86	4.93	11.60	11.49	11.60	29.6	29.2	29.6	30.0	7	3	
617	4.44	4.19	4.44	1.42	2.02	1.42	.16	.24	.16	9.62	9.57	9.62	6.04	5.85	6.04	30.3	29.1	30.3	30.8	5	3	
618	8.16	8.33	8.16	10.44	10.77	10.44	.64	.65	.64	7.50	7.44	7.50	7.61	7.63	7.61	29.0	29.9	29.0	29.0	3	2	
619	3.27	3.28	3.27	3.27	3.77	3.27	.50	.58	.50	14.55	14.01	14.55	3.22	2.90	3.22	28.1*	29.4	28.1	23.6	2	1	
620	11.40*	10.43	9.99**	15.96*	15.03	13.99**	.70	.72	.70	4.79	4.75	4.79	12.20	11.89	12.20	28.4*	29.0	28.4	28.8	2.5	2	↑
622	4.40	4.13	4.40	1.67	1.56	1.67	.19	.19	.19	7.15	6.75	7.15	8.55	8.29	8.55	28.8	30.0	28.8	30.0	5	3	CAL
623	5.95	6.19	5.95	1.31	1.58	1.31	.11	.13	.11	4.97	4.87	4.97	11.20	11.49	11.20	32.5	30.2	32.5	29.8	6.5	3.5	
624	11.87*	10.46	10.22*	16.52*	14.89	14.72**	.72*	.71	.72	7.33	7.54	7.33	7.70	7.51	7.70	29.8*	29.8	29.8	29.4	2	1.5	
625	9.12	9.50	9.12	12.95	12.74	12.96	.71	.67	.71	8.70	8.34	8.70	6.68	6.74	6.68	29.5	30.2	29.5	29.5	3	2	
626	11.39*	10.90	10.51**	16.17*	15.17	14.92**	.71*	.70	.71	6.81	6.86	6.81	8.66	8.23	8.66	29.2*	30.1	29.2	29.7	2.5	1.5	
627	2.94	2.54	2.94	2.12	2.22	2.12	.36	.44	.36	6.29	6.58	6.29	8.78	8.61	8.78	30.1*	30.3	30.1	29.8	4.5	2	
628	4.38	4.15	4.38	1.40	1.34	1.40	.16	.16	.16	5.10	5.12	5.10	11.31	10.92	11.31	29.4	29.8	29.4	30.2	6	2.5	
629	—	—	—	—	—	—	—	—	—	—	—	—	—	—	—	—	—	—	—	3	2	
630	13.17*	11.89	11.49**	19.76*	16.84	17.21**	.75*	.71	.75	3.06	3.04	3.06	18.21	18.56	18.21	30.2*	30.4	30.2	29.7	5.5	3.5	
632	11.02*	10.91	11.02	13.22*	15.42	13.22	.60*	.71	.60	5.05	4.97	5.05	4.97	5.05	11.31	11.35	11.31	29.2	29.6	4	2	↑

* VALUES NOT USED IN LEAST-SQUARES FIT

** BEST VALUE COMPUTED USING STEADY-STATE(SS) PARAMETERS

Table IX

PARAMETERS SIMULATED
LONGITUDINAL SHORT PERIOD AND PIO CONFIGURATIONS

V = 365 KTS(IAS)

FLT NO.	ω_{sp} RAD/SEC			$\zeta_{sp}\omega_{sp}$ RAD/SEC			ζ_{sp}			α/δ_{es} DEG/IN.			F_{es}/n_s LB/g			n_s/α g/RAD			$\omega_{n_s}^2/\delta_{es}$	PR	PIOR	PILOT
	MEAS.	COMP LSF	BEST EST. VALUE	MEAS.	COMP LSF	BEST EST. VALUE	MEAS.	COMP LSF	BEST EST. VALUE	MEAS.	COMP LSF	BEST EST VALUE	MEAS.	COMP LSF	BEST EST. VALUE	MEAS.	COMP LSF	BEST EST. VALUE	LB/IN.			
564		13.58	11.25**		17.82	17.82		.67	.79**	3.18*	3.27	3.18	8.8*	8.45	8.8	60.2*	64.5	60.2	29.1	6.5	-	CAL
565	3.75	3.76	3.75	6.08	5.31	6.08	.81	.71	.81	3.38	3.54	3.38	8.38	7.23	8.38	60.3*	61.9	60.3	29.7	5	-	
566	2.00*	2.42	2.00	3.36*	4.4	3.36	.84*	.91	.84	1.99*	3.13	1.99	14.7	7.2	14.7	58.3	63.6	58.3	29.0	8	4	
568	7.94	8.72	7.94	11.27	11.83	11.27	.71	.68	.71	4.28	4.22	4.28	6.42	6.53	6.42	62.4	62.7	62.4	30.2	3.5		
570	13.8*	12.5	10.53**	19.32*	15.02	14.75*	.7*	.6	.7	4.45*	4.7	4.45	6.29*	5.94	6.29	62.5*	62.3	62.5	30.1	7	5	
571	9.86	10.03	9.86	14.2	13.31	14.2	.72	.67	.72	3.96	4.05	3.96	6.71	6.83	6.71	64.5	63.5	64.5	30.2	4	2	
572	3.05	3.28	3.05	5.98	5.74	5.98	.98	.88	.98	3.07*	2.14	3.07	8.8*	11.71	8.8	64.8	63.2	64.8	30.5	7	1.5	
574	4.05	4.7	4.42**	5.51	6.98	6.00**	.68	.74	.68	3.29	2.76	3.29	8.1	9.61	8.31**	66.8	64.8	66.8	30.3	5	2	
575	12.2	11.97	12.2	17.08	15.85	17.08	.7	66	.7	2 95	3.1	2.95	9.3	9.0	9.3	62.5	62.8	62.5	29.8	4.5	2	
576	4.62	4.65	4.62	6.84	7.87	6.84	.74	.85	.74	3.3	2.92	3.3	8.42	9.16	6 42	64.3	64.6	64.3	30.0	7	3	
577	5.62	4.62	4.64**	8.21	7.82	6.77*	.73	.85	.73	2.84	2.63	2.84	9.4	10.18	9.4	66.8	65.4	66.8	30.7	7	3.5	
580	1.36*	1.2	1.36	1.88*	3.26	1.88	.69*	1.36	.69	12.9*	4.79	12.9	2.07*	4.02	2.07	61.0	63.3	61.0	30.1	8	3	CAL
581	4.98	4.69	4.98	6.57	7.92	6.57	.66	.84	.66	6.98	5.84	6.98	4.3	4.58	4.3	62.8	63.7	62.8	32.4	2	1	
583	8.98	9.08	8.98	11.85	12.33	11.85	.66	.68	.66	5.09	5.49	5.09	4.86	5.03	4.86	66.6	62.9	66.6	28.4	3	4	
584	4.07	4.01	4.07	5.45	6.12	5.45	.67	.76	.67	7.87	6.58	7.87	3.04	3.91	4.07**	62.5	61.1	62.5	35.5	6	2	
585	1.92*	1.19	1.9**	4.99*	3.94	4.99	1.3*	1.67	1.31**	9.43*	4.73	9.43	3.05	4.38	3.05	59.0	62.8	59.0	28.9	7	1	
586	15.1*	14.4	15.1*	18.12*	19.46	18.12	.6	.68	.6	4.94*	4.05	4.94	5.65*	5.91	5.65	60.8	62.4	60.8	29.3	5	3	
587	7.14	6.82	7.14	9.71	10.37	9.71	.68	.76	.68	5.7	4.72	5.7	5.61	5.79	5.61	59.1	61.7	59.1	32.4	3	3	
588	4.02	3.69	4.02	6.59	5.6	6.59	.82	.76	.82	7.45*	6.06	7.45	3.8*	4.22	3.8	60.8	62.7	60.8	29.1	3	2	
591	4.16	4.43	4.16	5.99	6.54	5.99	.72	.74	.72	2.48	2.22	2.48	11.47	11.85	11.47	62.5	65.5	62.5	29.8	7	2.5	AF
592	16.7*	14.37	12.03**	24.05**	18.42	17.35**	.72*	.64	.72	3.75	4.37	3.75	6.8	6.41	6.8	65.4	64.4	65.4	30.1	6.5	3	
593	4.16	4.58	4.16	7.16	6.78	7.16	.86	.74	.86	2.73	2.25	2.73	9.61	11.71	9.61	63.5	62.1	63.5	28.9	7	3	
595	3.72*	3.31	3.72	1.79*	1.76	1.79	.24*	.27	.24	-	1.429	-	-	17.95	-	-	65.8	-	-	9	4.5	
596	7.31	6.91	7.31	10.38	10.66	10.38	.71	.77	.71	2.27	2.37	2.27	11.7	11.58	11.7	65.0	65.5	65.0	29.9	6.5	2	
598	15.2	15.21	15.2	17.61	18.4	17.6	.58	.61	.58	2.85	3.38	3.06**	8.99	8.31	8.99	68.6	66.7	68.6	30.5	6	3	
599	3.78	3.25	3.78	4.0	3.25	4.0	.52	.5	.52	2.15	2.01	2.15	12.28	12.67	12.28	65.5	63.8	65.5	30.5	6	2.5	
601	2.0*	1.2	2.16**	1.76*	2.21	1.9**	.44*	.92	.44	1.46	1.35	1.46	16.2	15.32	16.2	68.8	63.9	68.8	33.4	9	4.5	
503	14.9	14.45	14.9	18.76	18.66	18.76	.63	.65	.63	3.51	3.68	3.51	8.3	7.6	8.3	60.6	60.7	60.6	30.5	4	3	AF
604	1.8*	1.21	1.8	1.87*	2.21	1.87	.52	.92	.52	5.6*	2.7	5.6	5.85*	7.66	5.85	62.1*	63.9	62.1	31.7	9	3	
605	3.72	3.46	3.72	1.41	1.91	1.41	.19	.28	.19	5.86	5.71	5.86	4.15	4.49	4.15	63.5	63.5	63.5	29.5	7.5	4	
606	12.25	11.43	12.25	17.89	15.23	17.89	.73	.67	.73	5.35	5.39	5.35	5.73	5.16	5.01**	56.6	56.8	56.6	29.7	2.5	2	

*VALUE NOT USED IN LEAST-SQUARE FIT

**BEST VALUE COMPUTED USING STEADY-STATE (SS) PARAMETERS

Table IX (CONT'D)

FLT NO.	ω_{sp} - RAD/SEC			$2\zeta_{sp}\omega_{sp}$ - RAD/SEC			ζ_{sp}			α/δ_{es} - DEG/IN.			F_{es}/n_g - LB/g			n_g/α g/RAD			F_{es}/δ_{es}	PR	PIOR	PILOT
	MEAS.	COMP. LSF	BEST EST. VALUE	MEAS.	COMP. LSF	BEST EST. VALUE	MEAS.	COMP. LSF	BEST EST. VALUE	MEAS.	COMP. LSF	BEST EST. VALUE	MEAS.	COMP. LSF	BEST EST. VALUE	MEAS.	COMP. LSF	BEST EST. VALUE	LB/IN.			
607	6.39	5.47	5.12**	7.8	8.77	6.23**	.61	.8	.61	8.11	7.4	7.87**	3.46	3.65	3.46	61.0	63.6	61.0	30.2	2.5	2	AF
608		10.19	8.64**		13.44	13.44		.66	.78**	5.2 *	5.17	5.2	5.95*	5.36	5.27**	59.8*	61.9	59.8	30.4	2	2	
609	2.32	2.03	2.32	3.99	4.11	3.99	.86	1.01	.86	21.3 *	9.14	21.3	1.44*	2.39	1.44	58.6*	59.1	58.6	31.8	7	1	
610	5.47	5.32	5.47	.55	.93	.55	.05	.09	.05	3.72	4.07	3.72	8.12	8.78	8.12	54.0	62.2	54.0	27.9	8.5	6	
612	11.91	12.43	11.91	16.74	16.66	16.74	.62	.67	.62	3.57	3.82	3 57	7.77	7.31	7.77	59.6	58.3	59.6	29.4	2	2	
613	2.8 *	1.69	2.17**	4.58*	3.94	3.56**	.81*	1.17	.82	27.2 *	16.04	27.7 *	.98*	1.37	.98	62.9*	61.8	62.9	23.8	7	3	
614	10.08	10.35	10.08	14.52	13.59	14.52	.75	.66	.75	6.3	6.25	6.3	4.77	4.44	4.77	57.4	58.0	57.4	29.9	1.5	1	
615	12.71	13.3	12.71	15.74	17.28	15.74	.62	.65	.62	4.82	5.02	4.82	6.23	5.57	5.64**	60.5	58.1	60.5	30.1	3	2	
616	2.73	3.21	3.46**	3.55	5.02	4.5**	.65	.78	.65	11.9	10.25	11.9	2.23	2.36	2.23	60.6*	56.3	60.6	27.7	7	2	
617	12.24*	10.88	9.36**	17.6*	14.33	13.5**	.72*	.66	.72	6.35	6.05	6.35	4.29	4.06	4.29	64.6*	63.1	64.6	29.7	2.5	2	
618	7.27*	8.04	7.02**	9.89*	11.75	9.55**	.68	.73	.68	7.77*	7.27	7.77	3.97*	3.31	3.39**	55.2*	55.6	55.2	29.2	3	2	
619	12.49*	13.36	11.04**	14.24*	17.46	12.60**	.57	.65	.57	3.91	3.92	3.91	5.94	5.03	5.17**	54.7*	55.2	54.7	22.4	3	2	
620	16.0	15.7	16.0	18.88	18.8	18.88	.59	.6	.59	4.22*	4.52	4.22	7.3*	6.21	6.19**	53.6	52.4	53.6	29.0	3	2	↓
622	11.05*	12.38	11.05	13.26*	16.48	13.26	.8 *	.67	.6	4.57	4.68	4.57	6.26	5.96	6.26	59.0	61.2	59.0	29.4	3.5	2.5	CAL
623	5.3	5.22	5.3	.85	.79	.85	.08	.08	.08	1.44	1.58	1.44	16.8	17.09	16.8	65.6	66.5	65.6	30.7	7	2	
624	9.6	10.12	9.6	14.21	13.57	14.21	.74	.66	.74	4.1 *	4.56	4.1	6.89*	6.83	6.89	60.1	58.4	60.1	29.5	4	2	
625	13.78	13.92	13.78	18.47	18.07	18.46	.67	.65	.67	2.98	3.18	2.98	8.9	8.8	8.9	62.8	61.6	62.8	29.7	4	2	
626	3.4	3.47	3.4	1.29	1.59	1.29	.19	.23	.19	1.25*	.97	1.25	15.5*	26.52	21.5 **	67.1	63.2	67.1	29.9	7	3.5	
627	5.89	5.2	4.38**	10.72	8.51	7.97**	91	.82	.91	3.12	2.14	3.12	9.01*	12.57	9.01	62.9	62.1	62.9	30.7	4.5	2	
628	17.05*	15.96	17.05**	23.56*	17.63	22.5**	.66*	.55	.66	2.55	2.85	2.55	11.08	10.23	11.08	63.6	63.5	63.6	30.1	4.5	3	
630	17.9 *	16.63	17.9	23.6*	21.6	23.6	.66*	.65	.66	2.13*	2.35	2.13	12.28	11.96	12.28	65.3	64.5	65.3	30.2	5	3.5	↓

* VALUE NOT USED IN LEAST-SQUARES FIT

** BEST VALUE COMPUTED USING STEADY-STATE (SS) PARAMETERS

Table X

LONGITUDINAL SHORT PERIOD HANDLING QUALITIES PARAMETERS SIMULATED AND PILOT RATINGS

V = 220 KTS (IAS)

FLT NO.	ω_{sp} RAD/SEC	ζ_{sp}	n_g/α g/RAD	F_{es}/n_g LB/g	CAP (1)	$(\theta_{nd})_{max}$ (2)	(CAP)' (3)	$(\theta)_{max}/F_{es}$ (4)	$\dot{\theta}_{max}/\theta_{ss}$ (5)	PR	PILOT PIOR	PILOT
564	8.34	.68	16.1	15.8	4.32	.50	2.16	.137	3.18	6	-	CAL
565	1.71	.72	16.7	11.0	.18	.95	.17	.015	1.16	7	-	
566	2.03	.79	15.4	5.4	.27	.91	.24	.045	1.22	5	3	
568	3.60	.58	16.1	7.0	.81	.76	.61	.087	1.65	3.5	1	
570	8.39	.67	17.1	11.5	4.12	.50	2.06	.179	3.20	4	2	
571	5.00	.60	17.7	7.1	1.41	.66	.93	.131	2.08	3.5	2	
572	1.73	.83	16.5	16.5	.18	.95	.17	.010	1.17	7	1.5	
573	6.25	.64	18.8	11.1	2.08	.59	1.23	.112	2.50	4	1.5	
574	2.22	.72	18.0	12.0	.27	.89	.24	.020	1.25	7	2.5	
576	8.84	.78	17.6	14.1	4.45	.48	2.12	.151	3.35	6.5	3	
577	3.04	.70	17.9	9.9	.52	.81	.42	.042	1.47	7	2	
579	8.29	.73	17.4	11.2	3.94	.50	1.96	.176	3.17	7	2.5	
581	6.13	.68	17.4	13.8	2.16	.60	1.30	.094	2.46	5	2	AF
582	2.30	.69	17.7	6.9	.30	.88	.26	.037	1.27	7	3	
583	9.44	.79	17.6	28.0	5.06	.46	2.33	.083	3.52	7	3	
584	3.82	.68	16.2	10.1	.90	.74	.67	.066	1.68	2	1	
585	2.19	.84	16.8	6.0	.29	.89	.25	.042	1.25	4	1	
586	6.09	.63	17.6	12.8	2.11	.60	1.27	.098	2.45	4	2	
587	8.68	.62	17.1	18.1	4.40	.49	2.15	.119	3.30	5	2	
588	5.48	.68	16.6	16.0	1.81	.64	1.15	.072	2.25	4.5	2	
591	10.02	.76	18.5	13.5	5.44	.44	2.37	.176	3.70	4	1.5	CAL
592	2.96	.59	17.6	7.4	.50	.81	.40	.055	1.45	6	2.5	
595	5.52	.60	17.9	9.4	1.70	.63	1.07	.114	2.25	5	2.5	
596	1.94	.76	18.5	14.9	.20	.92	.19	.013	1.21	7.5	2	
597	4.97	.61	18.9	8.4	1.31	.66	.86	.103	2.09	4	2	
599	8.36	.73	17.2	11.4	4.06	.50	2.02	.178	3.18	7.5	1	
600	5.83	.70	18.1	12.7	1.88	.62	1.16	.092	2.35	3	1.5	
601	2.16	.56	18.5	11.5	.25	.88	.22	.019	1.25	5.5	3	
602	8.85	.75	16.5	17.6	4.81	.48	2.28	.130	3.35	5	2	AF
603	1.93	.79	16.8	7.5	.22	.92	.20	.027	1.20	7	2	
604	5.08	.66	16.8	10.9	1.54	.66	1.01	.093	2.12	3	3	
605	10.20	.71	16.9	21.9	6.16	.44	2.65	.121	3.45	5	2	
606	7.22	.67	16.2	14.2	3.22	.55	1.77	.125	2.82	4	2	
608	2.93	.86	16.7	8.3	.51	.82	.42	.050	1.43	2.5	1	
610	2.89	.66	16.9	8.7	.50	.82	.40	.047	1.43	2	1	
612	9.12	.70	16.4	20.8	5.07	.47	2.40	.115	3.42	4.5	2	
613	7.18	.66	16.9	14.7	3.06	.55	1.68	.115	2.82	3.5	2	
614	2.75	.93	16.3	3.9	.46	.84	.39	.100	1.40	4	1	
617	4.68	.70	15.8	9.8	1.38	.68	.94	.096	2.00	2	1	
621	4.27	.64	17.9	9.4	1.02	.71	.72	.077	1.86	3	2	CAL
624	6.97	.73	15.8	7.0	3.07	.56	1.71	.243	2.75	2	1.5	
625	2.83	.74	16.4	11.5	.50	.83	.40	.035	1.40	6	2	
627	8.71	.72	16.6	16.6	4.57	.49	2.23	.134	3.30	3.5	2	
629	10.59	.66	18.3	19.0	6.13	.43	2.61	.137	3.87	3.5	2	
630	9.54	.65	16.5	19.9	5.53	.46	2.55	.129	3.55	4	2.5	
632	9.71	.75	16.0	13.6	5.91	.45	2.68	.197	3.60	4	2	

(1) $CAP = \dfrac{\omega_{sp}^2}{n_g/\alpha}$

(2) - OBTAINED FROM FIGURES 4 AND 6

(3) $(CAP)' = \dfrac{\omega_{sp}^2 (\ddot{\theta}_{nd})_{max}}{n_g/\alpha}$

(4) $\dfrac{\ddot{\theta}_{max}}{F_{es}} = \dfrac{\omega_{sp}^2 (\ddot{\theta}_{nd})_{max}}{(n_g/\alpha)(F_{es}/n_g)}$

(5) - OBTAINED FROM FIGURE 5

Table XI

LONGITUDINAL SHORT PERIOD HANDLING QUALITIES PARAMETERS SIMULATED AND PILOT RATINGS

V = 300 KTS (IAS)

FLT NO.	ω_{sp} RAD/SEC	ζ_{sp}	n_{α}/α g/RAD	F_{es} n_{α} LB/g	(1) CAP	(2) $(\theta_{nd})_{MAX}$	(CAP)' (3)	(4) $(\ddot{\theta})_{MAX}/F_{es}$	(5) $\ddot{\theta}_{MAX}/\ddot{\theta}_{ss}$	PR	PIOR	PILOT
564	3.04	.68	30.0	7.0	.31	.83	.26	.037	1.30	6	-	CAL
565	9.70	.84	30.1	9.2	3.12	.46	1.44	.156	2.86	7	-	
566	6.30	.63	28.2	6.2	1.41	.61	.86	.139	2.02	2	-	
568	9.99	.72	30.8	8.9	3.21	.45	1.46	.164	2.93	4.5		
570	9.15	.65	31.0	7.0	2.70	.48	1.30	.186	2.73	4.5	2 2.5	
571	8.14	.63	30.1	6.7	2.20	.52	1.14	.171	2.48	4	2.5	
572	2.28	1.08	30.8	11.2	.17	.91	.15	.014	1.18	7	5	
573	9.75	.69	30.3	7.4	3.14	.46	1.44	.196	2.87	5	3	
574	4.67	.63	31.1	7.4	.70	.70	.49	.066	1.65	3	1.5	
575	3.67	.58	29.1	6.3	.46	.78	.36	.057	1.43	3.5	1.5	
576	6.36	.60	30.6	6.9	1.33	.60	.79	.115	2.03	3	1.5	
577	9.95	.70	32.0	9.2	3.10	.45	1.40	.153	2.92	6	3	
578	6.29	.57	32.0	7.1	1.23	.61	.75	.106	2.02	5.5	2.5	
580	10.68	.69	32.0	12.0	3.56	.43	1.53	.127	3.10	5	3	AF
581	3.02	.60	29.5	4.3	.31	.84	.26	.060	1.30	2	2 1.5	
582	5.43	.58	29.5	7.5	1.00	.66	.66	.088	1.80	3	2	
583	9.17	.65	31.6	11.0	2.66	.48	1.28	.116	2.72	4	3	
584	4.17	.60	30.7	5.1	.57	.74	.42	.082	1.53	2	2	
585	2.24	.93	29.3	6.5	.17	.91	.16	.024	1.17	5	2	
586	7.77	.68	29.4	11.2	2.05	.53	1.09	.098	2.38	4	2	
587	10.52	.83	30.6	15.7	3.62	.43	1.56	.099	3.05	5	2	
588	2.63	.81	29.4	6.1	.24	.88	.21	.034	1.23	4	2	
591	10.40	.64	31.0	8.6	3.48	.44	1.53	.177	3.02	3	5	CAL
592	8.23	.62	30.6	6.0	2.21	.52	1.15	.191	2.50	4	2	
593	10.00	.63	31.2	7.7	3.20	.45	1.44	.187	2.93	5	3	
594	2.59	.78	30.2	13.4	.22	.88	.20	.015	1.23	7	2	
595	5.23	.56	30.8	6.7	.89	.67	.59	.089	1.75	3	2	
597	9.72	.68	31.6	8.9	2.99	.46	1.38	.166	2.87	5	2	
600	1.59	.86	31.3	11.4	.08	1.00	.08	.007	1.09	8	3	
601	3.03	.66	30.8	7.0	.30	.84	.25	.036	1.31	5.5	2.5	
602	5.35	.58	29.7	6.9	.96	.66	.63	.092	1.78	4	2	AF
604	9.51	.69	29.5	10.3	3.08	.47	1.45	.141	2.81	4	3	
607	1.65	.88	30.3	5.8	.09	.99	.09	.015	1.10	7		
609	9.81	.69	29.0	8.5	3.32	.46	1.53	.179	2.89	2.5	2	
612	8.78	.75	29.7	11.2	2.60	.47	1.22	.109	2.62	3	2	
613	4.17	.71	30.2	6.0	.58	.74	.43	.071	1.54	3.5	2.5	
615	10.52	.64	30.3	9.5	3.66	.43	1.57	.165	3.05	3	2	
618	8.16	.64	29.0	7.6	2.30	.62	1.43	.188	2.47	3	2	
619	3.27	.50	28.1	3.2	.38	.81	.31	.096	1.35	2		
620	9.94	.70	28.4	12.2	3.52	.45	1.59	.130	2.92	2.5	2	
624	10.22	.72	29.8	7.7	3.52	.44	1.55	.201	2.97	2	2.5	CAL
625	9.12	.71	29.5	6.7	2.82	.48	1.35	.202	2.71	3	2	
626	10.51	.71	30.1	8.7	3.67	.43	1.58	.179	3.05	2.5	2	
630	11.49	.75	30.2	10.2	4.37	.41	1.79	.098	3.29	5.5	3.5	
632	11.02	.60	29.2	11.2	4.16	.42	1.75	.156	3.17	4	2	

(1) $CAP = \dfrac{\omega_{sp}^2}{n_{\alpha}/\alpha}$

(2) - OBTAINED FROM FIGURES 4 AND 6

(3) $(CAP)' = \dfrac{\omega_{sp}^2(\ddot{\theta}_{nd})_{max}}{n_{\alpha}/\alpha}$

(4) $\dfrac{(\ddot{\theta})_{max}}{F_{es}} = \dfrac{\omega_{sp}^2(\ddot{\theta}_{nd})_{max}}{(n_{\alpha}/\alpha)(F_{es}/n_{\alpha})}$

(5) - OBTAINED FROM FIGURE 5

Table XII

LONGITUDINAL SHORT PERIOD HANDLING QUALITIES PARAMETERS SIMULATED AND PILOT RATINGS

V = 365 KTS (IAS)

FLT NO.	ω_{sp} RAD /SEC	ζ_{sp}	n_α/α g /RAD	F_{es}/n_g LB /g	(1) CAP	(2) $(\theta_{nd})_{max}$	(3) (CAP)'	(4) $(\theta)_{max}/F_{es}$	(5) θ_{max}/θ_{ss}	PR	PIOR	PILOT
564	11.25	.79	60.2	8.8	2.10	.44	.93	.105	2.07	6.5	-	CAL
565	3.75	.8!	60.3	8.4	.23	.84	.20	.023	1.14	6	-	|
566	2.00	.84	58.3	14.7	.07	1.06	.07	.005	1.05	8	4	|
568	7.94	.71	62.4	6.4	1.01	.57	.57	.089	1.59	3.5	-	|
570	10.53	.70	62.5	6.3	1.78	.47	.83	.132	1.96	7	5	|
571	9.86	.72	64.5	6.7	1.51	.49	.73	.110	1.85	4	2	|
572	3.05	.98	64.8	8.8	.14	.92	.13	.015	1.10	7	1.5	|
574	4.42	.68	66.8	8.3	.29	.98	.29	.034	1.19	5	2	|
575	12.20	.70	62.5	9.3	2.38	.42	.99	.107	2.22	4.5	2	|
576	4.62	.74	64.3	8.4	.33	.76	.25	.030	1.20	7	3	|
577	4.64	.73	66.8	9.4	.32	.76	.26	.028	1.21	7	3.5	↑
580	1.36	.69	61.0	2.1	.03	1.16	.03	.017		8	3	AF
581	4.98	.66	62.8	4.3	.40	.74	.29	.068	1.24	2	1	|
583	8.98	.66	62.9	4.9	1.28	.52	.67	.137	1.72	3	4	|
584	4.07	.67	62.5	4.1	.27	.81	.21	.053	1.16	6	2	|
585	1.90	1.31	59.0	3.1	—					7	1	|
586	15.10	.60	60.8	5.7	3.75	.35	1.30	.229	2.55	5	3	|
587	7.14	.68	59.1	5.6	.86	.61	.53	.094	1.49	3	3	|
588	4.02	.82	60.8	3.8	.27	.81	.22	.058	1.16	3	2	↑
591	4.16	.72	62.5	11.5	.27	.81	.21	.019	1.17	7	2.5	CAL
592	12.03	.72	65.4	6.8	2.21	.42	.93	.137	2.20	6.5	3	|
593	4.16	.86	63.5	9.6	.27	.81	.22	.023	1.17	7	3	|
596	7.31	.71	65.0	11.7	.82	.60	.49	.042	1.50	6.5	2	|
598	15.20	.58	68.6	9.0	3.37	.35	1.16	.130	2.55	6	3	|
599	3.78	.52	65.5	12.3	.22	.84	.18	.015	1.14	6	2.5	↑
603	14.90	.63	60.6	8.3	3.66	.35	1.05	.126	2.52	4	3	AF
606	12.25	.73	56.8	5.0	2.64	.42	1.10	.219	2.24	2.5	2	|
607	5.12	.61	61.0	3.5	.44	.73	.32	.092	1.25	2.5	2	|
608	8.64	.78	59.8	5.3	1.25	.53	.66	.126	1.68	2	2	|
609	2.32	.86	58.6	1.4	.09	1.02	.09	.065	1.06	7	1	|
612	11.91	.62	59.6	7.8	2.38	.43	1.01	.130	2.18	2	2	|
613	2.17	.82	62.9	1.0	.07	1.03	.08	.079	1.06	7	3	|
614	10.08	.75	57.4	4.8	1.77	.48	.85	.178	1.90	1.5	1	|
615	12.71	.62	60.5	5.6	2.67	.40	1.07	.190	2.29	3	2	|
616	3.46	.65	60.6	2.2	.20	.87	.17	.077	1.12	7	2	|
617	9.36	.72	64.6	4.3	1.36	.50	.68	.159	1.77	2.5	2	|
618	7.02	.68	55.2	3.4	.89	.61	.54	.161	1.46	3	2	|
619	11.04	.57	54.7	5.2	2.23	.44	.98	.190	2.05	3	2	|
620	16.00	.59	53.6	6.2	4.78	.33	1.57	.253	2.62	3	2	↑
622	11.05	.60	59.0	6.3	2.07	.45	.33	.149	2.05	3.5	2.5	CAL
624	9.60	.74	60.1	6.9	1.53	.50	.76	.110	1.81	4	2	|
625	13.78	.67	62.8	8.9	3.03	.38	1.14	.128	2.41	4	2	|
627	4.38	.91	62.9	9.0	.31	.75	.23	.026	1.19	4.5	3	|
628	17.05	.66	63.6	11.1	4.57	.31	1.42	.128	2.71	4.5	3	|
630	17.90	.66	65.3	13.3	5.03	.30	1.48	.121	2.78	5	3.5	↑

(1) $CAP = \dfrac{\omega_{sp}^2}{n_\alpha / \alpha}$

(2) - OBTAINED FROM FIGURES 4 AND 6

(3) $(CAP)' = \dfrac{\omega_{sp}^2 (\ddot{\theta}_{nd})_{max}}{n_\alpha / \alpha}$

(4) $\dfrac{(\theta)_{max}}{F_{es}} = \dfrac{\omega_{sp}^2 (\ddot{\theta}_{nd})_{max}}{n_\alpha / \alpha \; F_{es}}$

(5) - OBTAINED FROM FIGURE 5

Table XIII

PIO HANDLING QUALITIES PARAMETERS
SIMULATED AND PILOT RATINGS

FLT NO.	V(IAS) KTS	ω_{sp} RAD/SEC	ζ_{sp}	n_z/α g/RAD	L_α 1/SEC	F_{es}/n_z LB/g	$2\zeta_{sp}\omega_{sp}$ RAD/SEC	$\frac{2\zeta_{so}\omega_{sp}}{L_\alpha}$	PR	PIOR	PILOT
568	220	3.60	.58	16.1	1.36	7.0	4.18	3.07	3.5	1	CAL
571	↓	5.00	.60	17.7	↓	7.1	6.00	4.42	3.5	2	↓
592		2.96	.59	17.6		7.4	3.49	2.57	6	2.5	
598		6.95	.22	18.2		10.9	3.06	2.25	7	2	
601		2.16	.56	18.5		11.5	2.42	1.85	5.5	3	↓
607		5.95	.06	18.3		20.4	.74	.54	7	3	AF
609		3.17	.13	17.9		8.3	.82	.61	7	3	
615		1.99	.28	16.1		12.0	1.11	.82	6	2	
616		5.89	.07	16.0		9.8	.78	.57	7	1	
618		2.42	.10	18.2		10.0	.48	.36	7	3	
620		5.95	.05	16.0		15.9	.60	.43	8	3	↓
622		2.61	.10	16.8		12.1	.52	.38	6.5	3.5	CAL
626		5.90	.07	17.1		17.9	.77	.57	7	3	
628	↓	2.17	.28	17.2	↓	15.0	1.22	.89	6.5	3	↓
575	300	3.67	.58	29.1	1.78	6.3	4.26	2.39	3.5	1.5	
[illegible]		6.36	.60	30.6		6.9	7.03	4.28	3	1.5	
578		6.29	.57	32.0		7.1	7.16	4.03	5.5	2.5	↓
581		3.02	.60	29.5		4.3	3.55	2.00	2	2TO1.5	AF
582		5.43	.58	31.6		7.5	6.30	3.54	3	2	
584		4.17	.60	30.7		5.1	5.00	2.81	2	2	↓
595		5.23	.56	30.8		6.7	5.86	3.29	3	2	CAL
596		6.08	.13	33.0		15.8	1.58	.89	8	5	
598		4.43	.33	31.8		10.7	2.93	1.64	7	3	
599		5.94	.16	31.5		15.2	1.90	1.07	7	3	
602		5.35	.58	29.7		6.9	6.21	3.48	4	2	↓
603		6.07	.16	29.7		16.7	1.94	1.09	5	3.5	AF
605		4.43	.31	30.7		8.2	4.43	2.49	3	2	
606		4.30	.22	30.7		7.7	1.89	1.06	3	2	
608		4.11	.24	26.8		6.9	1.97	1.11	4	2	
610		6.05	.09	30.1		8.5	1.09	.61	7	2	
614		5.91	.12	30.4		7.9	1.42	.80	7	3	
616		5.95	.11	29.6		11.6	1.31	.74	7	3	
617		4.44	.16	30.3		6.0	1.42	.80	5	3	
619		3.27	.50	28.1		3.2	3.27	1.84	2	1	↓
622		4.40	.19	28.8		8.6	1.67	.94	5	3	CAL
623		5.95	.11	32.5		11.2	1.31	.74	6.5	3.5	
627		2.94	.36	30.1		8.8	2.12	1.20	4.5	2	
628		4.38	.16	29.4		11.3	1.40	.79	6	2.5	
632	↓	11.02	.60	29.2	↓	11.3	13.22	7.44	4	2	↓
586	365	15.10	.60	60.8	3.07	5.7	18.12	5.90	5	3	AF
595		3.72	.24	65.8		17.9	1.79	.58	9	4.5	CAL
598		15.20	.28	66.7		9.0	17.61	5.74	6	3	
599		3.78	.52	65.5		12.3	4.00	1.30	6	2.5	
601		2.16	.44	68.8		16.2	1.90	.62	9	4.5	↓
604		1.80	.52	62.1		5.9	1.87	.61	9	3	AF
605		3.72	.19	63.5		4.2	1.42	.46	7.5	4	
610		5.47	.05	54.0		8.1	.55	.18	8.5	4	
619		11.04	.57	54.7		5.2	12.60	4.10	3	2	
620		16.00	.59	53.6		6.2	18.88	6.15	3	2	↓
622		11.05	.60	59.0		6.3	13.26	4.32	3.5	2.5	CAL
623		5.30	.08	65.6		16.8	.85	.28	7	2	
626	↓	3.40	.19	67.1	↓	21.5	1.29	.42	7	3.5	↓

BLANK PAGE

Appendix I

PARAMETER IDENTIFICATION AND CORRELATION TECHNIQUES

A least-squares-fit method for correlating the measured values of stability parameters to the T-33 airplane variable stability gain settings is presented in this appendix. The stability parameters correlated are ω_{sp}, $2\zeta_{sp}\omega_{sp}$, ζ_{sp}, and the steady-state values $(\alpha/\delta_{Es})_{ss}$, $(F_{Es}/n_z)_{ss}$, $(n_z/\alpha)_{ss}$, and $(F_{Es}/\delta_{Es})_{ss}$. The results of these correlation techniques are next used to establish alternate ways of identifying some of the parameters such as undamped natural frequency, ω_{sp}.

I.1 CORRELATION EQUATIONS

The two-degree-of-freedom longitudinal equations of motion for the T-33 airplane can be written as:

$$-\dot{\alpha} + z_{\alpha_{T-33}}\alpha + \dot{\theta} + z_{\delta_{e_{T-33}}}\delta_e = 0 \tag{I.1}$$

$$M_{\dot{\alpha}_{T-33}}\dot{\alpha} + M_{\alpha_{T-33}}\alpha - \ddot{\theta} + M_{\dot{\theta}_{T-33}}\dot{\theta} + M_{\delta_{e_{T-33}}}\delta_e = 0 \tag{I.2}$$

$$n_z = \frac{V_o}{g}(\dot{\theta} - \dot{\alpha}) \tag{I.3}$$

Equation (I.3) is not an independent equation but merely relates the normal acceleration in g's to two variables in the equations, α and θ. The derivatives and symbols are defined in the List of Symbols. Equation (I.1) differs from Equation (3.1) of Section 3.2 in that it contains an elevator lift term ($z_{\delta_{e_{T-33}}}\delta_e$). It is not assumed a priori in the correlation that elevator lift of the T-33 is negligible.

The elevator deflection angle in terms of the independent gain settings (δ_e/α), $(\delta_e/\dot{\alpha})$, $(\delta_e/\dot{\theta})$, and the stick gearing (δ_e/δ_{Es}) can be written as follows:

$$\delta_e = \left(\frac{\delta_e}{\alpha}\right)\alpha + \left(\frac{\delta_e}{\dot{\alpha}}\right)\dot{\alpha} + \left(\frac{\delta_e}{\dot{\theta}}\right)\dot{\theta} + \left(\frac{\delta_e}{\delta_{Es}}\right)\delta_{Es} \tag{I.4}$$

Equation (I.4) assumes that the gain settings are constant and a function of the variable stability gain settings of the T-33 airplane. Equation (I.4) is true only if the elevator servo frequency is quite high compared to the airplane frequency and the sensor lags are quite small. The effects of this assumption on the simulation and the correlation of measured parameters will be discussed later.

By substituting Equation (I. 4) in Equations (I. 1) and (I. 2), and rearranging terms we have:

$$\left[z_{\delta_{e_{T-33}}}\left(\frac{\delta_e}{\dot{\alpha}}\right)-1\right]\dot{\alpha}+\left[z_{\alpha_{T-33}}+z_{\delta_{e_{T-33}}}\left(\frac{\delta_e}{\alpha}\right)\right]\alpha+\left[z_{\delta_{e_{T-33}}}\left(\frac{\delta_e}{\dot{\theta}}\right)+1\right]\dot{\theta}=-z_{\delta_{e_{T-33}}}\left(\frac{\delta_e}{\delta_{ES}}\right)\delta_{ES} \tag{I. 5}$$

$$\left[M_{\dot{\alpha}_{T-33}}+M_{\delta_{e_{T-33}}}\left(\frac{\delta_e}{\dot{\alpha}}\right)\right]\dot{\alpha}+\left[M_{\alpha_{T-33}}+M_{\delta_{e_{T-33}}}\left(\frac{\delta_e}{\alpha}\right)\right]\alpha-\ddot{\theta}+\left[M_{\dot{\theta}_{T-33}}+M_{\delta_{e_{T-33}}}\left(\frac{\delta_e}{\dot{\theta}}\right)\right]\dot{\theta}=-M_{\delta_{e_{T-33}}}\left(\frac{\delta_e}{\delta_{ES}}\right)\delta_{ES} \tag{I. 6}$$

The coefficients of the responses in these equations are the stability derivatives simulated by the variable stability system of the T-33 airplane based on the variable stability gains and the T-33 airplane derivatives for a particular flight condition. By taking Laplace transforms, the transfer functions $\alpha(s)/\delta_{ES}(s)$ and $\theta(s)/\delta_{ES}(s)$ can easily be derived.

$$\frac{\alpha(s)}{\delta_{ES}(s)}=\frac{A_\alpha s+B_\alpha}{C_1 s^2+C_2 s+C_3} \tag{I. 7}$$

$$\frac{\theta(s)}{\delta_{ES}(s)}=\frac{A_\theta s+B_\theta}{s\left(C_1 s^2+C_2 s+C_3\right)} \tag{I. 8}$$

where

$$A_\alpha = z_{\delta_{e_{T-33}}}\left(\frac{\delta_e}{\delta_{ES}}\right)$$

$$B_\alpha = \left(M_{\delta_e} - z_{\delta_e}\ M_{\dot{\theta}}\right)_{T-33}\left(\frac{\delta_e}{\delta_{ES}}\right)$$

$$A_\theta = \left(M_{\delta_e} + z_{\delta_e}\ M_{\dot{\alpha}}\right)_{T-33}\left(\frac{\delta_e}{\delta_{ES}}\right)$$

$$B_\theta = \left(z_{\delta_e}\ M_\alpha - M_{\delta_e}\ z_\alpha\right)_{T-33}\left(\frac{\delta_e}{\delta_{ES}}\right)$$

$$C_1 = \left[1 - Z_{\delta_e}{}_{T-33}\left(\frac{\delta_e}{\dot{\alpha}}\right)\right]$$

$$C_2 = -\left[\left(M_{\dot{\alpha}} + M_{\dot{\theta}} + Z_{\alpha}\right)_{T-33} + \left(M_{\delta_e} - M_{\dot{\theta}} Z_{\delta_e}\right)_{T-33}\left(\frac{\delta_e}{\dot{\alpha}}\right) + Z_{\delta_e}{}_{T-33}\left(\frac{\delta_e}{\alpha}\right) + \left(M_{\delta_e} + M_{\dot{\alpha}} Z_{\dot{\delta}_e}\right)_{T-33}\left(\frac{\delta_e}{\dot{\theta}}\right)\right]$$

$$C_3 = \left[\left(M_{\dot{\theta}} Z_{\alpha} - M_{\alpha}\right)_{T-33} + \left(M_{\dot{\theta}} Z_{\delta_e} - M_{\delta_e}\right)_{T-33}\left(\frac{\delta_e}{\alpha}\right) + \left(M_{\delta_e} Z_{\alpha} - M_{\alpha} Z_{\delta_e}\right)_{T-33}\left(\frac{\delta_e}{\dot{\theta}}\right)\right]$$

From Equation (I. 3), we can write the following transfer function:

$$\frac{n_z(s)}{\delta_{ES}(s)} = \frac{V_o}{g}\left[\frac{\dot{\theta}(s)}{\delta_{ES}(s)} - \frac{\dot{\alpha}(s)}{\delta_{ES}(s)}\right] \qquad \text{(I. 9)}$$

Using Equations (I. 7) and (I. 8), this transfer function assumes the following form:

$$\frac{n_z(s)}{\delta_{ES}(s)} = \frac{A_{n_z} s^2 + B_{n_z} s + C_{n_z}}{C_1 s^2 + C_2 s + C_3} \qquad \text{(I. 10)}$$

where

$$A_{n_z} = -\frac{V_o}{g} Z_{\delta_e}{}_{T-33}\left(\frac{\delta_e}{\delta_{ES}}\right)$$

$$B_{n_z} = \frac{V_o}{g} Z_{\delta_e}{}_{T-33}\left(M_{\dot{\alpha}} + M_{\dot{\theta}}\right)_{T-33}\left(\frac{\delta_e}{\delta_{ES}}\right)$$

$$C_{n_z} = \frac{V_o}{g}\left(Z_{\delta_e} M_{\alpha} - M_{\delta_e} Z_{\alpha}\right)_{T-33}\left(\frac{\delta_e}{\delta_{ES}}\right)$$

From the above transfer functions, it is also possible to write the following:

$$\frac{n_z(s)}{\alpha(s)} = \frac{A_{n_z} s^2 + B_{n_z} s + C_{n_z}}{A_{\alpha} s + B_{\alpha}} \qquad \text{(I. 11)}$$

$$\frac{n_z(s)}{F_{ES}(s)} = \frac{n_z(s)}{\delta_{ES}(s)}\,\frac{\delta_{ES}(s)}{F_{ES}(s)} = \frac{A_{n_z} s^2 + B_{n_z} s + C_{n_z}}{C_1 s^2 + C_2 s + C_3}\,\frac{\delta_{ES}(s)}{F_{ES}(s)} \qquad \text{(I. 12)}$$

ω_{SP} and ζ_{SP}, in terms of the T-33 stability derivatives and the gain settings, can easily be determined from the longitudinal short period characteristic equation:

$$s^2 + \frac{C_2}{C_1} s + \frac{C_3}{C_1} = 0 \tag{I. 13}$$

$$\omega_{SP}^2 = \frac{C_3}{C_1} = \frac{\left[(M_{\dot\theta} Z_\alpha - M_\alpha)_{T-33} + (M_{\dot\theta} Z_{\delta_e} - M_{\delta_e})_{T-33}\left(\frac{\delta_e}{\alpha}\right) + (M_{\delta_e} Z_\alpha - M_\alpha Z_{\delta_e})_{T-33}\left(\frac{\delta_e}{\theta}\right)\right]}{\left[1 - Z_{\delta_e}{}_{T-33}\left(\frac{\delta_e}{\dot\alpha}\right)\right]} \tag{I. 14}$$

$$2\zeta_{SP}\omega_{SP} = \frac{C_2}{C_1} = \frac{-\left[(M_{\dot\alpha} + M_{\dot\theta} + Z_\alpha)_{T-33} + (M_{\delta_e} - M_{\dot\theta} Z_{\delta_e})_{T-33}\left(\frac{\delta_e}{\alpha}\right) + Z_{\delta_e}\left(\frac{\delta_e}{\alpha}\right) + (M_{\delta_e} + M_\alpha Z_{\delta_e})_{T-33}\left(\frac{\delta_e}{\theta}\right)\right]}{\left[1 - Z_{\delta_e}{}_{T-33}\left(\frac{\delta_e}{\dot\alpha}\right)\right]} \tag{I. 15}$$

It is also possible to determine certain steady-state responses from the transfer functions. Assuming a step control input of magnitude δ_{ES} or F_{ES}, we can write the following:

$$\left(\frac{\alpha}{\delta_{ES}}\right)_{ss} = \lim_{s\to 0} \frac{\alpha(s)}{\delta_{ES}(s)} = \frac{B_\alpha}{C_3} = \frac{(M_{\delta_e} - Z_{\delta_e} M_{\dot\theta})_{T-33}\left(\frac{\delta_e}{\delta_{ES}}\right)}{\left[(M_{\dot\theta} Z_\alpha - M_\alpha)_{T-33} + (M_{\dot\theta} Z_{\delta_e} - M_{\delta_e})_{T-33}\left(\frac{\delta_e}{\alpha}\right) + (M_{\delta_e} Z_\alpha - M_\alpha Z_{\delta_e})_{T-33}\left(\frac{\delta_e}{\dot\theta}\right)\right]} \tag{I. 16}$$

$$\left(\frac{n_z}{\alpha}\right)_{ss} = \lim_{s\to 0} \frac{n_z(s)}{\alpha(s)} = \frac{C_{n_z}}{B_\alpha} = \frac{\frac{V_o}{g}\left(Z_{\delta_e} M_\alpha - M_{\delta_e} Z_\alpha\right)_{T-33}}{\left(M_{\delta_e} - Z_{\delta_e} M_{\dot\theta}\right)_{T-33}} \tag{I. 17}$$

$$\left(\frac{n_z}{F_{ES}}\right)_{ss} = \lim_{s\to 0} \frac{n_z(s)}{F_{ES}(s)} = \frac{C_{n_z}}{C_3}\left(\frac{\delta_{ES}}{F_{ES}}\right)_{ss} = \frac{\frac{V_o}{g}\left(Z_{\delta_e} M_\alpha - M_{\delta_e} Z_\alpha\right)_{T-33}\left(\frac{\delta_e}{\delta_{ES}}\right)\left(\frac{\delta_{ES}}{F_{ES}}\right)_{ss}}{\left[(M_{\dot\theta} Z_\alpha - M_\alpha)_{T-33} + (M_{\dot\theta} Z_{\delta_e} - M_{\delta_e})_{T-33}\left(\frac{\delta_e}{\alpha}\right) + (M_{\delta_e} Z_\alpha - M_\alpha Z_{\delta_e})_{T-33}\left(\frac{\delta_e}{\dot\theta}\right)\right]} \tag{I. 18}$$

The equations as shown above are quite complex. It is possible to introduce certain simplifications. A check of the T-33 stability derivatives for the flight conditions used in this program indicates that it is reasonable to make the following assumptions:

$$|Z_{\delta_e} M_{\dot\theta}| << |M_{\delta_e}|$$

$$|M_\alpha Z_{\delta_e}| << |M_{\delta_e} Z_\alpha|$$

$$\left| M_{\dot{\alpha}} \; Z_{\delta_e} \right| << \left| M_{\delta_e} \right|$$

$$\left| Z_{\delta_e} \left(\frac{\delta_e}{\dot{\alpha}} \right) \right| << 1$$

The T-33 stability derivatives were estimated using the data in Reference 17. On the basis of the above assumptions, Equations (I. 14), (I. 15), (I. 16), (I. 17), and (I. 18) assume the following form:

$$\omega_{sp}^2 = \left(M_{\dot{\theta}} Z_\alpha - M_\alpha \right)_{T-33} - M_{\delta_e}{}_{T-33} \left(\frac{\delta_e}{\dot{\alpha}} \right) + \left(M_{\delta_e} Z_\alpha \right)_{T-33} \left(\frac{\delta_e}{\dot{\theta}} \right) \tag{I. 19}$$

$$2\zeta_{sp}\omega_{sp} = -\left(M_{\dot{\alpha}} + M_{\dot{\theta}} + Z_\alpha \right)_{T-33} - M_{\delta_e}{}_{T-33} \left(\frac{\delta_e}{\dot{\alpha}} \right) - Z_{\delta_e}{}_{T-33} \left(\frac{\delta_e}{\alpha} \right) - M_{\delta_e}{}_{T-33} \left(\frac{\delta_e}{\dot{\theta}} \right) \tag{I. 20}$$

$$\left(\frac{\delta_{ES}}{\alpha} \right)_{ss} = \left(\frac{M_{\dot{\theta}} Z_\alpha - M_\alpha}{M_{\delta_e}} \right)_{T-33} \left(\frac{\delta_{ES}}{\delta_u} \right) - \left(\frac{\delta_e}{\alpha} \right) \left(\frac{\delta_{ES}}{\delta_e} \right) + Z_{\alpha_{T-33}} \left(\frac{\delta_e}{\dot{\theta}} \right) \left(\frac{\delta_{ES}}{\delta_e} \right) \tag{I. 21}$$

$$\left(\frac{n_z}{\alpha} \right)_{ss} = - \frac{V_o}{g} Z_{\alpha_{T-33}} \tag{I. 22}$$

$$\left(\frac{F_{ES}}{n_z} \right)_{ss} = - \frac{g}{V_o} \left(\frac{M_{\dot{\theta}} Z_\alpha - M_\alpha}{M_{\delta_e} Z_\alpha} \right)_{T-33} \left(\frac{\delta_{ES}}{\delta_e} \right) \left(\frac{F_{ES}}{\delta_{ES}} \right)_{ss} + \frac{g}{V_o} \left(\frac{1}{Z_\alpha} \right)_{T-33} \left(- \frac{\delta_e}{\alpha} \right) \left(\frac{\delta_{ES}}{\delta_e} \right) \left(\frac{F_{ES}}{\delta_{ES}} \right)_{ss} - \frac{g}{V_o} \left(\frac{\delta_e}{\theta} \right) \left(\frac{\delta_{ES}}{\delta_e} \right) \left(- \frac{F_{ES}}{\delta_{ES}} \right)_{ss} \tag{I. 23}$$

Equations (I. 19) through (I. 23) establish the relationship between the T-33 stability derivatives, the gain settings, and the simulated parameters in the flight program. These equations are strictly true, and the coefficients of the gain settings are the indicated combinations of T-33 stability derivatives only when the servo and sensor lags are negligibly small. This is only true in the case of the simulated frequencies and dampings when the simulated frequencies are small compared to the servo and sensor frequencies. The steady-state equations, Equations (I. 21) to (I. 23), are reasonably accurate, since the only airplane angular rate is the constant pitch rate. Equation (I. 19) does not contain a term with the gain setting δ_e/α . Because of sensor and elevator servo lags, Equation (I. 19) will be valid over a larger simulated frequency range if it contains a term with this gain. Equation (I. 19) now becomes:

$$\omega_{sp}^2 = \left(M_{\dot{\theta}} Z_\alpha - M_\alpha \right)_{T-33} + K_{\omega\dot{\alpha}} \left(\frac{\delta_e}{\dot{\alpha}} \right) - M_{\delta_e}{}_{T-33} \left(\frac{\delta_e}{\alpha} \right) + \left(M_{\delta_e} Z_\alpha \right)_{T-33} \left(\frac{\delta_e}{\dot{\theta}} \right) \tag{I. 24}$$

How these equations are used in fitting all the measured stability parameters to the gain settings used in flight will be discussed later. It is interesting to note that certain relationships exist between the stability parameters. By multiplying Equation (I. 21) by M_{δ_e} (δ_e / δ_{ES}) and substituting in Equation (I. 24) we have:

$$\omega_{sp}^2 = M_{\delta_{e_{T-33}}} \left(\frac{\delta_e}{\delta_{ES}}\right)\left(\frac{\delta_{ES}}{\alpha}\right)_{ss} + K_{\omega_{\dot{\alpha}}} \left(\frac{\delta_e}{\dot{\alpha}}\right) \qquad \text{(I. 25)}$$

Multiplying Equation (I. 23) by $-\frac{V_o}{g} Z_\alpha M_{\delta_{e_{T-33}}} \left(\frac{\delta_e}{\delta_{ES}}\right)\left(\frac{\delta_{ES}}{F_{ES}}\right)_{ss}$ or $\left(\frac{n_z}{\alpha}\right)_{ss} M_{\delta_{e_{T-33}}} \left(\frac{\delta_e}{\delta_{ES}}\right)\left(\frac{\delta_{ES}}{F_{ES}}\right)_{ss}$,

and substituting in Equation (I. 24), we have:

$$\omega_{sp}^2 = M_{\delta_{e_{T-33}}} \left(\frac{\delta_e}{\delta_{ES}}\right)\left(\frac{n_z}{\alpha}\right)_{ss}\left(\frac{\delta_{ES}}{F_{ES}}\right)_{ss}\left(\frac{F_{ES}}{n_z}\right)_{ss} + K_{\omega_{\dot{\alpha}}}\left(\frac{\delta_e}{\dot{\alpha}}\right) \qquad \text{(I. 26)}$$

It is possible to relate Equations (I. 21) and (I. 23). If Equation (I. 23) is multiplied by $-\frac{V_o}{g} Z_{\alpha_{T-33}} \left(\frac{\delta_{ES}}{F_{ES}}\right)_{ss}$ or $\left(\frac{n_z}{\alpha}\right)_{ss}\left(\frac{\delta_{ES}}{F_{ES}}\right)_{ss}$ and substituted in Equation (I. 21) the result is:

$$\left(\frac{\delta_{ES}}{\alpha}\right)_{ss} = \left(\frac{n_z}{\alpha}\right)_{ss}\left(\frac{\delta_{ES}}{F_{ES}}\right)_{ss}\left(\frac{F_{ES}}{n_z}\right)_{ss} \qquad \text{(I. 27)}$$

By multiplying Equation (I. 21) by $-\frac{g}{V_o}\left(\frac{1}{Z_\alpha}\right)_{T-33}\left(\frac{F_{ES}}{\delta_{ES}}\right)_{ss}$ or $\left(\frac{\alpha}{n_z}\right)_{ss}\left(\frac{F_{ES}}{\delta_{ES}}\right)_{ss}$

and substituting in Equation (I. 23):

$$\left(\frac{F_{ES}}{n_z}\right)_{ss} = \left(\frac{\alpha}{n_z}\right)_{ss}\left(\frac{F_{ES}}{\delta_{ES}}\right)_{ss}\left(\frac{\delta_{ES}}{\alpha}\right)_{ss} \qquad \text{(I. 28)}$$

Equations (I. 27) and (I. 28) are merely a way of combining the various measured steady-state responses to obtain the steady-state responses $(\delta_{ES}/\alpha)_{ss}$ and $(F_{ES}/n_z)_{ss}$. These responses can also be measured directly from the oscillograph traces and the consistency of the measured steady-state responses can be established based on the above relationships. Equations (I. 25) and (I. 26) are alternate ways of determining the undamped frequency from measured steady-state values, the elevator gearing, and the T-33 M_{δ_e}. The last term in these equations is usually a small term and represents the effect of ($\delta_e/\dot{\alpha}$) gain on the simulated frequency. How this term and the M_{δ_e} of the T-33 are determined through a least-squares-fit process is discussed in Section I. 2.

I. 2 CORRELATION TECHNIQUES

Equations (I. 20) through (I. 24) were the basic equations used to correlate the measured frequencies, damping, and steady-state values to the gain settings used in the simulation for each of the flight conditions. There was some effect of differences in fuel remaining during the simulation on the basic T-33 stability derivatives, and, therefore, the simulated derivatives vary with fuel remaining for a given set of gain settings. As stated in Section IV, these effects were kept to a minimum for any given flight condition by always performing simulations using the same flight condition sequence, 300 kts, 220 kts, and 365 kts IAS. The effect of small differences on fuel remaining can be adequately accounted for by adding a term to the equations that accounts for the changes in the basic (unaugmented) T-33 characteristics with fuel remaining. Equations (I. 24), (I. 20), and (I. 22) now become:

$$\omega_{sp}^2 = \left(M_{\dot\theta} Z_\alpha - M_\alpha\right)_{o_{T-33}} + \left[\frac{\partial(M_{\dot\theta} Z_\alpha - M_\alpha)}{\partial(FR)}\right]_{T-33}(\Delta FR) + K_{\omega_{\dot\alpha}}\left(\frac{\delta_e}{\dot\alpha}\right) - M_{\delta_{e_{T-33}}}\left(\frac{\delta_e}{\alpha}\right) + \left(M_{\delta_e} Z_\alpha\right)_{T-33}\left(\frac{\delta_e}{\theta}\right) \quad \text{(I. 29)}$$

$$2\zeta_{sp}\omega_{sp} = -\left(M_{\dot\alpha} + M_{\dot\theta} + Z_\alpha\right)_{o_{T-33}} + \left[\frac{\partial(M_{\dot\alpha} + M_{\dot\theta} + Z_\alpha)}{\partial(FR)}\right]_{T-33}(\Delta FR) - M_{\delta_{e_{T-33}}}\left(\frac{\delta_e}{\dot\alpha}\right) - Z_{\delta_{e_{T-33}}}\left(\frac{\delta_e}{\alpha}\right) - M_{\delta_{e_{T-33}}}\left(\frac{\delta_e}{\theta}\right) \quad \text{(I. 30)}$$

$$\left(\frac{n_z}{\alpha}\right)_{ss} = -\left(\frac{V_o}{g} Z_\alpha\right)_{o_{T-33}} + \frac{\partial\left(\frac{V_o}{g} Z_\alpha\right)}{\partial(FR)}(\Delta FR) \quad \text{(I. 31)}$$

The quantities with subscript 0 refer to the basic T-33 values of ω_{sp}^2, $2\zeta_{sp}\omega_{sp}$, and $\left(\frac{n_z}{\alpha}\right)_{ss}$ for a particular flight condition at a specified average value of fuel remaining (FR). The quantity (ΔFR) is the change in fuel remaining from this average value.

The response parameters measured from oscillograph traces and the variable stability gain settings used in the simulation were fitted to the gain setting equations[(Equations (I. 21), (I. 23), (I. 29), (I. 30), and (I. 31)]. The fit was a least-squares fit, and the quantities determined were the constant coefficients of the gain setting terms. These coefficients are composed of the basic T-33 stability derivatives.

Once the least-squares-fit coefficients of the equation for a particular parameter, such as ω_{sp}^2 , have been determined, it is possible to compute the parameter from the equation using the proper gains and the determined coefficients. These least-squares-fit parameters can then be compared to the actual measured parameter to determine the degree of correlation based on the assumed fit equation.

The correlations in general were quite good as indicated by Figures I. 1 to I. 30. The least-squares-fit parameters and the measured parameters are presented in Tables VII, VIII, and IX.

I. 3 DISCUSSION OF CORRELATIONS - ALTERNATE METHODS OF IDENTIFICATION

The discussion and explanation presented here will be concerned only with the flight condition of 220 kts IAS, but applies equally as well to the results at 300 kts and 365 kts.

Figure I. 1 compares the least-squares-fit undamped frequencies using Equation (I. 29) to the actual measured frequencies for the simulated configurations at 220 kts IAS. The solid points represent data not used in the fit, since preliminary fits indicated these data to be poor. Once the fit was determined however, the frequency was computed for these poor correlation points and compared to the measured frequency to show the degree of deviation of the poor point from the correlation line.

A similar comparison (Figure I. 3) is made for $2\zeta_{sp}\omega_{sp}$ at 220 kts IAS by fitting Equation (I. 30). Using least-squares-fit values of ω_{sp}^2 and $2\zeta_{sp}\omega_{sp}$, it is next possible to determine a least-squares-fit value for ζ_{sp}. Comparisons of ζ_{sp} are made in Figure I. 4 for 220 kts IAS.

Least-squares-fit (LSF) values of the steady-state parameters α/δ_{es}, n_z/α, and F_{es}/n_z were determined by fitting the measured data and the gain settings to Equations (I. 21), (I. 31), and (I. 23). Measured and LSF steady-state values are compared for 220 kts IAS in Figures I. 5, I. 7, and I. 8. The points not used in the least-squares fitting process are again shown as solid points.

In some cases, LSF values of the steady-state parameters compare well with the measured values, even though the measured and LSF frequencies do not compare well. This is especially true at the higher frequencies simulated. (Compare Figures I. 10 and I. 15.) Under such conditions, it is possible to determine a "best estimate" value of frequency using the measured steady-state parameters, the elevator gearing (δ_e/δ_{es}), and the T-33 M_{δ_e} from Equation (I. 25) or (I. 26). The T-33 value of M_{δ_e} is determined from the LSF values of $(M_{\dot\theta} z_\alpha - M_\alpha)/M_{\delta_e}$ and $(M_{\dot\theta} z_\alpha - M_\alpha)$ for the T-33 airplane obtained from the fit of Equations (I. 21) and (I. 29), respectively.

$$M_{\delta_e} = \frac{(M_{\dot\theta}\, z_\alpha - M_\alpha)_{T-33}}{\left(\dfrac{M_{\dot\theta}\, z_\alpha - M_\alpha}{M_{\delta_e}}\right)_{T-33}}$$

Incidentally, frequencies determined from Equation (I. 25) or (I. 26) compare well with frequencies measured directly from the oscillograph traces when such measurements can be accurately made (i.e., the frequencies are not too high or too low). Frequencies determined from measured steady-state values are shown as the solid points in Figure I. 2 for 220 kts IAS. The "best estimate" frequencies plotted in Figure I. 2 are the best estimate values shown in Table VII, and represent the best estimate of the measured frequencies determined either directly from flight data, or indirectly using Equations (I. 25) or (I. 26). The indirectly determined best estimate frequencies are indicated in Table VII with a double asterisk.

From the best estimate values of ω_{sp} and the measured ζ_{sp}, best estimate values of $2\zeta_{sp}\omega_{sp}$ have been determined and compared to least-squares-fit values in Figure I. 13 for 300 kts IAS.

In a few instances, steady-state values of $(\delta_{es}/\alpha)_{ss}$ or $(F_{es}/n_z)_{ss}$ do not compare well with the LSF or computed values based on the gain settings. Alternate ways of checking $(\delta_{es}/\alpha)_{ss}$ or $(F_{es}/n_z)_{ss}$ based on the other steady-state values are indicated by Equations (I. 27) and (I. 28). When the checked values of $(\delta_{es}/\alpha)_{ss}$ or $(F_{es}/n_z)_{ss}$ appeared to be better than the directly measured values, they were used as the best estimate values in Tables VII, VIII, and IX, and are plotted as Figures I. 6 and I. 9 for 220 kts IAS.

A similar procedure was used in correlating and fixing the values of the parameters simulated at the other two flight conditions -- 300 kts and 365 kts IAS. Comparisons between measured and LSF values and between best estimate and LSF values are shown as Figures I. 10 through I. 30. The best estimate values of the parameters simulated are tabulated in Tables VIII and IX.

It is obvious from the correlations and alternate methods of identification used, that the parameters simulated in flight have been reasonably well identified. Some specific questionable points still exist, and these are discussed in conjunction with the pilot rating and comments for these specific configurations in Section VII.

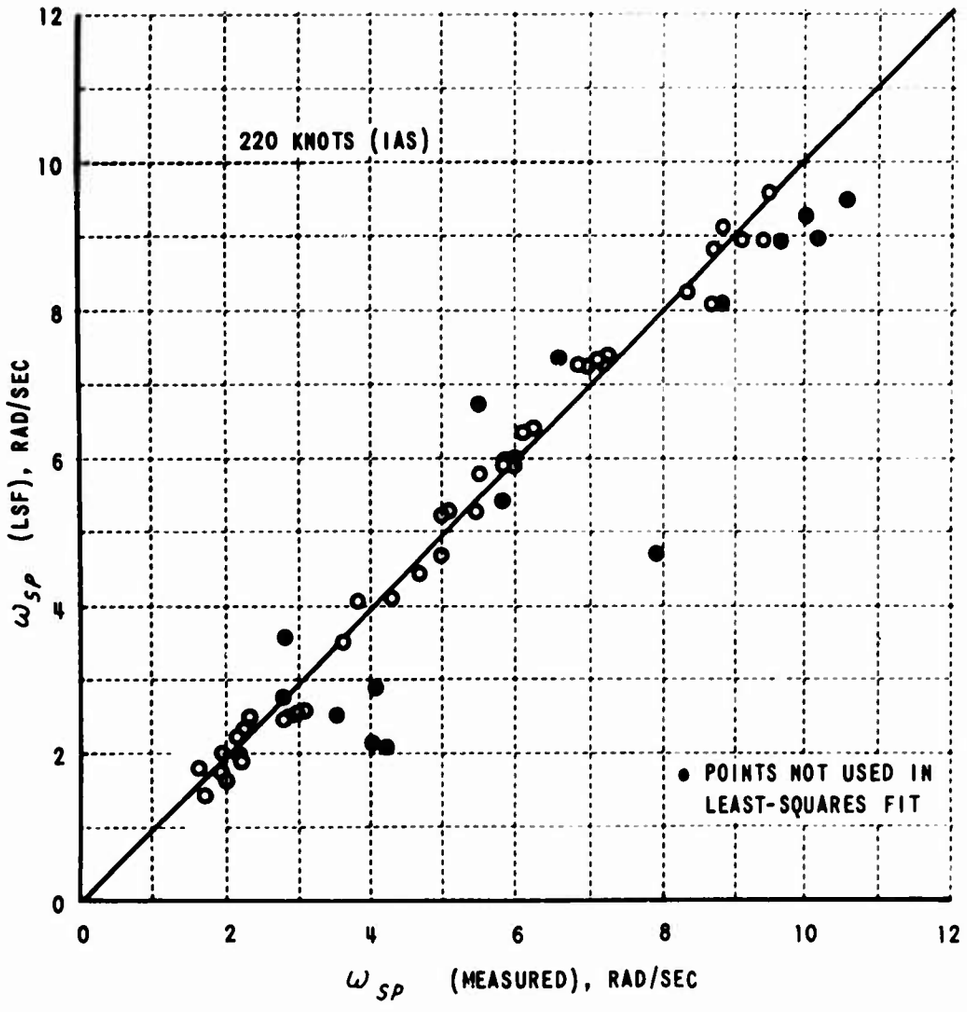

Figure I.1 COMPARISON OF LEAST-SQUARES FIT (LSF) AND MEASURED UNDAMPED FREQUENCIES (ω_{SP}) SIMULATED

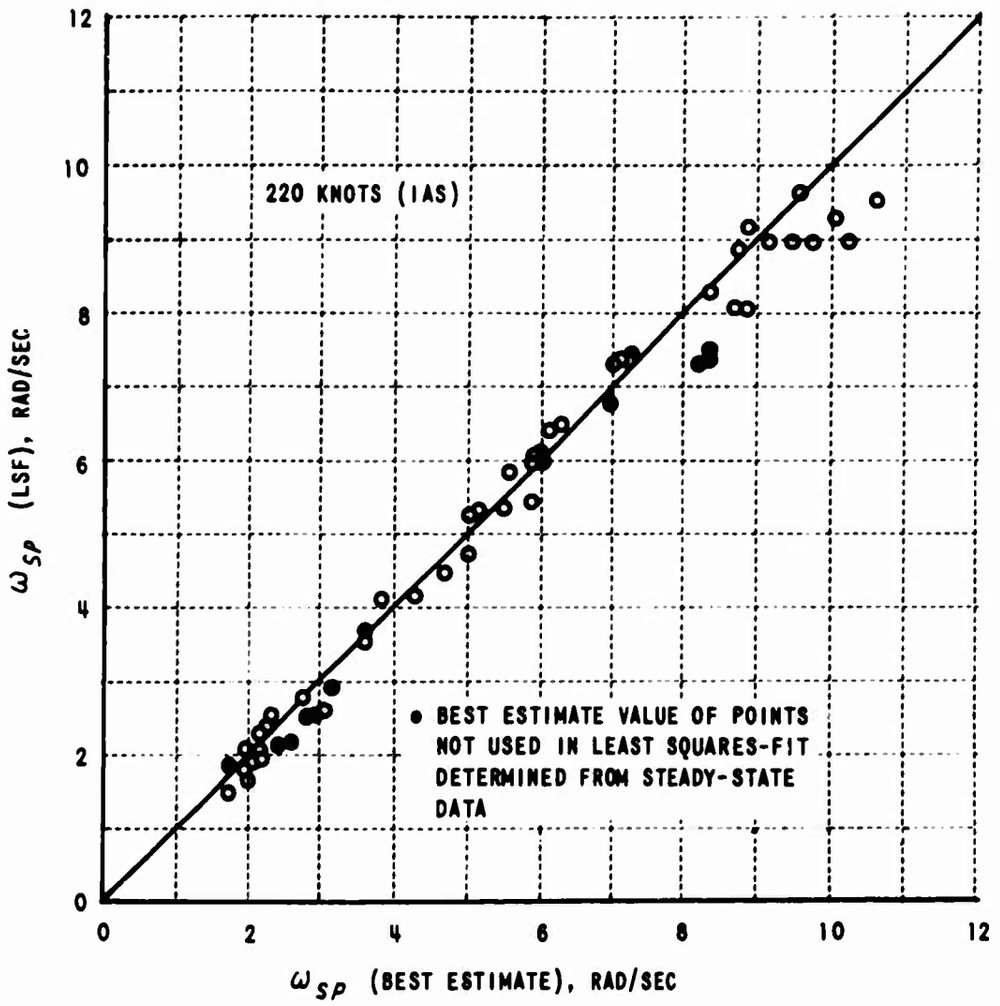

Figure I.2 COMPARISON OF LEAST-SQUARES FIT (LSF) AND BEST ESTIMATE UNDAMPED FREQUENCIES (ω_{sp}) SIMULATED

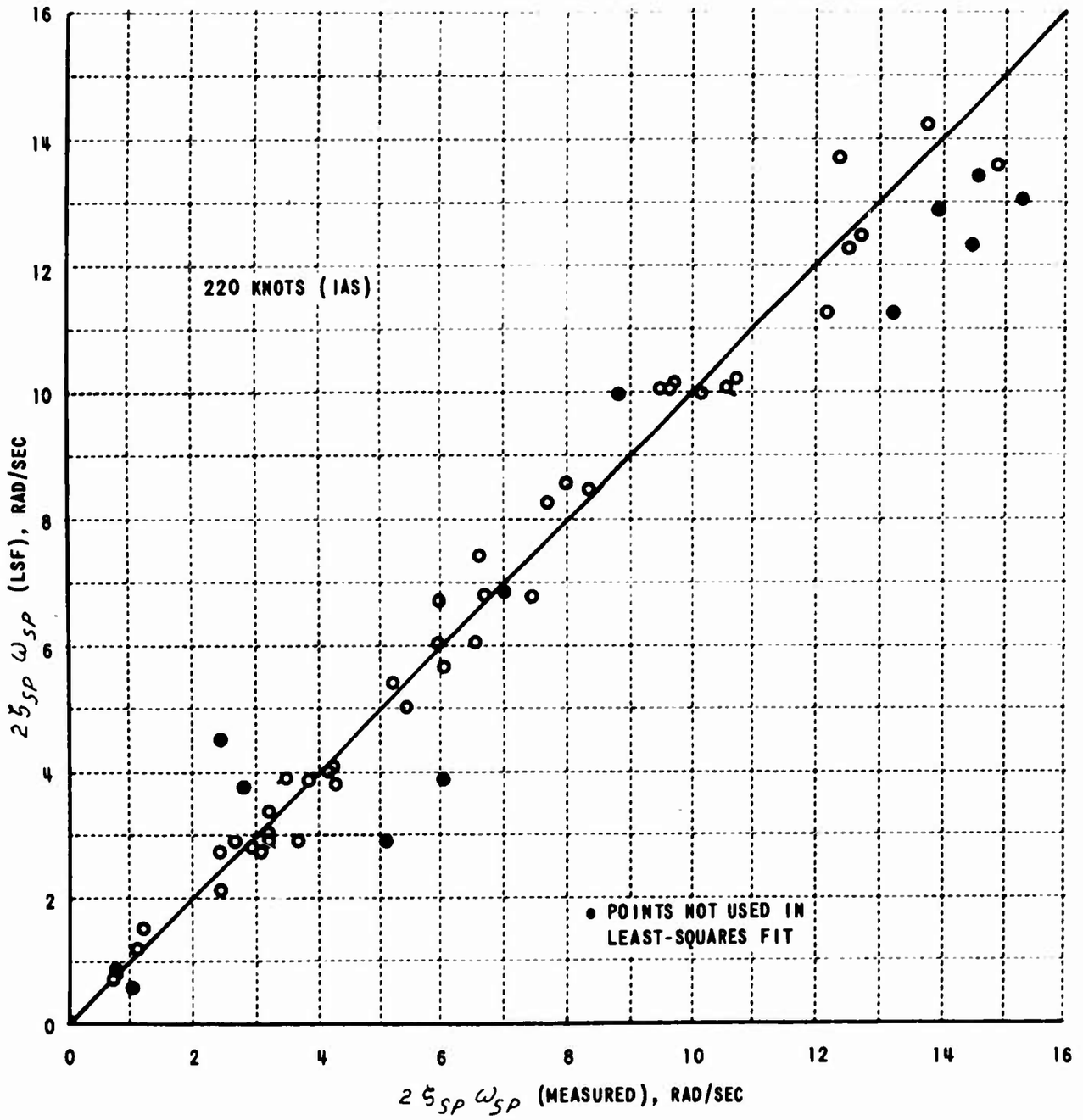

Figure I.3 COMPARISON OF LEAST-SQUARES FIT (LSF) AND MEASURED $2\zeta_{SP}\omega_{SP}$ SIMULATED

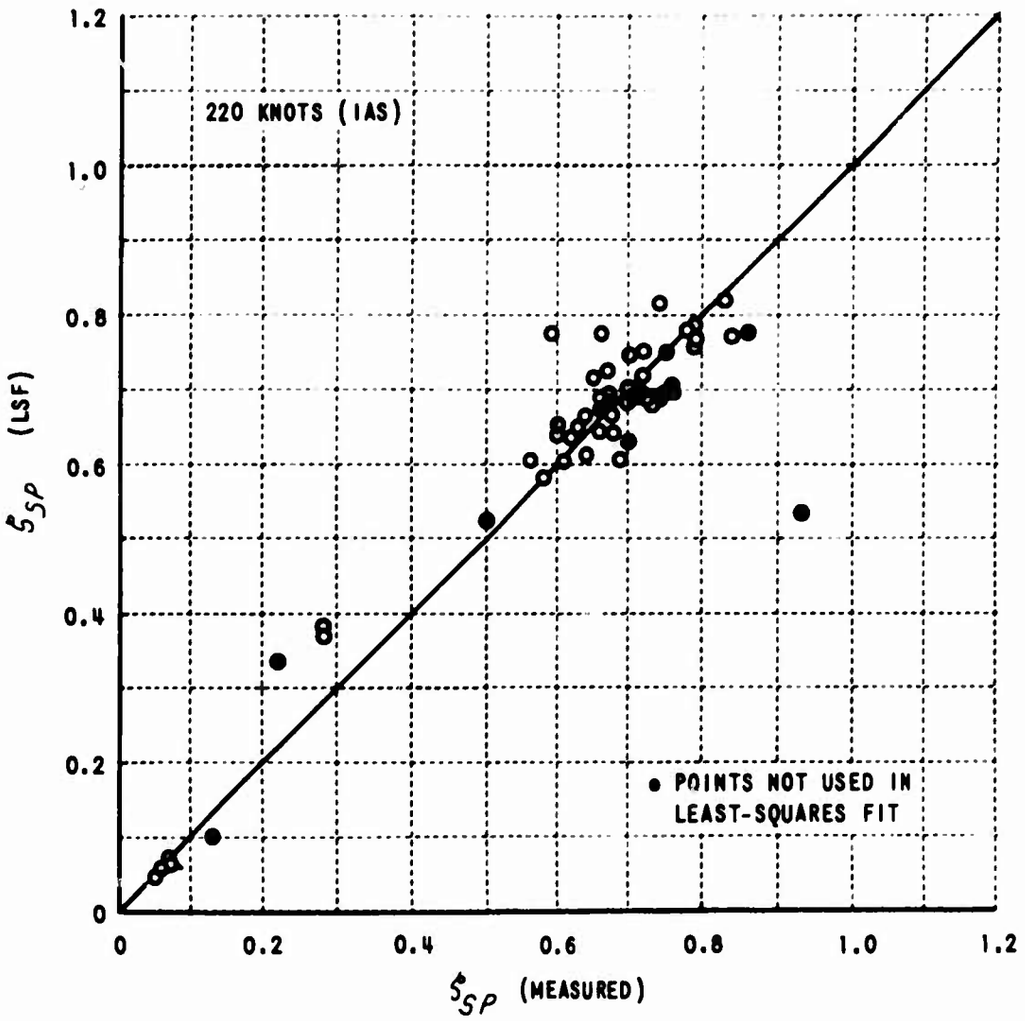

Figure I.4 COMPARISON OF LEAST-SQUARES FIT (LSF) AND MEASURED VALUES OF DAMPING RATIO (ζ_{SP}) SIMULATED

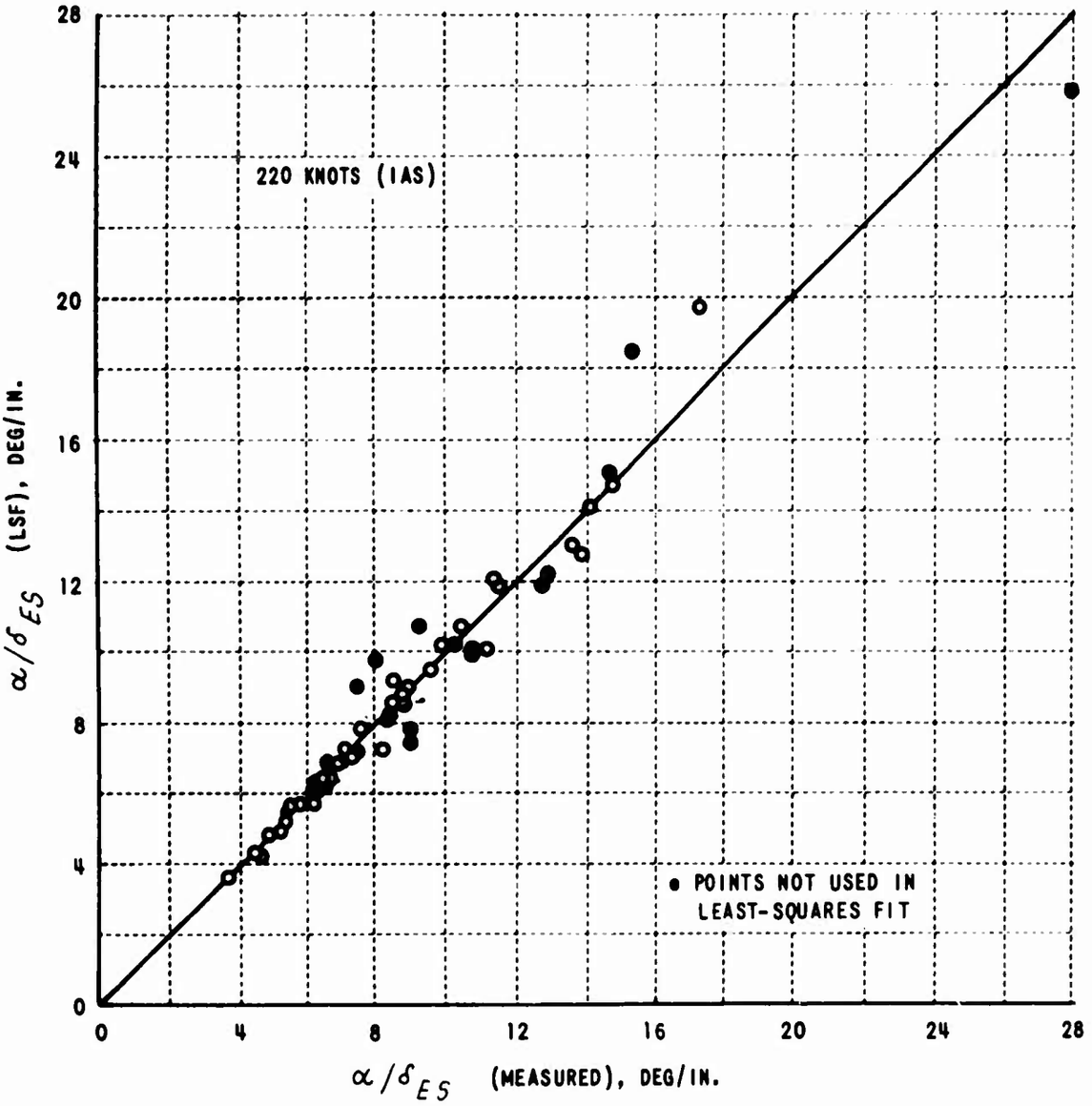

Figure I.5 COMPARISON OF LEAST-SQUARES FIT (LSF) AND MEASURED VALUES OF STEADY-STATE α/δ_{ES} SIMULATED

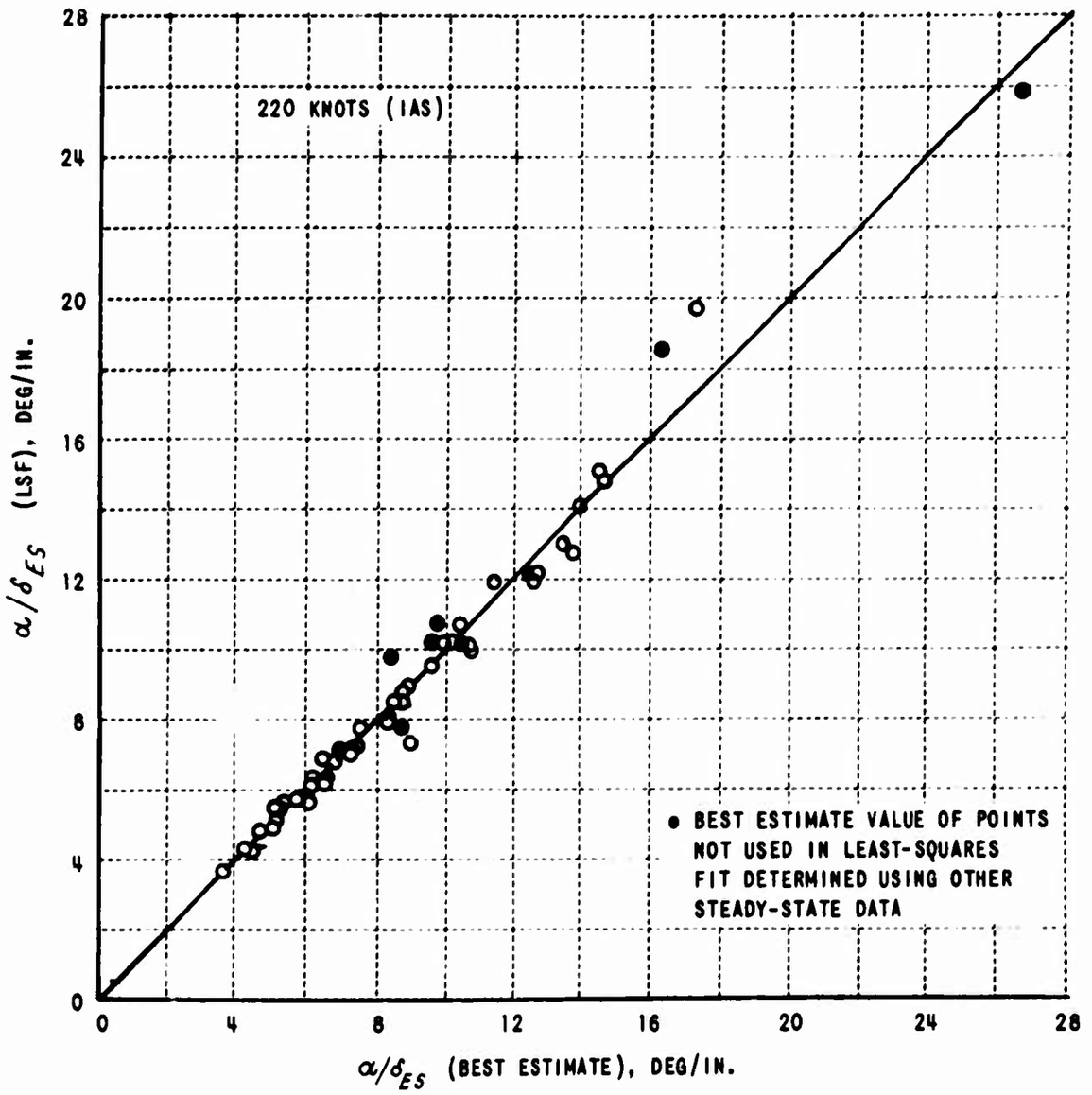

Figure I.6 COMPARISON OF LEAST-SQUARES FIT AND BEST ESTIMATE STEADY-STATE α/δ_{ES} SIMULATED

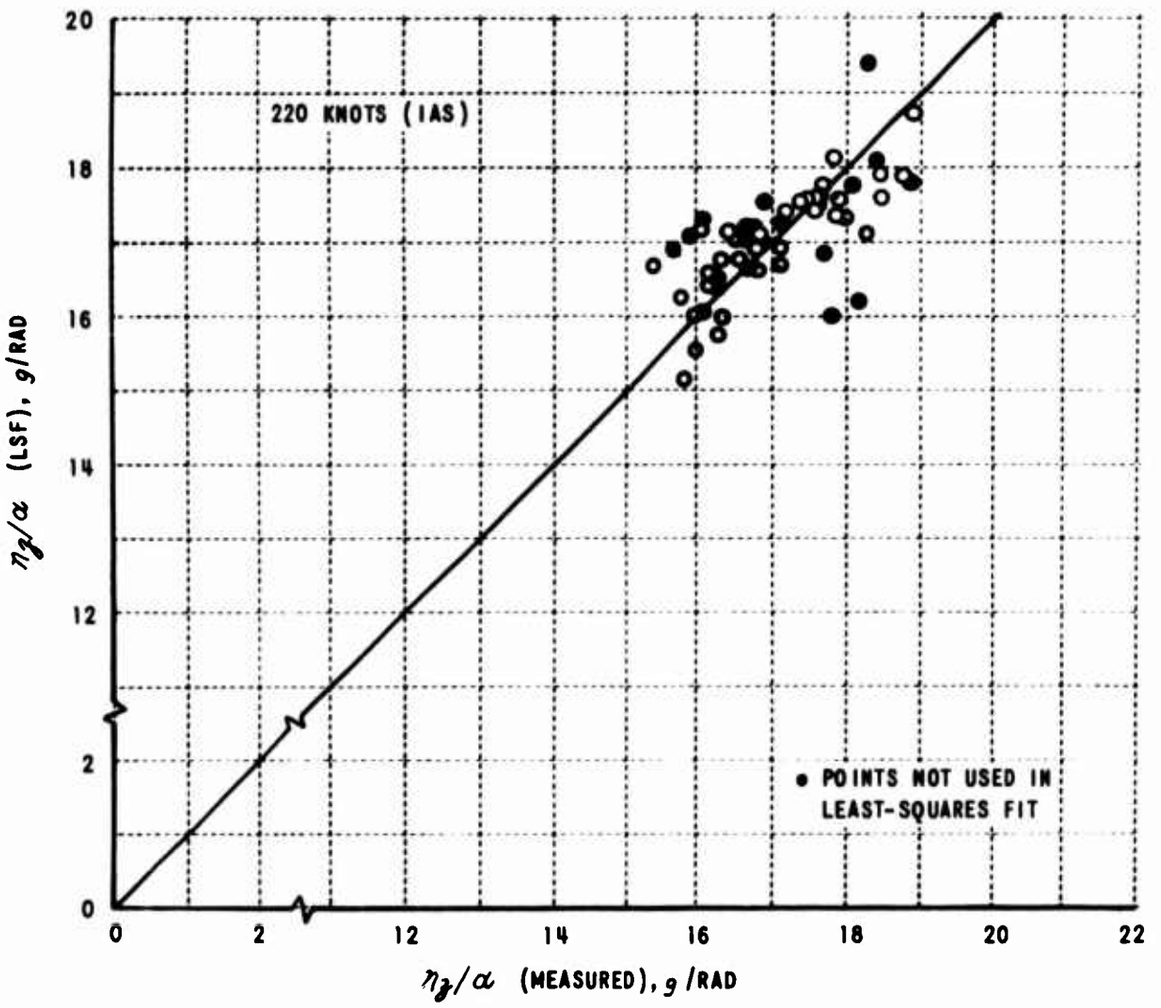

Figure I.7 COMPARISON OF LEAST-SQUARES FIT (LSF) AND MEASURED STEADY-STATE n_z/α SIMULATED

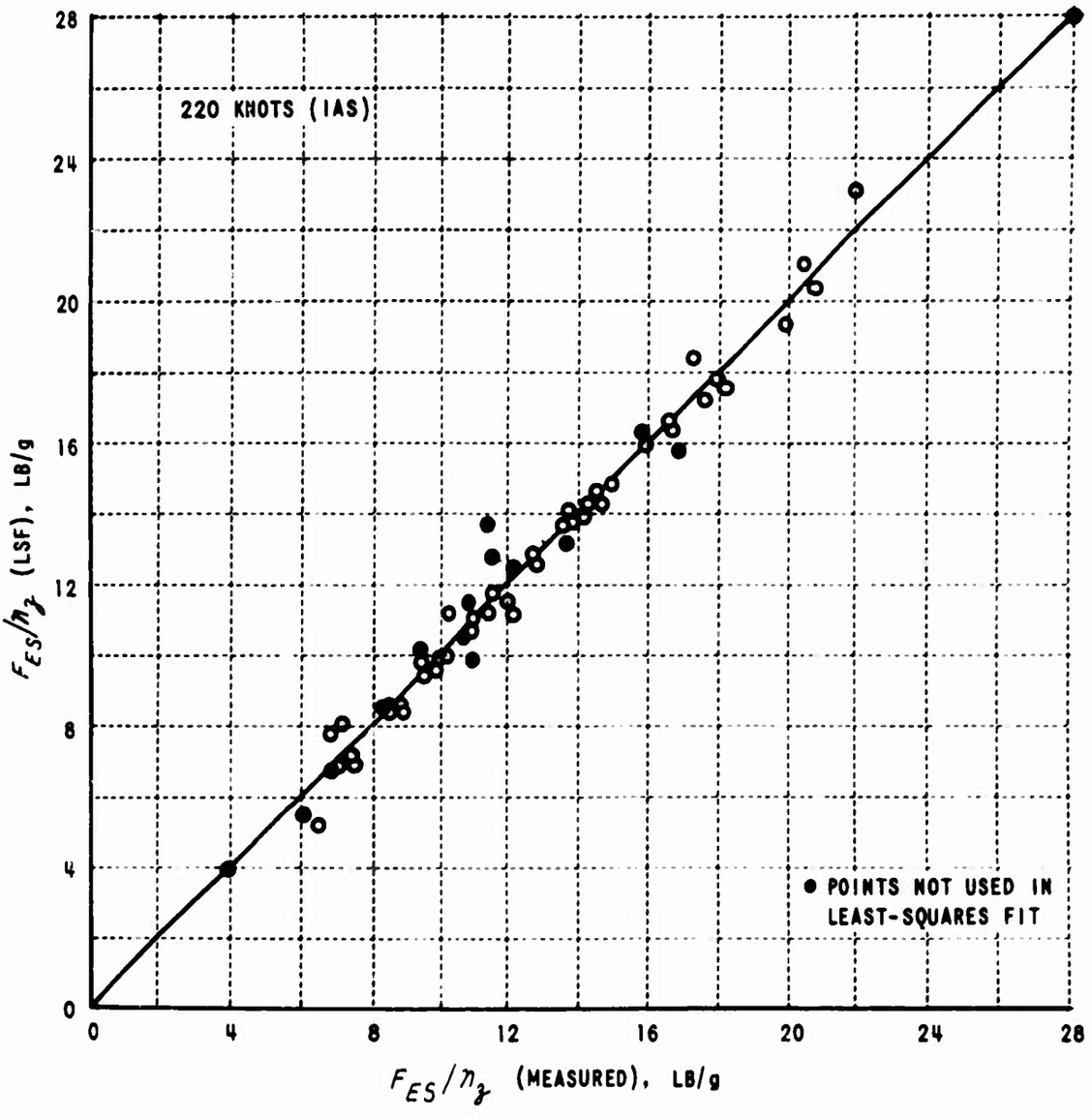

Figure I.8 COMPARISON OF LEAST-SQUARES FIT (LSF) AND MEASURED STEADY-STATE F_{ES}/n_z SIMULATED

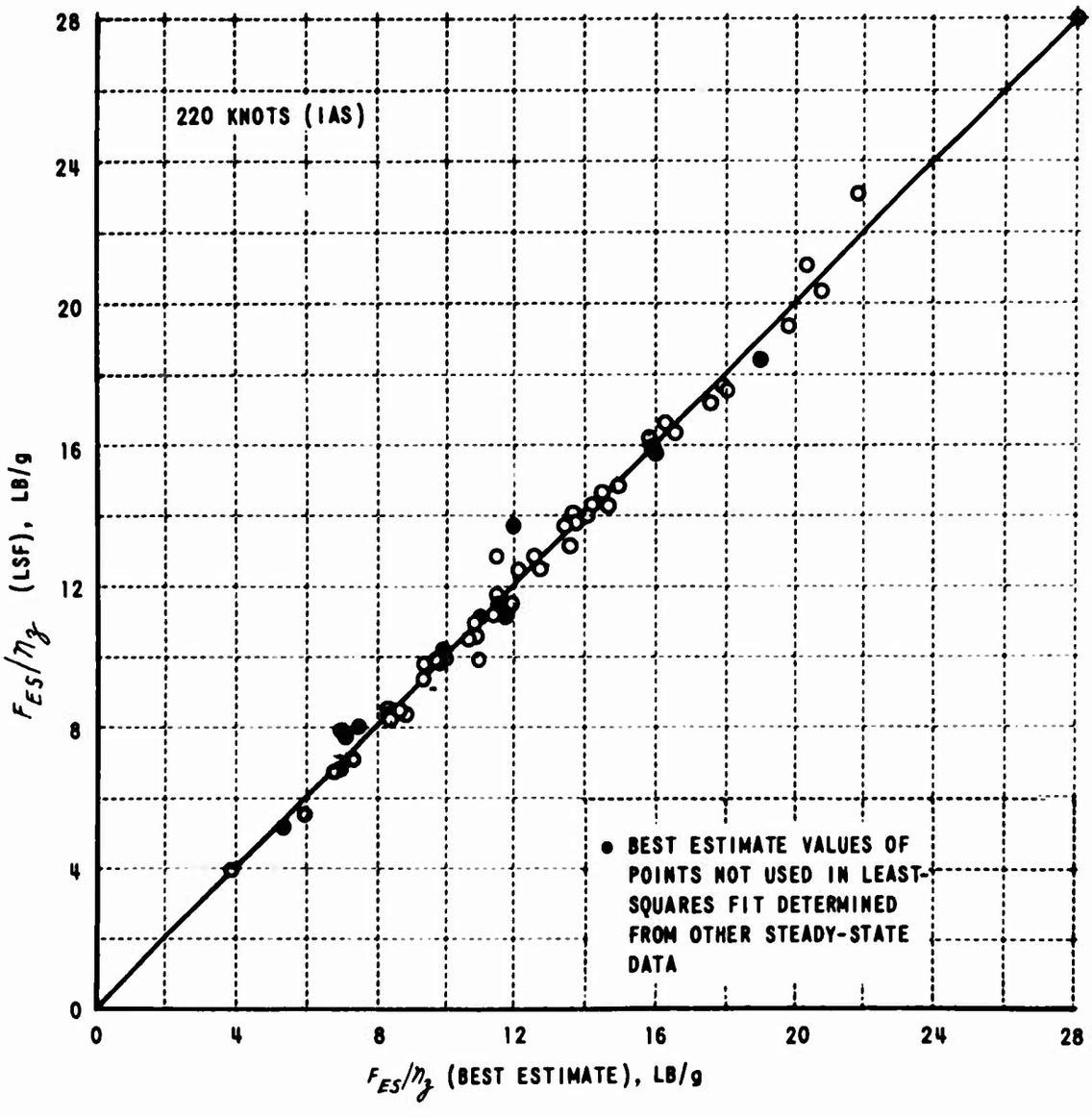

Figure I.9 COMPARISON OF LEAST-SQUARES FIT (LSF) AND BEST ESTIMATE VALUE OF STEADY-STATE F_{ES}/n_z SIMULATED

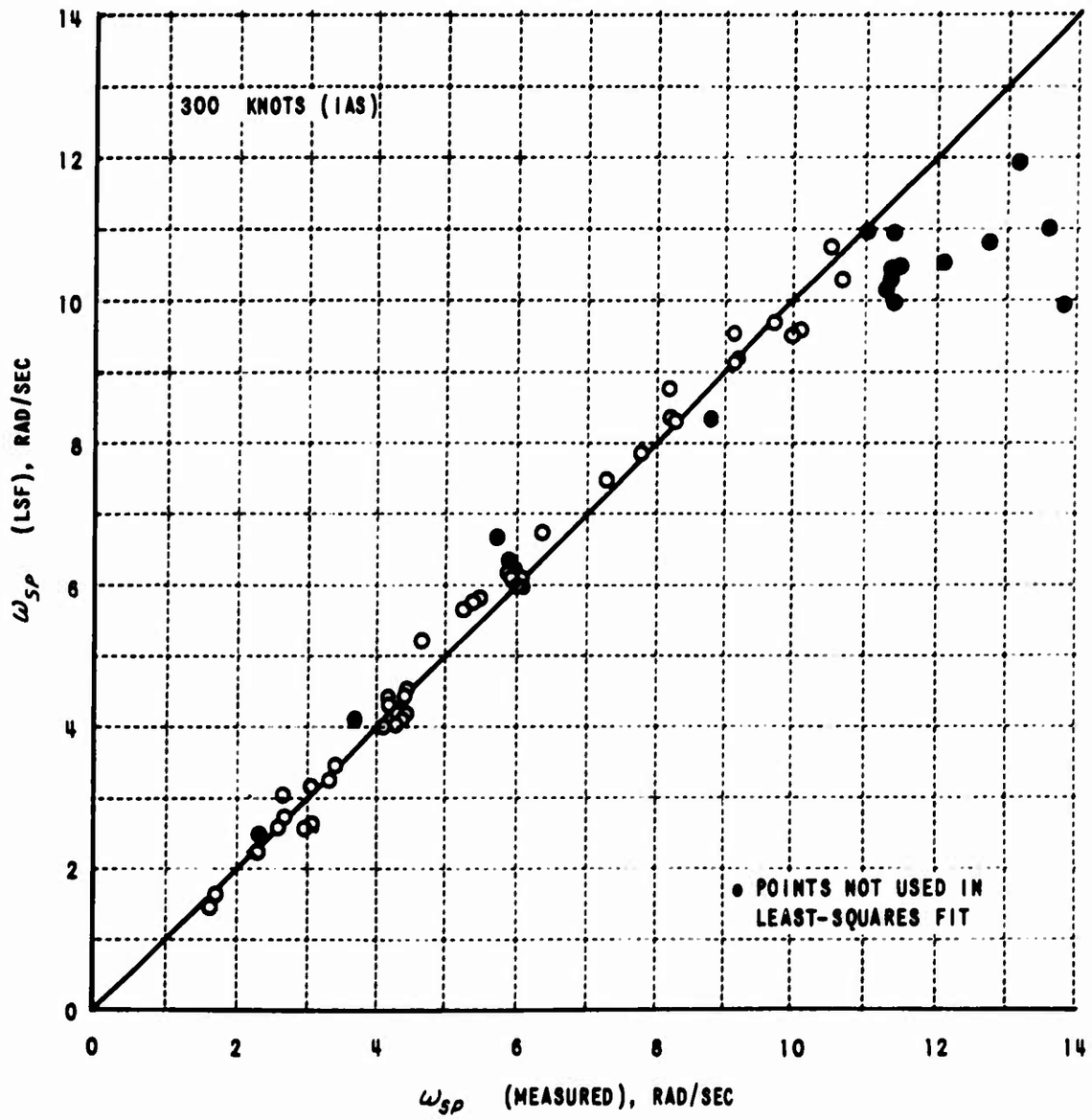

Figure I.10 COMPARISON OF LEAST-SQUARES FIT (LSF) AND MEASURED UNDAMPED FREQUENCIES ω_{sp} SIMULATED

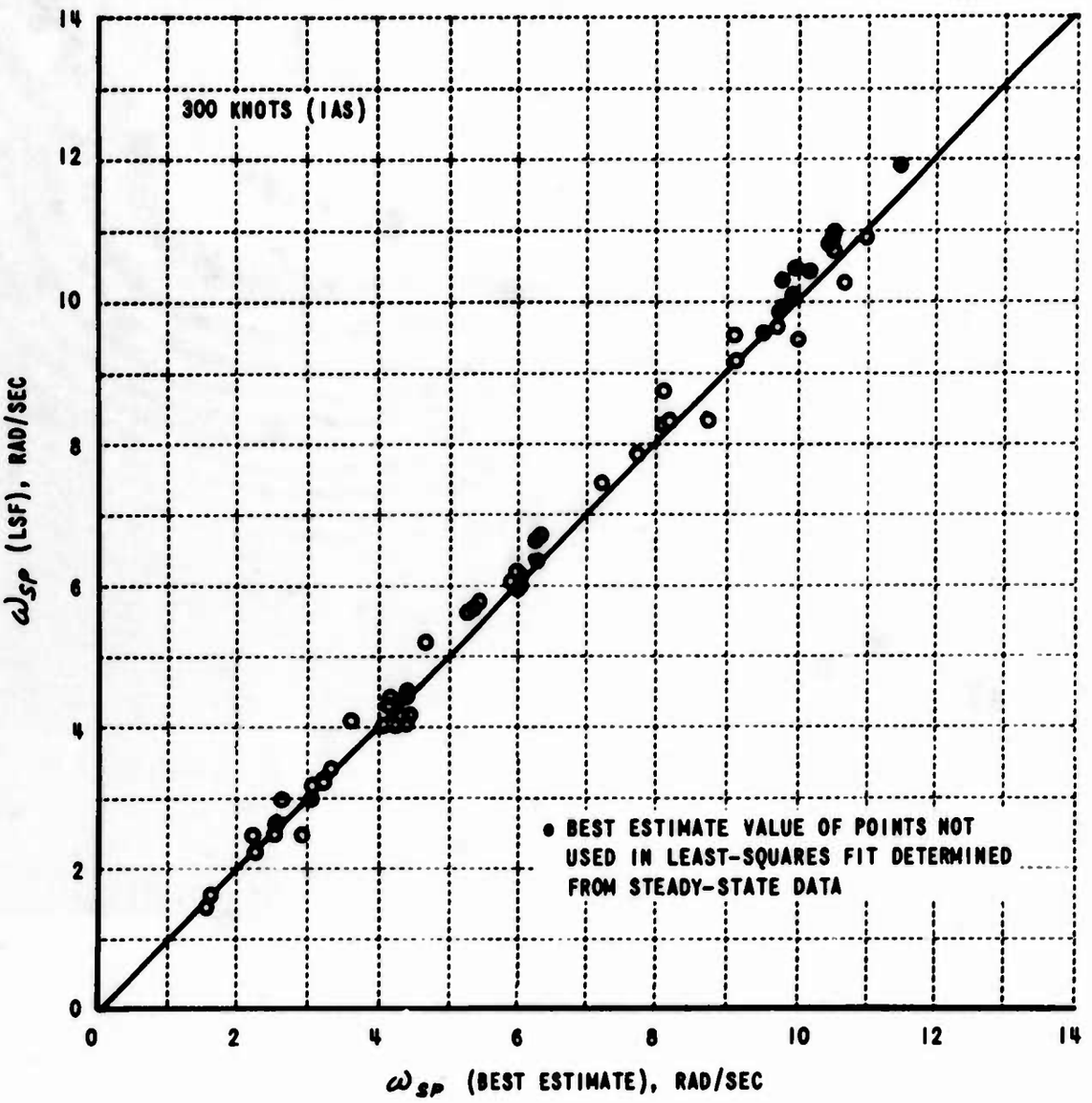

Figure I.11 COMPARISON OF LEAST-SQUARES FIT (LSF) AND BEST ESTIMATE UNDAMPED FREQUENCIES (ω_{sp}) SIMULATED

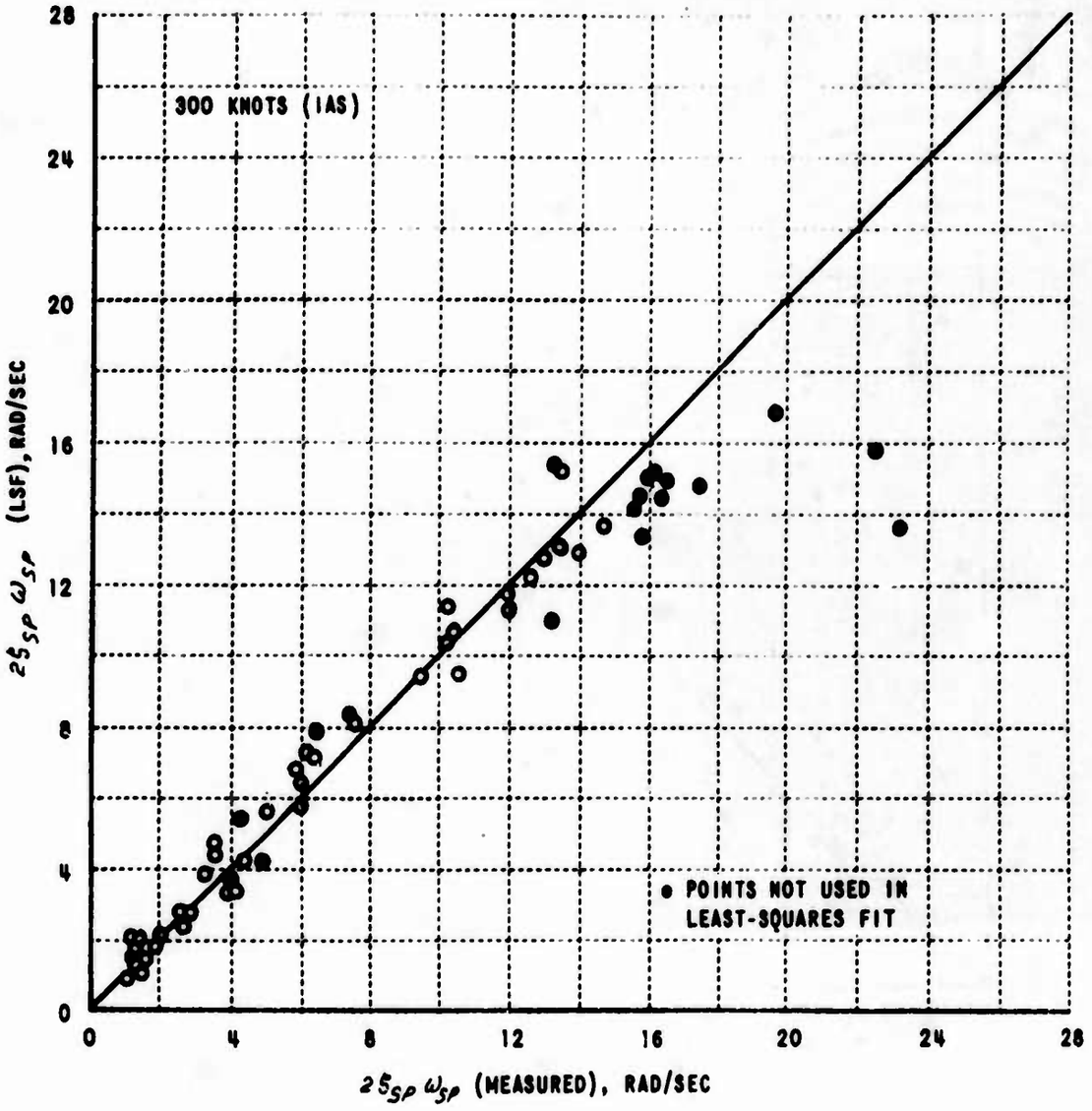

Figure I.12 COMPARISON OF LEAST-SQUARES FIT (LSF) AND MEASURED $2\zeta_{SP}\omega_{SP}$ SIMULATED

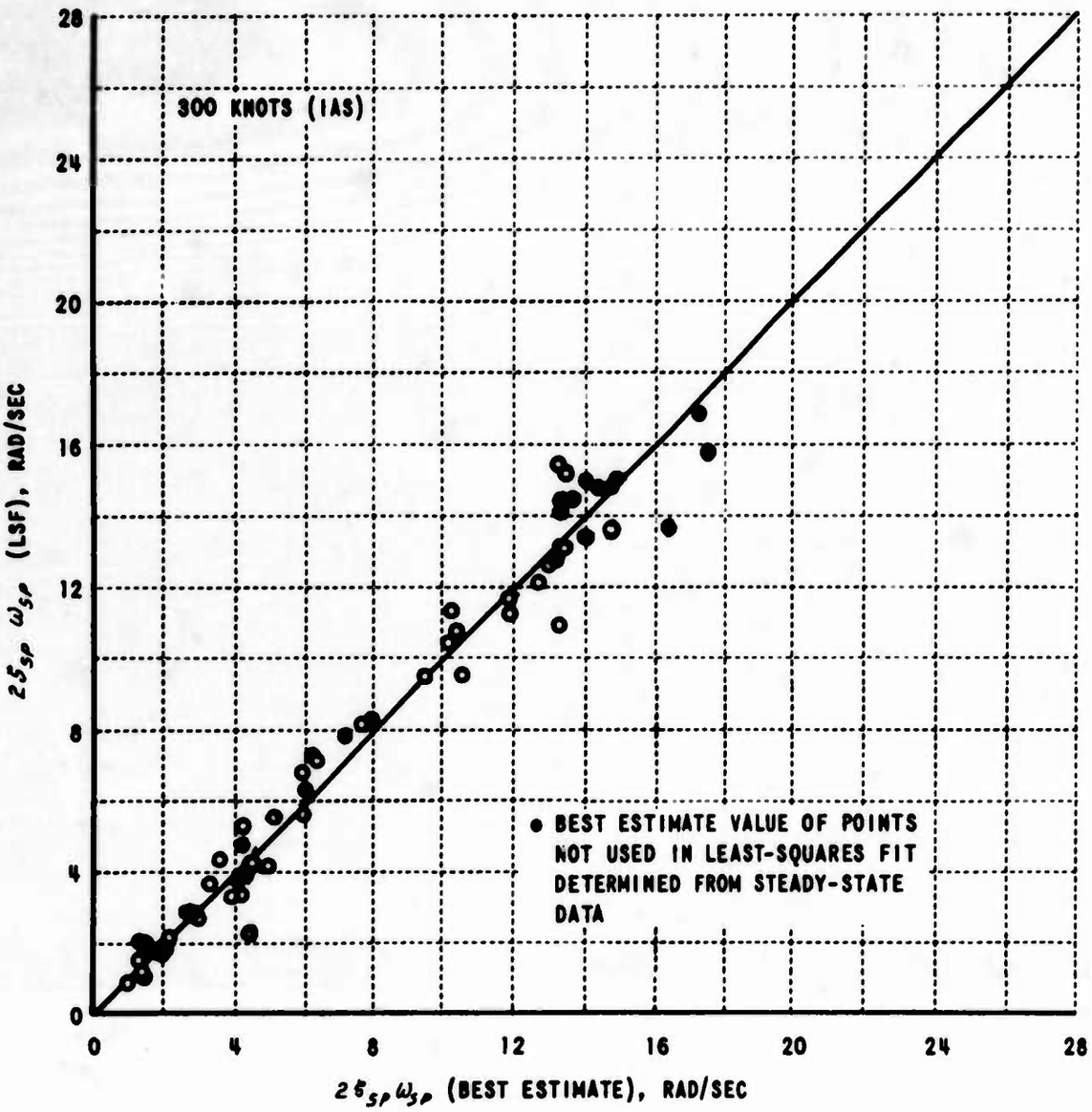

Figure I.13 COMPARISON OF LEAST-SQUARES FIT (LSF) AND BEST ESTIMATE $2\zeta_{sp}\,\omega_{sp}$ SIMULATED

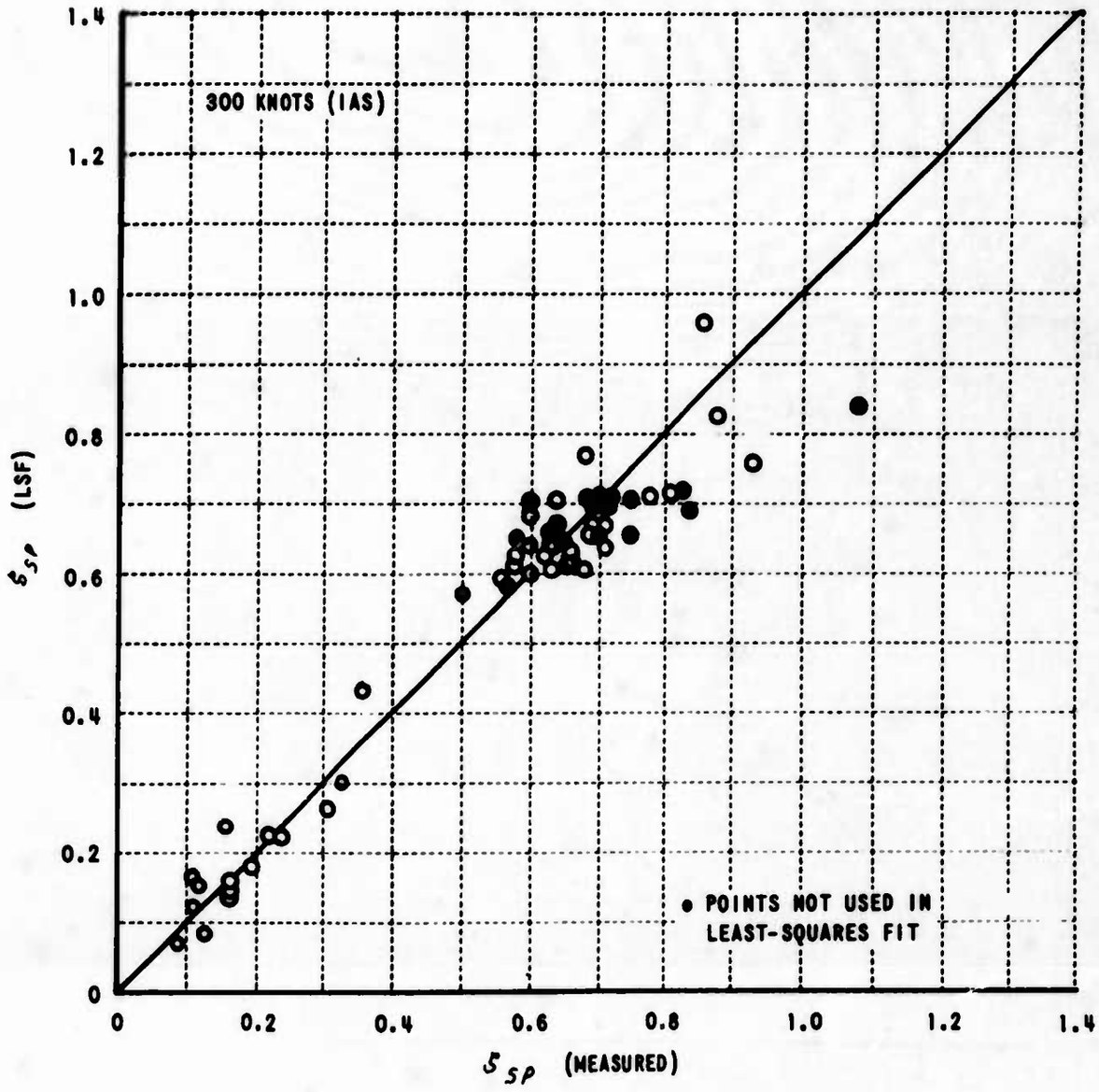

Figure I.14 COMPARISON OF LEAST-SQUARES FIT (LSF) AND MEASURED VALUES OF DAMPING RATIO (ζ_{sp}) SIMULATED

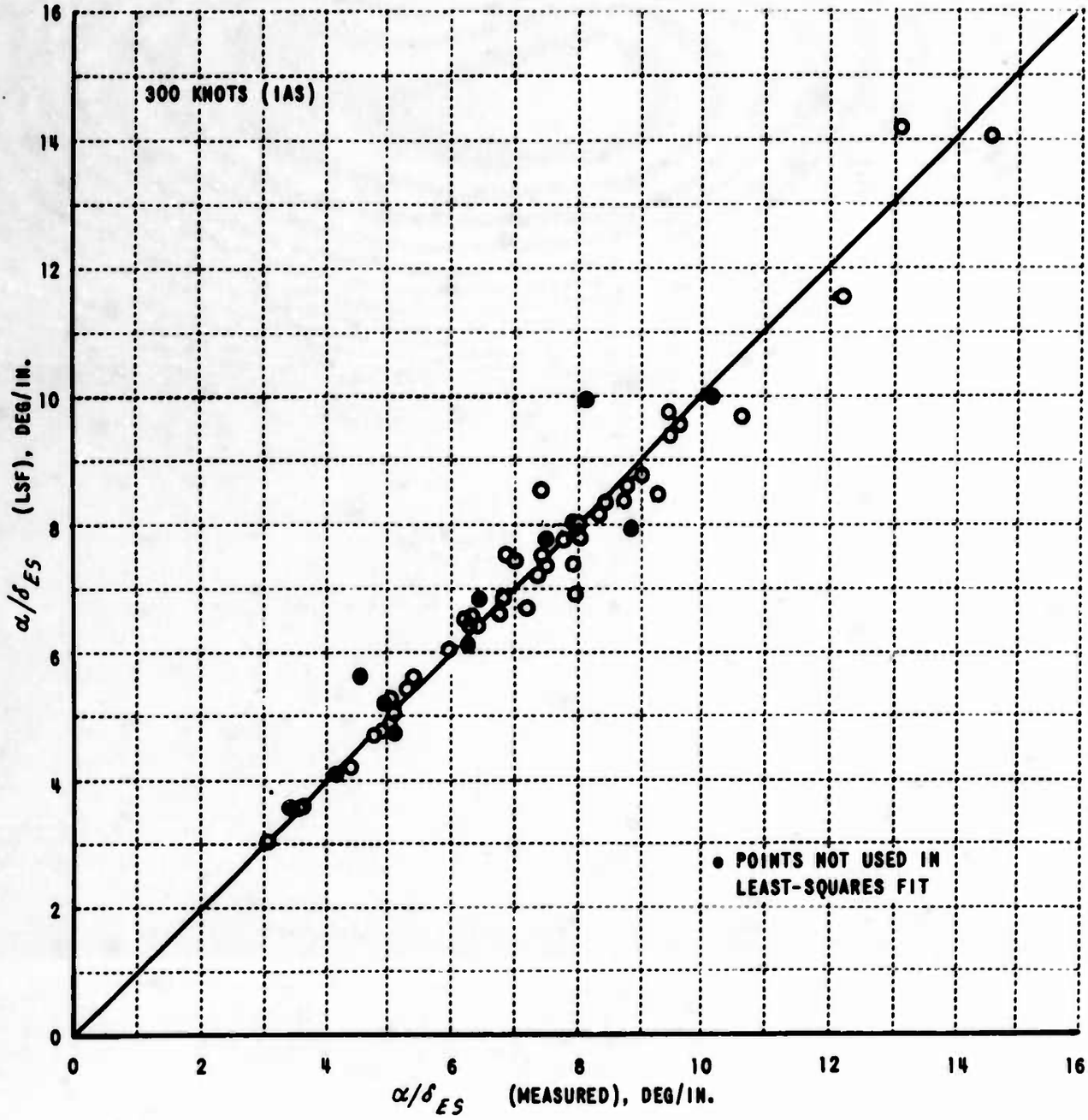

Figure I.15 COMPARISON OF LEAST-SQUARES FIT (LSF) AND MEASURED VALUE OF STEADY-STATE α/δ_{ES} SIMULATED

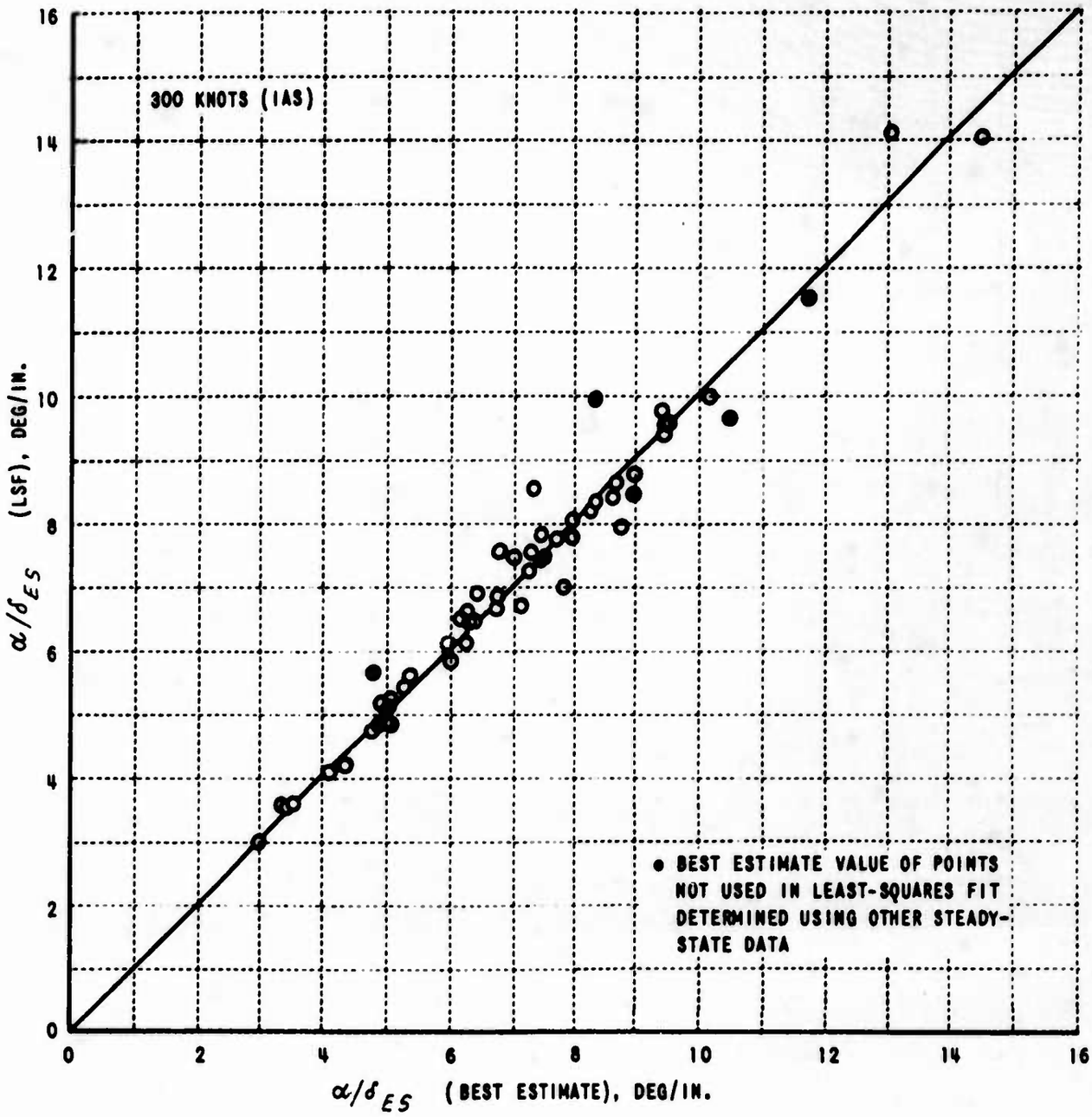

Figure I.16 COMPARISON OF LEAST-SQUARES FIT (LSF) AND BEST ESTIMATE VALUE OF STEADY-STATE α/δ_{ES} SIMULATED

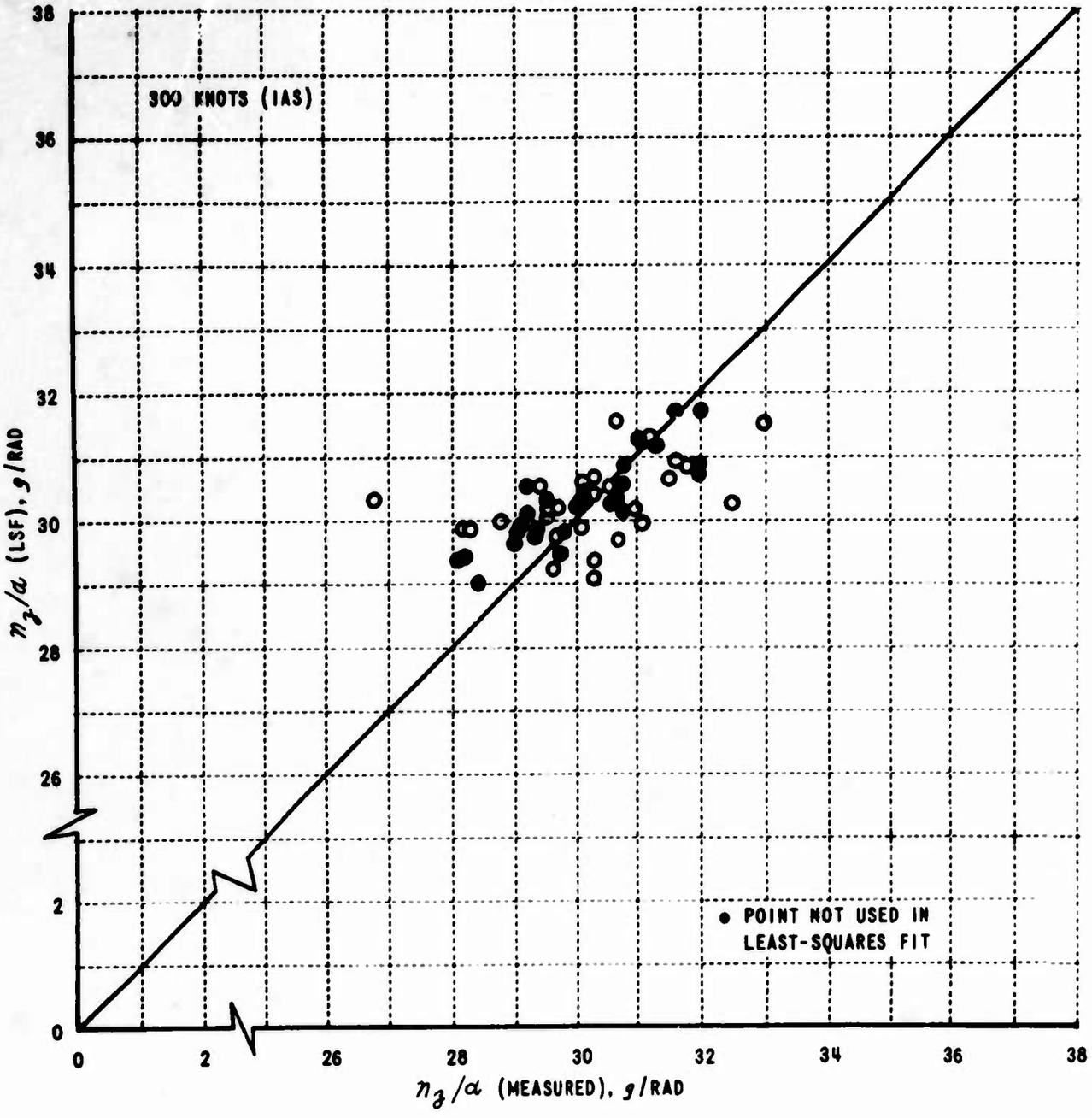

Figure I.17 COMPARISON OF LEAST-SQUARES FIT (LSF) AND MEASURED STEADY-STATE n_z/α SIMULATED

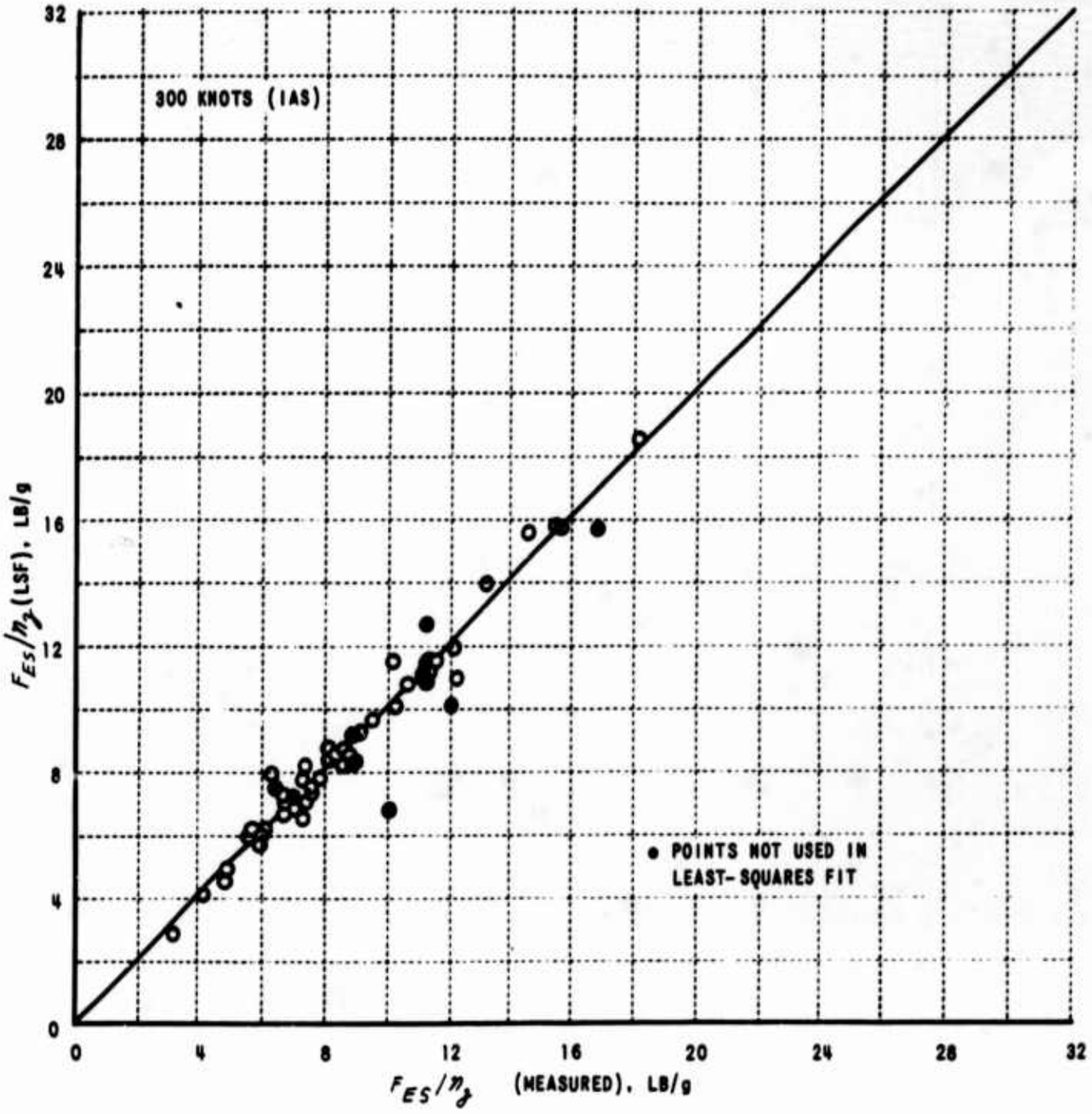

Figure I.18 COMPARISON OF LEAST-SQUARES FIT (LSF) AND MEASURED STEADY-STATE F_{ES}/n_z SIMULATED

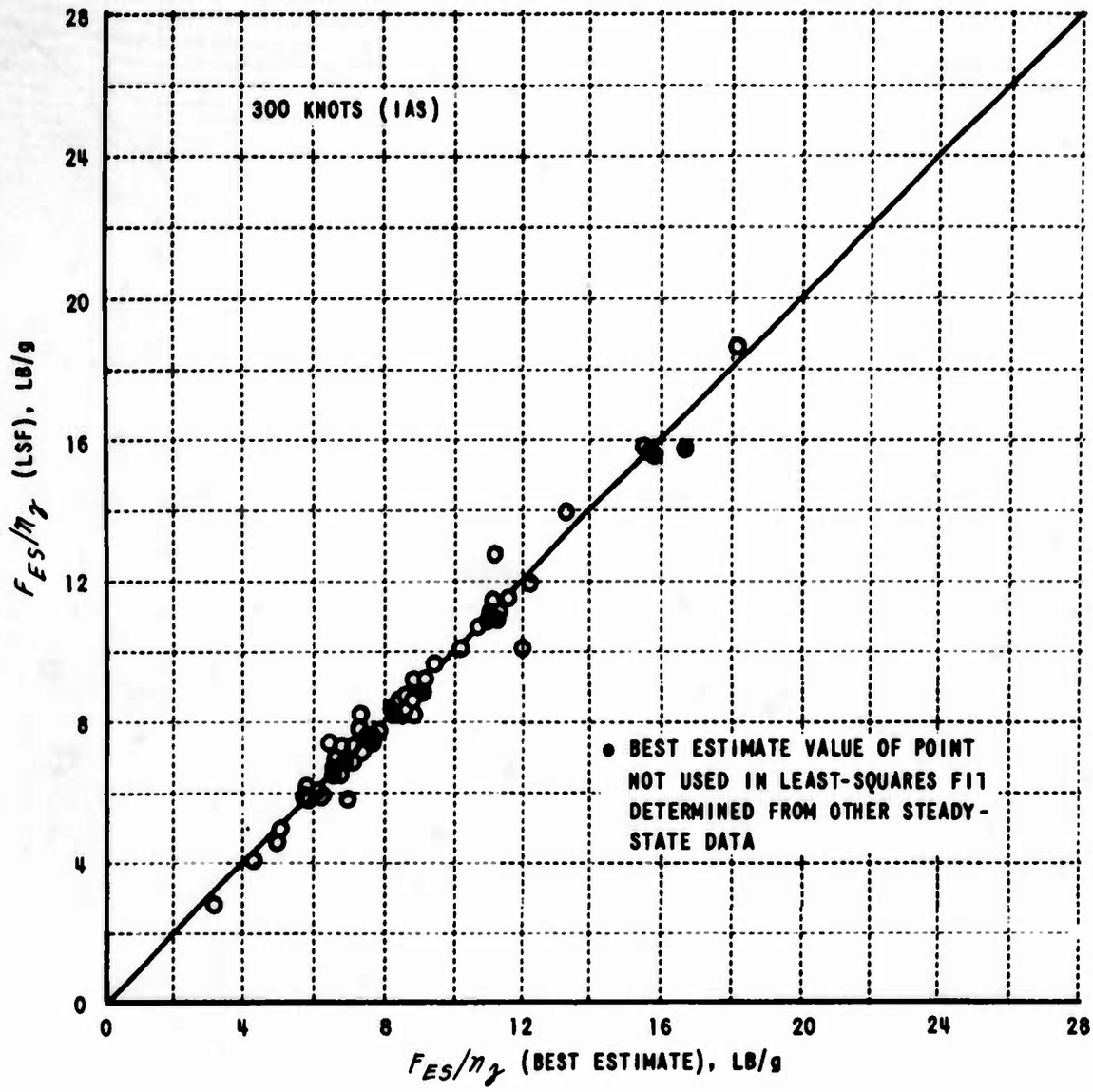

Figure I.19 COMPARISON OF LEAST-SQUARES FIT (LSF) AND BEST ESTIMATE VALUE OF STEADY-STATE F_{ES}/η_g SIMULATED

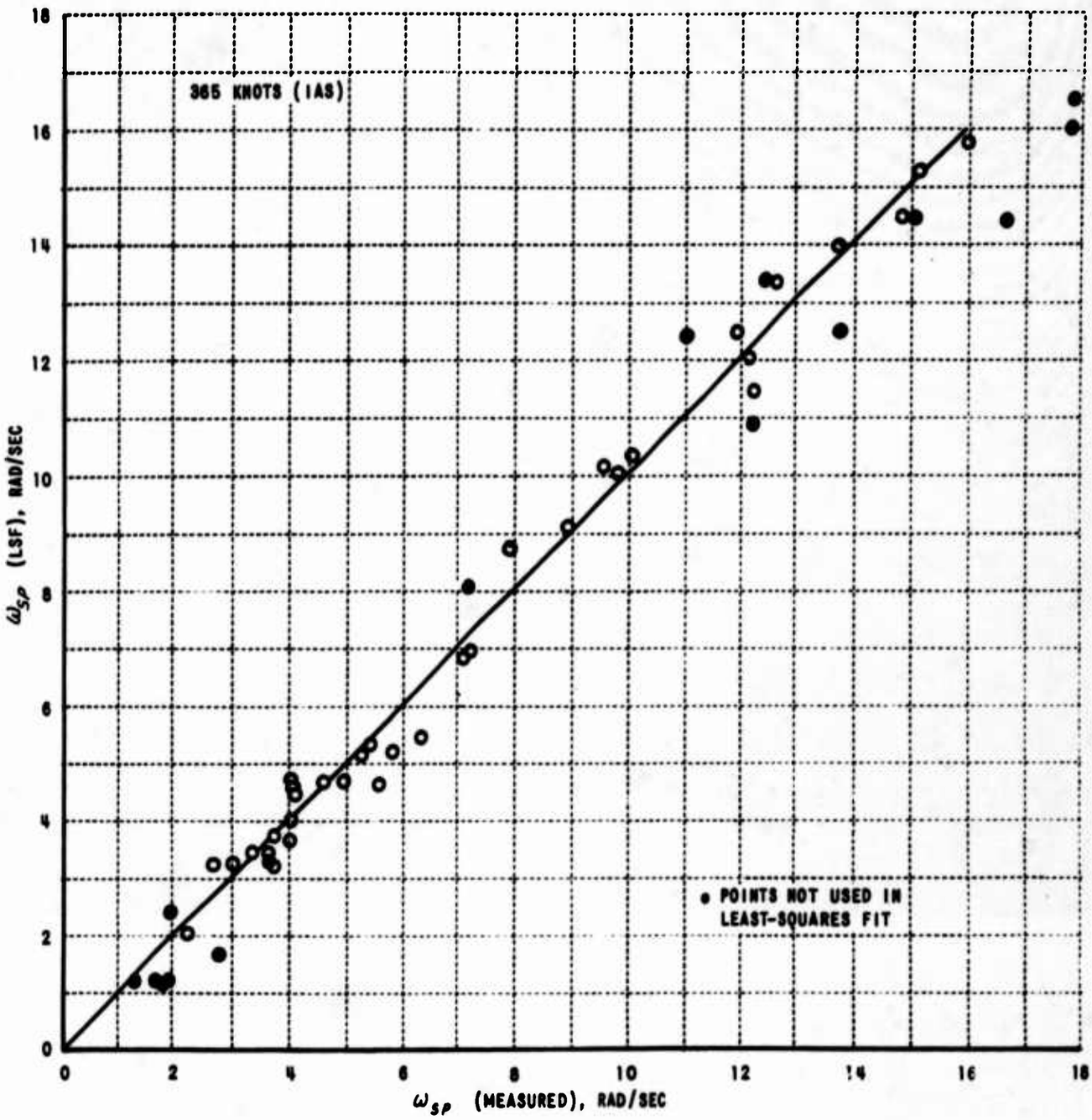

Figure I.20 COMPARISON OF LEAST-SQUARES FIT (LSF) AND MEASURED UNDAMPED FREQUENCIES (ω_{sp}) SIMULATED

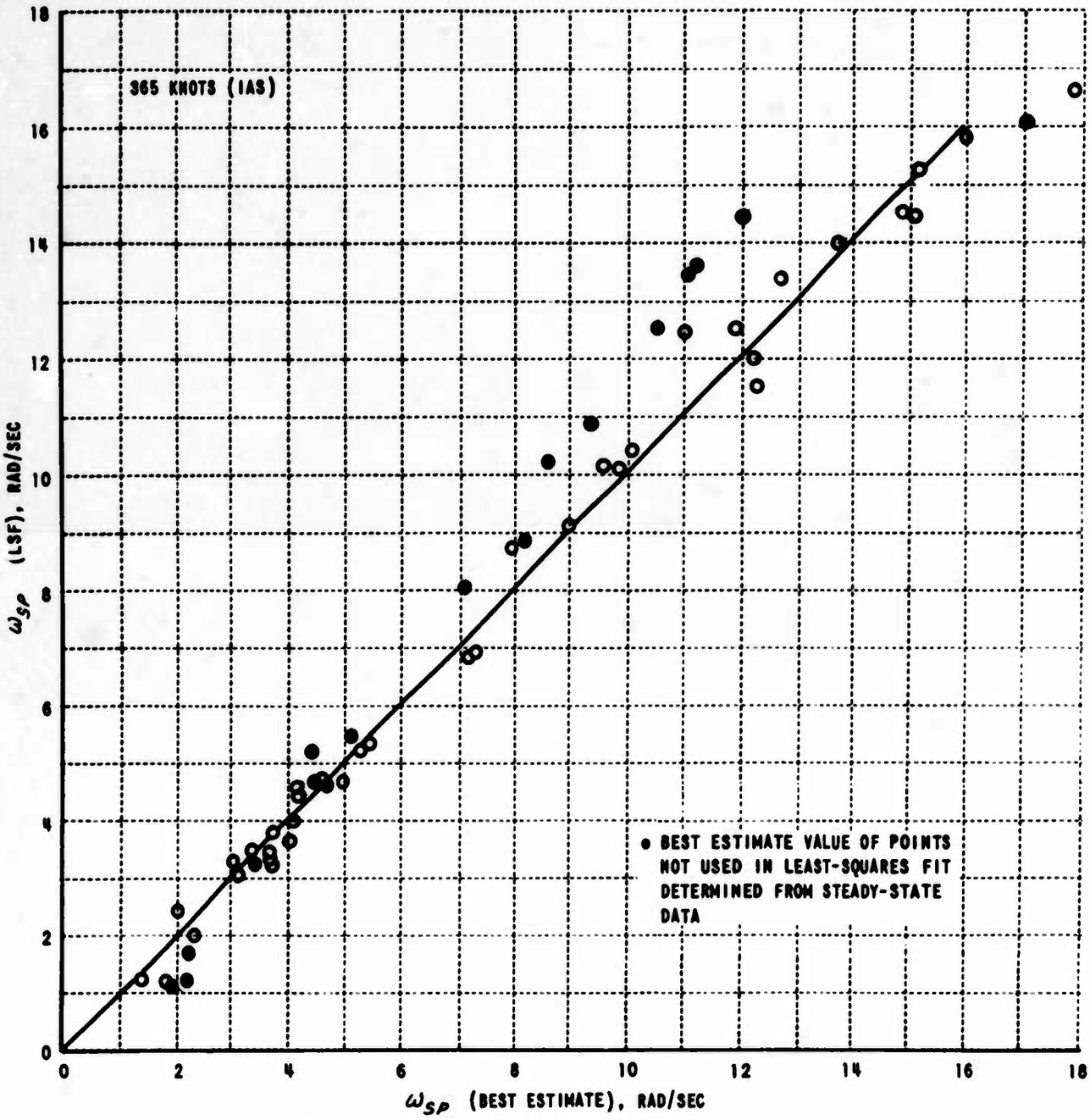

Figure I.21 COMPARISON OF LEAST-SQUARES FIT (LSF) AND BEST ESTIMATE UNDAMPED FREQUENCIES (ω_{sp}) SIMULATED

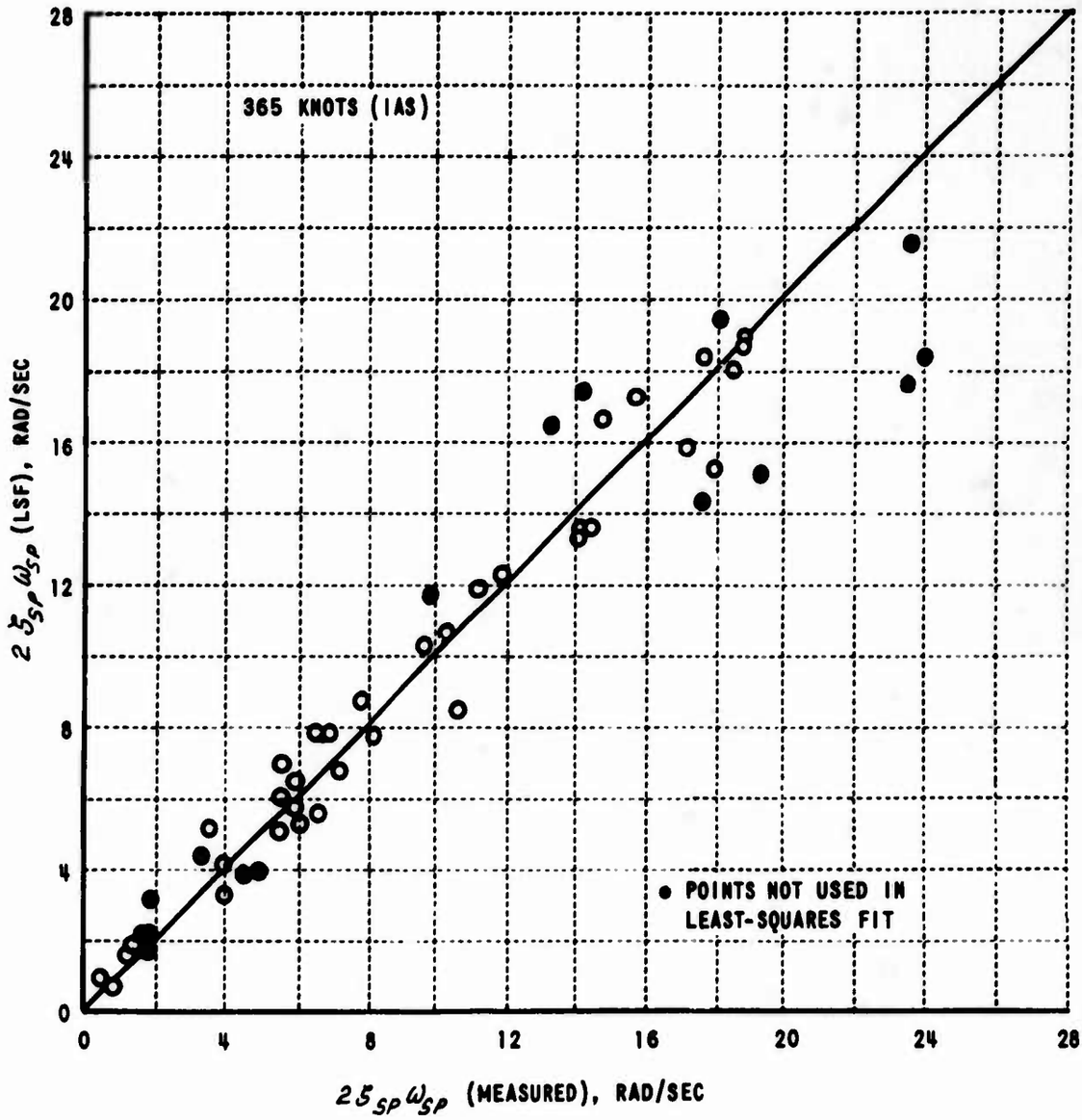

Figure I.22 COMPARISON OF LEAST-SQUARES FIT (LSF) AND MEASURED $2\zeta_{sp}\omega_{sp}$ SIMULATED

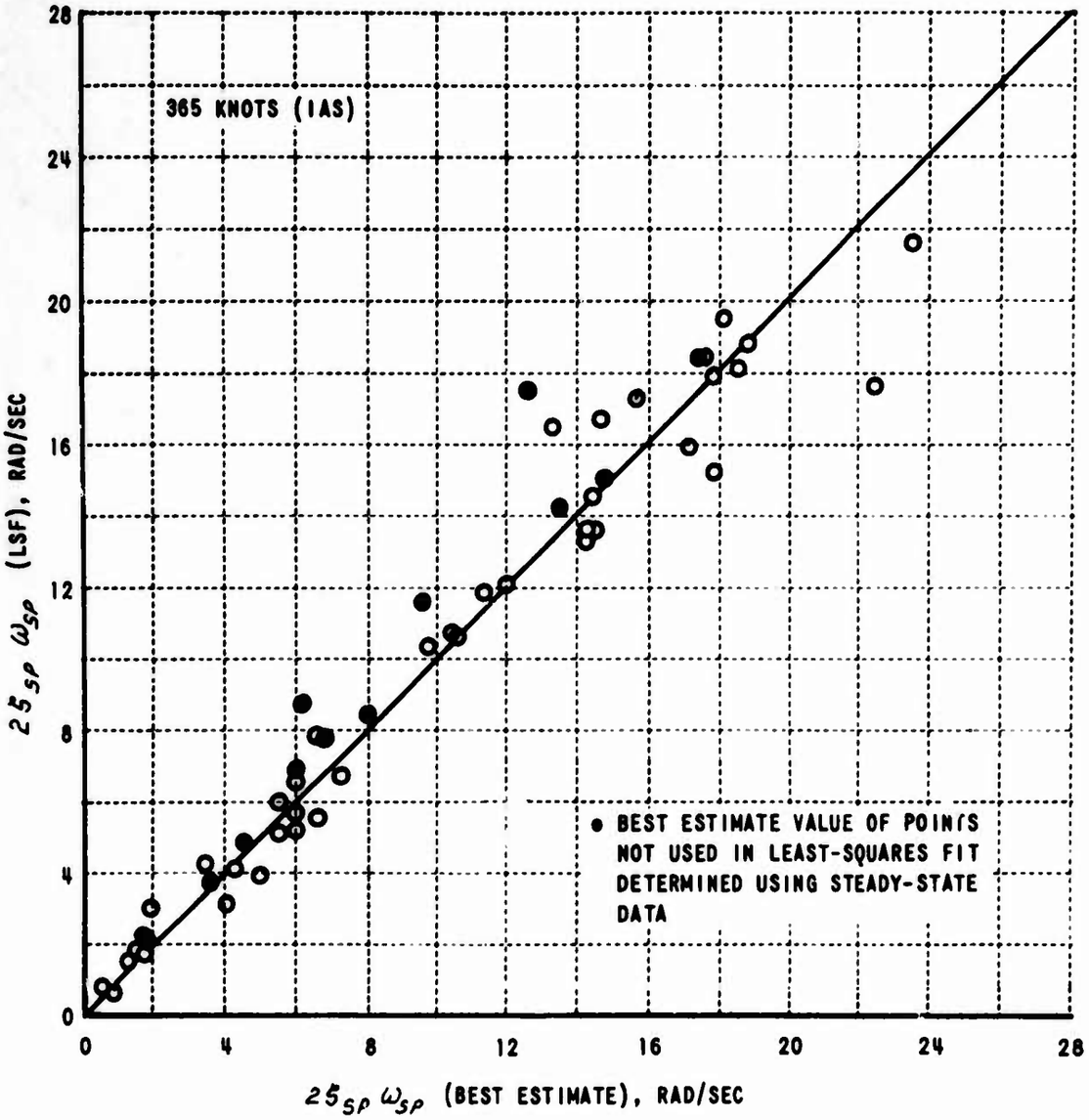

Figure I.23 COMPARISON OF LEAST-SQUARES FIT (LSF) AND BEST ESTIMATE VALUES OF $2\zeta_{sp}\omega_{sp}$ SIMULATED

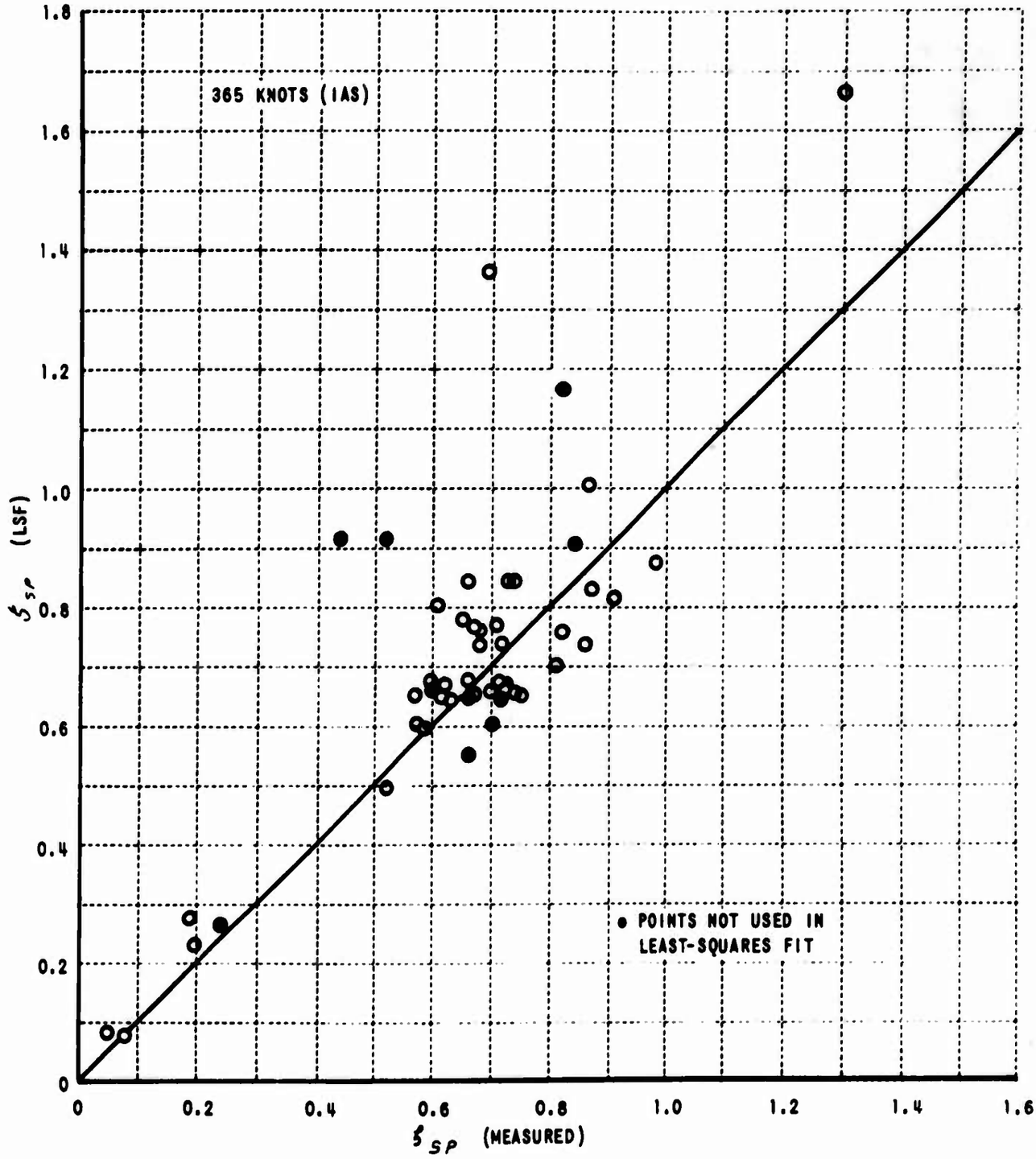

Figure I.24 COMPARISON OF LEAST-SQUARES FIT (LSF) AND MEASURED VALUES OF DAMPING RATIO (ζ_{sp}) SIMULATED

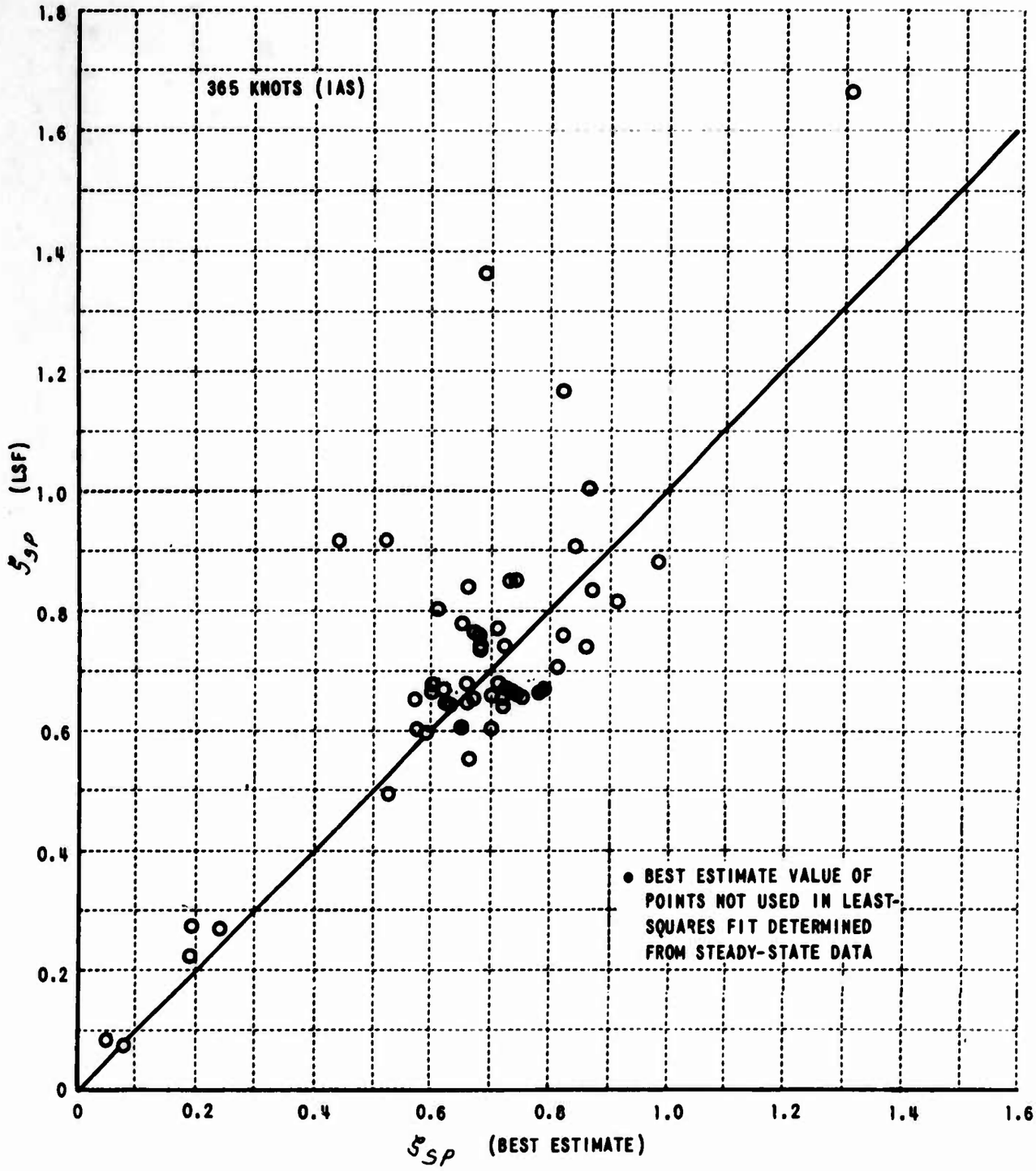

Figure I.25 COMPARISON OF LEAST-SQUARES FIT (LSF) AND BEST ESTIMATE DAMPING RATIO (ζ_{SP}) SIMULATED

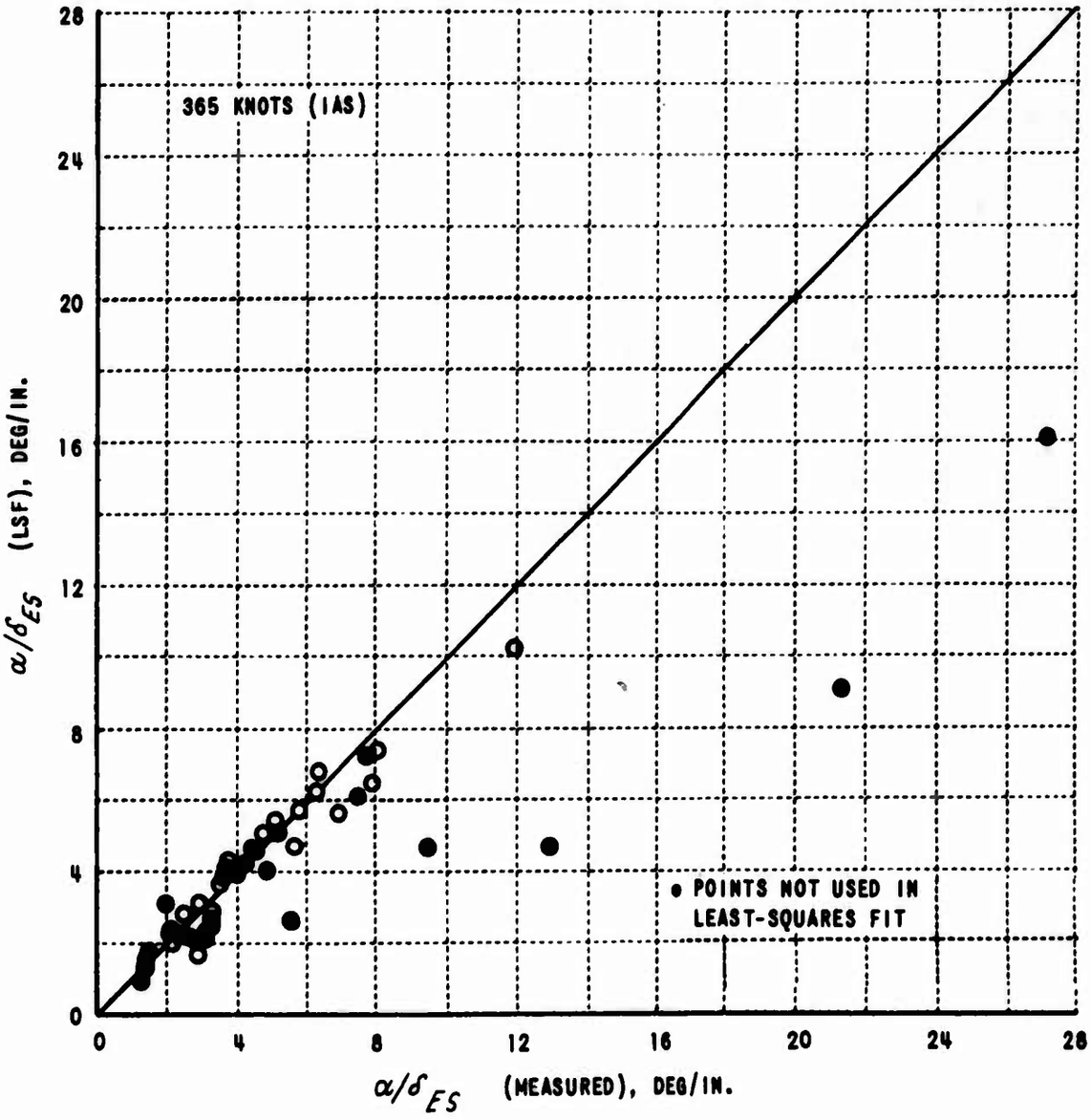

Figure I.26 COMPARISON OF LEAST-SQUARES FIT (LSF) AND MEASURED VALUES OF STEADY-STATE α/δ_{es} SIMULATED

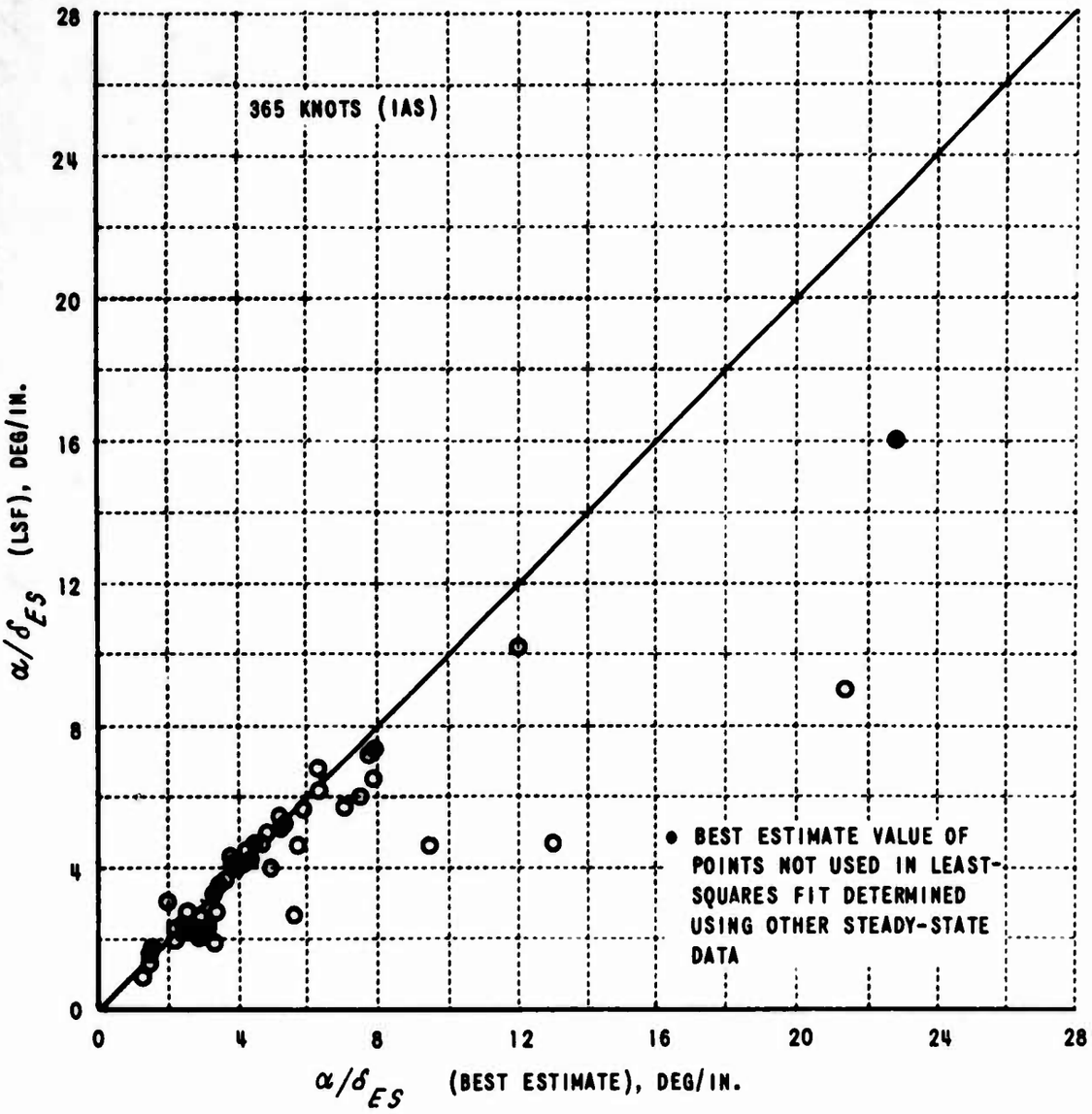

Figure I.27 COMPARISON OF LEAST-SQUARES FIT (LSF) AND BEST ESTIMATE VALUE OF STEADY-STATE (α /δ_{ES}) SIMULATED

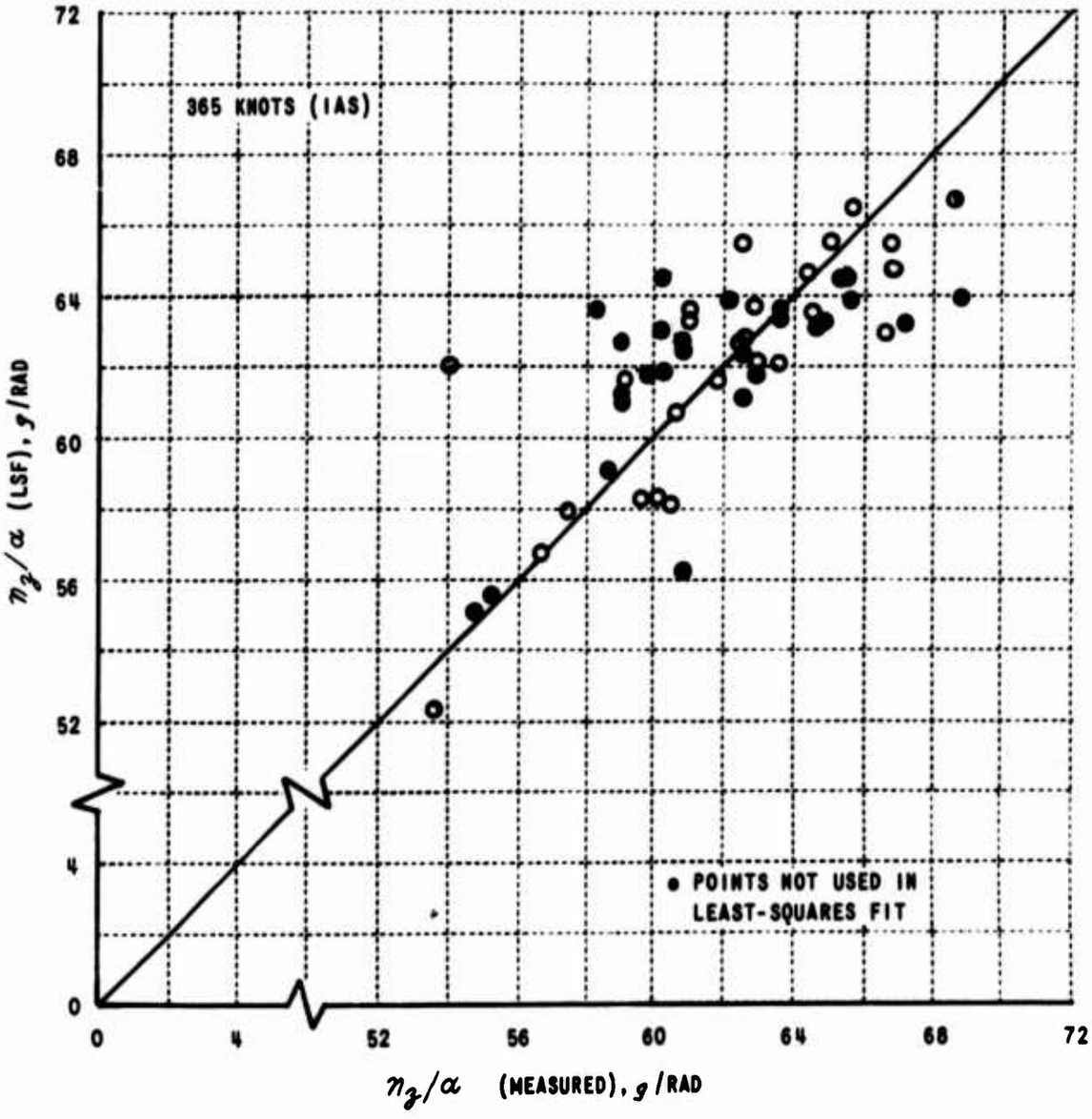

Figure I.28 COMPARISON OF LEAST-SQUARES FIT (LSF) AND MEASURED STEADY-STATE (n_z/α) SIMULATED

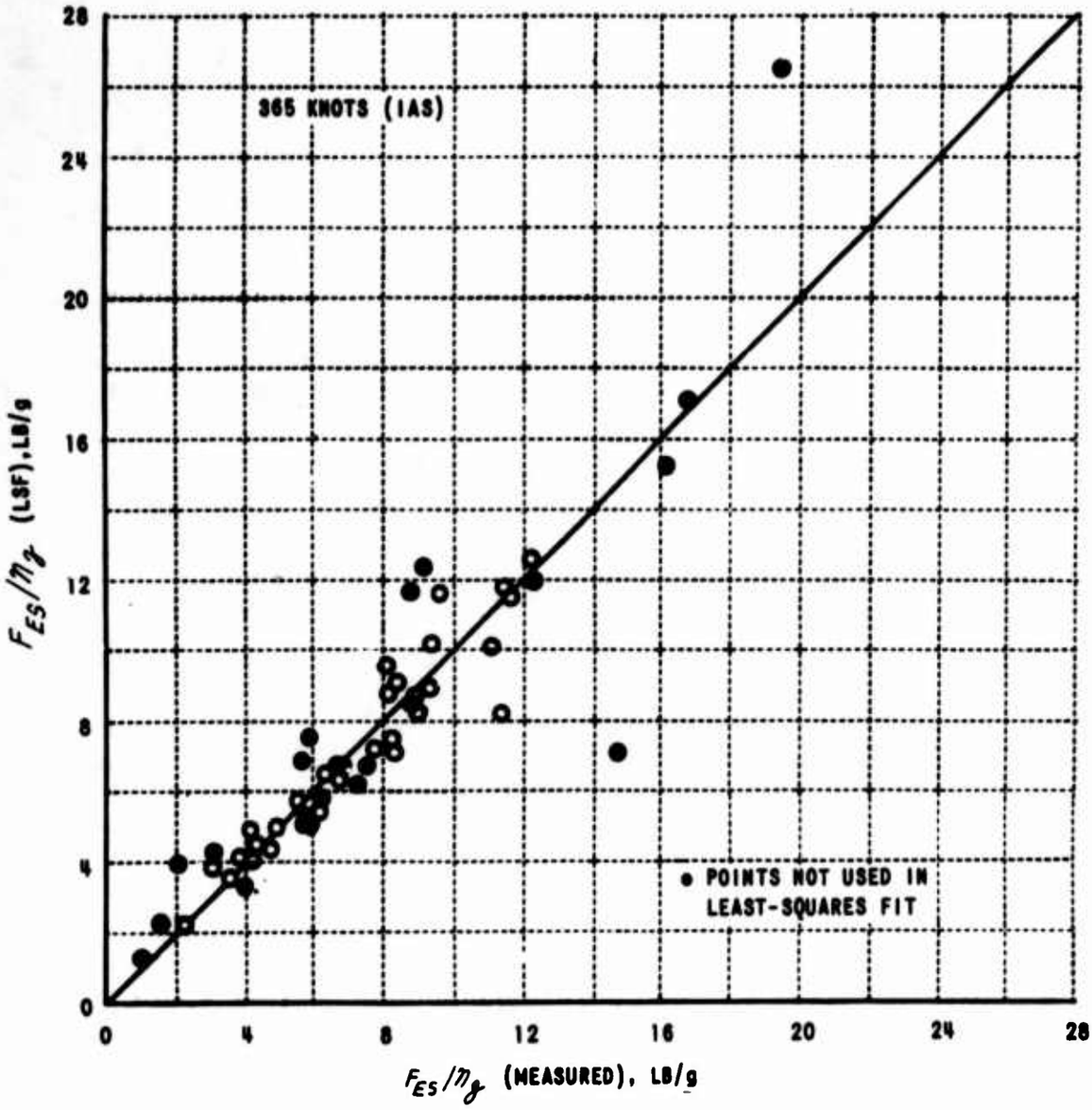

Figure I.29 COMPARISON OF LEAST-SQUARES FIT (LSF) AND MEASURED VALUE OF STEADY-STATE F_{ES}/η_g SIMULATED

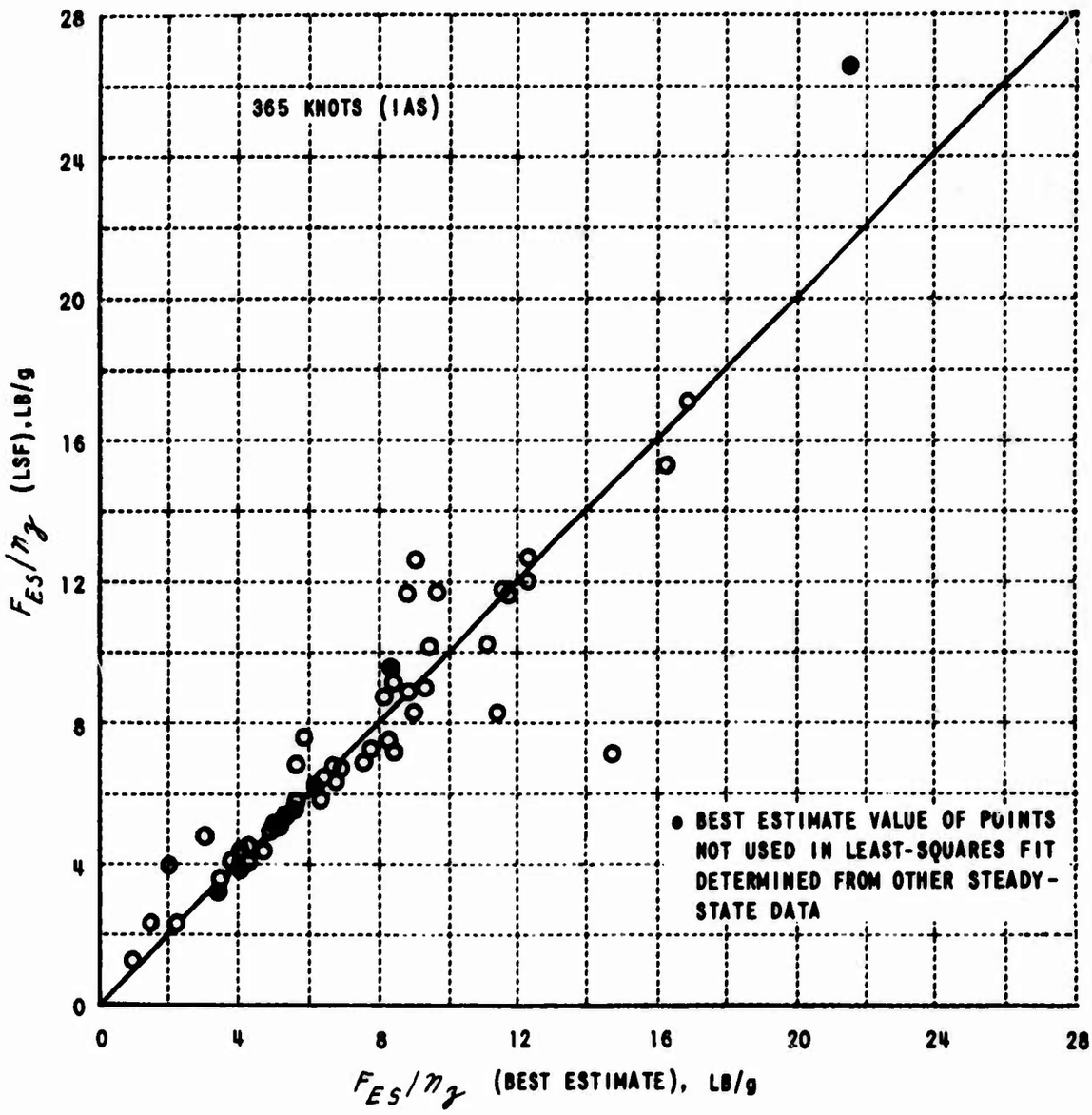

Figure I.30 COMPARISON OF LEAST-SQUARES FIT (LSF) AND BEST ESTIMATE VALUE OF STEADY-STATE F_{ES}/n_z

Appendix II

DYNAMICS OF ELEVATOR FEEL SYSTEM

The importance of elevator feel system dynamics in determining the initial pitch response of the short period frequency configurations simulated has been discussed in Section VI.

It has been demonstrated in Reference 17 that the elevator feel system can be adequately approximated as a second-order system with a transfer function of the following form:

$$\frac{\delta_{ES}(s)}{F_{ES}(s)} = \frac{\omega_{FS}^2 \left(\frac{\delta_{ES}}{F_{ES}}\right)_{ss}}{s^2 + 2\zeta_{FS}\,\omega_{FS}\,s + \omega_{FS}^2} \qquad \text{(II. 1)}$$

Rather than approximate the feel system dynamic characteristics from the limited data of Reference 17, it was thought best to determine the characteristics using data obtained in the present flight test program.

One method used was the analysis of ground records of elevator stick responses to stick force inputs based on the transient response of a second-order system. A second method consisted of the harmonic analysis of actual flight records to determine the frequency response of the transfer function $\delta_{ES}(s)/F_{ES}(s)$. Using the same techniques, some indication was also obtained of the frequency response of the elevator servo $\delta_e(s)/\delta_{ES}(s)$ transfer function.

II. 1 AUTOMATIC STEP INPUTS ON THE GROUND

At the completion of the flight test program, records were taken of step inputs applied at the elevator stick feel strain gage to simulate step stick force inputs (see Reference 17). These were electrical step stick force inputs. Elevator stick and elevator motions were recorded on an oscillograph. Data were taken for the most frequently used feel system gains of the flight test program. Records for three different size steps were taken in both the positive and negative direction.

These records were analyzed using the so called "time ratio" method applied to a well damped second-order step response. The results of this analysis are presented in Table III for the feel system characteristics simulated during most of the flights. It is interesting to note that the feel system characteristics simulated did not vary significantly during the flight program.

It was not possible to analyze the elevator servo transfer function, $\delta_e(s)/\delta_{ES}(s)$, in this way because of the very small lag in the elevator servo. The elevator servo frequency is of the order of 10 cps.

II. 2 HARMONIC ANALYSIS OF FLIGHT RECORDS

An alternate method used to identify the feel system characteristics was to harmonically analyze several actual flight records to determine the frequency response of the feel system.

Figures II. 1, II. 2, II. 3, and II. 4 are the frequency response (amplitude and phase) of the $\delta_{es}(s)/F_{es}(s)$ transfer function following a stick force doublet input. The four figures are based on the harmonic analysis of four different records obtained during the simulations of flights 604 and 591. Faired through the data are frequency response curves based on the frequency and damping determined from the previously discussed ground records.

Reasonable agreement exists between the ground and flight records. The agreement is better for phase shift than amplitude ratio. As is to be expected, considerable noise or scatter exist in the data at the higher frequencies. The feel system characteristics for all three flight conditions (220 kts, 300 kts, and 365 kts IAS) of flight 604 also agree reasonably well, as they should.

Using the same harmonic analysis technique, a check was made of elevator servo frequency response using a flight record for flight 556 at 300 kts IAS (Figure II. 5). Also shown on Figure II. 5 is the frequency response of a second-order system with ω_e = 63 rad/sec, ζ_e = 0. 7. It is evident from the comparison that the elevator servo frequency is of the order of 10 cps.

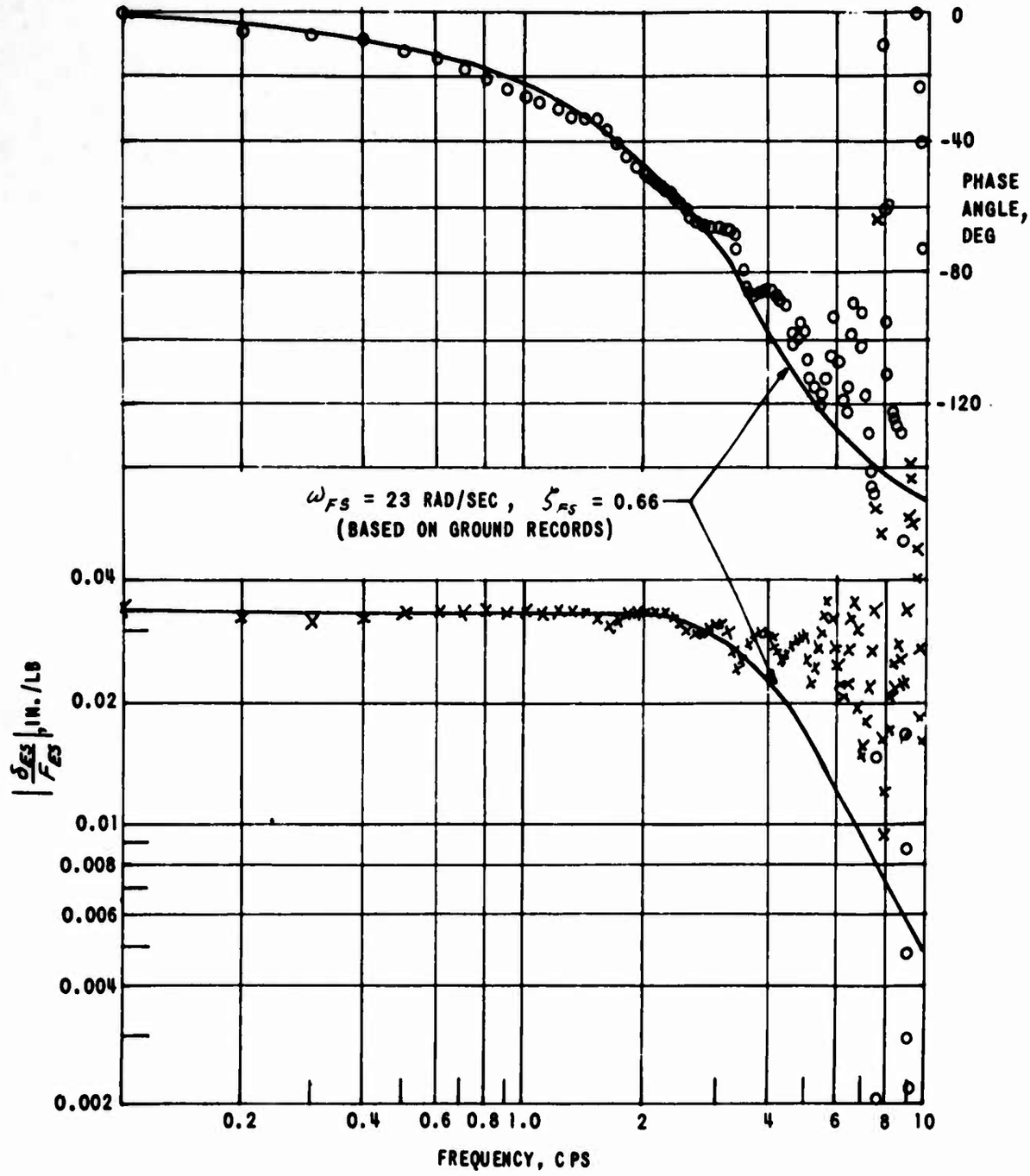

Figure II.1 δ_{ES}/F_{ES} TRANSFER FUNCTION FREQUENCY RESPONSE BASED ON HARMONIC ANALYSIS OF FLIGHT RECORDS (FLIGHT 604, V = 220 KTS IAS, DOUBLET INPUT)

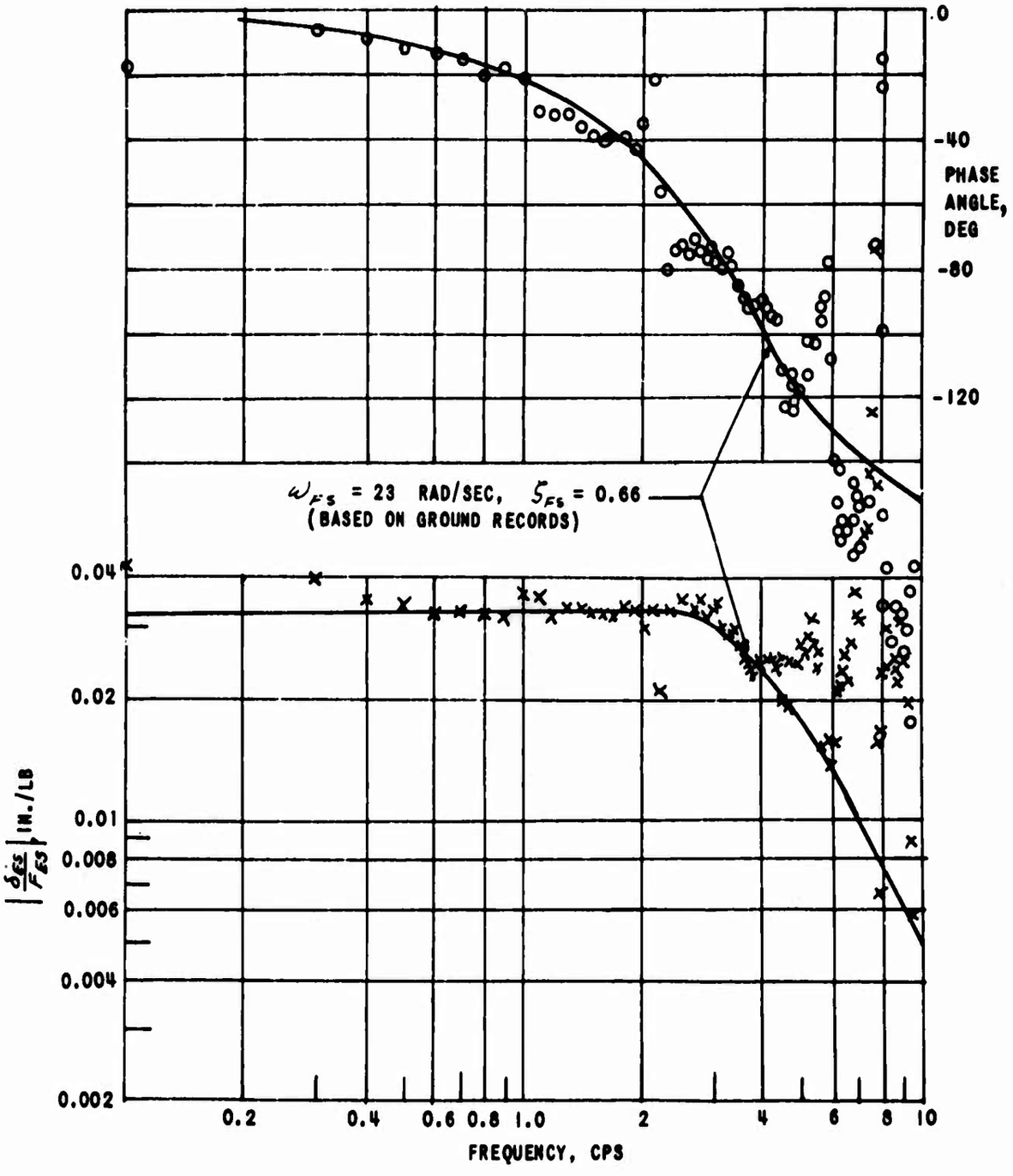

Figure II.2 δ_{Es}/F_{Es} TRANSFER FUNCTION FREQUENCY RESPONSE BASED ON HARMONIC ANALYSIS OF FLIGHT RECORDS (FLIGHT 604, V = 300 KTS IAS, DOUBLET INPUT)

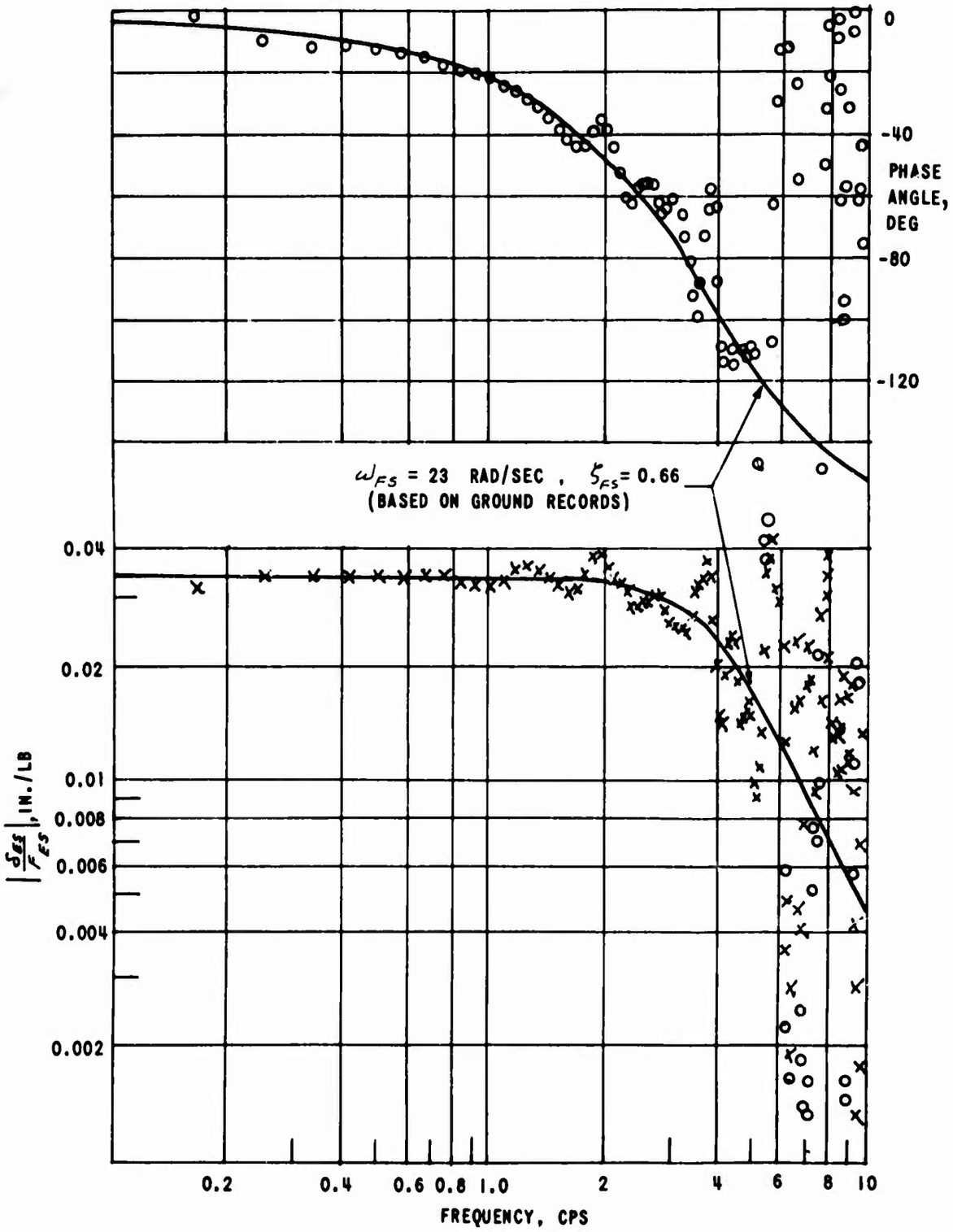

Figure II.3 δ_{ES}/F_{ES} TRANSFER FUNCTION FREQUENCY RESPONSE BASED ON HARMONIC ANALYSIS OF FLIGHT RECORDS (FLIGHT 604, V = 365 KTS IAS, DOUBLET INPUT)

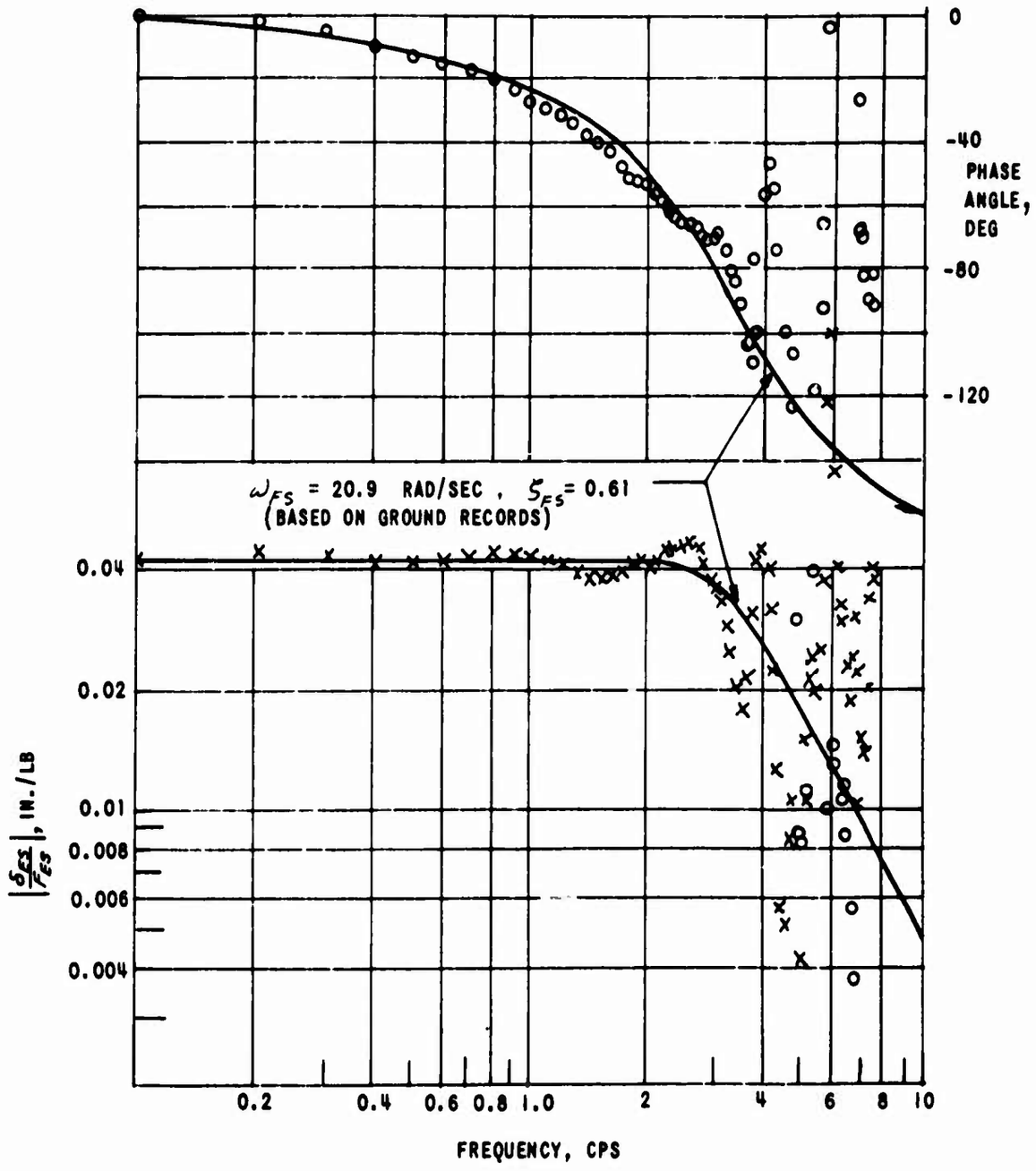

Figure II.4 δ_{ES}/F_{es} TRANSFER FUNCTION FREQUENCY RESPONSE BASED ON HARMONIC ANALYSIS OF FLIGHT RECORDS (FLIGHT 591, V = 220 KTS IAS, DOUBLET INPUT)

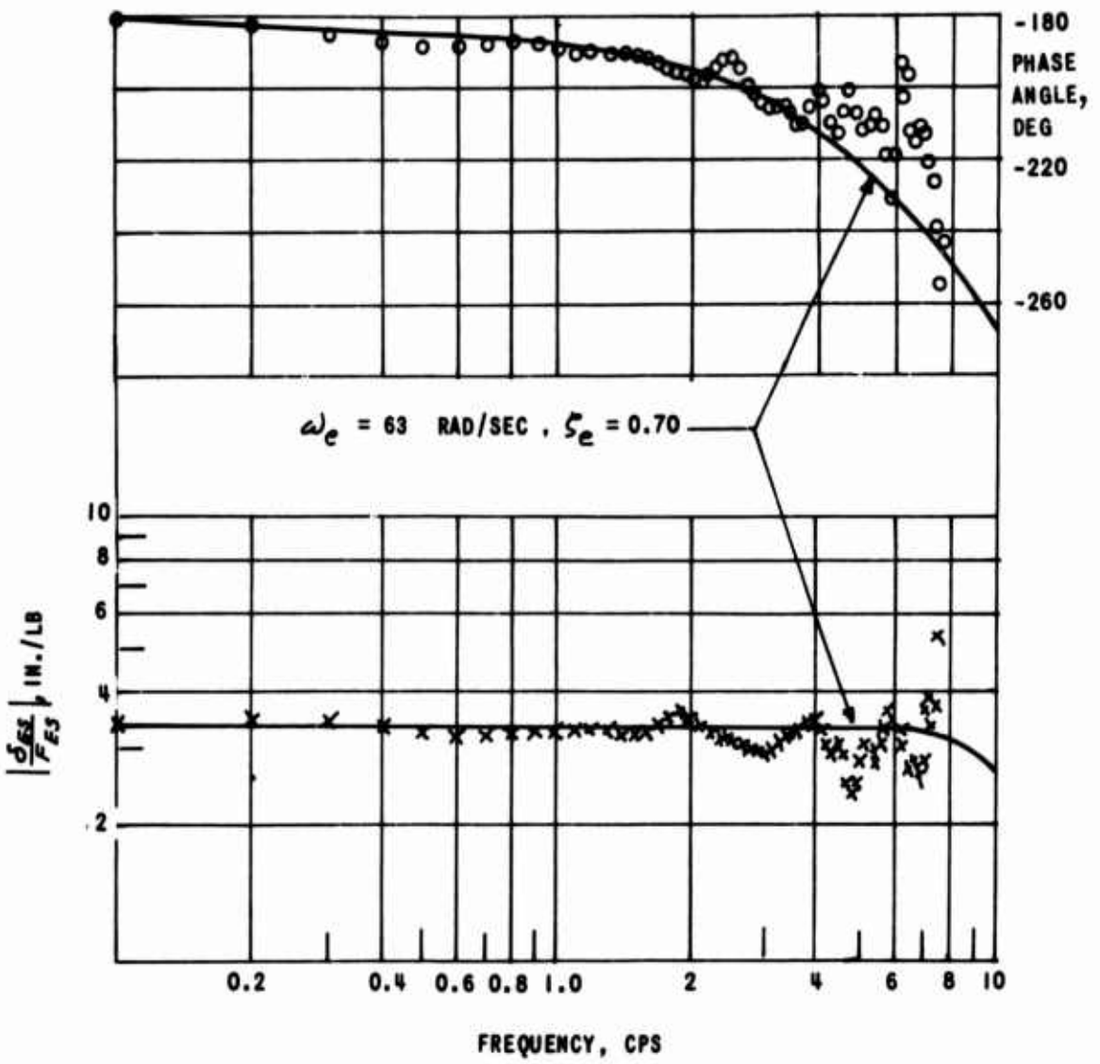

Figure II.5 δ_e/δ_{ES} TRANSFER FUNCTION FREQUENCY RESPONSE BASED ON HARMONIC ANALYSIS OF FLIGHT RECORDS (FLIGHT 556, V = 300 KTS IAS, DOUBLET INPUT)

UNCLASSIFIED
Security Classification

DOCUMENT CONTROL DATA - R & D

(Security classification of title, body of abstract and indexing annotation must be entered when the overall report is classified)

1 ORIGINATING ACTIVITY (Corporate author)	2a. REPORT SECURITY CLASSIFICATION
Cornell Aeronautical Laboratory, Inc. P. O. Box 235 Buffalo, New York 14221	Unclassified
	2b. GROUP

3 REPORT TITLE

Flight Investigation of Longitudinal Short Period Frequency Requirements And PIO Tendencies

4 DESCRIPTIVE NOTES (Type of report and inclusive dates)

Final Report 12 August 1966

5 AUTHOR(S) (First name, middle initial, last name)

DiFranco, Dante A.

6. REPORT DATE	7a. TOTAL NO. OF PAGES	7b. NO. OF REFS
June 1967	138	18

8a. CONTRACT OR GRANT NO.	9a. ORIGINATOR'S REPORT NUMBER(S)
AF33(615)-2536 b. PROJECT NO. 8219 c. Task No. 821905 d.	AFFDL-TR-66-163 9b. OTHER REPORT NO(S) (Any other numbers that may be assigned this report) TC-2083-F-1

10 DISTRIBUTION STATEMENT

Distribution of this document is unlimited.

11. SUPPLEMENTARY NOTES	12. SPONSORING MILITARY ACTIVITY
	AFFDL (FDCC) Wright-Patterson AFB, Ohio 45433

13 ABSTRACT

The results of a flight test program to investigate longitudinal short peroid frequency requirements and PIO tendencies are presented and discussed. Short period frequency requirements were investigated with a damping ratio (ζ_{sp}) of approximately 0.7 at three fixed values of n_z/α (16.9, 30.4, 63.4 g/rad). PIO tendencies were investigated with various values of the parameter $2\zeta_{sp}\omega_{sp}/L_\alpha$. The feel system dynamic characteristics were held essentially constant throughout the program. A variable stability T-33 airplane was used as an in-flight simulator. Each configuration was evaluated as a fighter in "up and away" flight. The evaluation pilots commented on each configuration and rated each numerically. An analysis of pilot ratings and pilot comments was made, and these in turn were related to various handling qualities parameters. In the analysis and interpretation of the handling qualities results, feel system dynamics and pilot-selected stick force gradients (F_{fs}/n_z) were also important considerations.

DD FORM 1 NOV 65 1473

UNCLASSIFIED
Security Classification

14. KEY WORDS	LINK A		LINK B		LINK C	
	ROLE	WT	ROLE	WT	ROLE	WT
Handling qualities PIO (pilot induced oscillations) Longitudinal handling qualities Short period requirements In-flight simulations						